OPTIMAL CONTROL OF FLUID CATALYTIC CRACKING PROCESSES

by

HIROFUMI KURIHARA

Kogakushi, Tokyo University
(1963)

S.M., Massachusetts Institute of Technology
(1966)

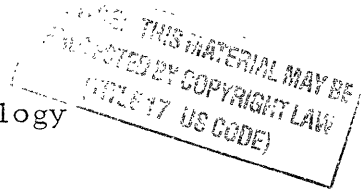

SUBMITTED IN PARTIAL FULFILLMENT OF THE
REQUIREMENTS FOR THE DEGREE OF
DOCTOR OF SCIENCE

at the

MASSACHUSETTS INSTITUTE OF TECHNOLOGY
June , 1967

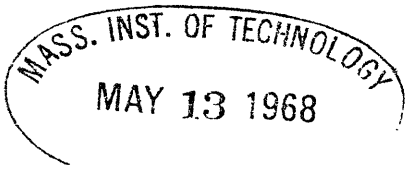

Signature of Auth
Department of Chemical Engineering, June 15, 1967

Certified by _____
Thesis Supervisor

Certified by _____
Thesis Supervisor

Accepted by _____
Chairman, Departmental Committee on Graduate Students

OPTIMAL CONTROL OF FLUID CATALYTIC CRACKING PROCESSES

by

HIROFUMI KURIHARA

Submitted to the Department of Chemical Engineering June 1967 in partial fulfillment of the requirements for the degree of Doctor of Science.

ABSTRACT

An investigation was made of the applicability of optimal control theory to the design of control systems for nonlinear multivariable chemical processes. A hypothetical fluid catalytic cracking process, which is of great economic significance in the modern petroleum refinery, was selected as a typical representative of such a chemical process and was used to test and evaluate alternative approaches to the problem.

Mathematical models describing the dynamic behavior of the process in varying degrees of detail were developed from unsteady-state heat and material balances about the reactor and regenerator. The models utilized semiempirical equations to describe the kinetics of the cracking and carbon burning reactions. The kinetic equations were based upon experimental work reported in the literature.

The dynamic models were used to simulate the process on a digital computer. An extensive investigation was conducted to determine the degree of detail in the mathematical models that would be required for the optimal control studies. It was found that, for the purposes of this work, each fluidized bed could be considered perfectly mixed with respect to spent or regenerated catalyst and that the gas could be assumed to move in plug flow through the bed with negligible time delay. Although there is apparently no quantitative data publicly available describing the dynamic behavior of a commercial cracking unit, the general dynamic characteristics of such units are well known and qualitative descriptions are available. The simulations carried out in this work predicted all of the important dynamic characteristics that have been attributed to commercial units.

The major result from this thesis investigation was the development of a new approach to the design of control systems for highly nonlinear multivariable chemical processes based on optimal feedback control theory. This approach involves obtaining explicit solutions numerically for the open-loop control policy which restores the process from a disturbed state to a steady state in an optimal fashion. These explicit

solutions are obtained for a range of initial disturbed states and they are then converted into implicit closed-loop control policies that can be implemented as an optimal feedback control law. The new approach to control system design was demonstrated for the design of a control system for the hypothetical fluid cracking process.

The objective function is based on an economic balance for the process and incorporates penalties for exceeding safe temperature and oxygen levels in the regenerator. The optimal control problem, with air rate and catalyst rate as control variables, was formulated using the maximum principle of Pontryagin and the explicit numerical solutions for the open-loop control policies were obtained by the method of steepest ascent of the Hamiltonian (or gradient method in function space).

In the feedback control law which resulted from converting the explicit solutions into implicit solutions, the regenerator temperature is controlled by the air rate and the oxygen level is controlled by the catalyst rate. This control scheme is quite different from that which is typically used in refinery operation where the reactor temperature is controlled by the catalyst rate and the oxygen level is controlled by the air rate. The performances of this new control scheme was demonstrated by dynamic simulation to be significantly better at controlling the hypothetical cracking process in the face of disturbances than was the conventional control scheme.

The new design approach was found to have significant advantages over conventional trial and error methods, because it is systematic, and because it provides information to evaluate the desirability of each design step, since the ultimate performance of the system is known from the optimal control theory.

Thesis Supervisor: Leonard A. Gould

Title: Associate Professor of Electrical Engineering

Thesis Supervisor: Lawrence B. Evans

Title: Assistant Professor of Chemical Engineering

ACKNOWLEDGEMENT

The author wishes to acknowledge with deep gratitude the help and advice of his thesis supervisors, Professor L. A. Gould of the Electrical Engineering Department, and Professor L. B. Evans of the Chemical Engineering Department.

This work was supported by National Science Foundation Grant NSF GK-563, M.I.T. Project DSR 74994. The computational work reported here was performed at the M.I.T. Computation Center.

Finally the efforts of the Drafting and Publications Staffs of the Electronic Systems Laboratory are greatly appreciated.

CONTENTS

CONTENTS (Contd.)

LIST OF FIGURES

LIST OF FIGURES (Contd.)

LIST OF FIGURES (Contd.)

LIST OF TABLES

CHAPTER I

SUMMARY

Introduction

Although recent advances in the theory of optimal control have been remarkable, the application of the theory to the control of chemical processes has been restricted largely to overly simplified situations of limited practical significance. A major difficulty in designing control systems for chemical processes is the complicated nature of most processes. Chemical processes are generally highly nonlinear, multivariable systems, and receive a wide range of disturbances. Furthermore, the operating goal for most chemical plants is not only the regulation of process variables, but also the realization of maximum profit.

The purpose of this work is to investigate the applicability of optimal control theory to the problem of control system design for a typical example of multivariable, nonlinear chemical process. A hypothetical fluid catalytic cracking unit was selected as the process to be studied. It provides a challenging control problem, and also is of great economic significance in a modern petroleum refinery.

Until the late 1950's fluid catalytic crackers were relatively easy to operate. However, as refineries became more complex, greater efficiency has been required. Removal of the catalyst-deactivating influence of regenerator spray water has increased regenerator temperatures 100-150^{o}F, to above 1200^{o}F. Afterburning of CO to CO_2 will occur readily at these temperatures, if there is any significant content of oxygen in the flue gas. Afterburning results in rapid and excessive temperature rises. All of these actions influence the carbon content of the circulating fluidized catalyst and the heat balance in the unit to produce a potentially unstable operation.

This can easily result in an upset condition, unless the control system is properly designed or operators remain alert.[32*]

Theoretical Background for a New Approach in Control System Design

In recent years great attention has been given to the theory of optimal control.[6, 39, 58, 60] The theory assumes a plant described by a set of ordinary differential equations:

$$\dot{\underline{x}} = \underline{f}(\underline{x}, \underline{u}) \tag{1.1}$$

where $\underline{x}$ represents a vector of state variables (dependent variables) and $\underline{u}$ represents a vector of control variables (independent variables). An objective functional (or performance criterion), which may consist of profit, cost, or other artificial measure of performance of operating the plant from time $t = 0$ to $t = t_1$, is given by:

$$J(\underline{u}) = \int_0^{t_1} L(\underline{x}, \underline{u})\, dt \tag{1.2}$$

where L may be an arbitrary function. Optimal control theory asks how $\underline{u}$ should be chosen as a function of t, $0 \leq t \leq t_1$, to make the objective functional J a maximum (or a minimum).

Once the problem is posed, the optimal control can be derived by mathematical techniques, such as the calculus of variation,[38] or its extension, the maximum principle of Pontryagin.[58] If an explicit result is needed, however, the computations are severe. Results have been obtained thus far only for relatively simple functions of L, and for plants defined by small sets of equations.[60] Most of the work in optimal control theory has been directed toward obtaining an explicit solution, or an open-loop structure of the optimal system.

---

* Superscripts refer to numbered items in the Literature Citations.

In some cases, it is possible to obtain the structure of the optimal control system without explicitly solving the equations for the optimal control, $\underline{u}$. For example, if the plant is operated continuously for a sufficiently long period between shutdowns, then t_1 in Eq. 1.2 becomes so large that the optimal control $\underline{u}$ is effectively independent of t_1. Then, $\underline{u}(t)$ for $0 \leq t \leq t_1$ will depend only on the initial condition (initial state) of the plant $\underline{x}(0)$. This can be simplified further by using the principle of optimality, namely--Whatever the previous state and previous decision, the remaining decision must constitute an optimal policy with respect to the state resulting from the previous decision. Thus, in general, if t_1 is infinite the optimal functional relation between $\underline{u}(t)$ and $\underline{x}(t)$ at any instance t is

$$\underline{u} = \underline{h}(\underline{x}) \tag{1.3}$$

This relation, if it exists, is called a closed-loop structure of the optimal control system, and may be considered an implicit solution (or optimal control law).

This closed-loop structure essentially has the following advantages over the open-loop structure:

1. A closed-loop structure does not require extensive on-line computations to implement it in a real-time operation. According to Eqs. 1.1 and 1.3, the plant should obey the differential equations:

$$\dot{\underline{x}} = \underline{f}\{\underline{x}, \underline{h}(\underline{x})\} \tag{1.4}$$

and the resulting behavior corresponds to optimal operation. An open-loop structure requires an optimizing computation for an operation with a different initial condition.

2. Generally, real plant performance will be affected less by disturbances and by errors in the mathematical model when a closed-loop structure is implemented than when an open-loop structure is implemented.

A result of this thesis investigation is a proposed new approach to control system design based on the above closed-loop structure of the optimal system. However, with this new approach the optimal control system will not be implemented directly, but an alternative closed-loop control system will be implemented which approximates the resulting implicit solution (or optimal control law) by a simple relation for practical use. And if the performance of this alternative closed-loop control is tested for various disturbances with the use of dynamic simulation, then the evaluation of this new approach is possible.

An implicit solution, however, can not be obtained analytically except certain idealized cases.[6,36] Therefore it is necessary first to obtain an explicit solution and then to convert it into an implicit solution. In order to obtain an explicit solution, there exist two groups of computational algorithms. One group uses necessary conditions for optimality derived from the calculus of variation or the maximum principle and transforms a dynamic optimization problem into a two-point boundary value problem, which is very difficult to solve because a set of differential equations must be solved in a direction in which their behavior is unstable.[60] The other group essentially uses a hill climbing approach. The method of steepest ascent of the Hamiltonian (or gradient method in function space) belongs to this second group and has been used successfully.[33,39,60] The method will be summarized briefly.

First, the problem of optimizing an objective functional, Eq.1.2, while observing Eq. 1.1 as constraints, can be reduced to the problem of optimizing the following Lagrangean functional with respect to $\underline{x}$, and $\underline{u}$:

$$\mathcal{L}\ (\underline{x}, \underline{p}, \underline{u}) = J(\underline{u}) + \int_0^{t_1} \underline{p}'\{\underline{f}(\underline{x}, \underline{u}) - \dot{\underline{x}}\}\ dt \qquad (1.5)$$

where $\underline{p}$ represents a vector of costate variables (or Lagrange multipliers). After certain mathematical manipulations,[60] it is possible to state that if $\underline{p}$ is chosen such that

$$\dot{\underline{p}} = -\partial H/\partial \underline{x} \text{ with } \underline{p}(t_1) = \underline{0} \tag{1.6}$$

where H is referred to as the Hamiltonian function and defined by

$$H(\underline{x}, \underline{p}, \underline{u}) = L(\underline{x}, \underline{u}) + \underline{p}' \underline{f}(\underline{x}, \underline{u}) \tag{1.7}$$

and if Eq. 1.1 is satisfied with a certain initial condition, then the variation of the Lagrangean functional with respect to $\underline{u}$ is expressed by

$$\delta \mathcal{L}(\underline{u}) = \int_0^{t_1} (\partial H/\partial \underline{u})' \delta \underline{u} dt \tag{1.8}$$

Equation 1.8 is the basis of the method of steepest ascent of the Hamiltonian, since it is possible to insure positive $\delta \mathcal{L}(\underline{u})$ by setting

$$\delta \underline{u} = e(\partial H/\partial \underline{u}) \tag{1.9}$$

where e is a positive relaxation parameter, until $\partial H/\partial u_i$ becomes zero or u_i is found on the boundary at which the free choice of u_i is limited.

A typical computing algorithm for this method is the following:

1. For a specified time t_1 of operation, choose a nominal $u(t)$ as a first approximation. This $\underline{u}(t)$ will be nonoptimal.

2. Integrate Eq. 1.1 from 0 to t_1 for the assumed $\underline{u}(t)$.

3. Now integrate Eq. 1.6 from t_1 back to 0, which is possible because the $\underline{x}$ are known along the trajectory.

4. In the course of (3) evaluate $\partial H/\partial \underline{u}$ as a function of time.

5. Replace $\underline{u}(t)$ by $\underline{u}(t) + e\partial H/\partial \underline{u}$, and repeat from (2).

It should be noticed that Eqs. 1.1 and 1.6 are each integrated in the "natural" direction, that is, the direction in which each is expected to be stable. This eliminates the problem of stability which is encountered in a direct application of the variational method. There is, on the other hand, a problem in choosing e. If e is too small, progress will be slow. If it is too large, the iteration becomes unstable. The best method of selecting and varying e during the computations depends upon the particular problem.[39]

Specific Objectives

As was stated earlier, the purpose of this work is to investigate the applicability of optimal control theory to the problem of control system design for a hypothetical fluid catalytic cracker as a typical example of a multivariable nonlinear process. It is now possible to describe the specific goals of the work:

1. The first objective was to evaluate a new approach to control system design that was developed in the course of the thesis investigation and which, as described earlier, is based essentially on a closed-loop structure of the optimal control law. The performances of the resulting control system was tested for various disturbances with the use of dynamic simulation.

2. The second objective was to test a computational algorithm--the method of steepest ascent of the Hamiltonian--for dynamic optimization of a highly nonlinear multivariable process typified by a fluid catalytic cracking unit. In the work, the applicability of using penalty functions (artificial measures of process performance

under certain undesirable operating conditions which should be avoided) was tested to obtain an approximate solution for the problem of dynamic optimization with the allowable ranges of state variables restricted.

Control of Fluid Catalytic Cracking Processes

Catalytic cracking is a continuous process for converting high-boiling, high-molecular-weight components of distilled crude oil into lower-boiling, lower-molecular-weight materials such as gasoline. This processing adds economic value to the oil. A catalyst is used to effect the reaction, and in fluid catalytic cracking the catalyst is in a fine powder form and is maintained in a fluidized state.

The diagram of the process is shown in Fig. 1.1. The catalyst circuit consists of the reactor, stripper, spent catalyst slide valve, air riser, regenerator, standpipe, regenerated catalyst slide valve, oil riser and leads back into the reactor with the catalyst flowing in the same order.

Fresh feed and recycle feed are vaporized on contacting the regenerated catalyst at the base of the oil riser and lift the catalyst into the reactor where disengagement is accomplished both by gravity and with cyclone separators. The endothermic reaction commences at the moment of contact and is completed in the reactor. The product vapors pass overhead to the fractionator.

The catalyst, from the reactor, which has a layer of coke deposited on it as a result of the reaction, is stripped coutercurrently with steam to remove entrained oil vapors. Air moves the spent catalyst to the dense bed in the regenerator and burns off the carbonaceous deposit from the catalyst as H_2O, CO and CO_2. This reaction is exothermic, and the hot regenerated catalyst flows back into the reactor and provides the necessary heat for the cracking reaction.

As is shown in the figure, there are five controls which the operators may adjust: air blower adjustment, slide valve adjustment,

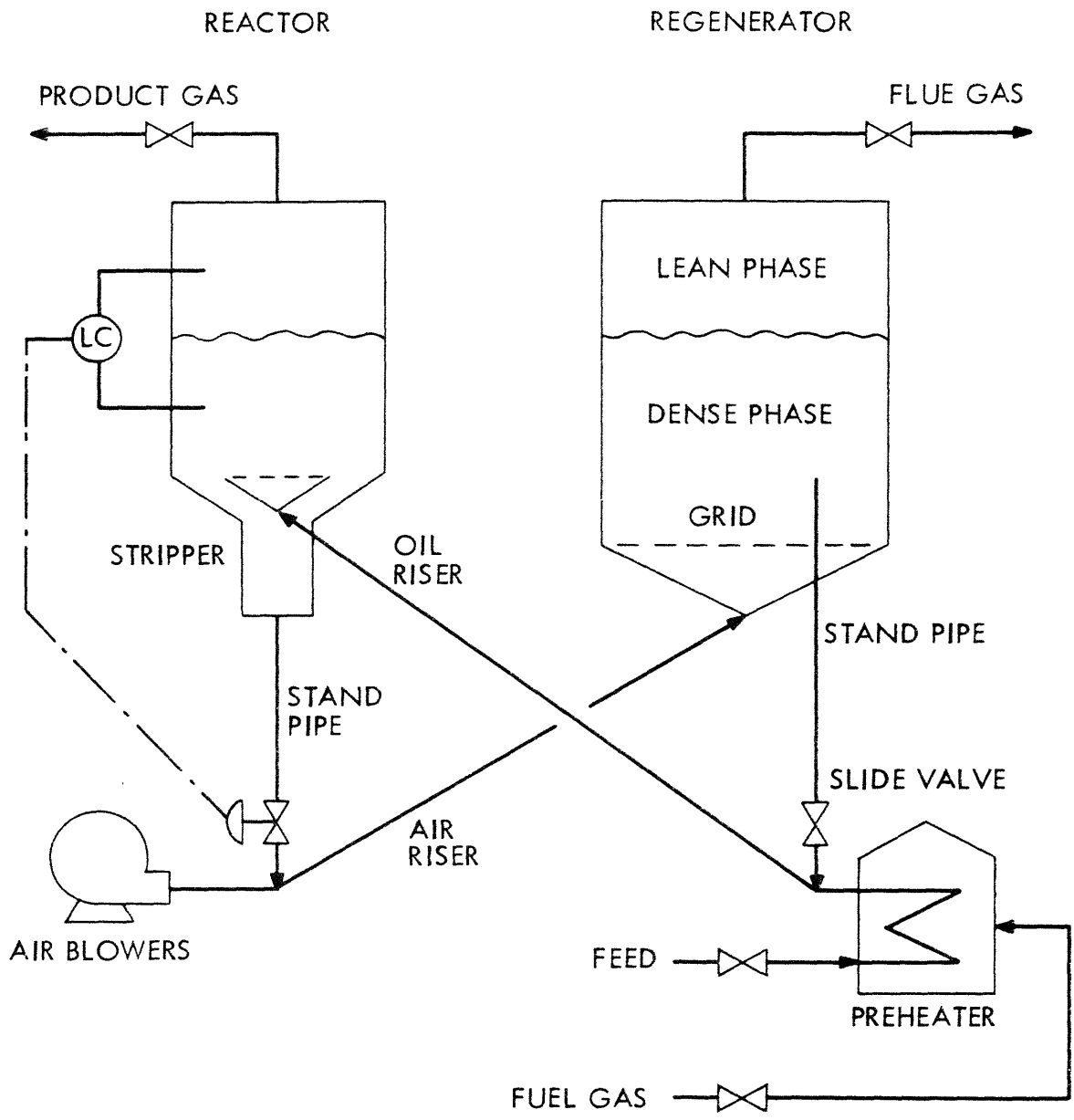

Fig. 1.1 A Typical Fluid Catalytic Cracking Unit

reactor level controller setting, fuel gas flow rate to the feed preheater, and feed rate. The air blower is adjusted to supply necessary air to the regenerator. The slide valve is adjusted to supply necessary catalyst flow to the reactor. The reactor level controller setting is adjusted to maintain a certain catalyst holdup. The fuel gas flow rate to the feed preheater is adjusted to maintain a certain feed temperature at the coil outlet. The feed rate is adjusted to maintain a satisfactory condition depending on the regenerator capacity, preheater capacity, etc.

The objective is to maintain a set of conditions which will result in the satisfactory operation of the process. Some of the problems involved in control of a fluid catalytic cracking unit may be explained in terms of the idealized representation (referred to as mathematical Model No. 1) shown in Fig. 1.2. (Symbols are listed in Table 1.2.) There are five independent variables which can be varied at will plus five dependent variables (of which only T_{rg}, O_{fg} and T_{ra} are continuously measurable). The principal disturbance which affects the operation of this process is the fluctuation of feed properties. This results from the unavoidable necessity of processing several different crude-oil stocks during a relatively brief period. Another aspect of the control problem is that O_{fg} and T_{rg} must be maintained below certain specified values to insure safe operation of the regenerator. Therefore the control problem is to manipulate some or all of the independent variables in order to maintain satisfactory performance in the face of disturbances, while restricting the variables within allowable ranges.

The dynamic mathematical Model No. 1 for a hypothetical fluid catalytic cracker with dense bed reactor was developed by isolating the reactor and regenerator systems from the fractionator and the feed preheater. The main assumptions were as follows:

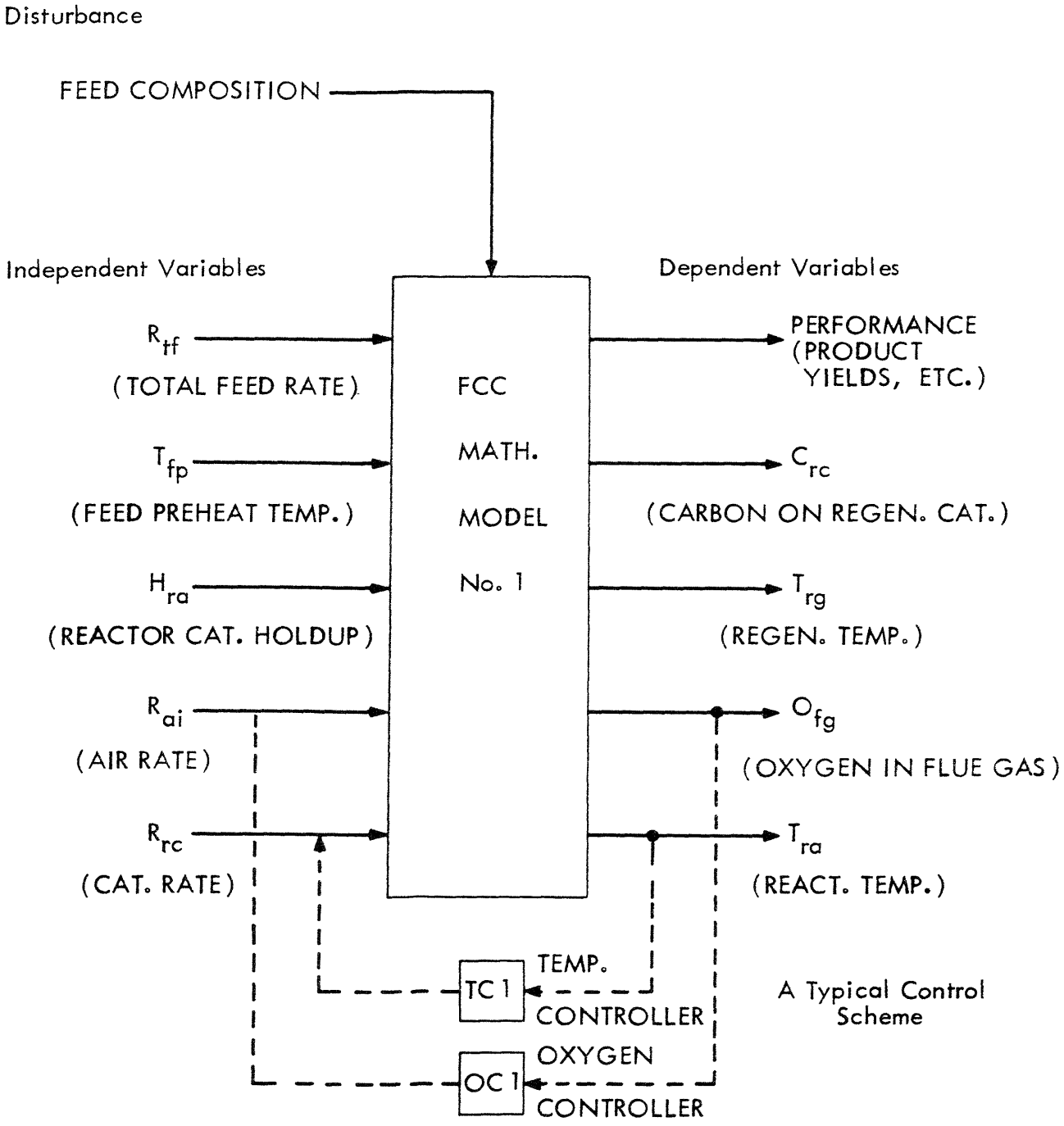

Fig. 1.2 Control Aspect of a FCC Mathematical Model

1. A fluidized bed is "perfectly mixed" with respect to spent and regenerated catalyst.

2. Gas passes through the bed in a plug-flow manner with negligible time lag.

3. Constant pressure is maintained in both vessels.

4. The heat capacity (per unit mass) of reactants and products are equal and constant in each vessel. Catalyst heat capacity is also constant.

5. Activation energies, heats of reaction and heat of vaporization of the feed are all constant.

The dynamic models of reactor and regenerator involve carbon balances, heat balances, and reaction rate equations; they are shown in Table 1.1. The equations are dimensional and their symbols are listed in Table 1.2. Equation 1.10 is a reactor carbon balance equation; accumulation equals carbon forming rate plus the difference between input and output due to catalyst circulation. Equation 1.11 is a reactor heat balance equation; accumulation equals the difference between input and output due to catalyst circulation and reactant gas carry over minus the heats of vaporization and cracking. Equations 1.12 and 1.13 were derived semiempirically utilizing the results of experimental studies reported in the literature. The basis for the derivation will be explained.

Gas oil is fed to the reactor, where it reacts to form product gas while depositing coke on the catalyst,

$$\text{Gas oil} \xrightarrow{\text{catalytic cracking}} \text{Product gas} + \text{Coke (catalytic plus additive)}$$

There are two mechanisms for depositing coke: as catalytic carbon and as additive carbon. The catalytic carbon is produced in the cracking reaction, while the additive carbon is present in most heavy gas oils and deposits without catalytic reaction.[3, 52] Therefore Eq. 1.13 allows for both mechanisms; the first term is for catalytic

Table 1.1

Equations for Mathematical Model No. 1

a. Reactor Section

Carbon Balance Equation $H_{ra}dC_{sc}/dt = (50)R_{cf} + (60)R_{rc}(C_{rc}-C_{sc})$ (1.10)

Heat Balance Equation

$$S_c H_{ra} dT_{ra}/dt = (60)S_c R_{rc}(T_{rg}-T_{ra}) - (.875)S_f D_{tf} R_{tf}(T_{ra}-T_{fp})$$

$$-(.875)\Delta H_{fv} D_{tf} R_{tf} - (.5)\Delta H_{cr} R_{oc} \quad (1.11)$$

Cracking Rate Equation

$$R_{oc} = (1.75)D_{tf}R_{tf}C_{tf} \quad (1.12)$$

where

$$\begin{cases} \dfrac{C_{tf}}{1-C_{tf}} = \dfrac{K_{cr}P_{ra}}{R_{tf}/H_{ra}} \\ K_{cr} = \dfrac{k_{cr}}{C_{cat}C_{rc}^{m}} \exp\left\{-\dfrac{\Delta E_{cr}}{R(T_{ra}+460)}\right\} \text{ with } m=0.15 \end{cases}$$

Carbon Forming Rate Equation

$$R_{cf} = K_{cc}P_{ra}H_{ra} + F_{tf}R_{tf} \quad (1.13)$$

where $K_{cc} = \dfrac{k_{cc}}{C_{cat}C_{rc}^{n}} \exp\left\{-\dfrac{\Delta E_{cc}}{R(T_{ra}+460)}\right\}$ with $n=0.06$

Catalytic Carbon Balance Equation

$$H_{ra}dC_{cat}/dt = (50)K_{cc}P_{ra}H_{ra} - (60)R_{rc}C_{cat} \quad (1.14)$$

Table 1.1

Equations for Mathematical Model No. 1 (Contd.)

b. Regenerator Section

Carbon Balance Equation $$H_{rg}dC_{rc}/dt = (60)R_{rc}(C_{sc}-C_{rc})-(50)R_{cb} \tag{1.15}$$

Heat Balance Equation

$$S_c H_{rg} dT_{rg}/dt = (.5)\Delta H_{rg} R_{cb} - (60)S_c R_{rc}(T_{rg}-T_{ra}) - (.5)S_a R_{ai}(T_{rg}-T_{ai}) \tag{1.16}$$

Carbon Burning Rate Equation

$$R_{cb} = \frac{R_{ai}}{C_1}(21 - O_{fg})/(100) \tag{1.17}$$

where

$$\begin{cases} O_{fg} = 21 \exp\left\{ - \dfrac{P_{rg}H_{rg}/R_{ai}}{1/K_{od}+(100)/K_{or}C_{rc}} \right\} \\ K_{od} = C_2 R_{ai}^2 \\ K_{or} = C_3 \exp\left\{ \dfrac{\Delta E_{or}}{R(1560)} - \dfrac{\Delta E_{or}}{R(T_{rg}+460)} \right\} \end{cases}$$

c. Control System

Reactor Temperature Controller

$$R_{rc}-R_{rc}^s = K_p^t(T_{ra}-T_{ra}^s) + K_I^t \int_0^t (T_{ra}-T_{ra}^s)dt \tag{1.18}$$

Oxygen Controller

$$R_{ai}-R_{ai}^s = K_p^o(O_{fg}-O_{fg}^s) + K_I^o \int_0^t (O_{fg}-O_{fg}^s)dt \tag{1.19}$$

where superscript s represents steady-state (or equilibrium) value.

Table 1.2

Symbols for Mathematical Model No. 1

C_1	Stoichiometric coefficient (2.0)	lb. oxygen/lb.coke
C_2	Coefficient for K_{od} (5.0×10^{-6})	(M lb. oxygen/hr., psia, ton cat.) $(hr./M\ lb.)^2$
C_3	Coefficient for K_{or} (57.5)	M lb. Oxygen/hr., psia, ton coke
C_{cat}	Catalytic carbon on spent catalyst (0.9)	wt. %
C_{rc}	Carbon on regenerated catalyst (0.6)	wt. %
C_{sc}	Carbon (total) on spent catalyst (1.5)	wt. %
C_{tf}	Conversion on total feed (0.5)	vol. fract.
D_{tf}	Density of total feed (7.30)	lb./gal.
F_{tf}	Coke formation factor of total feed (0.0)	(M lb. carbon/hr.)/ (M bbl./day)
H_{ra}	Reactor catalyst holdup (60)	ton
H_{rg}	Regenerator catalyst holdup (200)	ton
K_{cc}	Velocity constant for catalytic carbon formation	
k_{cc}	Constant for K_{cc} *	
K_{cr}	Velocity constant for catalytic cracking	
k_{cr}	Constant for K_{cr} **	

---

* k_{cc} was calculated by setting derivatives in Eqs. 1.10 and 1.15 equal to zero, and solving simultaneously with Eqs. 1.13 and 1.17 at the assumed steady-state condition.

** k_{cr} was calculated from Eq. 1.12 at the assumed steady-state condition.

Table 1.2

Symbols for Mathematical Model No. 1 (Contd.)

K_I^o	Integral gain for oxygen controller (-10)	(M lb. air/hr.)/ mol % oxygen, hr.
K_I^t	Integral gain for temperature controller (-0.1)	(ton cat./min.)/ ^oF, hr.
K_{od}	Oxygen diffusion coefficient	M lb. oxygen/ton cat., psia, hr.
K_{or}	Oxygen reaction coefficient	M lb. oxygen/ton cat., psia, hr.
K_p^o	Proportional gain for oxygen controller (-40)	(M lb. air/hr.)/ mol % oxygen
K_p^t	Proportional gain for temperature controller (-0.2)	(ton cat./min)/^oF
M	1,000	
O_{fg}	Oxygen in flue gas (0.2)	mol %
P_{ra}	Reactor pressure (40)	psia
P_{rg}	Regenerator pressure (25)	psia
R	Gas law constant (2)	Btu./lb.mole, ^oF
R_{ai}	Air rate (400)	M lb./hr.
R_{cb}	Coke burning rate	M lb./hr.
R_{cf}	Carbon (total) forming rate	M lb./hr.
R_{oc}	Gas-oil cracking rate	M lb./hr.
R_{rc}	Catalyst circulation rate (40)	ton/min.
R_{tf}	Total feed rate (100)	M bbl./day
S_a	Specific heat of air (0.27)	Btu./lb., ^oF
S_c	Specific heat of catalyst (0.25)	Btu./lb., ^oF

Table 1.2

Symbols for Mathematical Model No. 1 (Contd.)

S_f	Specific heat of feed (0.75)	Btu./lb., ^oF
T_{ai}	Air inlet temperature (250)	^oF
T_{fp}	Feed preheater temperature (700)	^oF
T_{ra}	Reactor temperature (930)	^oF
T_{rg}	Regenerator temperature (1,160)	^oF
t	Time	hr.
ΔE_{cc}	Activation energy (intrinsic) of catalytic carbon formation (18,000)	Btu./lb.mole
ΔE_{cr}	Activation energy (intrinsic) of catalytic cracking (27,000)	Btu./lb. mole
ΔE_{or}	Activation energy of oxygen reaction (63,000)	Btu./lb. mole
ΔH_{cr}	Heat of cracking (200)	Btu./lb.
ΔH_{fv}	Heat of feed vaporization (75)	Btu./lb.
ΔH_{rg}	Heat of regeneration (13,000)	Btu./lb.

carbon. For the catalytic carbon, Voorhies[74] found that a velocity constant for catalytic carbon (K_{cc}) is approximately inversely proportional to the catalytic carbon content on catalyst (C_{cat}) because of its temporal catalyst deactivation, and it is shown in Eq. 1.13 where a modification is made for the effect of residual carbon (C_{rc}), which is left unburned in the regenerator, and the effect of which is assumed to be somewhat different from that of C_{cat}.

Equation 1.12 was also derived by using the same assumptions as in Eq. 1.13, except that the relation between a conversion on total feed (C_{tf}) and a velocity constant for catalytic cracking (K_{cr}) was assumed to follow the relation, shown in Eq. 1.12, which was derived by Blanding.[10] Effects of C_{rc} in Eqs. 1.12 and 1.13 are known as an effect on product selectivity and were determined from the data reported by Oden, et al.[52] Equation 1.14 is a catalytic carbon balance equation; accumulation equals catalytic carbon forming rate minus output due to catalyst circulation.

Equation 1.15 is a regenerator carbon balance equation; accumulation is equal to the difference due to catalyst circulation minus carbon burning rate. Equation 1.16 is a regenerator heat balance equation; accumulation is equal to the heat of regeneration minus the difference between input and output due to catalyst circulation and air stream carry-over. In order to derive Eq. 1.17, a semiempirical approach based upon data from the literature was used again. By hypothesizing that the carbon burning reaction is controlled by a diffusion mechanism from a bubble phase to an emulsion phase of the fluidized bed and that the reaction rate is proportional to carbon content and oxygen partial pressure, Pansing[56] derived the relation shown in Eq. 1.17.

Thus far all equations necessary for dynamic simulation have been described. In Fig. 1.2 a typical control scheme, where reactor temperature is controlled by catalyst rate and oxygen level is controlled by air rate, is shown by broken lines. Since this scheme is

frequently found in the literature,[25, 57] it will be referred to as the "conventional control scheme" and is shown in Fig. 1.3. Controller functions for this scheme are assumed to be "proportional plus integral" and their equations are given by Eqs. 1.18 and 1.19 in Table 1.1. The dynamic behavior of this catalytic cracker with the conventional control scheme was illustrated by simulating the process and control system on a digital computer (IBM 7094) with DYNAMO (a dynamic simulation-purpose computer program).[59] DYNAMO obtains a solution to the differential equations by using Euler's method. Steady-state operating conditions were chosen that satisfy all equations in Table 1.1 with time derivatives set equal to zero. These values are shown inside the parentheses of Table 1.2. The values of k_{cc} and k_{cr} were adjusted to satisfy the assumed steady-state operating condition.

A dynamic simulation of this conventional control scheme, where the initial carbon level is slightly higher than the steady-state level, is shown in Fig. 1.4. The performance with the best controller parameter tunings (selected by trial-and-error adjustment), which are also listed in Table 1.2, is shown by solid lines. The performances for different tunings are also shown by broken lines. For reduced controller gains, as shown by symbols a and c, the response of the control system becomes more sluggish, while for increased controller gains, as shown by symbols b and d, the response of the control system becomes more oscillatory or unstable. Figure 1.5 shows the case where the carbon production is suddenly increased by a certain mechanism, which is due to feed composition variation; in the computer model, F_{tf} in Eq. 1.13 is suddenly raised. This dynamic behavior is explained by the following step-by-step analysis:

1. The increased carbon production results in an increased carbon content.

2. The increased carbon content tends to increase the conversion of oxygen. Then, because of the decreased oxygen level, the oxygen controller raises the air rate.

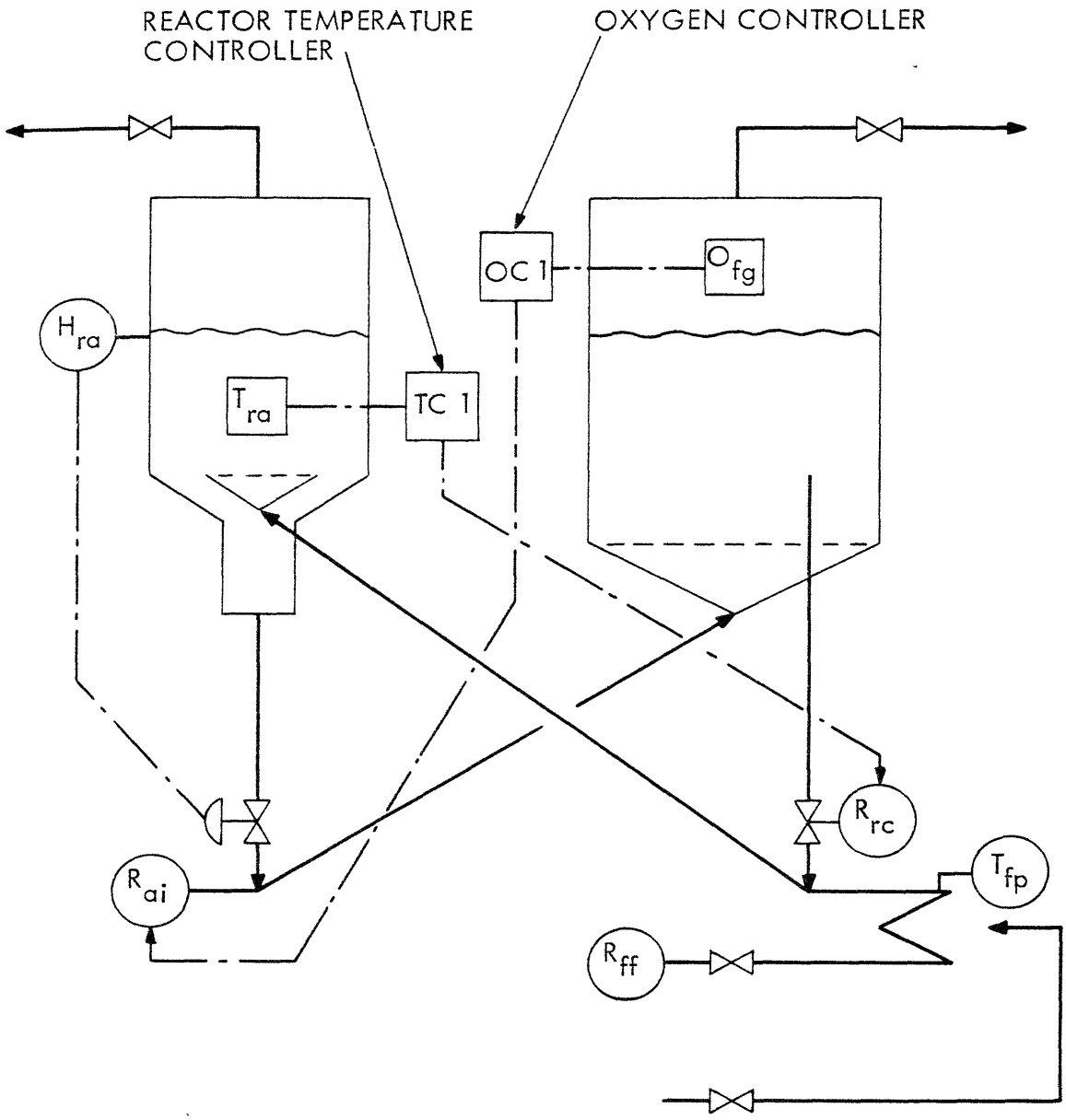

Fig. 1.3 Idealized Conventional Closed Loop Control Scheme of FCC

(HIGH INITIAL CARBON LEVEL)

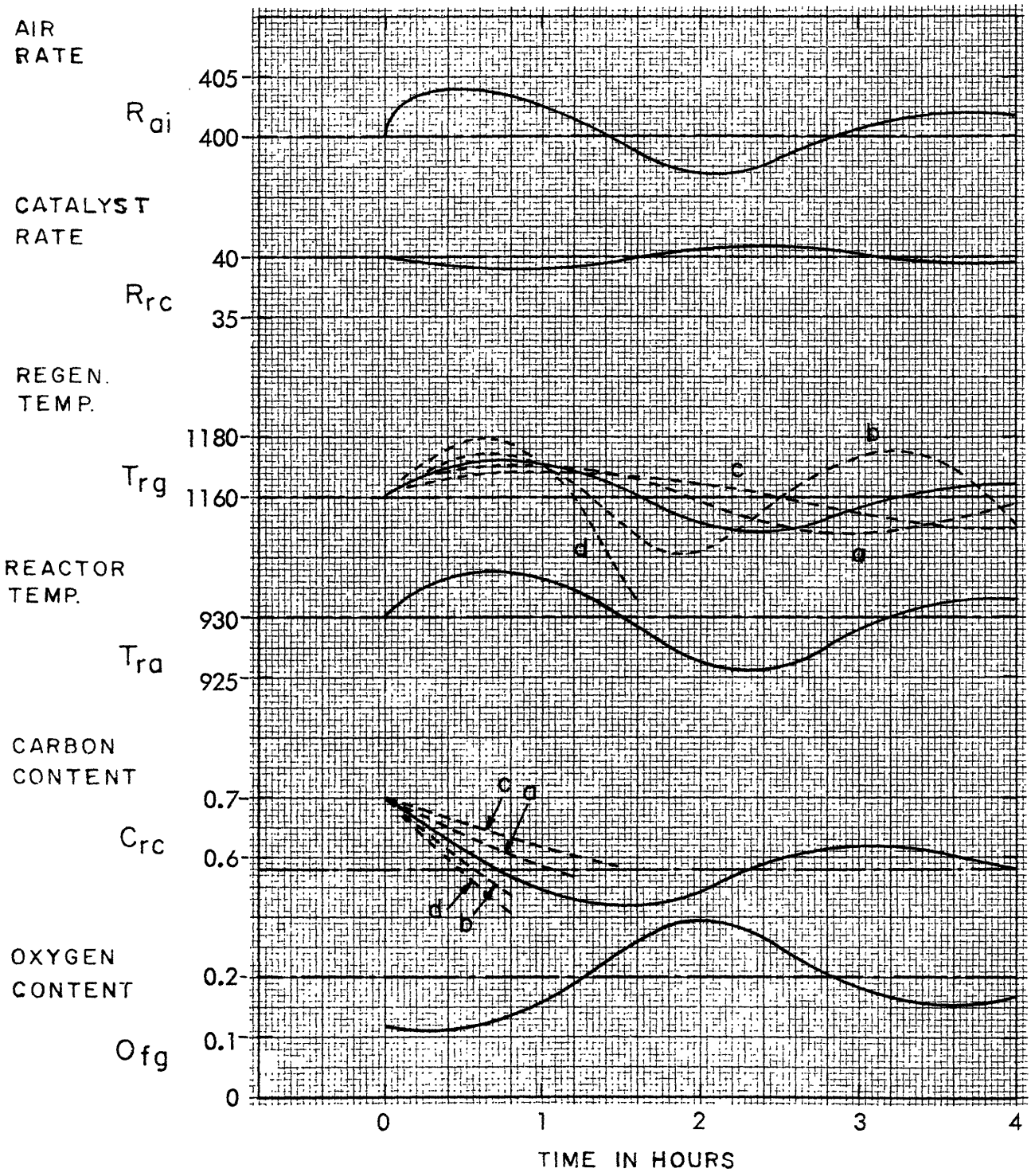

a = FOR HALVED TC1 GAIN
b = FOR TWICED TC1 GAIN
c = FOR HALVED TC1 and OC1 GAIN
d = FOR TWICED OC1 GAIN

Fig. 1.4 Conventional Control Scheme for Initial Condition No. 1

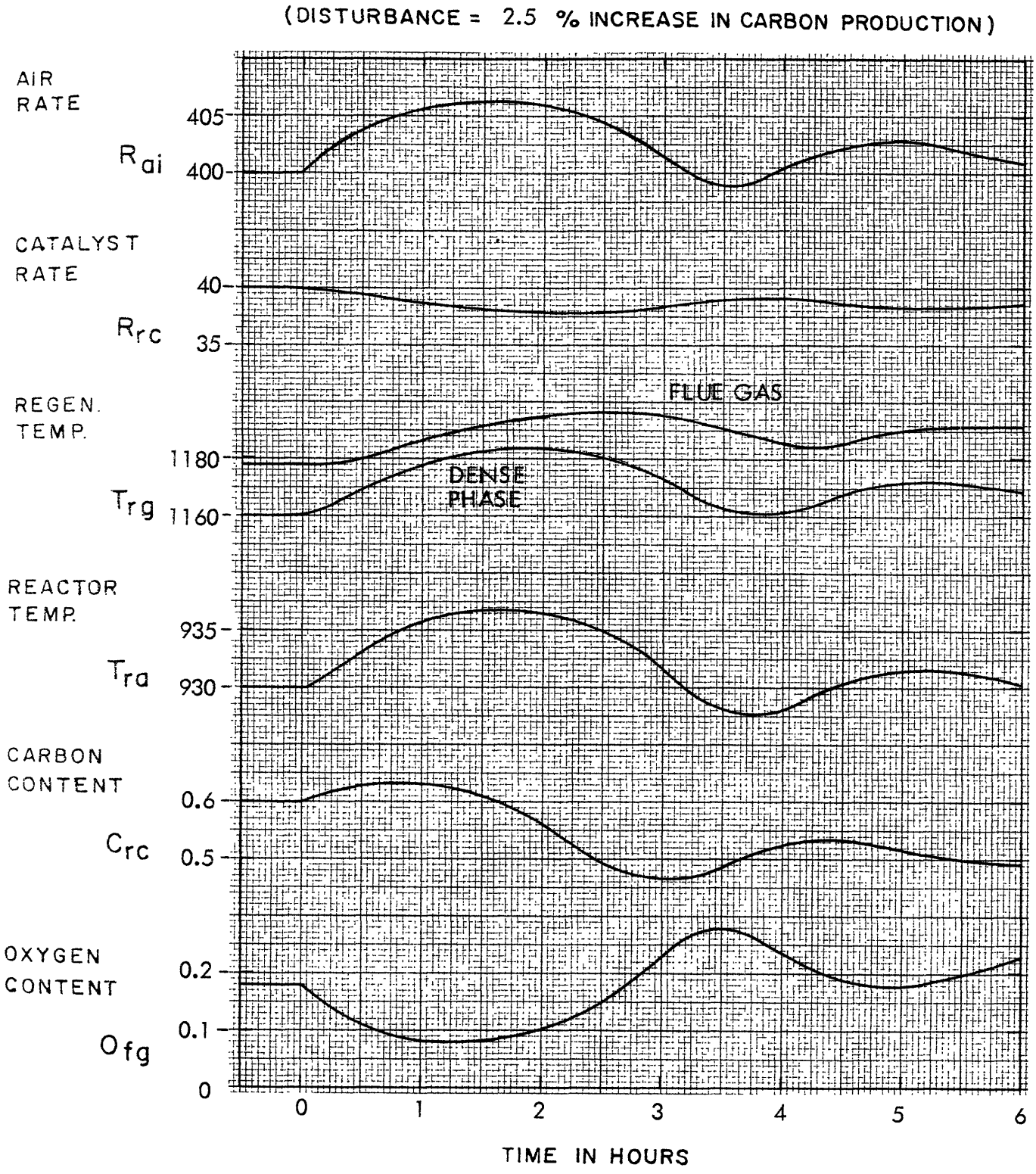

Fig. 1.5 Performances of Conventional Control Scheme (No. 2)

3. The increased air rate, together with the increased carbon level, results in higher regenerator and reactor temperatures.

4. Because of the increased reactor temperature, the temperature controller reduces the catalyst rate, and hence accelerates the regenerator temperature increase.

5. The increased air rate, together with the high regenerator temperature, tends to decrease the carbon level which, in turn, tends to increase the oxygen level.

6. The increased oxygen level reduces the air rate and so on.

The disadvantages of this conventional control scheme are summarized as follows:

1. This control scheme can not eliminate the relatively large variation in the regenerator temperature and the oxygen level. These phenomena are extremely undesirable when the regenerator is operated at an allowable maximum temperature.

2. This control scheme has a relatively small damping ratio or small degree of stability and the tunings of controllers are not trivial but require great care.

3. The period of oscillation is relatively long; in other words, the control system is very sluggish, and a quick recovery from an upset condition can not be achieved.

Thus far the general background and conventional means of control of catalytic crackers has been described. Next, the results of the optimal control study will be discussed.

Results of the Optimal Control Study

An outline of the optimal control study for this hypothetical fluid catalytic cracking unit is shown diagrammatically in Fig. 1.6. First,

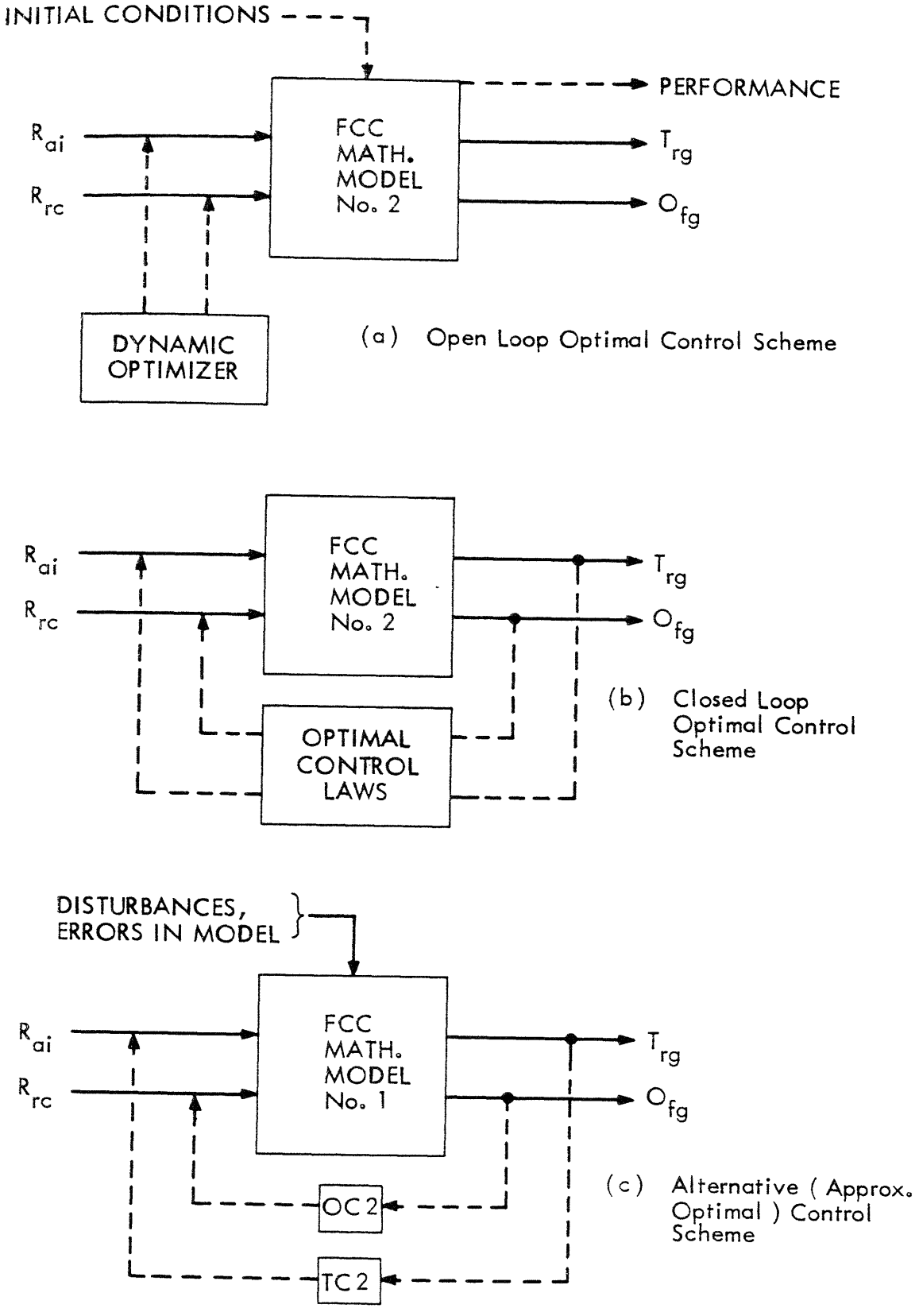

Fig. 1.6 An Approach for Control System Design

the mathematical Model No. 1 is reduced to a simpler one, because the computations for dynamic optimization are more time consuming than those for dynamic simulation, and this simplified model is denoted Model No. 2. Figure 1.6a shows an open-loop optimal control scheme where optimal air rate and catalyst rate will be determined as two functions of time for a given initial condition and for a given objective function. Because of the essential disadvantages of this open-loop structure, which were discussed before, it is desirable to convert this open-loop structure into a closed-loop structure, as shown in Fig. 1.6b. Optimal feedback control laws can be estimated from a set of solutions for dynamic optimization with several initial conditions. Finally, an alternative control scheme will be designed, as shown in Fig. 1.6c, by simplifying the resulting optimal feedback control laws. The performance of this control scheme will be tested by using the original mathematical Model No. 1 with disturbances.

Equations used for dynamic optimization are listed in Table 1.3. They are dimensional equations and their symbols are listed in Table 1.4. Equation 1.20 is an objective function to be maximized, the integrand of which is an instantaneous gross profit rate minus two penalty functions for regenerator temperature and oxygen in flue gas which are restricted for reasons of safety. Equation 1.21 is an instantaneous gross profit rate and its derivation will be described. Gas oil is fed to the reactor, where it is partially cracked to form gasoline, gas, and coke with an unconverted part remaining as cycle oil,

$$\text{Gas oil} \longrightarrow \underbrace{\text{Gasoline + Gas + Coke}}_{\text{Converted}} + \underbrace{\text{Cycle oil}}_{\text{Unconverted}}$$

By defining a product value as the sum of the flow rates of all of the product streams multiplied by their respective unit values, with the corresponding value of the plant feed subtracted from the sum, Eq. 1.21 is derived. The derivation of gasoline yield ($Y^t_{g\ell}$) as a

Table 1.3

Equations for Dynamic Optimization

Objective Function $$J = \int_0^{t_1} L\,dt \quad \text{where} \quad L = P_{ig} - P_{e1} - P_{e2} \tag{1.20}$$

Instantaneous Gross Profit Rate

$$P_{ig} = \frac{R_{tf}}{(24)}\left\{(42)D_{tf}Y^t_{gs}P_{gs} + Y^t_{g\ell}P_{g\ell} + Y^t_{co}P_{co} - P_{tf}\right\} \tag{1.21}$$

where

$$\begin{cases} Y^t_{g\ell} = \dfrac{F_{g\ell}}{1-I_{g\ell}}\left\{(1-C_{tf})^{I_{g\ell}} - (1-C_{tf})\right\} = \text{gasoline yield} \\ Y^t_{co} = 1 - C_{tf} = \text{cycle oil yield} \\ Y^t_{ck} = (.571)R_{cf}/R_{tf}D_{tf} = \text{coke yield} \\ Y^t_{gs} = 1 - Y^t_{g\ell}D_{g\ell}/D_{tf} - Y^t_{co}D_{co}/D_{tf} - Y^t_{ck} = \text{gas yield} \end{cases}$$

where superscript t represents a total feed base.

Penalty Function for Regenerator Temperature

$$P_{e1}(T_{rg}) = \begin{cases} G_1\{T_{rg} - (T_{rg})_{max}\}^{m_1} & \text{if } T_{rg} > (T_{rg})_{max} \\ 0 & \text{if } T_{rg} \leq (T_{rg})_{max} \end{cases} \tag{1.22}$$

where G_1 is a positive constant and m_1 is an integer.

Penalty Function for Oxygen in Flue Gas

$$P_{e2}(O_{fg}) = \begin{cases} G_2\{O_{fg} - (O_{fg})_{max}\}^{m_2} & \text{if } O_{fg} > (O_{fg})_{max} \\ 0 & \text{if } O_{fg} \leq (O_{fg})_{max} \end{cases} \tag{1.23}$$

where G_2 is a positive constant and m_2 is an integer.

Table 1.3

Equations for Dynamic Optimization (Contd.)

State Equations

$$d\,T_{rg}/dt = f_2(T_{rg},\ C_{rc},\ R_{ai},\ R_{rc}) \tag{1.24}$$

$$d\,C_{rc}/dt = f_4(T_{rg}\ C_{rc},\ R_{ai},\ R_{rc}) \tag{1.25}$$

Hamiltonian Function

$$H(T_{rg},\ C_{rc},\ p_2,\ p_4,\ R_{ai},\ R_{rc}) = L + p_2 f_2 + p_4 f_4 \tag{1.26}$$

where $$L = P_{ig} - P_{ei} - P_{e2} = L(T_{rg},\ C_{rc},\ R_{ai},\ R_{rc})$$

Costate Equations

$$\dot{p}_2 = -\partial H/\partial x_2 \quad \text{where } x_2 = T_{rg} \tag{1.27}$$

$$\dot{p}_4 = -\partial H/\partial x_4 \quad \text{where } x_4 = C_{rc} \tag{1.28}$$

Steepest Ascent of the Hamiltonian

$$u_1 \leftarrow u_1 + e_1\,\partial H/\partial u_1 \quad \text{where } u_1 = R_{ai} \tag{1.29}$$

$$u_2 \leftarrow u_2 + e_2\,\partial H/\partial u_2 \quad \text{where } u_2 = R_{rc} \tag{1.30}$$

Modifications for Relaxation Parameters

$$e_i \leftarrow \begin{cases} 2e_i & \text{if } J_{new} > J_{old} \\ \frac{1}{4}e_i & \text{if } J_{new} < J_{old} \end{cases} \qquad i=1,2 \tag{1.31}$$

Table 1.4

Symbols for Dynamic Optimization

D_{co}	Density of cycle oil (7.38)	lb./gal.
$D_{g\ell}$	Density of gasoline (6.40)	lb./gal.
$F_{g\ell}$	Gasoline yield factor (1.0)	lb.gasoline/lb. cracked
$I_{g\ell}$	Gasoline recracking intensity (0.9)	
G_1	Constant (5×10^{-4})	
G_2	Constant (1.0)	
m_1	Integer (2)	
m_2	Integer (1)	
$(O_{fg})_{max}$	Allowable maximum oxygen in flue gas (0.2)	mol %
P_{co}	Price of cycle oil (3.42)	$/bbl.
P_{e1}	Penalty function for regenerator temperature	M$/hr.
P_{e2}	Penalty function for oxygen in flue gas	M$/hr.
$P_{g\ell}$	Price of gasoline (4.59)	$/bbl.
P_{gs}	Price of gas (0.0112)	$/lb.
P_{ig}	Instantaneous gross profit rate	M$/hr.
P_{tf}	Price of total feed (3.15)	$/bbl.
$(T_{rg})_{max}$	Allowable maximum regenerator temperature (1,160)	^oF
Y^t_{ck}	Coke yield on total feed	wt. fract.
Y^t_{co}	Cycle oil yield on total feed	vol. fract.
$Y^t_{g\ell}$	Gasoline yield on total feed	vol. fract.
Y^t_{gs}	Gas yield on total feed	wt. fract.

function of conversion on total feed (C_{tf}) is as follows. Gasoline, cracked from gas oil, is still subjected to a further cracking (so called recracking) into gas and coke. By assuming that the ratio of cracking rate of gasoline divided by gasoline partial pressure and cracking rate of gas oil divided by gas oil partial pressure is constant and denoted by "gasoline recracking intensity" ($I_{g\ell}$), and that the yield of gasoline in an elemental gas oil cracking is constant and denoted by "gasoline yield factor" ($F_{g\ell}$), an integration of this relation for the total bed (plug flow equivalent) results in a gasoline yield as a function of conversion.

Equation 1.22 is a penalty function for regenerator temperature; if T_{rg} exceeds an allowable maximum limit $(T_{rg})_{max}$, then this function penalizes the objective function in order to avoid such a situation. Equation 1.23 is a penalty function for oxygen in flue gas which avoids an excessively high oxygen content. This concludes the description of the objective function for dynamic optimization.

The mathematical Model No. 1 was reduced to a simpler one (Model No. 2) as follows. If the reactor catalyst holdup is considerably smaller than the regenerator catalyst holdup, then the reactor equations may be simplified by setting the unsteady parts of Eqs. 1.10, 1.11, and 1.14 to zero and letting the total dynamics be governed by Eqs. 1.15 and 1.16 in Table 1.1. Thus, solving C_{sc}, T_{ra}, and C_{cat} from simultaneous algebraic equations, Eqs. 1.10, 1.11 and 1.14, and introducing them into Eqs. 1.15 and 1.16, state equations for T_{rg} and C_{rc} are obtained as Eqs. 1.24 and 1.25 in Table 1.3. Equation 1.26 is the Hamiltonian function derived from Eq. 1.7. Equations 1.27 and 1.28 are costate equations derived from Eq. 1.6. Equations 1.29 and 1.30 are procedures followed by the method of steepest ascent of the Hamiltonian. Equation 1.31 is an iterative modification for relaxation parameters adopted by Kurihara.[39]

A dynamic optimization of Model No. 2, where the initial carbon level is slightly higher than the optimal steady-state level, is shown

in Figs. 1.7, 1.8 and 1.9. In Fig. 1.7 solutions for the zero and second iterations are plotted with broken lines, and a solution for the eighth iteration is plotted with solid lines, while, chain lines show optimal steady-state levels. For the zeroth iteration, R_{ai} and R_{rc} are set to optimal steady state values, resulting in a very slow recovery of C_{rc} to an optimal steady state. As iterations proceed, R_{ai} and R_{rc} are changed so that the objective function is maximized, with the result that C_{rc} recovers quickly, without an excessive T_{rg} rise. As shown in the figure, the process approximately reaches the optimal steady-state condition at $t = 1$ (hr.) and starts to deviate at $t = 1.5$ (hr.). The latter phenomenon is essentially the end effect of dynamic optimization where the final time t_1 is arbitrarily truncated at a certain finite time (2 hrs. for this example), for purposes of computation, and should be neglected if the solution is understood to be an approximate solution of dynamic optimization with an infinite (or sufficiently large) final time.

In Fig. 1.8 supplemental data for the costate variables and gradients of the Hamiltonian function with respect to the control variables $u_1(=R_{ai})$ and $u_2(=R_{rc})$ are shown. As iteration proceeds, gradients converge to zeros for $0 < t < 2$, indicating that the objective function is almost maximized. Gross profit, which is an integration of the instantaneous gross profit rate for $0 < t < 2$, and relaxation parameters are also plotted against the iteration number. At each iteration, the relaxation parameters were modified, so that maximization is attained quickly. In Fig. 1.9, the solutions finally obtained are plotted together with the corresponding T_{ra} and O_{fg}. If one compares these solutions with the results of dynamic simulation of the conventional control scheme, as shown in Fig. 1.4, (considering the difference in time scale), then one can see that dynamic optimization results in considerably improved performance, since C_{rc} reaches the optimal steady-state condition very quickly without causing any excessively high T_{rg}.

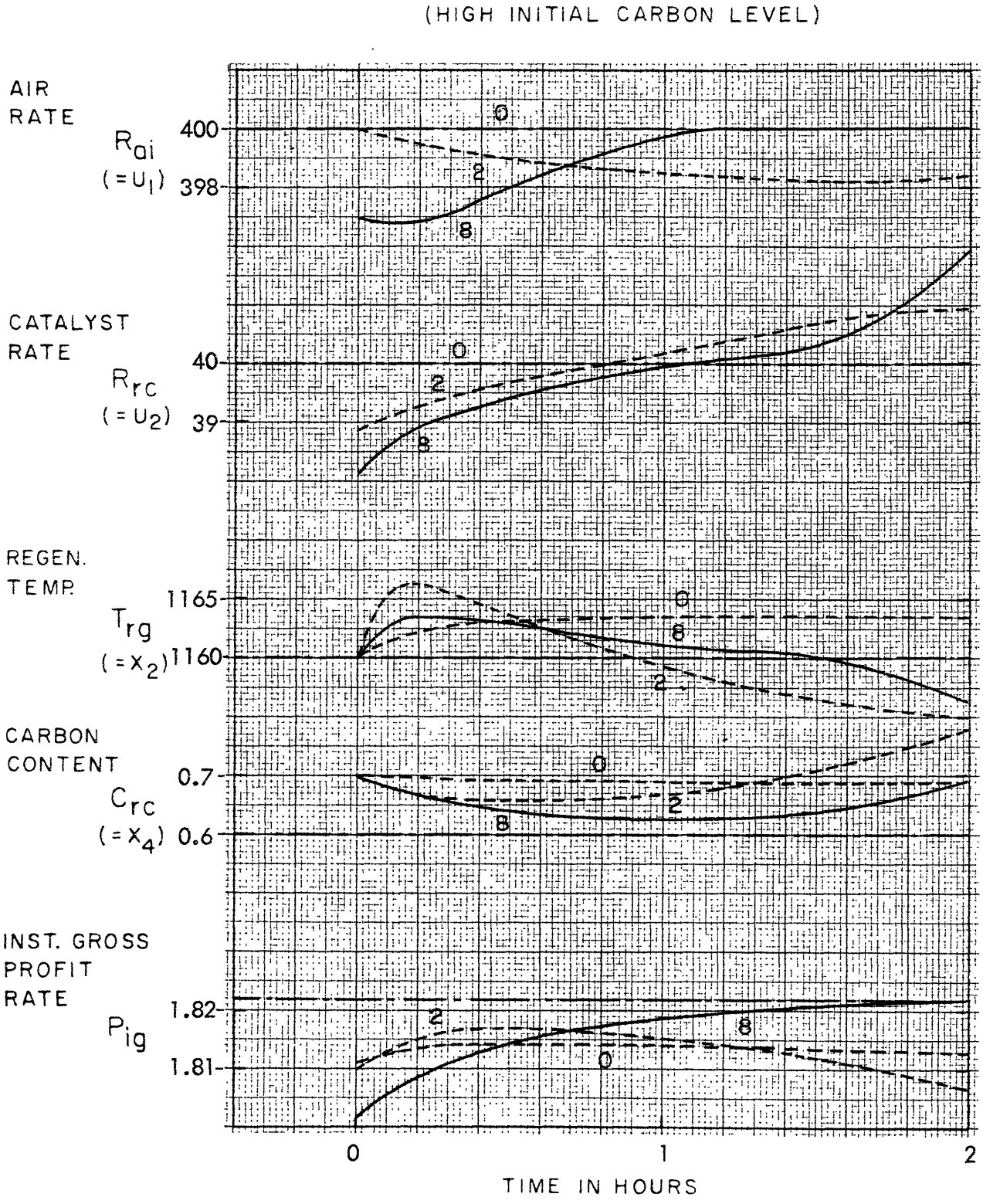

Fig. 1.7 Iterative Solutions (0,2 and 8-th) for Initial Condition No. 1

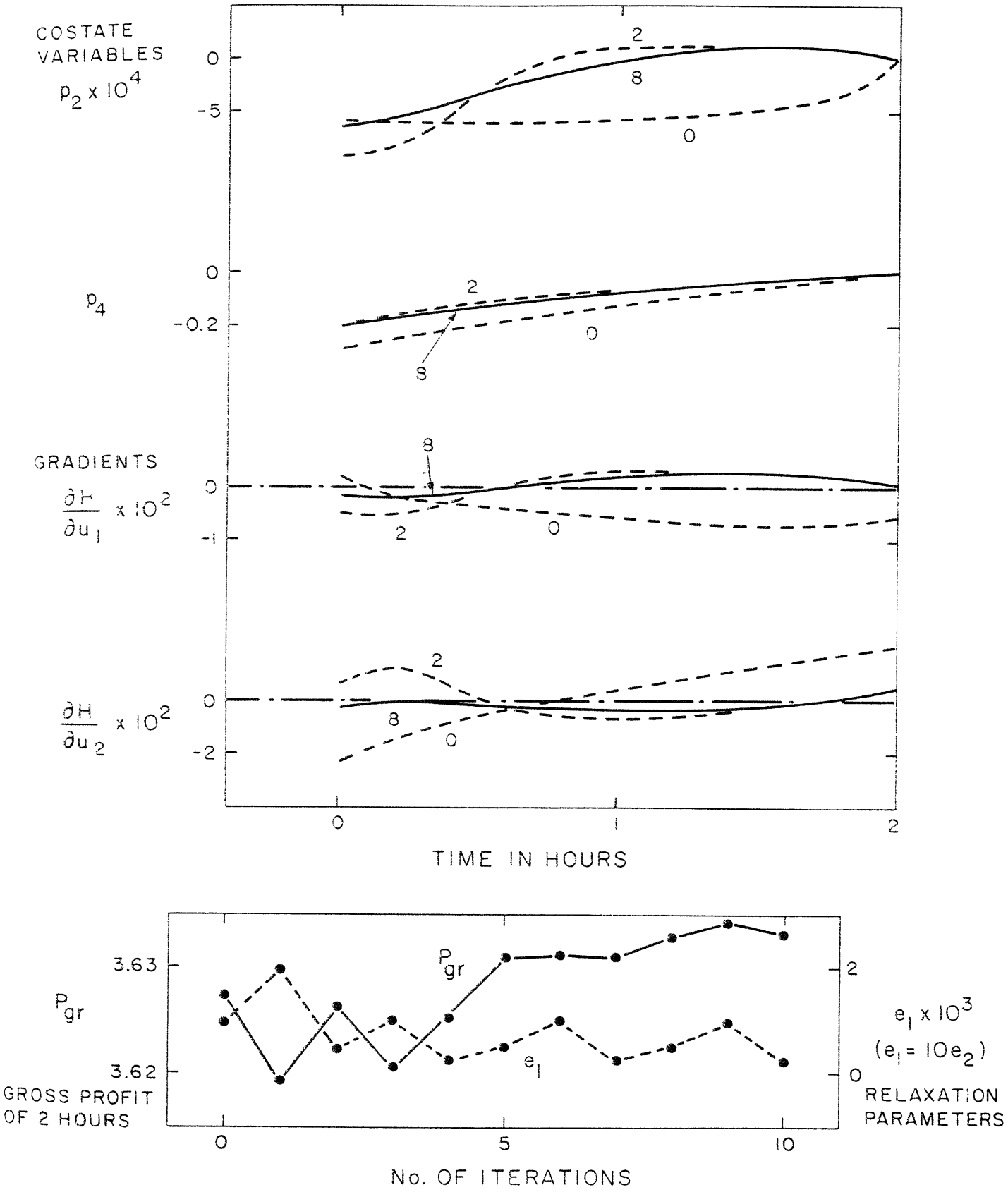

Fig. 1.8 Convergence Characteristics of Iteration

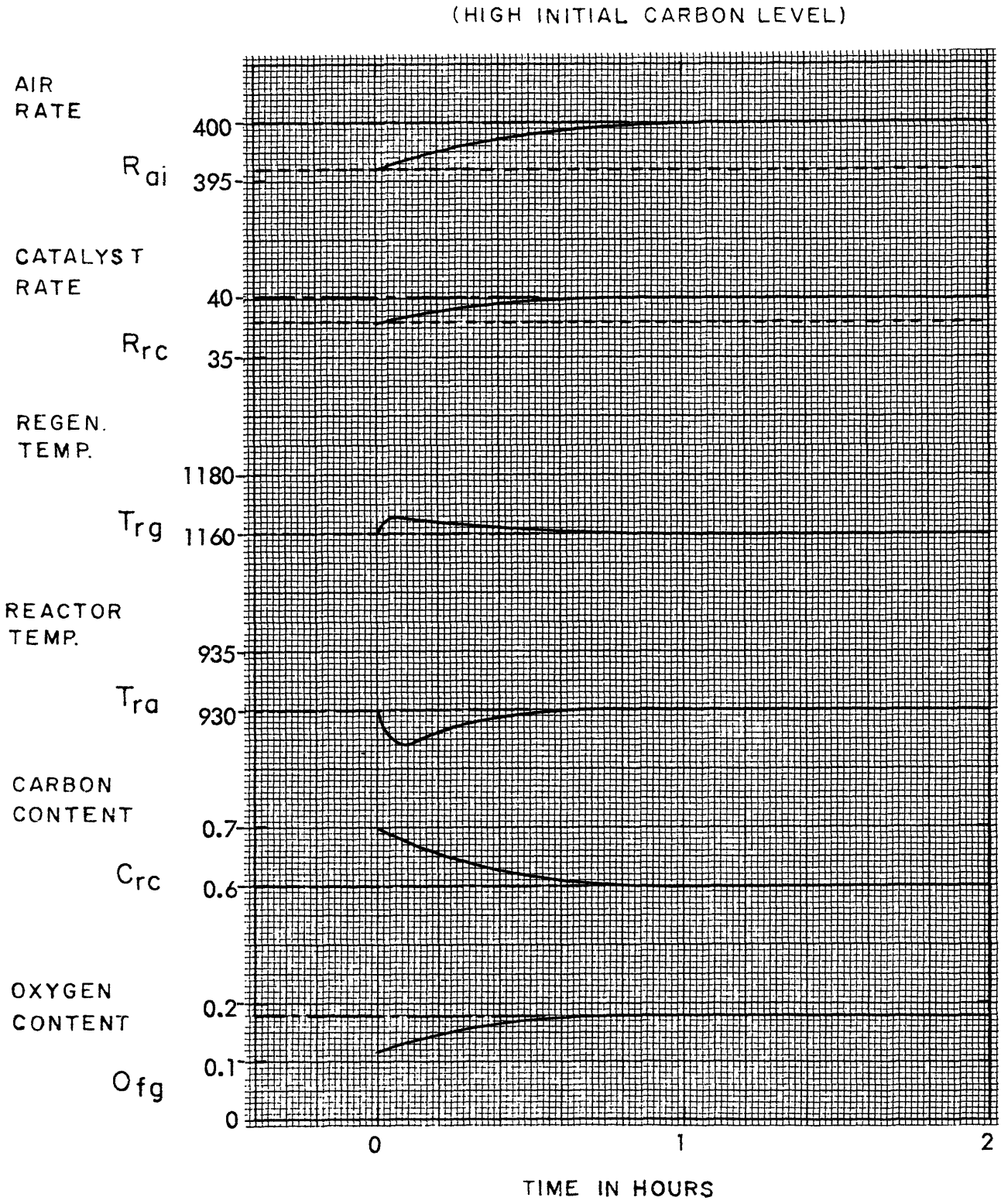

Fig. 1.9 Optimal Control Solution for Initial Condition No.1

This optimal control solution with initial condition No. 1 can be plotted in the phase plane, O_{fg} vs. T_{rg} and C_{rc} vs. T_{rg}, as shown in Fig. 1.10 by trajectories denoted by circles with the numeral 1 inside. Point S in the figure represents the optimal steady state. Dynamic optimizations with different initial conditions were solved in the same way and the solutions are plotted in Fig. 1.10 by trajectories denoted by circles with the numerals 2, 4, 5, 6, and 7 inside. Starting from several initial conditions, the trajectories move to an optimal steady state in an optimal manner (maximizing the objective function). A trajectory starting from any initial condition never crosses a trajectory starting from any other initial condition. In other words, an optimal trajectory is unique and depends only on the initial condition. This fact is known as the principle of optimality, as discussed before.

Now on this phase plane, it is possible to plot an optimal solution for R_{ai} as a function of O_{fg} and T_{rg}. For example, from Fig. 1.9 this functional relation at $t = 0.1$ is $R_{ai} \doteq 396$ at $T_{rg} \doteq 1,165$ and $O_{fg} \doteq 0.14$. Thus, one data point (shown by a square) can be plotted in Fig. 1.11. By plotting similar values at other times, one can obtain a sufficiently clear picture of R_{ai} as a function of T_{rg} and O_{fg}, as shown by contour lines in the figure. In a plot of T_{rg} vs. O_{fg}, a mountain is apparently located in the southwest, and a sea in the northeast. A plot of T_{rg} vs. C_{rc} is also shown for the purpose of reference. A similar functional relation for the R_{rc} is shown in Fig. 1.12. For a plot of T_{rg} vs. O_{fg}, a mountain is apparently located in the northeast and a sea in the southwest. These functional relations between control variables and state variables are called optimal feedback (or closed-loop) control laws.

Now we can design an alternative control scheme for this fluid catalytic cracker. We know the optimal feedback control laws, at least approximately. All that we have to do is to utilize the result of this optimal control study. First, we linearize the optimal control laws around the optimal steady state. This is done directly by

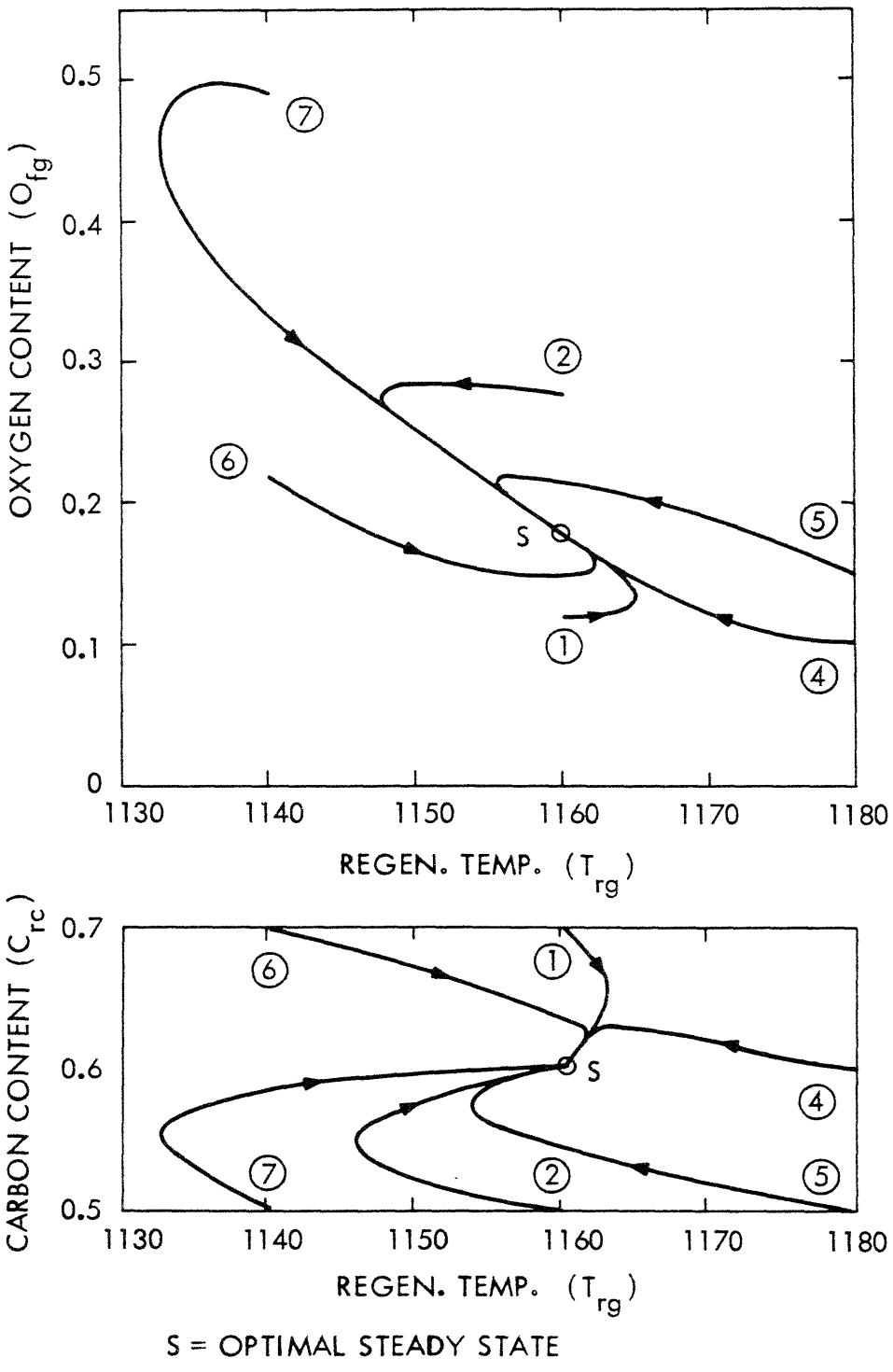

Fig. 1.10 Phase Plane Trajectories of Optimal Control Solutions

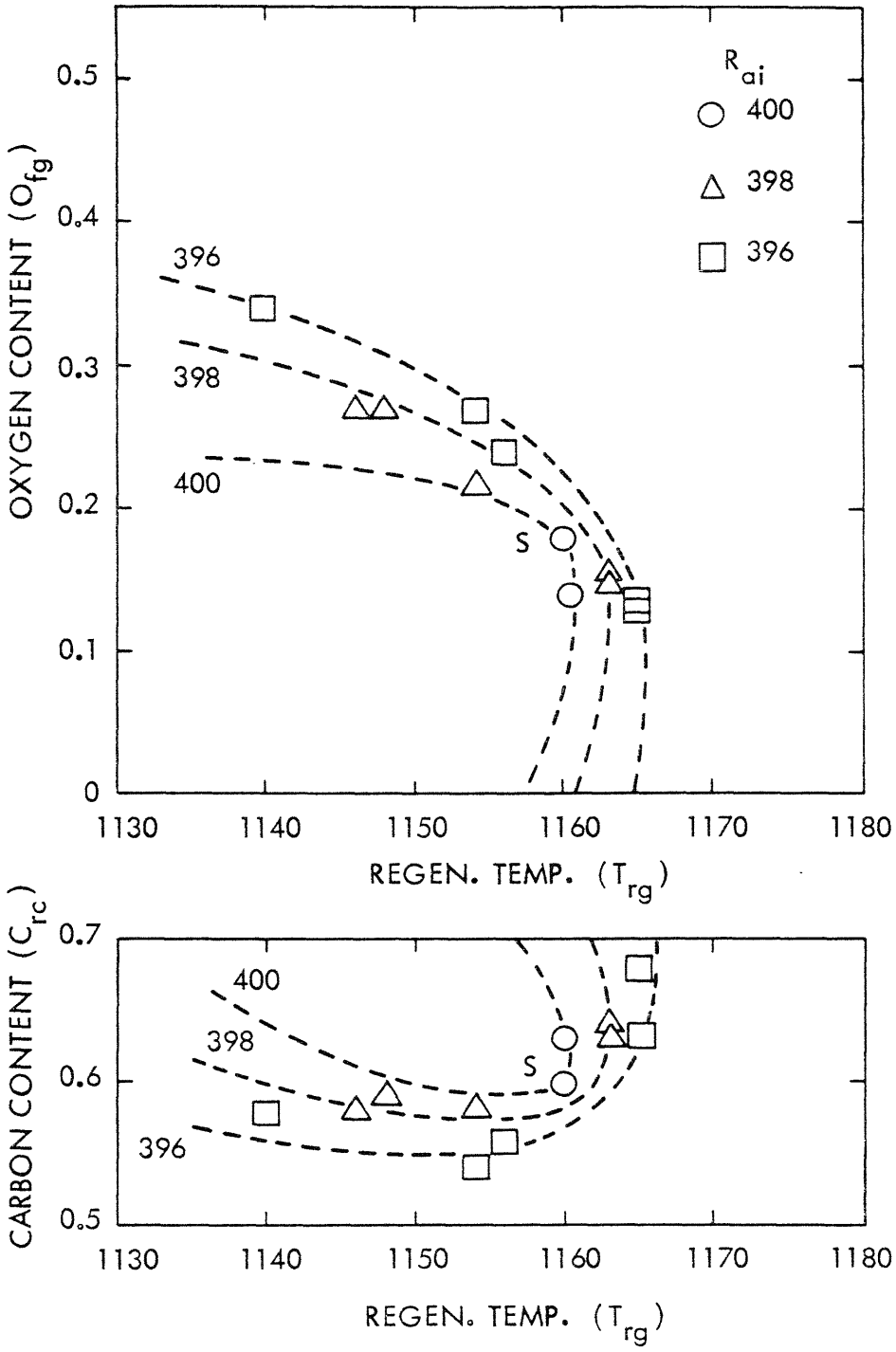

Fig. 1.11 Optimal Control Law for Air Rate

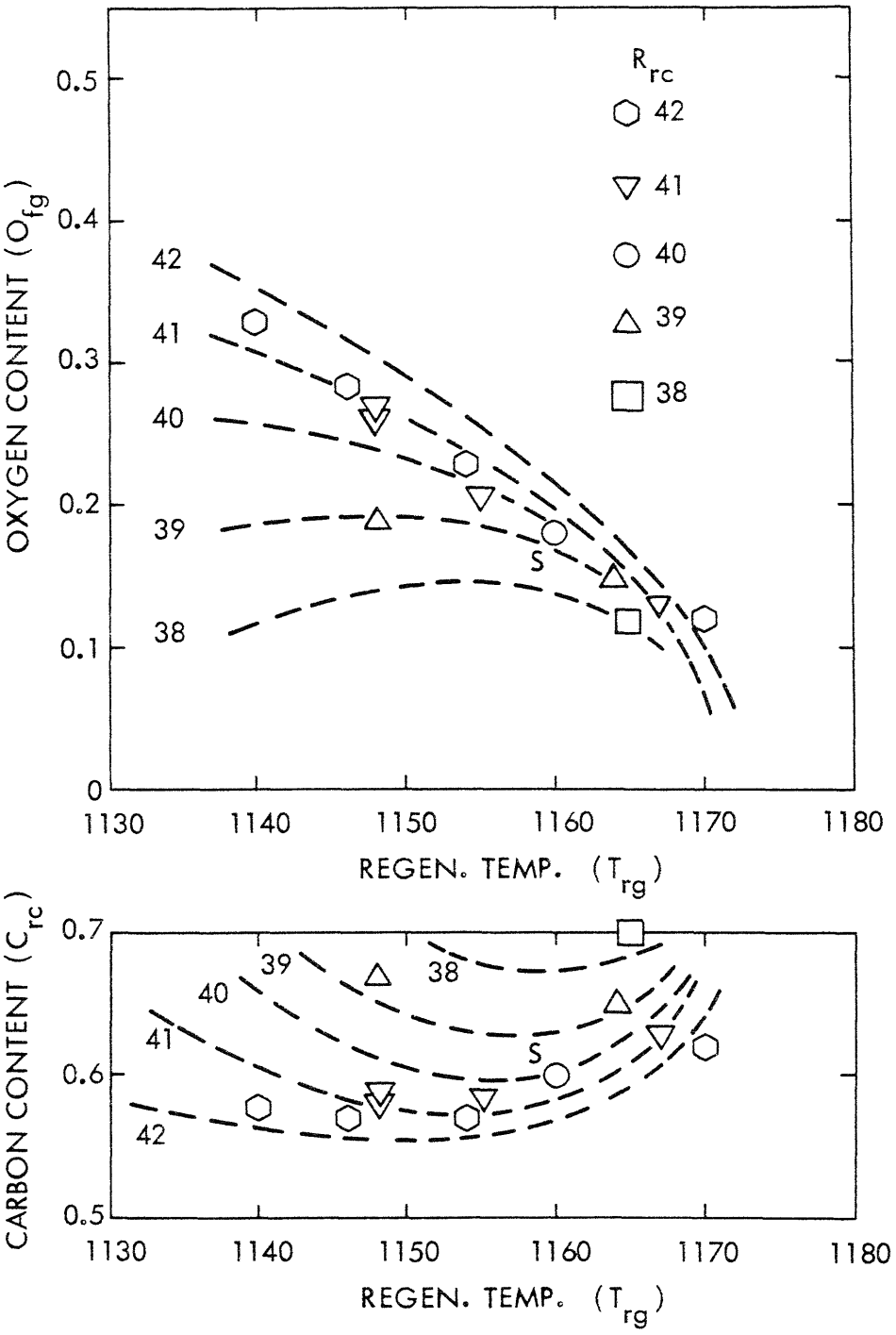

Fig. 1.12 Optimal Control Law for Catalyst Rate

measuring slopes around an optimal steady-state point of Figs. 1.11 and 1.12, to give

$$R_{ai} - R_{ai}^{s} = -1.0(T_{rg} - T_{rg}^{s}) - 100(O_{fg} - O_{fg}^{s}) \tag{1.32}$$

$$R_{rc} - R_{rc}^{s} = 0.5(T_{rg}\, T_{rg}^{s}) + 50(O_{fg} - O_{fg}^{s}) \tag{1.33}$$

where a superscript s represents optimal steady state. Secondly, we investigate the contribution of each term in Eqs. 1.10 and 1.11 to the overall performance of the optimal system by comparing the performances with and without each term. By neglecting the second term on the right side of Eq. 1.32 and the first term on the right side of Eq. 1.33, the control scheme was developed. This is referred to as the "alternative control scheme," shown in Fig. 1.13.

A dynamic simulation (with Model No. 1) of this alternative control scheme, where the initial carbon level is slightly higher than the steady-state level, is shown in Fig. 1.14. If this performance is compared with that of the conventional control scheme shown in Fig. 1.4, considering the difference in time scale, then one can see that the alternative control scheme results in a considerably better performance, since C_{rc} reaches an optimal steady-state condition very quickly without causing any excessively high T_{rg}. If this is compared with the optimal control solution shown in Fig. 1.9, then it can be seen that they are very similar.

Figure 1.15 shows the case where the carbon production is suddenly increased by a certain mechanism, which is due to feed composition variation. The resulting dynamic behavior will be explained by the following step-by-step analysis.

1. The increased carbon production causes the carbon level to increase.

2. The increased carbon level causes the regenerator temperature to increase and simultaneously decreases the oxygen level.

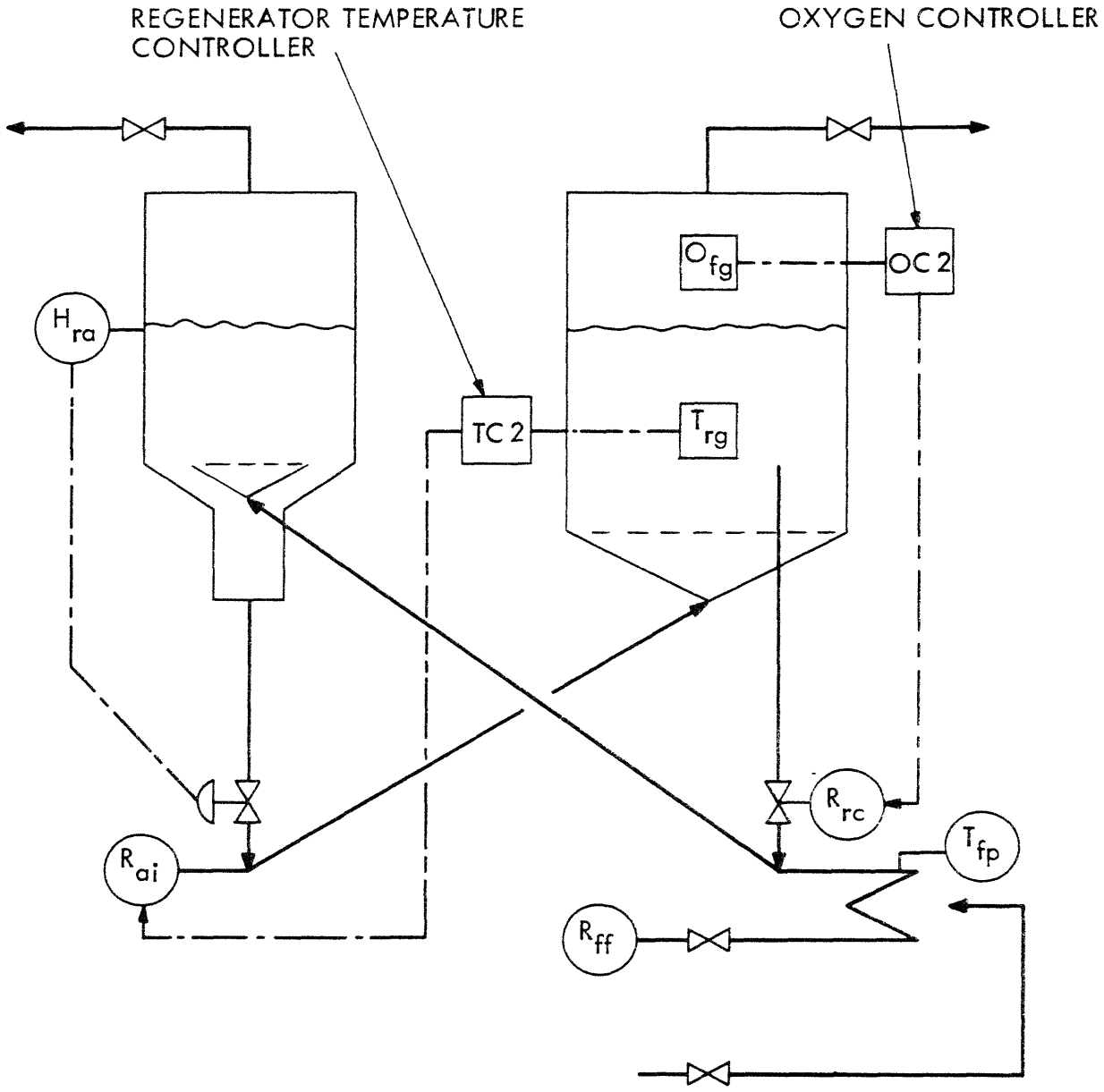

Fig. 1.13 Alternative Closed Loop Control Scheme of FCC

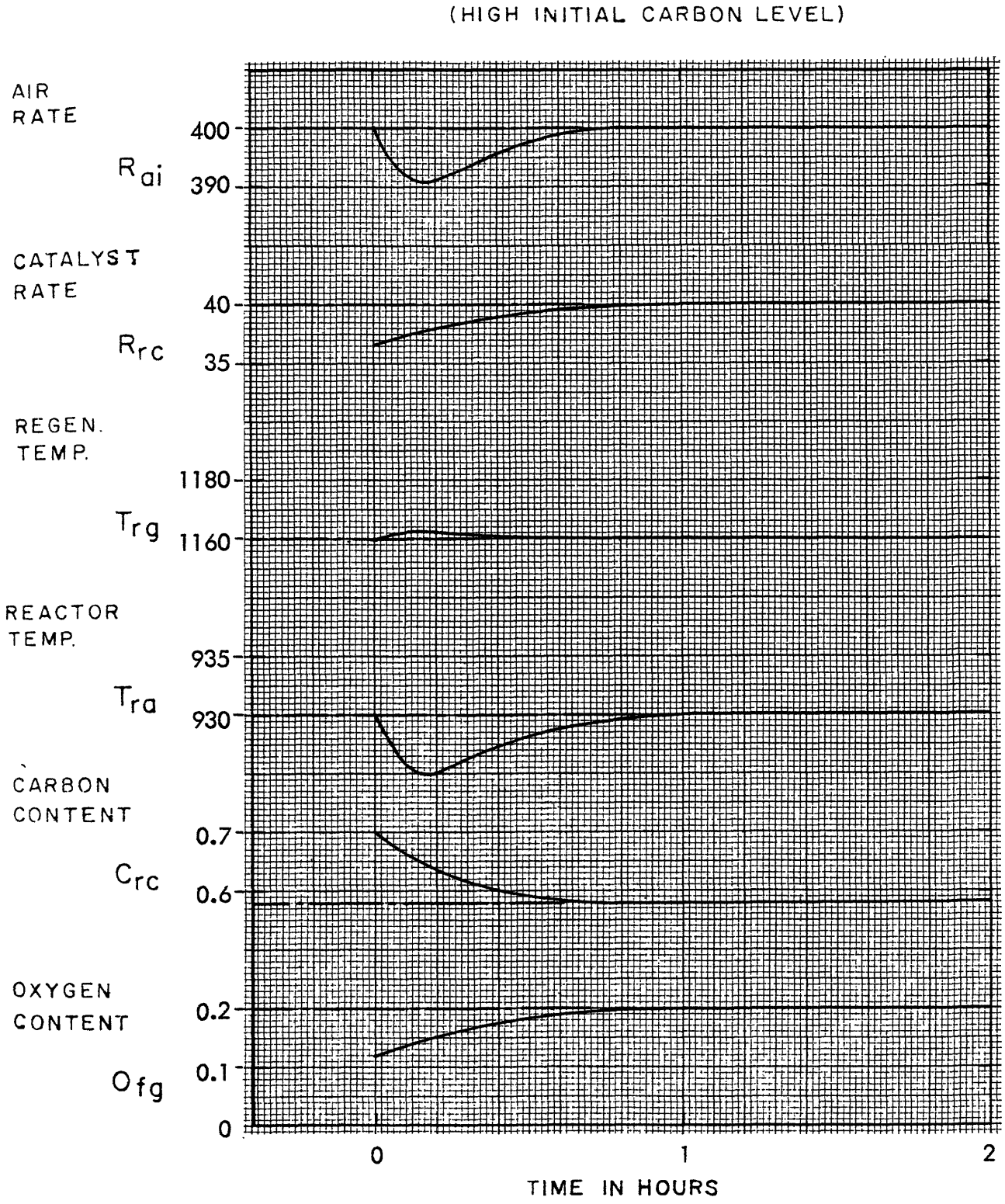

Fig. 1.14 Alternative Control Scheme for Initial Condition No. 1

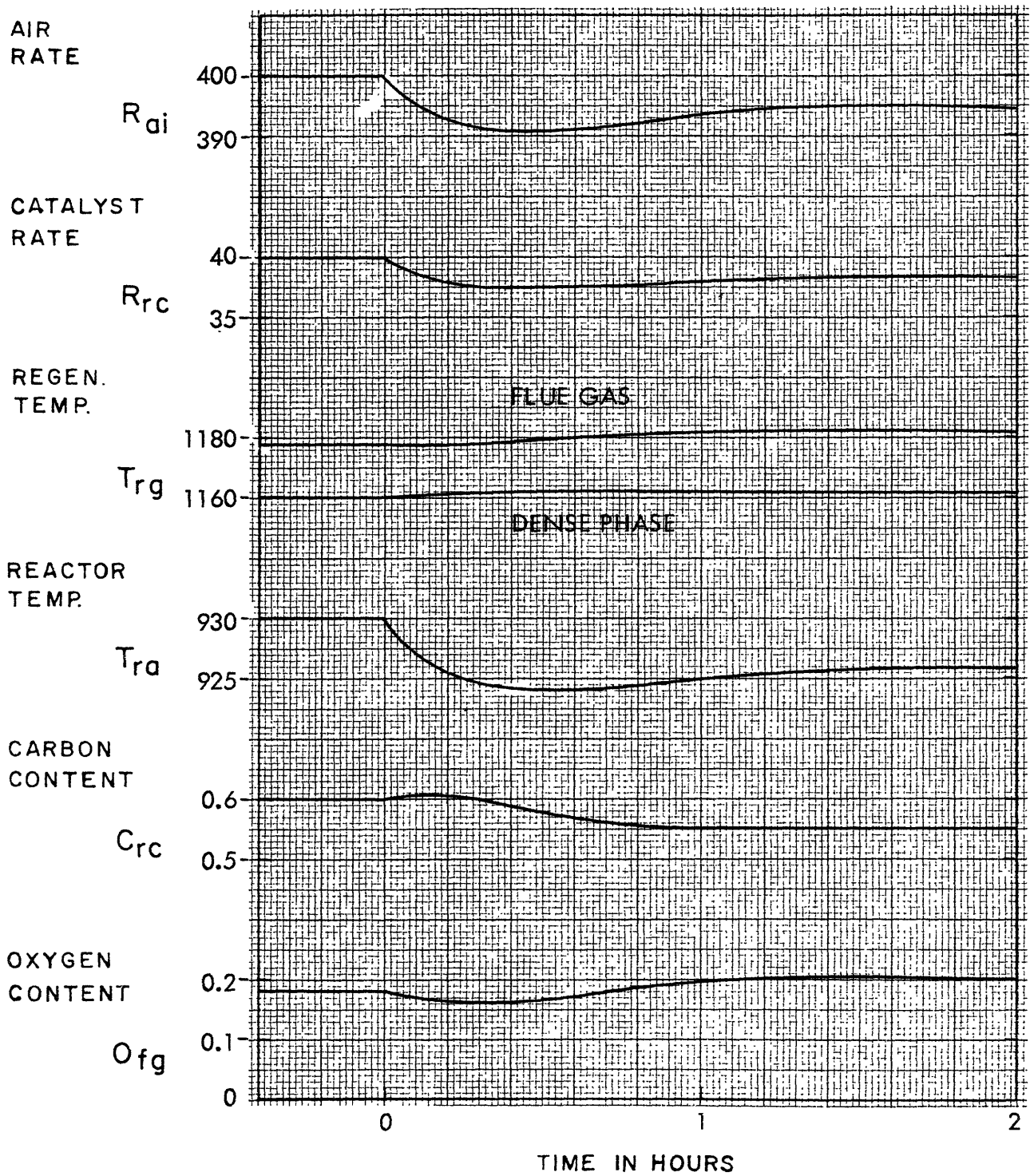

Fig. 1.15 Performances of Alternative Control Scheme (No. 2)

3. The decreased oxygen level causes the catalyst rate to decrease by action of the oxygen controller, and simultaneously the increased regenerator temperature decreases the air rate by action of the temperature controller.

4. The decreased catalyst rate compensates for the increased carbon production.

As shown in the figure, this scheme is practically insensitive to this disturbance in carbon production. If this is compared with Fig. 1.5, the superiority of this scheme over the conventional one will be reconfirmed.

Conclusions

1. A new approach to the design of a control system for nonlinear multivariable processes was developed in the course of this work. The method was demonstrated for the design of a control system for a hypothetical fluid catalytic cracking unit and resulted in an entirely different control scheme from the one that is typically used in refinery operation. The performance of the new control scheme was demonstrated by dynamic simulation to be significantly better than the conventional system.

2. The new design approach was found to have significant advantages over conventional trial-and-error methods, because it is systematic, and because it provides information to evaluate the desirability of each design step, since the ultimate performance of the system is known from the optimal control theory. With the conventional trial-and-error method it is not possible to evaluate the desirability of each trial efficiently since the ultimate performance is unknown.

3. The method of steepest ascent of the Hamiltonian, with the utilization of penalty functions, was demonstrated to be satisfactory as a computing algorithm for the dynamic optimization of the fluid catalytic cracking unit considered in this study. This method is therefore

recommended for dynamic optimization studies of similar highly nonlinear and multivariable processes.

Supplementary Studies

In the course of the study, the following supplementary studies were also conducted.

1. Signal flow graphs for the conventional control scheme and the alternative control scheme of fluid catalytic cracking processes were developed, and the dynamic behavior of each of these control schemes was analyzed from an information feedback point of view. These analyses gave insight into reasons why the alternative control scheme was significantly better than the conventional one.

2. Several control schemes different from the conventional control scheme were also simulated and compared with an analog computer simulation studied by others.[32] On the basis of this comparison it was concluded that although there are various kinds of fluid catalytic cracking processes, the characteristics of their dynamic behavior are quite similar.

3. An analysis was made of the optimal steady-state operating conditions for fluid catalytic cracking processes in order to gain insight into optimal operation.

CHAPTER II

INTRODUCTION

2.1 PROBLEM BACKGROUND

The objective of this section is to provide basic information about the idea of work. First, basic problems in chemical process control will be discussed in order to realize the essential difficulties. Secondly, the idea of profit optimal control will be introduced in order to unify two essential considerations, namely dynamics and economics. Thirdly, a typical fluid catalytic cracker (FCC), which, was used throughout the study, will be described. Fourthly, incentives for improved FCC control systems, together with their essential difficulties, will be discussed.

Basic Problems in Chemical Process Control

Some aspects of the basic difficulties in the study of process control are summarized as follows:

1. Chemical processes are frequently found to be multivariable (or multi-input and multi-output) systems. Although the theory (i.e., optimal tuning) of so-called "PID controller" has been developed successfully for a univariable system, strictly speaking there does not exist any completely satisfactory method for the design of multivariable control systems. Together with the problem of selection of a control structure, this multivariable characteristic of chemical processes creates one of the most essential difficulties in the control problem.

2. Chemical processes are frequently found to be nonlinear. This fact gives us two vexing problems. One is that any control theory, based on the linear theory, is restricted to the range where the assumption of linearization is valid. The other is that it is impossible, strictly speaking, to generalize the results obtained for a particular condition of a nonlinear system to any other conditions.

3. Chemical processes are frequently found where their final goal is not only the regulation of process variables but also the realization of maximum profitability. Therefore, for a certain disturbance, the role of a control system should not necessarily be to compensate or suppress this disturbance, but to obtain an extra profit from it.

Because of items 1 and 2, plant engineers tend to develop their own "art of engineering" by essentially "trial and error" techniques. Item 3 points out another direction of art, namely "optimizing (computer) control." Although the recent developments in the area of optimal control and nonlinear stability theory are remarkable, the status of their application to process control is still limited to highly simplified situations which have very limited use.

The objective of this work is, in short, to investigate the applicability of optimal control theory to the problem of control system design for a typical example of a multivariable, nonlinear chemical process. A hypothetical fluid catalytic cracking unit was selected as the process to be studied because, in addition to providing a challenging control problem, it is also of great economic significance in a modern petroleum refinery.

The Basic Idea of Profit Optimal Control

The basic idea of optimal control assumes that control improvement can be realized by optimizing a certain criterion. An ultimate criterion will be a profit as far as the control of industrial process is concerned. In fact, the conventional regulating control philosophy is based on the assumption that either the optimum operating conditions do not change much or the effect on profit resulting from the change of the optimum is small. Here, the ultimate criterion was replaced by a subcriterion (e.g., minimum deviation) for simplicity.

To achieve a desired operation, there are two considerations--dynamics (e.g., accuracy and stability) and economics. Conventional

feedback control engineering deals mainly with problems of system accuracy and stability, but it bears little or no direct relationship with the economy of overall process operation, except that it is considered to be necessary for the operation of the process. On the other hand, static optimization is concerned mainly with economics. In the last decade, in fact, the importance of a steady-state optimization of chemical processes has been increasing as the technology of computer control improves. A steady-state optimization gives a set of operating conditions of a hypothetical optimal steady state, but it does not say how this optimal steady-state can be reached without serious runaways nor how to keep this optimal steady-state satisfactory. The implications of its extension to the dynamic situation, when the results of optimization are to be used to affect the control of the process on a dynamic basis, have not been fully investigated. The profit optimal control is concerned with both dynamics and economics. In this sense the profit optimal control is a unified approach to achieve a desired operation.

Of course, the profit optimal control study does not always provide a means of control improvement that can be directly implemented, but at least the study can provide a basis for evaluating the desirability of any imaginative control strategy.

Description of Fluid Catalytic Crackers

Although there are various types of FCC (fluid catalytic cracker), Fig. 1.1 shows one of the most common ones. The catalyst circuit is the reactor, stripper, spent catalyst slide valve, air riser, regenerator, standpipe, regenerated catalyst slide valve, and oil riser leading back into the reactor, with the catalyst flowing in the same order.

Fresh feed and recycle feed are vaporized on contacting regenerated catalyst at the base of the oil riser and lift the catalyst into the reactor where disengagement is accomplished both by gravity and

with cyclones. The reaction commences at the moment of contact, and is completed in the reactor.

Catalyst from the reactor is stripped countercurrently with steam to remove entrained oil vapors. Air moves the spent catalyst to the dense bed in the regenerator and removes the carbonaceous deposit from the catalyst as H_2O, CO, and CO_2.

Reactor products flow into the base of the fractionator (which is not shown in Fig. 1.1), where the products are fractionated into various streams. "Gasoline and lighter" is taken from overhead and is pumped into a gas-concentration unit where it is further separated, normally into three streams: a stabilized (partially debutanized) gasoline, a C_3 and C_4 fraction, and a gas composed principally of "C_2 and lighter."

Two side cut streams are produced from the fractionator, a light cycle oil which, in fact, is infrequently used as a recycle stream, and a heavy cycle oil. This latter is the principal component of the material recycled to the reactor. It is returned to the reactor section at any desired rate up to that at which there is no net yield.

Open-Loop Control Systems of FCC

For illustration purposes, a typical open-loop control scheme of FCC is shown in Fig. 2.1. The operator has at his disposal four primary manipulated variables: blower adjustment (R_{ai}), feed preheat temperature (T_{fp}), reactor catalyst level or holdup (H_{ra}), and regenerated catalyst slide valve position (R_{rc}).

Although certain targets such as reactor temperature, fresh feed, and recycle feed rate are set for the operator to hold, his most vexing problem is maintaining carbon balance. The regenerator must burn neither more nor less carbon than is produced in the reactor. The operator has indirect indications of whether the carbon level is rising, steady, or falling but no on-line measurement. He must usually be satisfied to operate at the lower end of a range of carbon

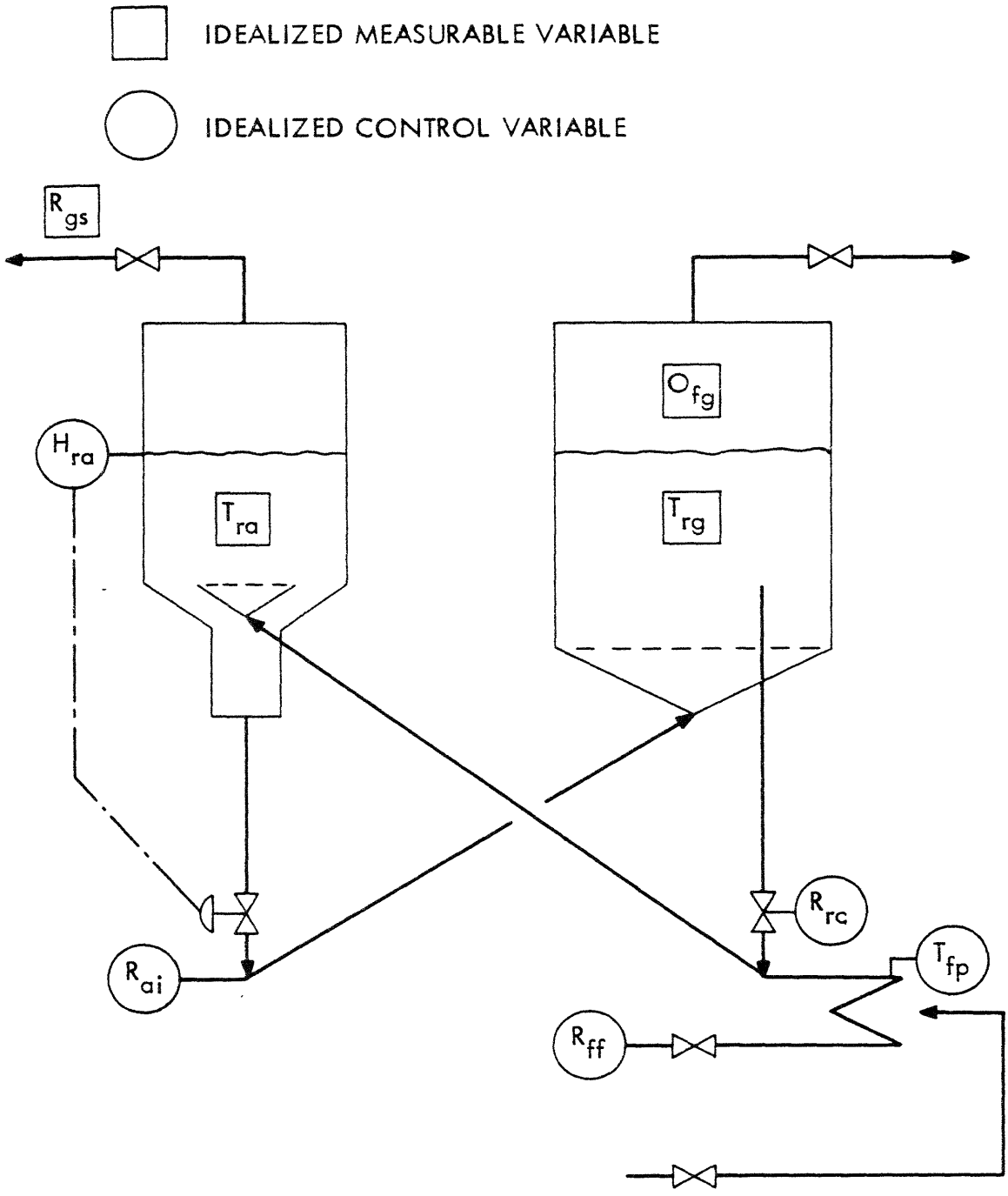

Fig. 2.1 An Idealized Open Loop Control Scheme of FCC

levels between a "snowballing" carbon buildup, which means poor selectivity for cracking on the high side and excessive afterburning above the regenerator dense bed on the low side.

Incentives for Improved FCC Control Systems

Until the late 1950's, fluid catalytic crackers were relatively easy to operate. Good cracking stocks, low cracking severity, non-extinction operation, 1-2% oxygen in the regenerator flue gas, and the use of regenerator lean phase spray water provided a high degree of self-regulation within the unit and gave the operators many "handles" to adjust when necessary.[32]

But as refineries have become more complex and greater efficiency has been required, one after another of these areas of operating freedom and inefficiency has been compressed. The variety of sources and types of cracking stocks has increased and the quality has deteriorated significantly. Conversion has been increased markedly, and heavy gas-oil production can no longer be tolerated with minimal heavy fuel production.[32]

Removal of the catalyst-deactivating influence of regenerator spray water (the use of spray water is undesirable because of potential damage to the catalyst by sintering or breakage due to thermal shock[57]) and higher severities have raised regenerator temperatures by about 100° to 150°F, to well above 1200°F. At these temperatures, afterburning of CO to CO_2 will readily occur if there is any significant amount of oxygen in the flue gas, with rapid and excessive temperature rises. For this reason the utilization of oxygen in the catalyst regeneration must be as complete as possible.[32]

All of these moves influence the carbon content of the circulating fluidized catalyst and the heat balance of the unit, creating a potentially unstable operation which can readily snowball into an upset condition.[32]

It is commonly observed that although cracking units may be designed for operation at equipment limits, operators tend to leave a comfortable margin and fail to operate the unit at the limits; in part this reflects their uncertainty about the process dynamics and the present control systems.[62]

The major role played by catalytic cracking and its larger contributions to overall refinery profitability, coupled with the necessity for keeping operations carefully controlled at close to critical conditions, has made catalytic cracking units prime candidates for any method of improved control.* On-line computer control of the process offers the promise of more efficient operation of the unit and maximizing of product values, not only for the unit itself but also for the integration of the unit into the overall refinery situation.[69]

2.2 PREVIOUS INVESTIGATIONS

The objective of this section is to summarize the previous works which are related to the study. First, several industrial efforts, directed to the improved control of FCC, will be discussed. Secondly, a short review of optimal control theory is introduced, and its open-loop and close-loop structure will be discussed from the point of view of control systems design. Thirdly, the profit optimal control problem of continuous flow process will be discussed in order to understand its significance and limitations.

Previous Control Studies of FCC

Because of the major role played by catalytic cracking and its larger contributions to overall refinery profitability, coupled with the necessity for keeping operations carefully controlled at close to critical conditions, numerous control studies have been attempted

---

* In fact, in the petroleum refining industry, the efficiency of the catalytic cracking unit contributes significantly to the refinery's competing capability.

for fluid catalytic crackers[25, 37, 32, 57] and for a moving-bed catalytic cracker.[75] Kane, et al.[37] and Gandsey[25] reported that their optimizing computer control systems improved their cat crackers significantly provided that computers and operators work together. This fact is very instructive. Since their optimizing systems concern only static optimizations, dynamic aspects of the control systems still require the operators' skill.

Pohlenz[57] describes a control scheme in which the reactor temperature is controlled by the catalyst rate and the oxygen level is controlled by the air rate. We are calling this the "conventional control scheme," since this scheme is frequently found in the literature. Although Pohlenz did not report any critical evaluation of his scheme, it is apparently satisfactory for certain limited situations. This scheme is analyzed in Chapter IV.

Hicks, et al.[32] reported on their analog computer simulation study of several control schemes:

1. the reactor and the flue gas temperature control scheme where the reactor temperature is controlled by the catalyst rate and where the flue gas temperature is controlled by the air rate, and

2. an alternative oxygen control scheme, where the oxygen level is controlled by the catalyst rate.

Although these schemes are apparently satisfactory for certain limited situations, they are essentially "incomplete" in the sense that they do not have any information feedback with respect to the oxygen level for scheme (1) and with respect to the reactor or the regenerator temperatures for scheme (2). However, their data as analog computer solutions serve as a basis to support the ideas that

1. although there are various kinds of FCC, the dynamic behavior of their controlled systems have, to a great extent, common characteristics which might be called the "dynamic similarities of FCC control systems," and therefore

2. the results obtained for an FCC can be generalized, to a certain extent, for most of the FCC.

These dynamic similarities are described in Appendix D and these incomplete control schemes are analyzed in Appendix E. These simulations are primary sources to support the validity of the dynamic mathematical models which will be described in Chapter III.

Background of Optimal Control Theory

During the past five years, an intense amount of research has been carried out in the area of optimal control.[6, 36, 58] The two main theoretical approaches to the optimal control problem have been (1) Bellman's dynamic programming method which is based on the principle of optimality, and (2) Pontryagin's maximum principle which can be viewed as an extension and application of the classical calculus of variations to the optimal control problem.

The dynamic programming method was originally developed for discrete-time problems and later on it was applied to continuous-time problems; in the latter form it is often referred to as the Hamilton-Jacobi-Bellman theory.[6] Its major disadvantage lies at the large computer memory requirements (the "curse of dimensionality").

The maximum principle was originally developed for continuous-time problems and, recently, has been extended to discrete-time problems. Its major disadvantage is that it provides, in general, only local necessary conditions for optimality. Its computational requirements, although nontrivial, are not as severe as those associated with dynamic programming.

The optimal control theory supposes that a plant can be described by a set of ordinary differential equations

$$\dot{\underline{x}} = \underline{f}(\underline{x}, \underline{u}) \qquad (2.1)$$

where $\underline{x}$ represents a vector of state variables and $\underline{u}$ represents a vector of control variables. An objective functional of operating the

plant from time $t=0$ to $t=t_1$, is given by

$$J(\underline{u}) = \int_0^{t_1} L(\underline{x}, \underline{u})\,dt \tag{2.2}$$

where L may be an arbitrary function. Optimal control theory asks how $\underline{u}$ should be chosen as a function of t, $0 \leq t \leq t_1$, in order to make the objective functional J a maximum (or a minimum).

Once the problem has been suitably posed, the optimal control can be derived by mathematical techniques. If an explicit result is needed, however, the computations are severe. The most work in optimal control theory has been directed towards obtaining an explicit solution or an open-loop structure of the optimal system.

In some cases it is possible to obtain the structure of the optimal control system without explicitly solving the equations for the optimal control $\underline{u}$. For example if the plant is operated continuously for a sufficiently long period between shut downs, then t_1 in Eq. 2.2 is so large that, in effect, the optimal control $\underline{u}$ is independent of t_1. In other words, $\underline{u}(t)$ for $0 \leq t \leq t_1$, in effect, depends only on the initial condition $\underline{x}(0)$. This situation can be further simplified by utilizing the principle of optimality (see Appendix H). Thus, in general, if t_1 is an infinity, there exists a certain optimal functional relation between $\underline{u}(t)$ and $\underline{x}(t)$ at any instance t, as follows:

$$\underline{u} = \underline{h}(\underline{x}) \tag{2.3}$$

This relation, if it exists, is called a closed-loop structure of the optimal control system, and may be considered as an implicit solution (or optimal control law).

This closed-loop structure has the following essential advantages over the open-loop structure:

1. A closed-loop structure does not require extensive on-line computations in order to implement in a real time operation, since, according to Eqs. 2.1 and 2.3, the plant should obey the differential equations:

$$\dot{\underline{x}} = \underline{f}\{\underline{x}, \underline{h}(\underline{x})\} \tag{2.4}$$

and the resulting behavior corresponds to optimal operation, while an open-loop structure requires an optimizing computation for an operation, with a different initial condition.

2. It is generally expected that the effect on real plant performance of disturbances and errors in the mathematical model will be less when a closed-loop structure is implemented than when an open-loop structure is implemented.

One of the most powerful control system design techniques that has been developed deals with the design of the optimal feedback system for a linear, time-invarying plant with respect to a quadratic performance index. The pioneering work in the area was done by Kalman[36] and resulted in the relation of Eq. 2.3. Details are included in Appendix H for the purpose of reference.

Now, as a result of this investigation, a new approach to control system design is proposed which is based on the above closed-loop structure of the optimal system. However, it should be emphasized that with this new approach the optimal control system will not be implemented directly, but instead an alternative closed-loop control system will be implemented, which approximates the resulting implicit solution (or optimal control law) by a simple relation for practical use. If the performance of this alternative closed-loop control is tested for various disturbances with the use of dynamic simulation, then the evaluation of this new approach is possible.

Profit Optimal Control of Continuous Flow Process

A profit optimal control, where the objective function is essentially the profitability of process operation, has important advantages over a steady-state optimization in the following area: batch reactors, cyclic reactors, or semi-batch reactors; start-up, shut down, and other unsteady operations (e.g., compensation of disturbances) of flow reactors.[39] Because of the nonlinearities in the process itself and in the objective function, there does not exist any analytical solution to these profit optimal control problems. Since the optimal control problem is, in general, reduced to the "two-point boundary value problem," it is impossible to solve the problem directly like the "initial value problem." Therefore, a "trial and error" method or, at best, an iterative computational algorithm is necessary.[39]

Among the batch reactor, cyclic reactor, and flow reactor, the last one is most important because most of the large scale processes are characterized by "continuous flow process." Kipiniak[38] initiated the study of profit optimal control of continuous process by the calculus of variation. His method is essentially a "trial and error" method and relatively inefficient.

Kurihara[39] formulated the profit optimal control problems of continuous flow process by the maximum principle of Pontryagin, and showed that the method of "steepest ascent of the Hamiltonian," which will be discussed in the next section, has a computational superiority over other numerical iterative methods.

The advantages of the profit optimal control problem formulation are as follows:

1. The process can be nonlinear
2. The objective function can be nonlinear
3. The control variables can be constrained
4. The steady-state optimal solution is automatically given as a by-product.

The limitations of the method are as follows:

1. The process is limited to the lumped parameter systems against the distributed parameter systems.

2. The problem is limited to the deterministic problem against the stochastic problem.

3. The method requires iteration.

Since most of the optimal control problems have these limitations, the advantages of the profit on optimal control are quite significant. This is the very reason why we use this method throughout the study. Furthermore, one of the objectives of this study is to add a fifth advantage to this method: (5) the state variables can be constrained practically by the use of appropriate penalty functions.

2.3 THE METHOD OF STEEPEST ASCENT OF THE HAMILTONIAN

The objective of this section is to describe the steepest ascent method without involving the maximum principle in details. First, the problem will be formulated. Secondly, the Hamiltonian function will be introduced. Thirdly, the steepest ascent method is described and its significance and limitations will be discussed.

Formulation of Optimal Control Problems

The profit optimal control problem is formulated in the form of a "fixed-time, free-end problem" which will be described in Appendix G.

The problem is to determine the control $\underline{u}$ which maximize the objective function

$$J(\underline{u}) = \int_0^{t_1} L(\underline{x}, \underline{u})dt \tag{2.5}$$

under the following conditions:

1. The system equations are

$$\dot{\underline{x}} = \underline{f}(\underline{x}, \underline{u}) \tag{2.6}$$

2. $\underline{u}$ is constrained by

$$\underline{u}_{min} \leq \underline{u} \leq \underline{u}_{max} \tag{2.7}$$

3. The initial condition is specified by

$$\underline{x}(o) = \underline{x}_o \tag{2.8}$$

4. The end condition is free, or unspecified.

Hamiltonian Function and Costate Equations

A few definitions of terms are necessary to describe the method of steepest ascent. The Hamiltonian function is defined by

$$H(\underline{x}, \underline{p}, \underline{u}) = L(\underline{x}, \underline{u}) + \sum_{i=1}^{n} p_i f_i(\underline{x}, \underline{u}) \tag{2.9}$$

where p_i's are costate variables associated with x_i. The costate equations are defined by

$$p_i = -\partial H/\partial x_i \qquad i=1, \ldots, n \tag{2.10}$$

The end conditions for costate variables are

$$\underline{p}(t_1) = \underline{0} \tag{2.11}$$

If we recall the Lagrange's multiplier method to solve the optimization problem with constrained equations, then the costate variables correspond to Lagrange's multipliers. The costate equations, i.e., Eq. 2.10, are just a part of necessary conditions for optimality. These points are described in Appendix G.

Steepest Ascent of the Hamiltonian

The necessary conditions and optimal control laws derived from the maximum principle are, in general, transformed into two-point boundary value problems which are, in general, very difficult to solve.[6,39,58] The steepest ascent method practically eliminates this difficulty.[39,60] The method may be explained by the following sequence of computations for one iteration:

1. Control variable, $\underline{u}$, is estimate for all t.

2. The system equations, Eq. 2.6, and the objective function, Eq. 2.5, are integrated with the initial condition, Eq. 2.8.

3. The costate equations, Eq. 2.10, are integrated with the end condition, Eq. 2.11, backwards in time.

4. New control variables are estimated by

$$\underline{u}_{new} = \underline{u}_{old} + \underline{e}\,\partial H/\partial \underline{u} \tag{2.12}$$

provided that Eq. 2.7 is satisfied, where $\underline{e}$ is a suitable positive relaxation parameter.

This iterative method is used until there is no further change in the objective function, J. The value of $\underline{e}$ should be small enough so that no instability will result, yet large enough so that the convergence will not be too slow.

In order to speed up the convergence, the following modifications

$$\underline{e}_{new} = \begin{cases} 2\,\underline{e}_{old} & \text{if } J_{new} > J_{old} \\ \frac{1}{4}\,\underline{e}_{old} & \text{if } J_{new} < J_{old} \end{cases} \tag{2.13}$$

were found effective.[39]

The main limitations of the method are as follows:

1. Although the convergence with respect to J and $\underline{x}$ is rapid, the convergence with respect to $\underline{u}$ is relatively slow.

2. The speed of convergence depends on the choice of $\underline{e}$ significantly, and it is nontrivial to choose a satisfactory one.

However, this method is one of the most practically useful methods for dynamic optimization,[39] and it will be used throughout the study.

2.4 STATEMENT OF OBJECTIVES

As was stated earlier, the objective of this work was to investigate the applicability of optimal control theory to the problem of control system design for a hypothetical fluid catalytic cracker as a typical example of multivariable, nonlinear processes. It is now possible to describe the specific goals of the work:

1. The first objective was to evaluate a new approach to control system design that was developed in the course of this investigation and which, as described earlier, is based essentially on a closed-loop structure of the optimal control law. The performance of the resulting control system is tested for various disturbances with the use of dynamic simulation.

2. The second objective was to test a computational algorithm--the method of steepest ascent of the Hamiltonian--for dynamic optimization of a highly-nonlinear, multivariable process typified by a fluid catalytic cracking unit. In the work, the applicability was tested by using penalty functions (artificial measures of process performance under certain undesirable operating conditions which should be avoided) to obtain an approximate solution for the problem of dynamic optimization with the allowable ranges of state variables restricted.

3. The third objective is to analyze the dynamic behavior of a fluid catalytic cracker from an information feedback point of view. This is expected to provide basic information which can be used to confirm the general conclusion, which will be drawn in the study, from a different aspect.

4. The fourth objective is to simulate and analyze several different control schemes which have appeared in the literature.[32]

5. The fifth objective is to analyze optimal steady-state operating conditions for fluid catalytic cracking processes, in order to derive several optimal operating criteria. These criteria are used to implement an adaptive optimizing control scheme which keeps the criteria automatically in the face of unknown disturbances. This is described in Appendix I.

CHAPTER III

COMPUTER PROGRAMS AND PROCEDURE

3.1 DYNAMIC SIMULATOR

The objective of this section is to derive a simplified set of dynamic mathematical models of FCC Model No. 1. First, basic dynamic models, which are derived in Appendix C in detail, will be summarized. Secondly, basic kinetic models, which are derived in Appendix A and B in detail, will be summarized. Thirdly, these models will be further transformed into a simplified set which will be used throughout the study. Fourthly, this simplified set of models will be used for a comparison of the dynamic behavior of the FCC control systems.

Basic Dynamic Models

There can be various kinds of dynamic mathematical models of FCC from the highly sophisticated ones to the very simple ones depending on the purpose for using them. For the objectives described in Section 2.4, simplified dynamic models are adequate. Simplified dynamic models can be obtained by isolating the reactor and regenerator systems from the fractionator and the feed preheater. Details in assumptions and derivations of models are described in Appendix C. The principal assumptions are that a fluidized bed is equivalent to a stirred tank with respect to catalysts, and that gas passes through the bed in a plug-flow manner with no time lag.

Basic dynamic models consisted of reactor material balances (catalyst, total carbon, catalytic carbon, and residual carbon), reactor heat balance, regenerator material balances (catalyst, carbon) and regenerator heat balance. They are summarized, in the same order as above, as follows

$$dH_{ra}/dt = (60)\,(R_{rc} - R_{sc}) \tag{3.1}$$

$$H_{ra}\,dC_{sc}/dt = (50)\,R_{cf} + (60)\,R_{rc}(C_{rc}-C_{sc}) \tag{3.2}$$

$$H_{ra}\,dC_{cat}/dt = (50)R_{cc}H_{ra} - (60)R_{sc}C_{cat} \tag{3.3}$$

$$H_{ra}\,dC_{res}/dt = (60)\,R_{rc}(C_{rc}-C_{res}) \tag{3.4}$$

$$\begin{aligned} S_c\,H_{ra}\,d\,T_{ra}/dt &= (60)\,S_c\,R_{rc}\,(T_{rg} - T_{ra}) \\ &-(.875)S_f\{D_{ff}R_{ff}(T_{ra} - T_{fp}) + D_{rf}R_{rf}(T_{ra}-T_{rf})\} \\ &-(.875)\Delta H_{fv}\{D_{ff}R_{ff} + D_{rf}R_{rf}\} - (.5)\,\Delta H_{cr}R_{oc} \end{aligned} \tag{3.5}$$

$$dH_{rg}/dt = (60)(R_{sc}-R_{rc}) \tag{3.6}$$

$$H_{rg}\,dC_{rc}/dt = (60)R_{sc}(C_{sc}-C_{rc}) - (50)R_{cb} \tag{3.7}$$

$$\begin{aligned} S_c\,H_{rg}\,dT_{rg}/dt &= (.5)\Delta H_{rg}R_{cb} - (60)S_c\,R_{sc}(T_{rg}-T_{ra}) \\ &-(.5)S_a\,R_{ai}(T_{rg}-T_{ai}) \end{aligned} \tag{3.8}$$

where

H_{ra} = reactor catalyst holdup

C_{sc} = (total) carbon on spent catalyst

C_{cat} = catalytic carbon

C_{res} = residual carbon

T_{ra} = reactor temperature

H_{rg} = regenerator catalyst holdup

C_{rc} = carbon on regenerated catalyst

T_{rg} = regenerator temperature

Other nomencaltures are described in Appendix C.

The above eight equations consist of a basic structure of dynamic models.

Basic Kinetic Models

Because of the complex nature of catalytic cracking and regeneration, any kinetic models are, at best, of empirical approximations. Details in assumptions and derivations of models are described in Appendices A and B. The principal assumptions are that an instantaneous reaction rate depends on the amount of catalysts, the condition of carbon deposition, and the temperature. Assuming that gas passes through the uniform catalyst bed in a plug-flow manner with no time lag, an instantaneous reaction rate is integrated for the total bed to provide an overall reaction rate.

Basic kinetic models consisted of reactor kinetics (gas oil cracking rate, total carbon forming rate, catalytic carbon forming rate) and regenerator kinetics. They are summarized, in the same order as above, as follows

$$R_{oc} = (1.75) D_{ff} R_{ff} C_{ff} = \text{gas oil cracking rate} \qquad (3.9)$$

where

$$\begin{cases} C_{ff} = C_{tf}(1+R_r) \\ C_{tf} = A/(A+1) \\ A = \dfrac{K_{cr} P_{ra}}{R_{tf}/H_{ra}} \\ K_{cr} = \dfrac{k_{cr}}{C_{cat} C_{res}^{m}} \exp\left\{ - \dfrac{\Delta E_{cr}}{R(T_{ra}+460)} \right\} \\ m = 0.15 \end{cases}$$

$$R_{cf} = R_{cc} + F_{tf} R_{tf} = \text{(total) carbon forming rate} \qquad (3.10)$$

$$R_{cc} = K_{cc} P_{ra} H_{ra} = \text{catalytic carbon forming rate} \tag{3.11}$$

where

$$\begin{cases} K_{cc} = \dfrac{k_{cc}}{C_{cat} C_{res}^{n}} \exp\left\{ - \dfrac{\Delta E_{cc}}{R(T_{ra}+460)} \right\} \\ \\ n = 0.06 \end{cases}$$

$$R_{cb} = \frac{R_{ai}}{C_1} (21 - O_{fg})/(100) = \text{carbon burning rate} \tag{3.12}$$

where

$$\begin{cases} O_{fg} = 21 \exp\left\{ - \dfrac{P_{rg} H_{rg}/R_{ai}}{1/K_{od} + (100)/K_{or} C_{rc}} \right\} \\ \\ K_{od} = C_2 R_{ai}^2 \\ \\ K_{or} = C_3 \exp\left\{ \dfrac{\Delta E_{or}}{R(1100 + 460)} - \dfrac{\Delta E_{or}}{R(T_{rg} + 460)} \right\} \end{cases}$$

These equations are dimensional and other nomenclatures are described in Appendices A and B.

The above four equations represent the basic structure of kinetic models.

Further Simplification of Models

It is generally observed that the reactor catalyst holdup is considerably smaller than the regenerator catalyst holdup. Their ratio is of the order of 1:4. If we recall that the effects of short-time constants on the overall dynamics are relatively negligible and the overall dynamic behavior of the system is controlled by a relatively few number of elements which have relatively large time constants, then it is expected that one can simplify the reactor dynamic models, Eqs. 3.1 through 3.5, without sacrificing the accuracy. However,

as far as the control systems which are actuated by the measurements of reactor variables are concerned, an accurate dynamic behavior of the variables is of critical importance. Therefore we avoid simplifying Eq. 3.5 with the consideration of the reactor temperature controller. For Eqs. 3.1, 3.3, and 3.4, the simplification of these equations are of great importance, since it results in a further simplified set of kinetic models, as follows. With the quasi-steady-state approximation, Eqs. 3.1, 3.3, and 3.4 result in

$$R_{rc} \doteqdot R_{sc} \tag{3.13}$$

$$R_{cc}H_{ra} \doteqdot (1.2)\, R_{sc}\, C_{cat} \doteqdot (1.2)R_{rc}C_{cat} \tag{3.14}$$

$$C_{res} \doteqdot C_{rc} \tag{3.15}$$

Eliminating R_{cc} from Eqs. 3.11 and 3.14, and solving for C_{cat},

$$C_{cat} \doteqdot \left\{\frac{H_{ra}P_{ra}k_{cc}}{R_{rc}C_{rc}^{n}}\right\}^{1/2} \exp\left\{-\frac{\Delta E_{cc}}{R(T_{ra}+460)}\right\} \tag{3.16}$$

Introducing Eq. 3.16 into 3.9,

$$R_{oc} = (1.75)\, D_{ff}\, R_{ff}\, C_{ff} \tag{3.17}$$

where
$$\begin{cases} C_{ff} = C_{tf}(1+R_r) \\ C_{tf} = A/(A+1) \\ A = A_1 \dfrac{\{R_{rc}H_{ra}P_{ra}\}^{1/2}}{R_{tf}\,C_{rc}^{m_1}} \exp\left[\left\{\dfrac{1}{R(900+460)} - \dfrac{1}{R(T_{ra}+460)}\right\}\Delta E'_{cr}\right] \\ m_1 = m - n/2 \\ \Delta E'_{cr} = \Delta E_{cr} - \Delta E_{cc}/2 \\ A_1 = \text{constant parameter for total feed and catalyst} \end{cases}$$

Introducing Eq. 3.16 into 3.10 or 3.11,

$$R_{cf} = A_2 \frac{\{R_{rc}H_{ra}P_{ra}\}^{1/2}}{C_{rc}^{n_1}} \exp\left[\left\{\frac{1}{R(900+460)} - \frac{1}{R(T_{ra}+460)}\right\}\Delta E'_{cc}\right] \qquad (3.18)$$

where
$$\begin{cases} n_1 = n/2 \\ \Delta E'_{cc} = \Delta E_{cc}/2 \\ A_2 = \text{constant parameter for total feed and catalyst} \end{cases}$$

Therefore, Eqs. 3.2, 3.5, 3.7, and 3.8 consist of a simplified set of dynamic models, and Eqs. 3.17, 3.18, and 3.12 consist of a simplified set of kinetic models. The overall model derived here will be referred to as mathematical Model No. 1.

Dynamic Similarities of FCC Control Systems

The basic ideas of the simulation study of an idealized hypothetical FCC are that although there are various kinds of FCC, the

dynamic behavior of their controlled systems have, to a great extent, common characteristics which might be called a "dynamic similarities of FCC control systems," and that therefore the results obtained for an FCC can be generalized, to a certain extent, for most of the FCC.

Although there are few published reports of dynamic behavior of any FCC control system, fortunately Hicks, et al.[32] reported their analog computer simulation study of an Atlantic's Orthoflow type FCC. In spite of the differences in capacity, size, configuration, and mechanism, between their FCC and the hypothetical FCC, the comparison of the dynamic behavior of the two systems can provide a basis to support the above ideas.

These comparisons are demonstrated in Appendix D, and showed the great possibility of supporting the above ideas, while they partially justified the adequacy of the models and the assumptions introduced in the study. Although the generalization of this conclusion is difficult to justify from these examples, with no additional information available this is the best that can be done now.

3.2 DYNAMIC OPTIMIZER

The objective of this section is to describe a basic structure of a dynamic optimization program of FCC. First, an objective function will be defined. Secondly, system equations will be derived (Model No. 2). Thirdly, a Hamiltonian function, costate equations, and gradients of the Hamiltonian function will be derived.

Objective Functions

In order to formulate an optimization problem of FCC, it is necessary to define an objective function and several constraints on dependent variables. Details in assumptions and derivations are described in Appendix F. The principal assumptions are that maximum profitability is synonymous with maximum product value, and that the

capacity of the process is limited not by the downstream processing capacity (e.g., gas compressor or alkylation unit, etc.) but by the regenerator capacity (e.g., air blower capacity and regenerator temperature).

Simplifying the product structure such that a fresh feed is converted into gas, gasoline, cycle oil, and coke, the following economic objective function is derived:

$$P_{gr} = \int_0^t \frac{R_{ff}}{(24)} \{ (42) D_{ff} Y_{gs} P_{gs} + Y_{g\ell} P_{g\ell} + Y_{co} P_{co} - P_{ff} \} dt \quad (3.19)$$

where
$$\begin{cases} Y_{g\ell} = (1+R_r) \frac{F_{g\ell}}{1-I_{g\ell}} \{ (1-C_{tf})^{I_{g\ell}} - (1-C_{tf}) \} = \text{gasoline yield} \\ Y_{co} = 1-C_{ff} = \text{cycle oil yield} \\ Y_{ck} = (.571)\, R_{cf}/R_{ff} D_{ff} = \text{coke yield} \\ Y_{gs} = 1 - Y_{g\ell} D_{g\ell}/D_{ff} - Y_{co} D_{co}/D_{ff} - Y_{ck} = \text{gas yield} \end{cases}$$

where P_{gr} = gross profit

Constraints on dependent variables consist of the regenerator safety models which are also described in Appendix F, and are expressed by

$$T_{rg} \leq (T_{rg})_{max} = \text{allowable maximum regenerator temperature}$$

$$O_{fg} \leq (O_{fg})_{max} = \text{allowable maximum oxygen level}$$

Although there are, in general, no direct methods to solve this problem, namely "dynamic optimization with state variables constrained," one of the most practically useful method is to use penalty functions (artificial measures of process performance under certain undesirable

operating conditions which should be avoided). Although there are various kinds of penalty functions,[38] the ones which we used are as follows:

$$P_1 = \int_0^t P_{e1}(T_{rg})dt \tag{3.20}$$

where $$P_{e1}(T_{rg}) = \begin{cases} G_1\{T_{rg}-(T_{rg})_{max}\}^{m_1} & \text{if } T_{rg} > (T_{rg})_{max} \\ 0 & \text{if } T_{rg} \leq (T_{rg})_{max} \end{cases}$$

and $$P_2 = \int_0^t P_{e2}(O_{fg})dt \tag{3.21}$$

where $$P_{e2}(O_{fg}) = \begin{cases} G_2\{O_{fg}-(O_{fg})_{max}\}^{m_2} & \text{if } O_{fg} > (O_{fg})_{max} \\ 0 & \text{if } O_{fg} \leq (O_{fg})_{max} \end{cases}$$

Parameters G_1, m_1, G_2, and m_2, govern the characteristics of penalty functions. Careful selections for these parameters are necessary in order to penalize the objective function efficiently and to avoid undesirable situations.

Therefore, an apparent objective function can be expressed by

$$J = P_{gr} - P_1 - P_2 \tag{3.22}$$

System Equations

The system equations, in the dynamic optimization problem of FCC, are essentially based on the dynamic mathematical models which

were described in the previous section as a dynamic simulator. However, if we recall that the real role of any optimization study is rarely to obtain the exact solution, which requires, in general, a great deal of computing time, but more often to obtain a certain approximate solution, then we must do our best to transform a set of dynamic models into a simpler set of system equations.

Among four equations, Eqs. 3.2, 3.5, 3.7, and 3.8, which constitute a set of dynamic models, quasi steady-state approximations will be made for Eqs. 3.2 and 3.5 with the expectation that these dynamic equations are less important than Eqs. 3.7 and 3.8, mainly because of the smaller time constant of the reactor. This simplification reduces active state variables to the regenerator temperature and the amount of carbon on the regenerated catalyst. In fact, we compared the models before and after this simplification by means of simulation and found that, although the latter is less accurate than the former, the latter is still useful, at least for the purpose of obtaining an approximate optimal solution.

After this process of approximation, the reactor temperature and the carbon on spent catalyst are expressed by the direct functions of other variables, and the system equations are reduced to

$$H_{rg}dC_{rc}/dt = (60)R_{rc}(C_{sc}-C_{rc}) - (50)R_{cb} \tag{3.23}$$

$$S_c H_{rg} dT_{rg}/dt = (.5)\Delta H_{rg} R_{cb} - (60)S_c R_{sc}(T_{rg}-T_{ra})$$

$$-(.5)S_a R_{ai}(T_{rg}-T_{ai}) \tag{3.24}$$

where C_{sc} and T_{ra} are determined by the following simultaneous equations:

$$\text{(right-hand side of Eq. 3.2)} = 0 \tag{3.25}$$

$$\text{(right-hand side of Eq. 3.5)} = 0 \tag{3.26}$$

The resulting simplified model will be referred to as mathematical Model No. 2. The principal reasons why this simplification is necessary are:

1. the smaller the number of state variables, then the smaller are the number of costate variables to be defined, and

2. the elimination of reactor dynamics which have a smaller time constant allows us to use a large time step for the numerical integration.

In fact, for the Euler's method of numerical integration, which is used throughout the study, an optimal (with respect to accuracy and computer time requirement) time step is about a half of the smallest time constant of the system equations.

Although there are five potential control variables, namely air rate, catalyst rate, reactor holdup, preheater temperature, and feed rate, we decided that our dynamic optimizer should include only two control variables, namely air rate and catalyst rate. The principal reasons for the above decision are

1. air rate and catalyst rate are common control variables for most of the FCC,

2. the smaller the number of control variables, then the faster is the convergence of the solution, and,

3. we intend to design a control system as simple as possible.

Hamiltonian Function and Costate Equations

In order to use the method of steepest ascent of the Hamiltonian, one must construct a Hamiltonian function. In order to avoid a complex mathematical manipulation, we discuss in an abstract form. Let

$$X_1 = T_{ra}$$

$$x_2 = T_{rg}$$

$$X_3 = C_{sc}$$

$$x_4 = C_{rc}$$

$$u_1 = R_{ai}$$

$$u_2 = R_{rc}$$

$$U_3 = H_{ra}$$

$$U_4 = T_{fp}$$

$$U_5 = R_{ff}$$

$$U_6 = R_{rf}$$

where x_2 and x_4 are state variables, u_1 and u_2 are control variables, X_1 and X_3 are functions, and U_3 through U_6 are parameters.

The integrand of the objective function, Eq. 3.22, in its complete form is expressed by

$$L = L(X_1, x_2, x_4, u_2, U_3, U_5, U_6) \tag{3.27}$$

System equations Eqs. 3.23 and 3.24 are expressed by

$$\dot{x}_2 = f_2(X_1, x_2, x_4, u_1, u_2, U_3) \tag{3.28}$$

$$\dot{x}_4 = f_4(x_2, X_3, x_4, u_1, u_2, U_3) \tag{3.29}$$

Equations 3.25 and 3.26 can be reduced to

$$X_1 = X_1(x_2 x_4, u_2, U_3, U_4, U_5, U_6) \tag{3.30}$$

$$X_3 = X_3(X_1, x_4, u_2, U_3, U_5, U_6) \tag{3.31}$$

A Hamiltonian function is defined by

$$H(x_2, x_4, u_1, u_2, U_3, U_4, U_5, U_6) = L + p_2 f_2 + p_4 f_4 \tag{3.32}$$

Costate equations are derived as follows:

$$\dot{p}_2 = -\frac{\partial H}{\partial x_2} = -\left\{\frac{\partial L}{\partial X_1}\frac{\partial X_1}{\partial x_2} + \frac{\partial L}{\partial x_2}\right\} - p_2\left\{\frac{\partial f_2}{\partial X_1}\frac{\partial X_1}{\partial x_2} + \frac{\partial f_2}{\partial x_2}\right\} - p_4\left\{\frac{\partial f_4}{\partial x_2} + \frac{\partial f_4}{\partial X_3}\frac{\partial X_3}{\partial X_1}\frac{\partial X_1}{\partial x_2}\right\} \tag{3.33}$$

$$\dot{p}_4 = -\frac{\partial H}{\partial x_4} = -\left\{\frac{\partial L}{\partial X_1}\frac{\partial X_1}{\partial x_4} + \frac{\partial L}{\partial x_4}\right\} - p_2\left\{\frac{\partial f_2}{\partial X_1}\frac{\partial X_1}{\partial x_4} + \frac{\partial f_2}{\partial x_4}\right\} - p_4\left\{\frac{\partial f_4}{\partial X_3}\left(\frac{\partial X_3}{\partial x_4} + \frac{\partial X_3}{\partial X_1}\frac{\partial X_1}{\partial x_4}\right) + \frac{\partial f_4}{\partial x_4}\right\} \tag{3.34}$$

Gradients of the Hamiltonian function are derived as follows:

$$\frac{\partial H}{\partial u_1} = p_2\frac{\partial f_2}{\partial u_1} + p_4\frac{\partial f_4}{\partial u_1} \tag{3.35}$$

$$\frac{\partial H}{\partial u_2} = \left\{\frac{\partial L}{\partial X_1}\frac{\partial X_1}{\partial u_2} + \frac{\partial L}{\partial u_2}\right\} + p_2\left\{\frac{\partial f_2}{\partial X_1}\frac{\partial X_1}{\partial u_2} + \frac{\partial f_2}{\partial u_2}\right\} + p_4\left\{\frac{\partial f_4}{\partial X_3}\left(\frac{\partial X_3}{\partial u_2} + \frac{\partial X_3}{\partial X_1}\frac{\partial X_1}{\partial u_2}\right) + \frac{\partial f_4}{\partial u_2}\right\} \tag{3.36}$$

System equations Eqs. 3.28 and 3.29, costate equations Eqs. 3.33 and 3.34, and the above gradients Eqs. 3.35 and 3.36 consist of a set of basic elements for a dynamic optimizer. Together with the iterative procedure described in Section 2.3, this dynamic optimizer provides optimal solutions as a set of functions of time, which lead a system from any initial condition to a final optimal steady-state condition.

3.3 PROCEDURE

The procedure of this study includes the following steps:

1. Dynamic simulation of the conventional control scheme is expected to disclose the principal control difficulties.

2. An information feedback analysis of the conventional control scheme is expected to disclose the principal cause of control difficulties.

3. Dynamic optimization of FCC will provide the ultimate performance and will evaluate the desirability of the conventional control scheme.

4. The optimal control solution and the principle of optimality provide optimal control laws as nonlinear functions of state variables.

5. An alternative control scheme will be determined by systematically approximating these optimal control laws.

6. Dynamic simulation of this alternative control scheme is expected to show a significant superiority over the conventional control scheme.

7. An information feedback analysis of this scheme is expected to disclose the principal cause of improvement.

CHAPTER IV

ANALYSIS OF THE CONVENTIONAL CONTROL SCHEME

4.1 DESCRIPTION OF THE CONVENTIONAL CONTROL SCHEME

The objective of this section is to describe a control scheme which is one of the most typical (or conventional) closed-loop schemes of FCC. First, as preparation, the pressure control scheme and oxygen detection scheme will be discussed. Secondly, an essential structure of this scheme is described in order to understand its significance.

Pressure Control Schemes

There are three types of pressure control schemes for FCC. They are shown in Fig. 4.1. Each scheme has its own advantages and disadvantages. In Scheme I and II, the top pressure in the reactor is not controlled directly; rather, the suction pressure to the gas compressor is controlled. The overhead gas in the reactor must flow through the cyclones, the fractionator, and the overhead condenser before it reaches the point of control. A considerable pressure drop, on the order of 10 psi, will occur due to flow through this equipment. Whenever a change occurs in the amount or nature of this overhead gas, such as would be caused by a change in conversion, the pressure drop, and hence reactor pressure, would also be expected to change.

In Scheme I, the regenerator top pressure is directly controlled by a slide valve in the flue gas line. This scheme has an advantage over other schemes; the regenerator pressure can be used to change the air rate by changing the air blower discharge pressure without changing the blower speed. However, this scheme has an essential disadvantage; any change in reactor pressure or regenerator pressure will affect catalyst circulation rate. In Scheme II, where the differential pressure is controlled by a slide valve in the flue gas line,

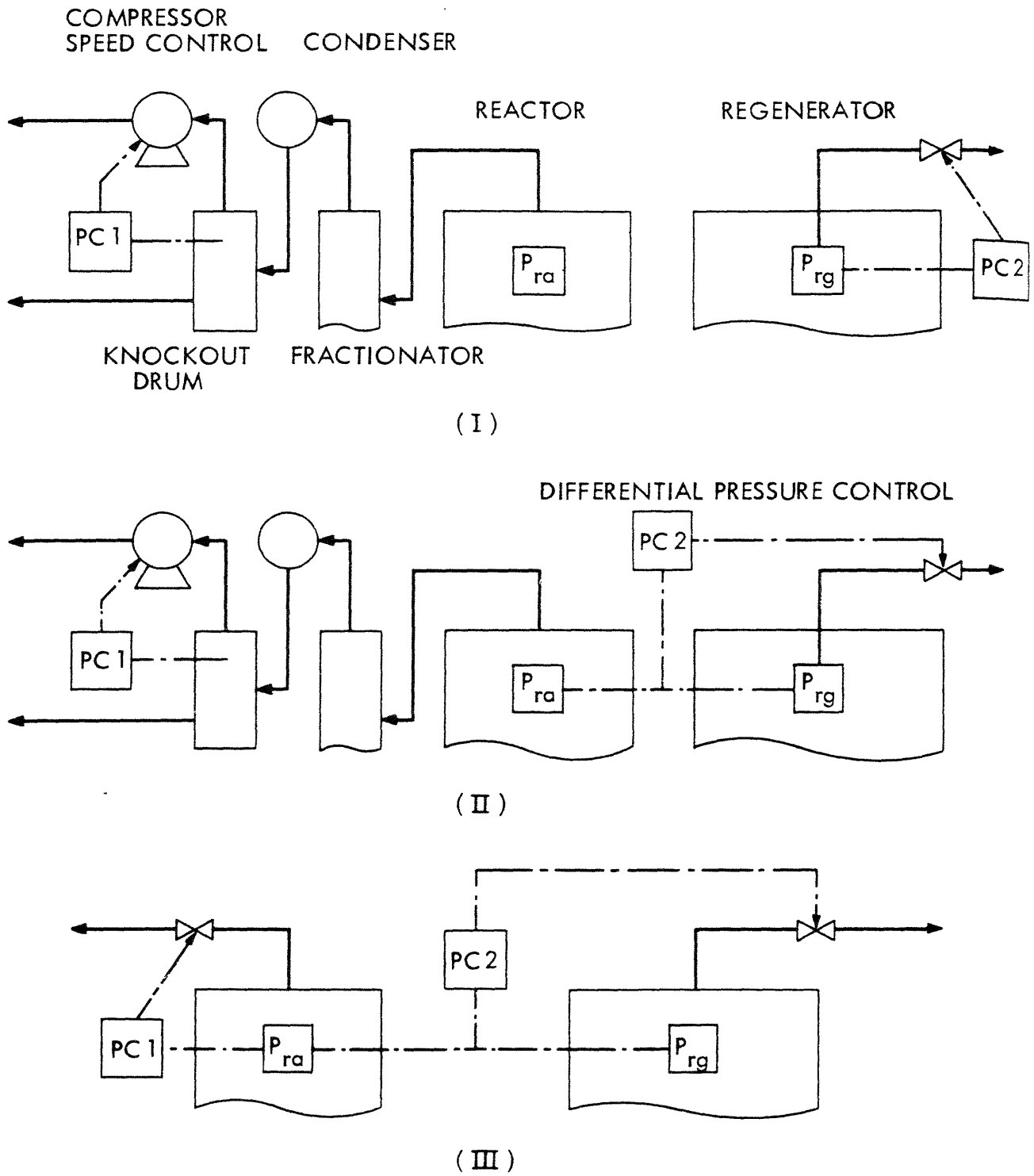

Fig. 4.1 Three Types of Pressure Control Scheme of FCC

the above disadvantage does not exist. In fact, this scheme is one of the most popular ones.[57] Scheme III, where the reactor pressure is directly controlled by a slide valve in the product gas line, is the simplest scheme and can be considered as an idealized, but rarely practical, one.

The effect of the difference in the pressure control scheme on the dynamic behavior of the total system is discussed in Appendix C. In short, it is relatively unimportant if the catalyst rate is used to control other operating variables (e.g., reactor temperature, etc.) automatically.

Oxygen Detection Schemes

Although the oxygen level in regenerator lean phase or in flue gas is one of the most important variables to be controlled carefully, it is impossible to measure it directly and accurately because of its extremely low level (order of 0.2%). Fortunately, regenerators are operated at such a high temperature (this is one of the most significant tendencies in the modern FCC operation) that an (approximately adiabatic) temperature rise due to the "afterburning" of CO to CO_2 can be used as a sensitive measure of oxygen level, although the accuracy is limited. There are two oxygen detection schemes as shown in Fig. 4.2.

In Scheme I, a lean phase differential temperature is measured.[57] In Scheme II, a cyclone differential temperature is measured.[32] The relation between differential temperature and oxygen level mainly depends on the residence time of gas, and will be described in Appendix B.

Structure of Conventional Control Scheme

Pohlenz[57] described his control systems of FCC, as follows:

1. The reactor temperature controls the regenerator slide valve to provide sufficient catalyst flow to maintain the reactor contents at the desired temperature.

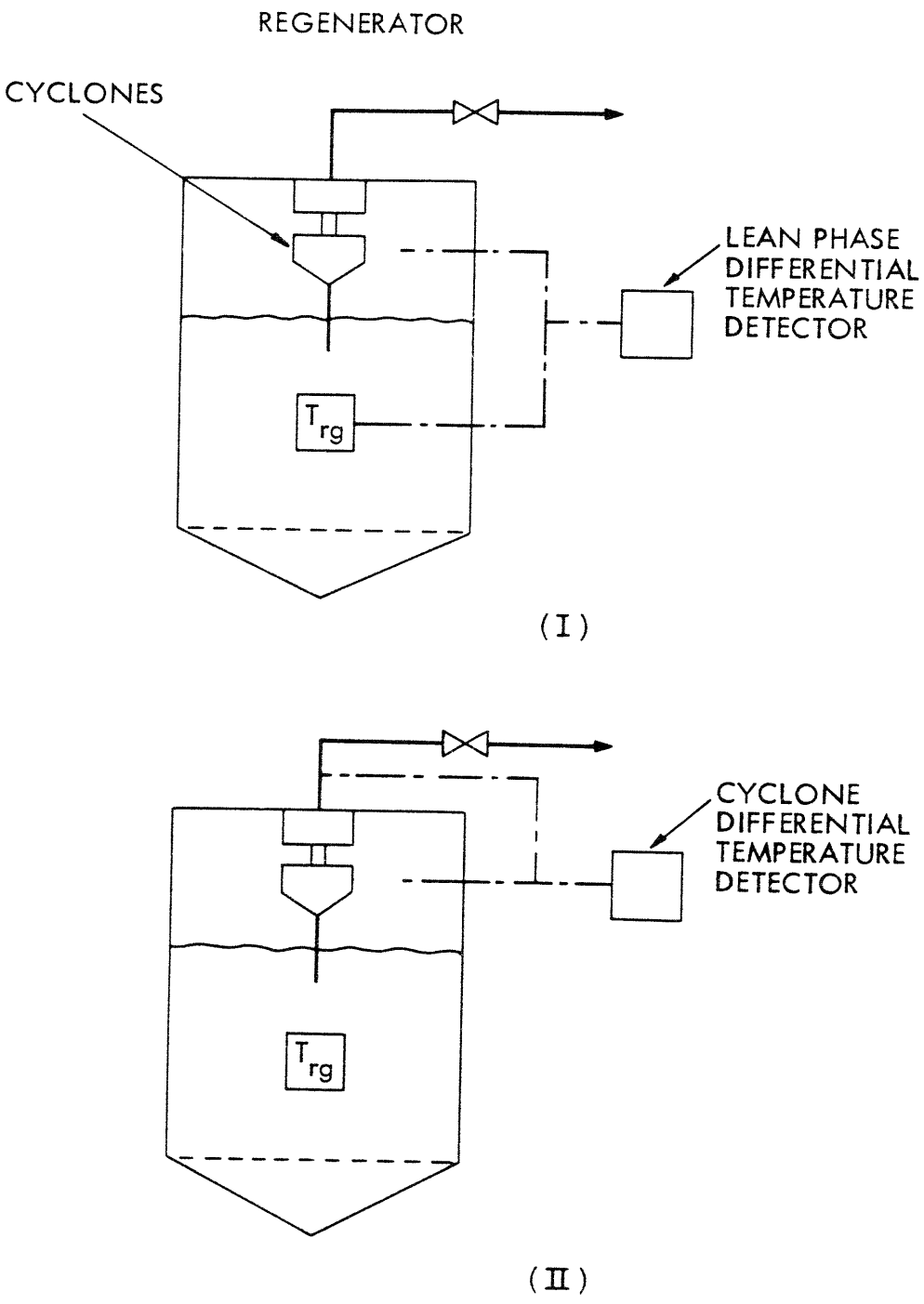

Fig. 4.2 Two Types of Oxygen Detection Scheme of FCC

2. The spent-catalyst slide valve is operated by a catalyst level control in the reactor.

3. Reactor pressure is held constant by pressure control of the main-column receiver.

4. The regenerator pressure is controlled, in turn, by a pressure-difference instrument between reactor and regenerator vessels which operates a double-acting slide valve in the flue-gas line.

5. The air rate to the regenerator is adjusted to provide air at a rate approximately 2% greater than that required for coke burnoff, and the excess is vented or "snorted" through a valve controlled by the temperature difference between dense and dilute regenerator catalyst phases, or between dense phase and flue gas.

6. The fresh feed and recycle streams operate on flow control as do the net yields of light cycle oil, heavy cycle oil, and clarified oil. With this system of instrumentation it is important to note that the catalyst circulation is not subject to direct control.

The main significance of the above systems lies in items 1 and 5, namely, the reactor temperature control by the catalyst rate and the oxygen control by the air rate. Since this scheme is one of the most practically important ones and is frequently found in the literature,[25,57] we denote it as a "conventional control scheme" which is shown in Fig. 1.3. Pohlenz claimed that, with this practice of controlling afterburning, the danger of temperature runaways is practically eliminated. This fact is of great significance. In fact, although Hicks, et al.[32] studied their control schemes, namely the control of the reactor and flue gas temperature by catalyst rate and air rate respectively, and the control of oxygen by catalyst rate, their control schemes are essentially "incomplete" in the sense that they can not prevent the runaway or extreme offset for regenerator temperature and oxygen level. These incomplete control schemes are analyzed in Appendix E.

Pohlenz explains, why the heat balance is automatic, as follows: For a given situation, the catalyst rate is expected to be relatively low if the regenerator temperature is high, and vice versa, because of the reactor temperature control. The net result is a coke rate which opposes the direction in which the regenerator temperature moves; this is the "flywheel" effect which stabilizes the regenerator temperature with respect to changes in charge stock and operating conditions.

The above fact obtained by Pohlenz is true at least for a long run or steady-state aspect. However, in a short run or dynamic aspect, it is frequently found that this conventional control scheme is not satisfactory. In fact, Hicks, et al.[32] reported that this scheme could not prevent upsets. Therefore, it is expected that there exists an essential problem about the dynamics in this control scheme, and, therefore, we decided to analyze the dynamic behavior of this conventional control scheme, and to provide a basis for comparison alternative improved control system.

4.2 DYNAMIC SIMULATION OF THE CONVENTIONAL CONTROL SCHEME

The purpose of this section is to demonstrate the performances of the conventional control scheme from the dynamics point of view. First, performances for unsteady-state initial conditions will be described. Secondly, performances for forced disturbances will be described. Thirdly, the performances of this control scheme will be summarized in order to understand its advantages and disadvantages.

Performances for Unsteady-State Initial Conditions

By "unsteady-state initial condition," we mean a set of dependent operating variables which are different from the steady-state conditions.

A dynamic simulation of the conventional control scheme, where the initial carbon level is slightly higher than the steady-state level,

is shown in Fig. 1.4. Figure 4.3 describes the case in which the initial carbon level is slightly lower than the steady-state level. We can observe that this carbon wave is dispersed by actuating the air rate and the catalyst rate, and that it tends to reach the final steady state. The best controller parameter tunings were selected by trial-and-error adjustment. In Fig. 1.4, the performances for different tunings are also shown by broken lines. For reduced controller gains, as shown by symbols a and c, the response of the control system becomes more sluggish, while for increased controller gains, as shown by symbols b and d, the response of the control system becomes more oscillatory or unstable.

Performances for Forced Disturbances

By "forced disturbance," we mean a change which occurred in the operating conditions in a step function manner. Since this forced disturbance does not decay by itself, any control system moves the process operating condition from one to another, while keeping a set of operating variables constant.

A dynamic simulation of the conventional control scheme, when the feed rate is suddenly reduced, is shown in Fig. 4.4. This dynamic behavior will be explained by the following step by step analysis:

1. The reduced feed rate tends to increase the reactor and regenerator temperatures because of the reduced heat requirement.

2. The increased reactor temperature causes the catalyst rate to decrease by means of the controller. Simultaneously, the increased regenerator temperature reduces the oxygen level which, in turn, increases the air rate by means of the controller.

3. The reduced catalyst rate and the increased air rate accelerates the regenerator temperature to increase.

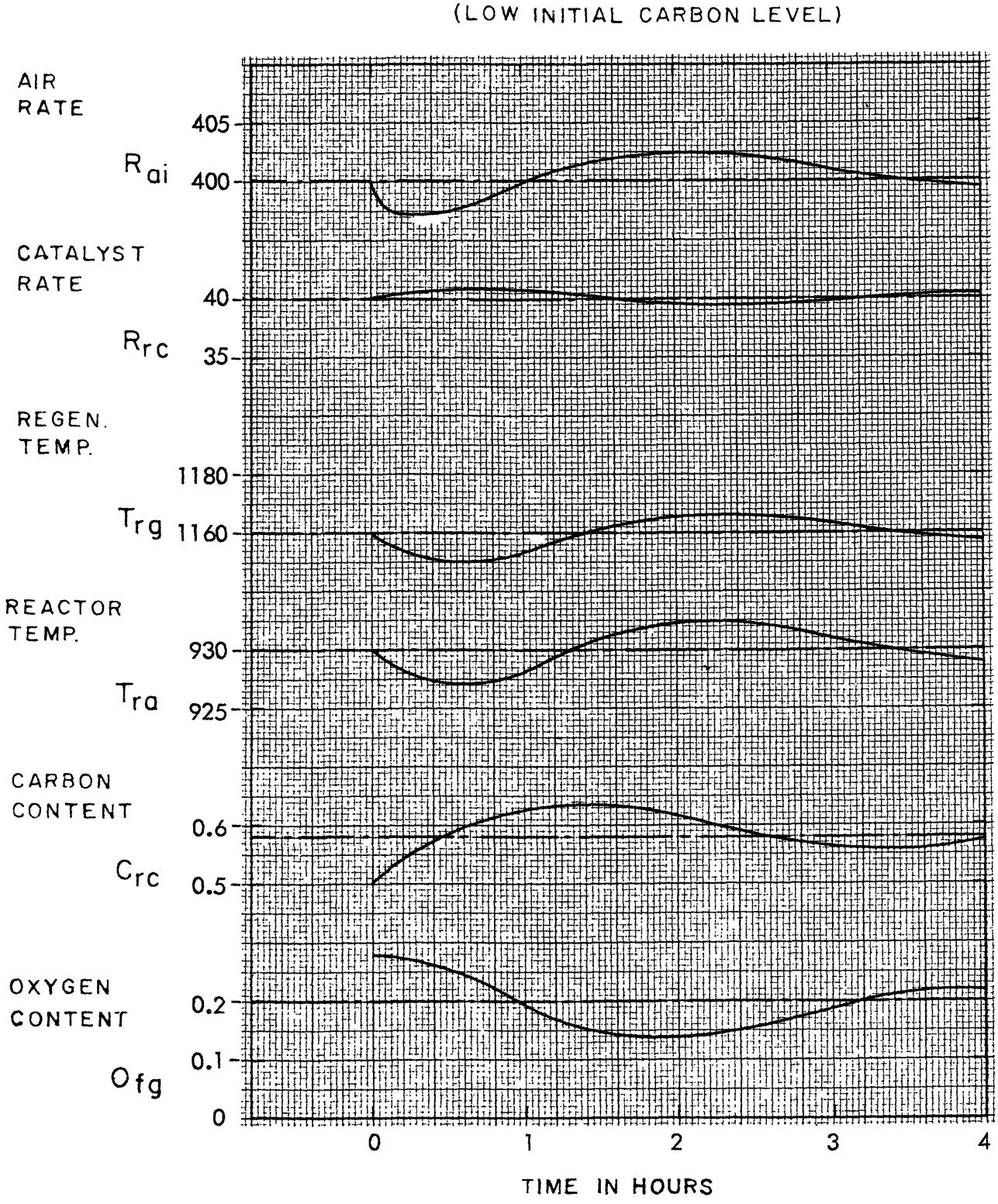

Fig. 4.3 Conventional Control Scheme for Initial Condition No. 2

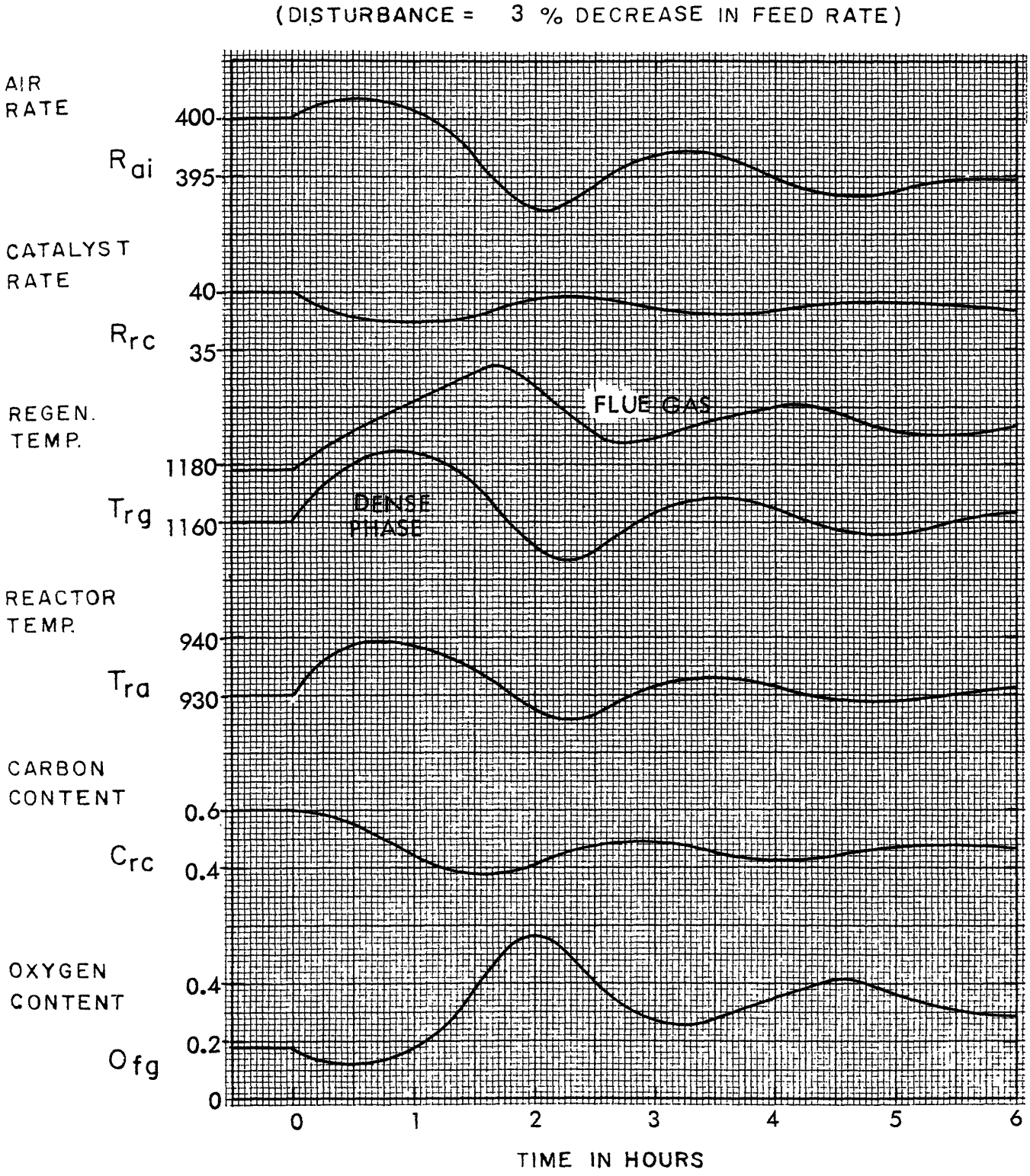

Fig. 4.4 Performances of Conventional Control Scheme (No. 1)

4. Because of the high regenerator temperature and the high air rate, carbon level tends to decrease, and hence the oxygen level starts to increase and so on.

5. The increased oxygen level reduces the air rate by means of the controller, and the regenerator temperature starts to decrease; hence, the carbon level starts to level off.

The resultant final steady-state condition is as follows:

1. The reactor temperature and the oxygen level are unchanged because of the essential role of this control scheme.

2. The air rate is significantly reduced because of the reduced heat requirement.

3. The catalyst rate is slightly reduced, and the resultant decrease in the carbon forming rate corresponds to the decreased carbon burning rate.

The principal phenomena during the transient are summarized as follows:

1. Variations in the regenerator and flue gas temperatures are extremely high.

2. The period of oscillation is relatively long (order of three hours).

3. The damping ratio is relatively small; in other words, the degree of stability is small.

Tunings of controllers were done in the follwing manner: (1) tuning of PI (proportional plus integral) for the reactor temperature controller while cutting the oxygen controller open, and (2) tuning of PI for the oxygen controller. The tuning was not trivial but required great care, which partly reflects the practical limitation of this control scheme. This is typical with interacting control schemes in general.

Figure 1.5 describes the case in which the carbon production is suddenly increased (by a certain probable mechanism such as the feed

composition variations). This dynamic behavior will be explained in the following step by step analysis:

1. The increased carbon production results in the increased carbon content.

2. The increased carbon content results in the decreased oxygen level, which increases the air rate by means of the controller.

3. The increased air rate, together with the increased carbon level, results in the increased regenerator and reactor temperatures.

4. The increased reactor temperature reduces the catalyst rate by means of the controller, and hence accelerates the regenerator temperature to increase.

5. The increased air rate, together with the high regenerator temperature, tends to decrease the carbon level, which, in turn, tends to increase the oxygen level.

6. The increased oxygen level reduces the air rate and so on.

The resultant final steady-state condition is as follows:

1. The reactor temperature and the oxygen level are unchanged because of the essential role of this control scheme.

2. The air rate is almost unchanged because the heat requirement is unchanged.

3. The catalyst rate is slightly reduced, and the resultant decrease in the carbon-forming rate compensates the increased carbon production.

Summary of Performances

Advantages of this conventional control scheme are summarized as follows:

1. This control scheme can compensate for the change in the heat requirement at least for a long-run aspect, as was shown in Fig. 4.4.

2. This control scheme can compensate for the change in the carbon production at least for a long-run aspect, as was shown in Fig. 1.5.

Disadvantages of this control scheme are summarized as follows:

1. This control scheme can not eliminate the relatively large variations in the regenerator temperature and the flue gas temperature. These phenomena are extremely undesirable when the regenerator is operated at an allowable maximum temperature.

2. This control scheme has a relatively small damping ratio or small degree of stability, and the tunings of controllers are not trivial but require great care.

3. The period of oscillation is relatively long, in other words very sluggish as a control system, and the quick recovery from the upset condition can not be expected.

In fact, Hicks, et al. reported that they could not use this scheme satisfactorily for their unit. It is expected that the disadvantages listed above were too serious for them.

4.3 ANALYSIS OF THE CONVENTIONAL CONTROL STRUCTURE

The aim of this section is to analyze the conventional control structure from an information feedback point of view. First, negative feedback loops will be discussed in order to understand the real role of this control scheme. Secondly, positive feedback loops will be discussed in order to understand the real limitation of this scheme.

Negative Feedback Loops

As was claimed by Pohlenz,[57] this conventional control scheme can stabilize the regenerator temperature with respect to changes in

charge stock and operating conditions. From an information feedback point of view, this scheme must have negative feedback loops.

A simplified information feedback structure of this scheme is shown in Fig. 4.5. There are two negative feedback loops, namely A and B. The loop A is just a reactor temperature control loop and will be explained by the following step by step analysis:

1. An increase in the reactor temperature causes the catalyst rate to decrease by means of the controller.

2. The decreased catalyst rate causes the reactor temperature to decrease.

Since the reactor temperature time constant with respect to the catalyst rate is relatively small (e.g., order of one min.), the response time of this loop is relatively short and it will be considered as a short-run negative feedback loop.

Loop B is essentially an oxygen control loop and will be explained by the following step-by-step analysis:

1. An increase in the oxygen level causes the air rate to decrease by means of the controller.

2. The decreased air rate causes the carbon level to increase since the carbon burning rate is decreased.

3. The increased carbon level causes the oxygen level to decrease since the conversion of oxygen is increased.

Since the regenerator carbon time constant with respect to the carbon removal rate (i.e., the time required for the carbon to shift to a two-thirds position of new equilibrium level when the change in the carbon removal rate occurs while the carbon production rate is kept constant.) is relatively large (e.g., order of one hour), the response time of this loop is relatively slow and it will be considered a long-run negative feedback loop. This time constant can be estimated as follows. Adding Eqs. 3.2 and 3.7 with the approximation of Eq. 3.13,

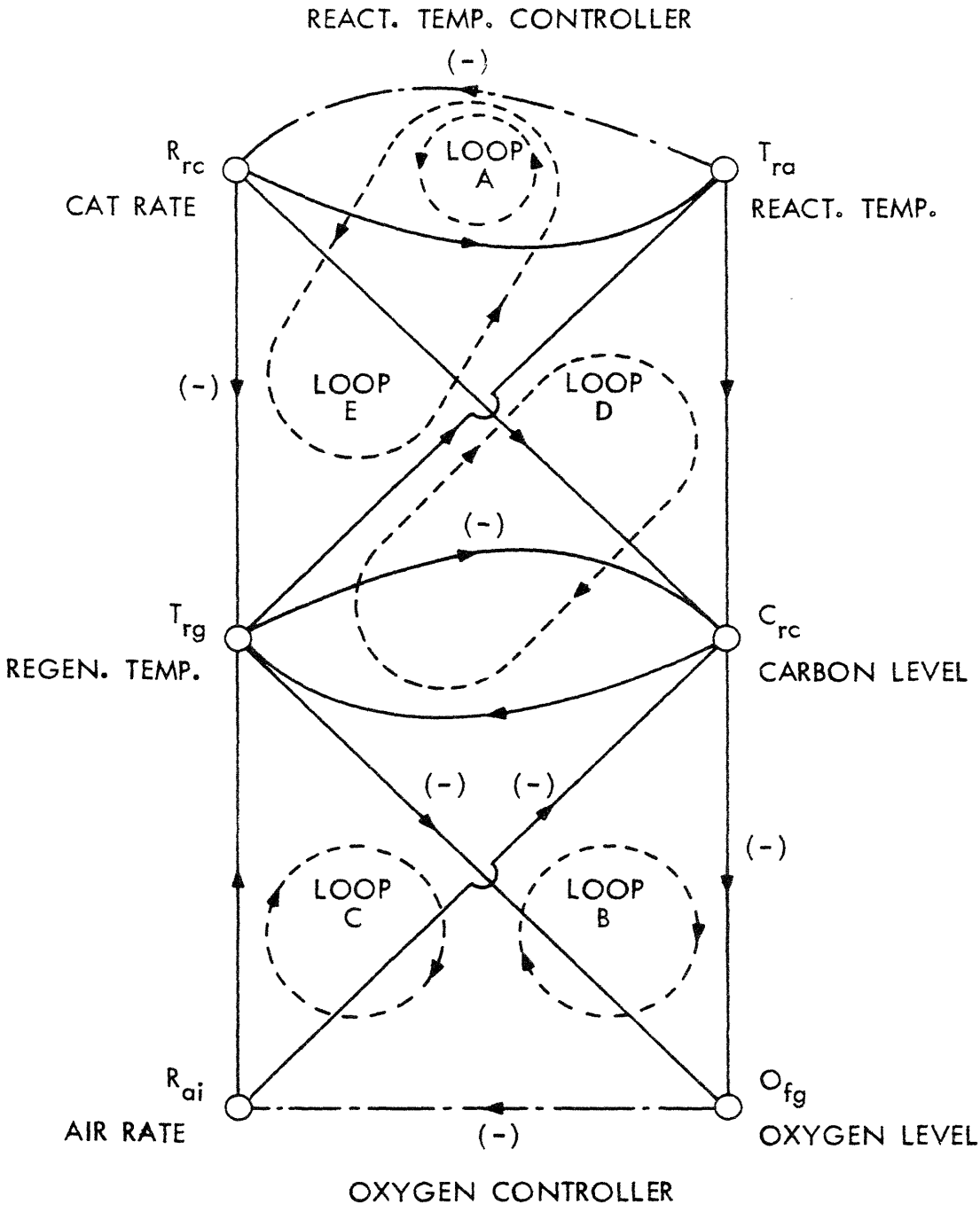

Fig. 4.5 Information Feedback Structure of Conventional Control Scheme

$$H_{ra} dC_{sc}/dt + H_{rg} dC_{rc}/dt = (50)(R_{cf}-R_{cb}) \qquad (4.1)$$

From Eq. 3.2, the time constant for C_{sc} is essentially equal to the reactor holdup divided by the catalyst rate and it is relatively small (e.g., order of one min.). If one neglects the first term of Eq. 4.1, then

$$H_{rg} dC_{rc}/dt \doteq (50)(R_{cf}-R_{cb}) \qquad (4.2)$$

Since R_{cb} is more sensitive to C_{rc} than R_{cf} is, a linearized equation of Eq. 4.2 is

$$H_{rg} dC_{rc}/dt \doteq (50) \frac{\partial R_{cb}}{\partial C_{rc}} (C^s_{rc} - C_{rc}) \qquad (4.3)$$

where C^s_{rc} is a steady-state value. Therefore the time constant for C_{rc} is estimated by

$$H_{rg} \Big/ \left\{ (50) \frac{\partial R_{cb}}{\partial C_{rc}} \right\}$$

Since $\partial R_{cb}/\partial C_{rc}$ is, in general, relatively small, the time constant for C_{rc} is relatively large.

These long-run negative feedback loops are an essential charactdristic of this conventional control scheme, and together with several positive feedback loops which will be described next, this characteristic will prove to be a serious limitation of this scheme.

Positive Feedback Loops

As was shown in the previous section, this conventional control scheme has several disadvantages which are of a dynamically poor nature. From an information feedback point of view, this scheme must have some poor structures. In fact there exist three positive feedback loops, namely C, D. and E in Fig. 4.5.

The loop C is associated with the oxygen control loop, and will be explained by the following step-by-step analysis:

1. An increase in the oxygen level causes the air rate to decrease by means of the controller.

2. The decreased air rate causes the regenerator temperature to decrease because the heat release due to carbon burning is decreased.

3. The decreased regenerator temperature causes the oxygen level to increase because the oxygen conversion is reduced.

Since the regenerator temperature time constant is relatively small (e.g., order of five min.), the response time of this loop is relatively short and it will be considered a short-run positive feedback loop.

Loop D is not directly associated with any control loop; in other words, it is built in the process itself and will be explained by the following step by step analysis:

1. An increase in the carbon level causes the regenerator temperature to increase because the heat release due to carbon burning is increased.

2. The increased regenerator temperature causes the reactor temperature to increase because the differential temperature between two vessels is increased.

3. The increased reactor temperature causes the carbon level to increase because the carbon production due to a high reactor temperature is increased.

Since this loop passes through the carbon level, the response time must be slow and it will be considered a long run positive feedback loop.

Loop E is associated with the reactor temperature control loop, and will be explained by the following step-by-step analysis:

1. An increase in the reactor temperature causes the catalyst rate to decrease by means of the controller.

2. The decreased catalyst rate causes the regenerator temperature to increase because the heat carry-over from the regenerator is reduced.

3. The increased regenerator temperature causes the reactor temperature to increase because the differential temperature between two vessels is increased.

Since the regenerator temperature time constant is relatively small, the response time of this loop is relatively short and it will be considered a short-run positive feedback loop.

Concluding Remarks

It has been described previously that this control scheme has several short-run positive feedback loops. It is not accidental but essential that the control scheme, which shows several dynamic inferiorities (as demonstrated in the previous section), has several positive feedback loops in its structure. (Although it is very difficult to determine which positive feedback loop is the main source of difficulty, it seems that all of them contribute to poor performance.) Therefore one can conclude that, although this control scheme has several important advantages, its dynamic disadvantages can not be eliminated by any improved tuning of controllers.

Also one can note that since this control scheme is not always satisfactory as was the case of Hicks, et al., there is a strong incentive for a better control scheme, not only from a practical point of view but also from a point of view of control engineering and science.

CHAPTER V

DESIGN OF ALTERNATIVE CONTROL SCHEME

An outline of the optimal control study for this hypothetical fluid catalytic cracking unit is shown diagrammatically in Fig. 1.6. First, the mathematical Model No. 1 is reduced to a simpler one (Model No. 2), because the computations for dynamic optimization are more time consuming than those for dynamic simulation. This process of simplification was described before in Section 3.2. Figure 1.6a shows an open-loop optimal control scheme where optimal air rate and catalyst rate will be determined as two functions of time for a given initial condition and for a given objective function. Because of the essential disadvantages of this open-loop structure, which were discussed before, it is desirable to convert this open-loop structure into a closed-loop structure, as shown in Fig. 1.6b. Optimal feedback control laws can be estimated from a set of solutions for dynamic optimization with several initial conditions. Finally, an alternative control scheme will be designed, as shown in Fig. 1.6c, by simplifying the resulting optimal feedback control laws. The performances of this control scheme will be tested by using the original mathematical Model No. 1 with disturbances.

The purpose of this chapter is to design an alternative control scheme, which is (hopefully) better than the conventional one, by an optimal control study. First, dynamic optimization problems will be formulated and solved. Secondly, optimal control laws will be determined with the basic idea of the principle of optimality. Thirdly, an alternative control scheme will be designed by the proposed design approach and its performances will be demonstrated by the use of dynamic simulation. Fourthly, this scheme will be examined from an information feedback point of view.

5.1 DYNAMIC OPTIMIZATION

The purpose of this section is to present the results of dynamic optimization. First, necessary specifications for dynamic optimization will be prepared. Secondly, the solutions for unsteady-state initial conditions will be shown in order to understand their performance and significance.

Preparation for Dynamic Optimization

A formulation of the dynamic optimization problem for FCC was already described in Section 3.2. It is summarized as follows:

1. An objective function is Eq. 3.22.
2. The system equations are Eq. 3.23 and 3.24 or, in an abstract form, Eq. 3.28 and 3.29.
3. Initial conditions for system equations will be specified later.
4. Operating time t_1 in Eq. 2.5 will be specified later.

A formulation for the method of steepest ascent of the Hamiltonian was already described in Section 3.2. It is summarized as follows:

1. A Hamiltonian function is Eq. 3.32.
2. Costate equations are Eqs. 3.33 and 3.34.
3. End conditions for costate equations will be specified later.
4. Gradients of the Hamiltonian function are Eqs. 3.35 and 3.36.

In the study presented in this section, the following specifications were made:

1. Operating time in two hours. The basis for this choice is that operating time must be sufficiently long so that the system can attain an optimal steady-state condition.

2. End conditions for costate equations are zeros.

3. Feed rate is kept constant; in other words, the problem is essentially a dynamic optimization with respect to two control variables, namely air rate and catalyst rate.

4. Control variables are constrained by

$$396 \leq u_1 (= R_{ai}) \leq 400 \text{ (M lbs. per hour)} \qquad (5.1)$$

$$38 \leq u_2 (= R_{rc}) \leq 42 \text{ (tons per min.)} \qquad (5.2)$$

(The basis for these choices is that the convergence of the iterative solution is relatively fast if the control variables are restricted in a narrow range.) Operating conditions are described in Appendix A and B. Other minor specifications regarding the relaxation parameters and penalty functions will be discussed later.

Optimal Solutions for Unsteady-State Initial Conditions

A dynamic optimization of Model No. 2 with an initial condition No. 1, where the initial carbon level is slightly higher than the optimal steady-state level, is shown in Figs. 1.7, 1.8, and 1.9. In Fig. 1.7, solutions for the zeroth and second iterations are plotted with broken lines, and a solution for the eighth iteration is plotted with solid lines, while chain lines show optimal steady-state levels. For the zeroth iteration, R_{ai} and R_{rc} are set to optimal steady-state values, resulting in a very slow recovery of C_{rc} to an optimal steady state. As iterations proceed, R_{ai} and R_{rc} are changed so that the objective function is maximized, resulting in a quick recovery of C_{rc} while avoiding an excessive T_{rg} rise. As shown in the figure, the process approximately reaches the optimal steady-state condition at $t = 1$ (hr.) and starts to deviate at $t = 1.5$ (hr.). The latter phenomenon is essentially the end effect of dynamic

optimization where the final time t_1 is arbitrarily truncated at a certain finite time (two hours for this example) for purposes of computation and should be neglected if the solution is understood to be an approximate solution of dynamic optimization with an infinite (or sufficiently large) final time.

In Fig. 1.8, supplemental data for the costate variables and gradients of the Hamiltonian function with respect to the control variables $u_1(=R_{ai})$ and $u_2(=R_{rc})$ are shown. As iteration proceeds, gradients converge to zeros for $0< t < 2$, indicating that the objective function is almost maximized. Gross profit, which is an integration of the instantaneous gross profit rate for $0 < t < 2$, and relaxation parameters are also plotted against the iteration number. At each iteration, the relaxation parameters were modified, resulting in a quick attainment of maximization. In Fig. 1.9, the solutions finally obtained are plotted together with the corresponding T_{ra} and O_{fg}. Although the high carbon level means, in general, a loss in profit because of its poor selectivity for gasoline, and a high regenerator temperature runaway because of its high heat release unless it is properly controlled, this optimal control solution shows that simultaneous reductions in air rate and catalyst rate avoid the regenerator temperature variation satisfactorily and guide the system to an optimal steady state within a half hour.

Figure 5.1 shows the case (No. 2) where carbon level is slightly lower. Although the low carbon level means, in general, a low regenerator temperature runaway and a high oxygen runaway (because of its low heat release unless it is properly controlled) a simultaneous reduction in air rate and increase in catalyst rate prevents variations in regenerator temperature and restores an optimal condition within a half hour.

Figure 5.2 shows the case (No. 4) in which the regenerator temperature is $20^{\circ}F$ higher than an allowable limit, and an optimal control regulates quickly. Figure 5.3 shows the case (No. 5) in

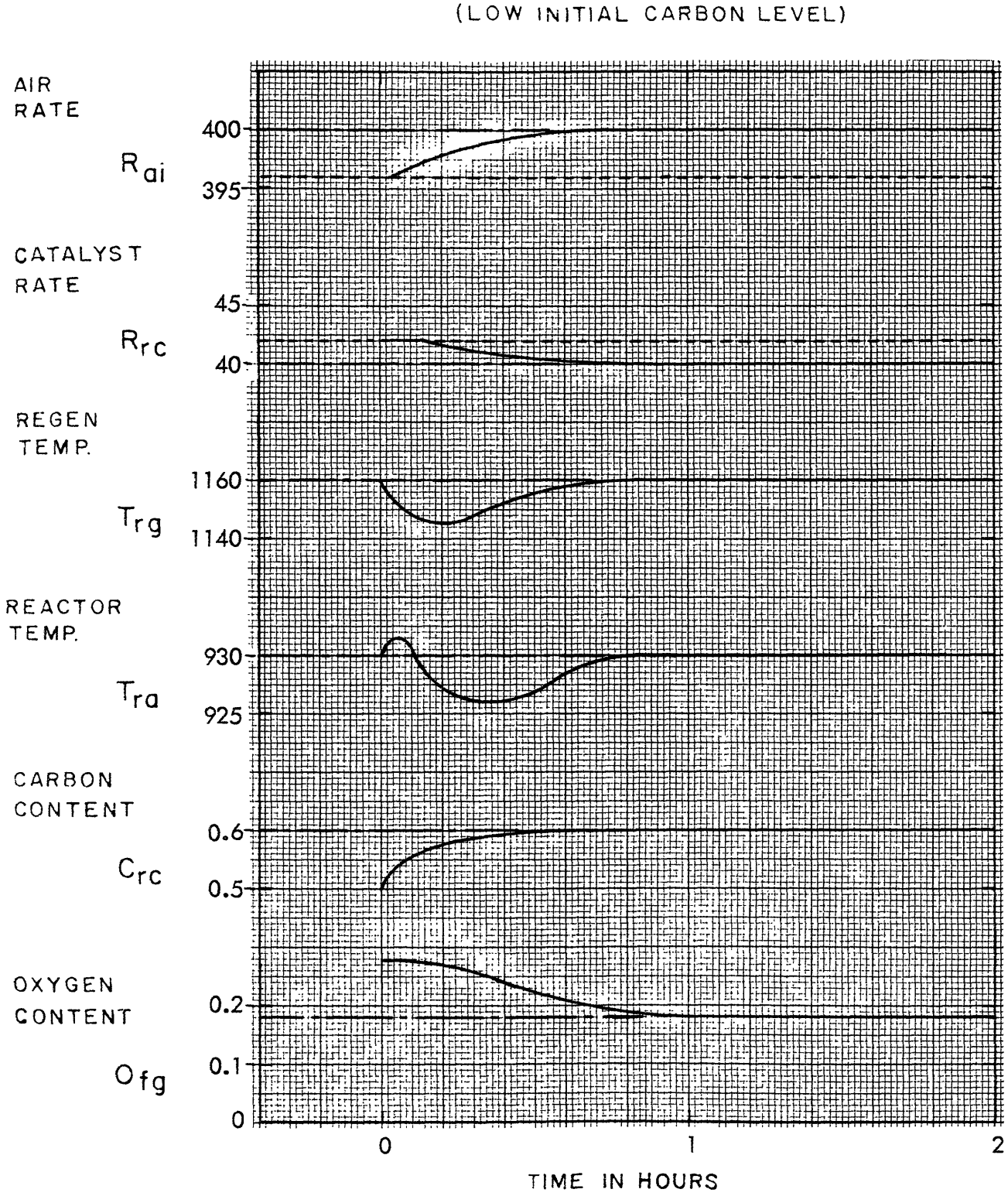

Fig. 5.1 Optimal Control Solution for Initial Condition No. 2

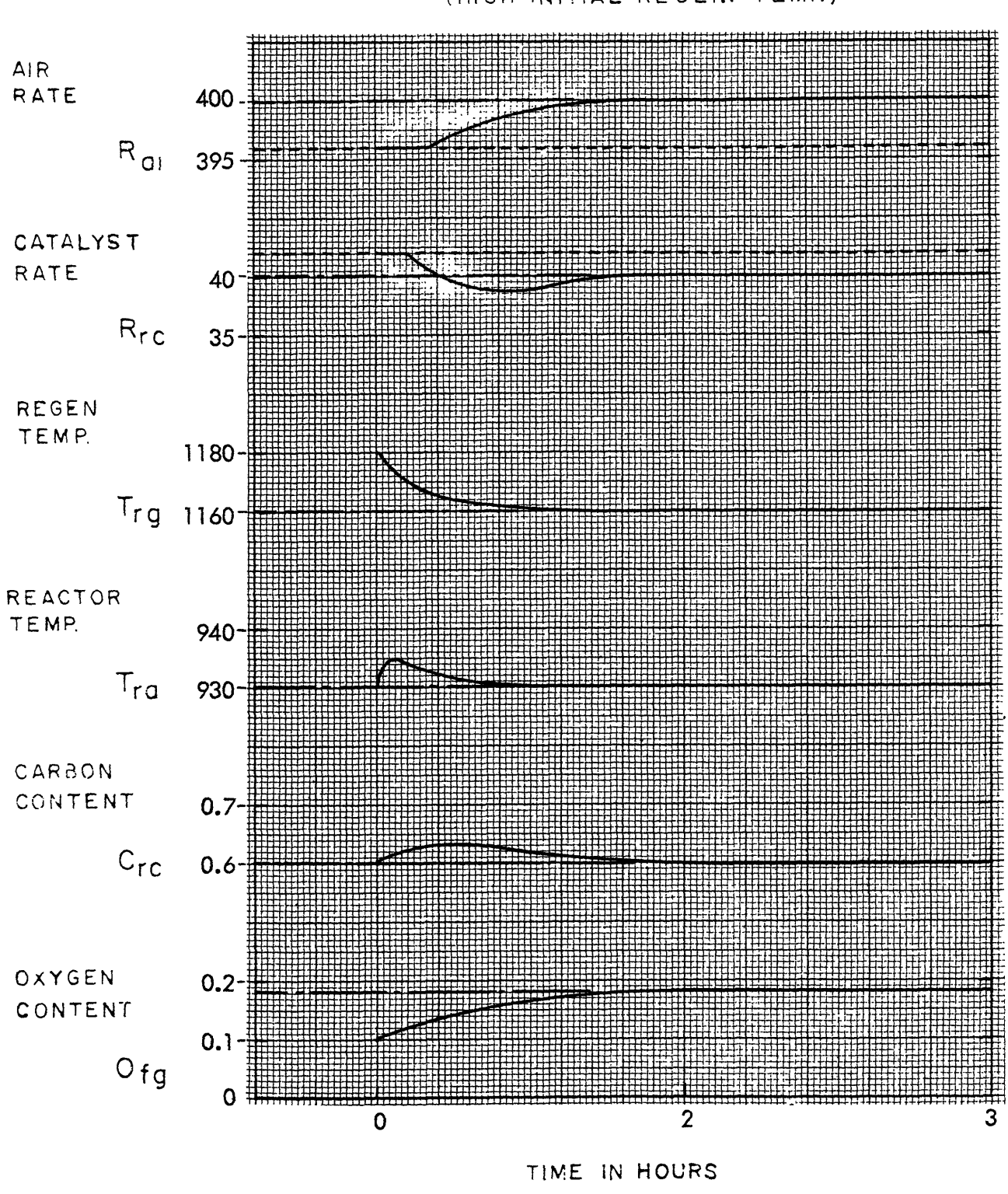

Fig. 5.2 Optimal Control Solution for Initial Condition No. 4

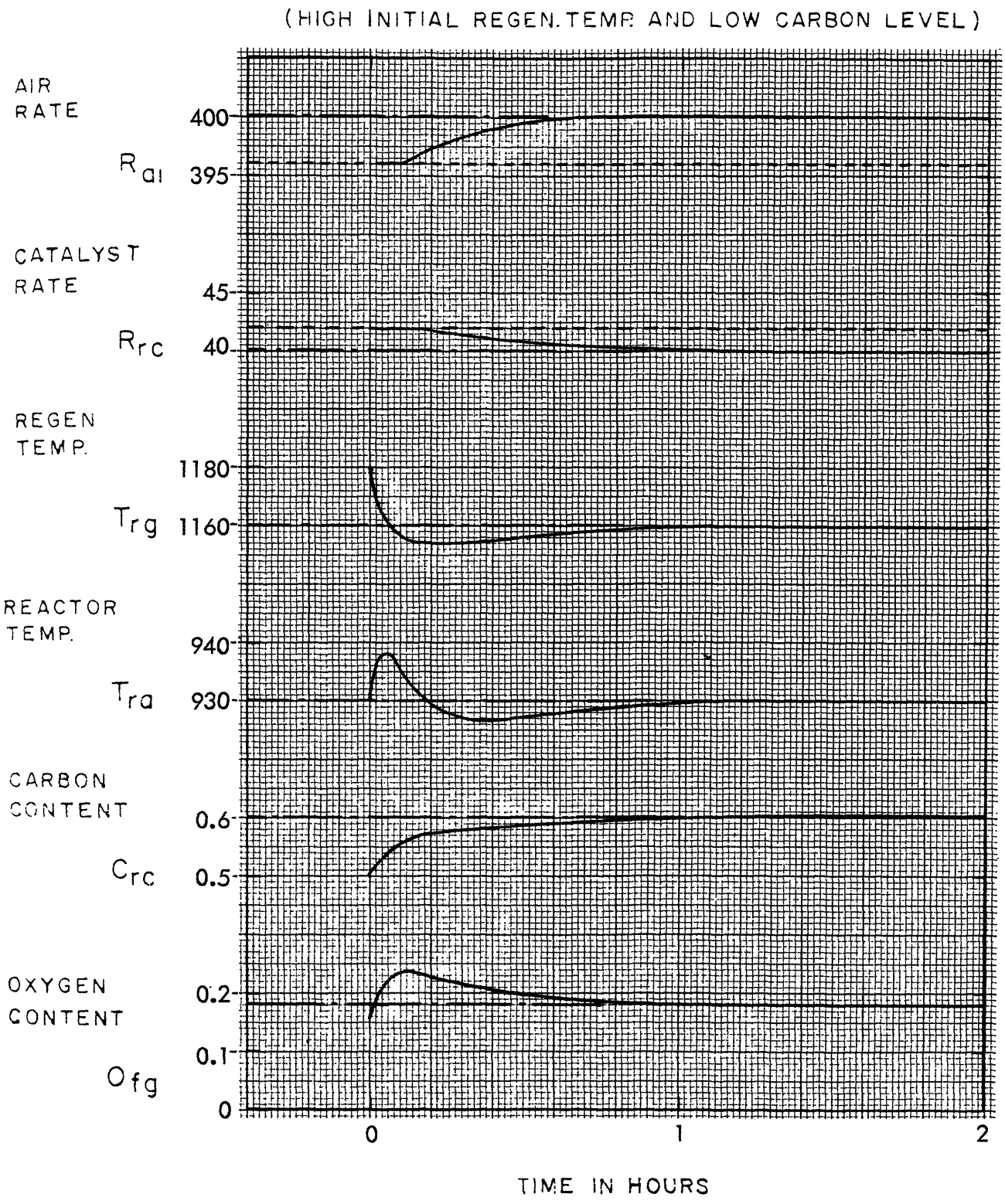

Fig. 5.3 Optimal Control Solution for Initial Condition No. 5

which the regenerator temperature is higher and carbon level is lower. Figure 5.4 shows the case (No. 6) in which the regenerator temperature is lower and carbon level is higher.

Figure 5.5 shows the case (No. 7) where regenerator temperature and carbon levels are lower. This is a very critical condition, since the low regenerator temperature and the low carbon level help each other to cause a low regenerator temperature runaway and a high oxygen runaway unless properly controlled. However, an optimal control regulates quickly.

These excellent performances of the optimal control system point out that the combination of control variables, namely air rate and catalyst rate, is satisfactory in the sense that they are sufficient to prevent any runaway and offset of operating variables at least when the disturbances are in the form of unsteady-state initial condition.

Furthermore it suggests that there is a possibility for an alternative control system that is better than the conventional one.

5.2 DETERMINATION OF OPTIMAL CONTROL LAWS

The purpose of this section is to determine optimal control laws in order to prepare a basis to design an alternative control system. First, phase plane trajectories of optimal control solutions will be analyzed in order to understand the significance of the principle of optimality. Secondly, the structure of an optimal closed-loop control system will be discussed from a theoretical point of view and a practical point of view. Thirdly, optimal control laws will be expressed with the use of contour lines.

Phase Plane Trajectories of Optimal Control Solutions

In order to provide another aspect of optimal control solutions obtained in the previous section, they are plotted in two phase planes, namely (1) regenerator temperature vs. oxygen level and (2) regenerator temperature vs. carbon level in Fig. 1.10. These phase

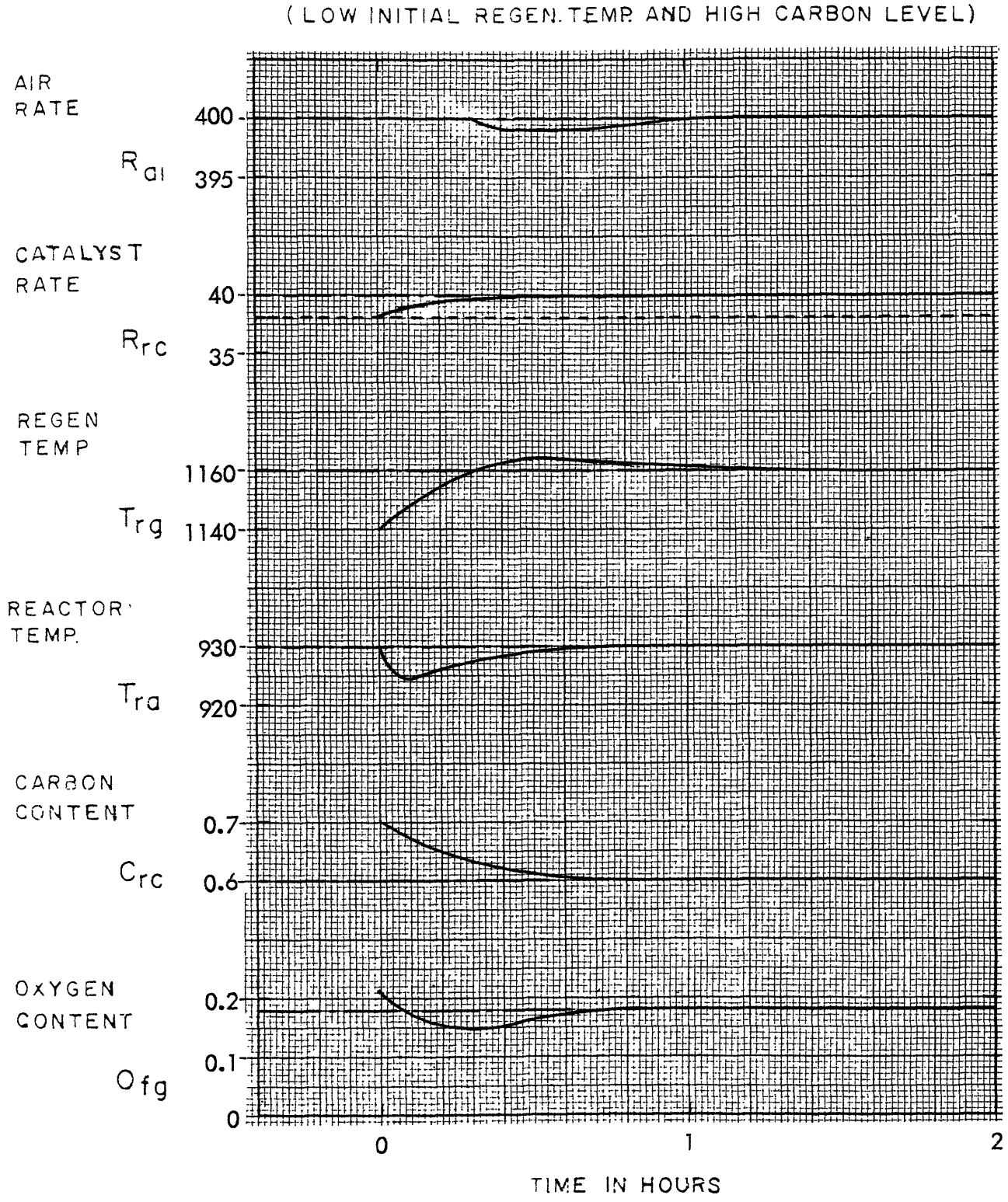

Fig. 5.4 Optimal Control Solution for Initial Condition No. 6

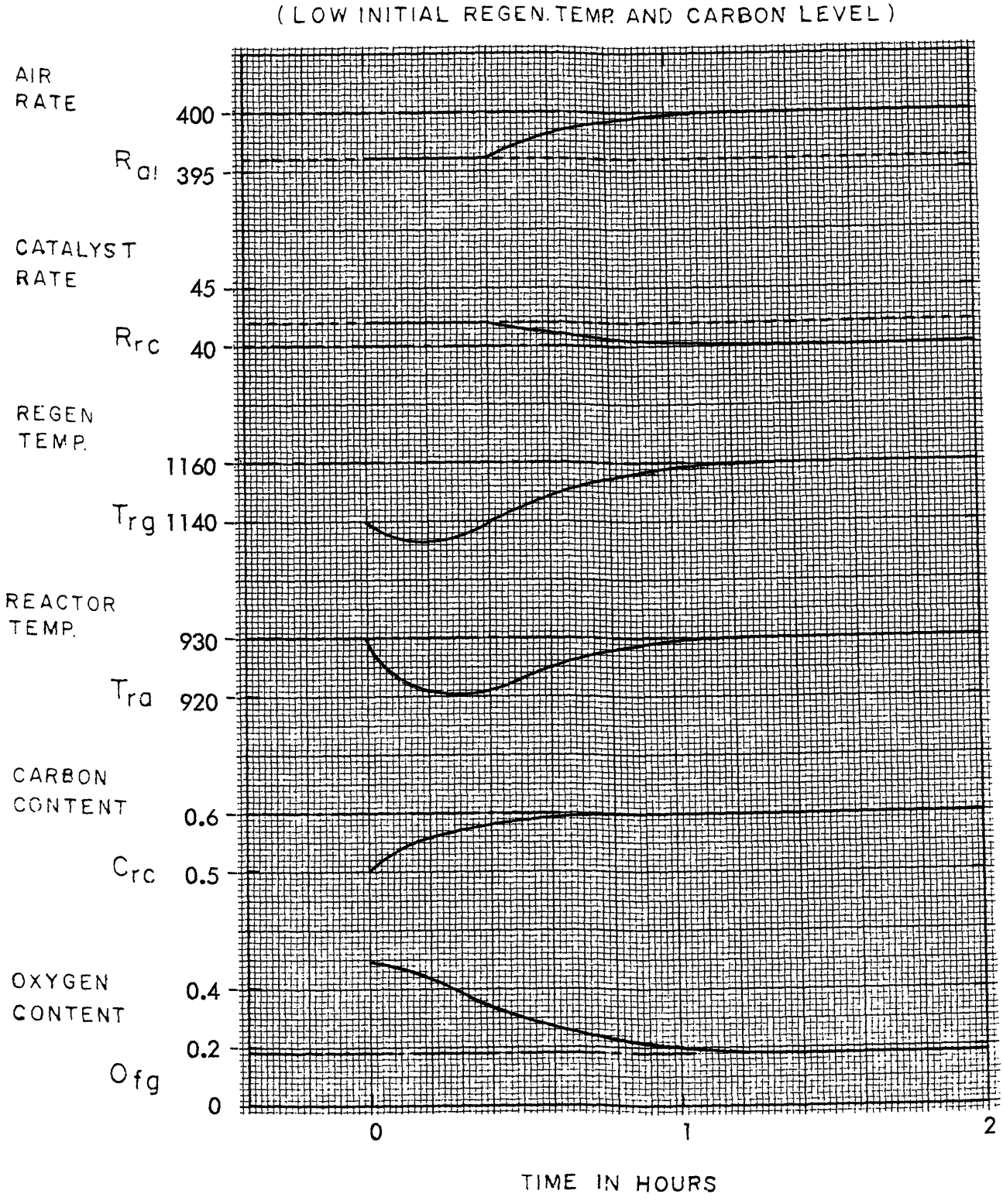

Fig. 5.5 Optimal Control Solution for Initial Condition No. 7

plane trajectories are equivalent in the sense that one trajectory can be transformed into the other. Starting from several initial conditions, they move to an optimal steady state (marked by S in the figure) in an optimal manner. It is significant that a trajectory starting from one initial condition never crosses a trajectory starting from any other initial condition. In other words, an optimal trajectory is unique and depends on only the initial condition. This fact is known as the principle of optimality. This figure shows that initial conditions are selected such that they surround an optimal steady state effectively and it shows that their trajectories cover almost total phase planes.

The Structure of Optimal Closed-Loop Control System

From the principle of optimality, which is discussed in Appendix H, an optimal control law can be expressed by the relation between control variables and state variables. In other words, optimal control variables are unique functions of state variables, namely regenerator temperature and carbon level. Theoretically speaking it is possible to design an optimal closed-loop control system where air rate and catalyst rate are manipulated as functions of regenerator temperature and carbon level. However, practically speaking, there are two limitations to this scheme as follows:

1. Continuous, instantaneous, and accurate measurement of carbon level is far beyond practicality.

2. There is no information feedback from the oxygen level. Therefore, if the system receives disturbances which shift an equilibrium point significantly, there is a possibility of oxygen offset, which can be dangerous.

Fortunately, the oxygen level is a function of carbon level and regenerator temperature; the optimal control law expressed by regenerator temperature and carbon level is equivalent to the one expressed by regenerator temperature and oxygen level. Theoretically

speaking, both schemes are equivalent, but practically speaking, there are two advantages to the latter scheme, as follows:

1. A continuous, instantaneous estimation of oxygen level is practically possible by means of temperature rise due to afterburning.

2. Since there is information feedback from the oxygen level, there is less possibility of oxygen offset than otherwise even if the system is faced with some forced disturbances.

This control scheme is shown in Fig. 1.6b where air rate and catalyst rate are manipulated by the information feedback from regenerator temperature and oxygen level.

Determination of Optimal Feedback Control Laws

Since the objective function and the system equations are highly nonlinear, optimal feedback control laws are expected to be nonlinear functions of two variables. Since they can not be expressed analytically, a three-dimensional diagram or a contour line method is necessary. Figure 1.11 shows contour lines for air rate. Data points come from the results obtained in the previous section. (For example, from Fig. 1.9 this functional relation at $t=0.1$ is $R_{ai} \doteq 396$ at $T_{rg} \doteq 1,165$ and $O_{fg} \doteq 0.14$. Thus one data point (shown by a square) can be plotted in Fig. 1.11.) Although these contour lines are not very accurate because of the noise in the data, they are still satisfactory because they provide a clear picture about the general characteristics of optimal feedback law. For a phase plane of regenerator temperature vs. oxygen level, a mountain is apparently located in the southwest and a sea is located in the northeast. A phase plane for regenerator temperature vs. carbon level is also shown for reference purposes.

Figure 1.12 shows contour lines for catalyst rate. For a phase plane of regenerator temperature vs. oxygen level, a mountain is apparently located in the northeast, and a sea is located in the southwest.

5.3 DYNAMIC SIMULATION OF AN ALTERNATIVE CONTROL SCHEME

The objectives of this section are to design and simulate an alternative control scheme and to show its superiority over the conventional control scheme. First, an alternative control scheme will be determined from the analysis of optimal feedback control structures. Secondly, the performance of this scheme for unsteady-state initial conditions will be demonstrated and it will be compared with the optimal control system and the conventional control scheme. Thirdly, the performance of this scheme for forced disturbances will be demonstrated and it will be compared with the conventional scheme.

The Design of An Alternative Control Scheme

Now we can design an alternative control scheme for this fluid catalytic cracker. We know the optimal feedback control laws at least approximately. All we have to do is to utilize the optimal control study. First, we linearize the optimal control laws around the optimal steady state. This is done directly by measuring slopes around an optimal steady-state point of Figs. 1.11 and 1.12 to give

$$R_{ai} - R^s_{ai} = -1.0(T_{rg} - T^s_{rg}) - 100(O_{fg} - O^s_{fg}) \qquad (5.3)$$

$$R_{rc} - R^s_{rc} = 0.5(T_{rg} - T^s_{rg}) + 50(O_{fg} - O^s_{fg}) \qquad (5.4)$$

where a superscript s represents optimal steady state. Secondly, we investigate the contribution of each term in Eqs. 5.3 and 5.4 to the overall performance of the optimal system by comparing the performance with and without each term. By neglecting the second term on the right side of Eq. 5.3 and the first term on the right side of Eq. 5.4, the control scheme was developed. This is referred to as the "alternative control scheme," and is shown in Fig. 1.13.

Performance for Unsteady-State Initial Conditions

A dynamic simulation of this alternative control scheme, where the initial carbon level is slightly higher than the steady-state level, is shown in Fig. 1.14. If this figure is compared with Fig. 1.9 it will be found that the performance of this scheme is as good as that of an optimal system. If this figure is compared with Fig. 1.4 (note the difference in time scale), it will be found that this scheme has a significant superiority over the conventional control scheme. Figure 5.6 shows the case where the initial carbon level is slightly lower. If this figure is compared with Fig. 5.1 and Fig. 4.3, the same results as in the previous case will be found.

Therefore one can conclude that, as far as the performance for unsteady-state initial conditions is concerned, this alternative control scheme is as desirable as the optimal control system and it has a significant superiority over the conventional control scheme.

Performance for Forced Disturbances

A dynamic simulation of the alternative control scheme, when the feed rate is suddenly reduced, is shown in Fig. 5.7. This dynamic behavior will be explained by the following step by step analysis:

1. The reduced feed rate tends to increase the reactor and regenerator temperatures because of reduced heat requirement.

2. The increased regenerator temperature causes the air rate to decrease by means of the controller, while it causes the oxygen level to decrease because of the higher oxygen conversion, which in turn causes the catalyst rate to decrease by means of the controller.

3. The decreased catalyst rate causes the carbon level to decrease because the carbon production is reduced.

4. The decreased carbon level causes the oxygen level to recover, and the decreased air rate causes the regenerator temperature to recover.

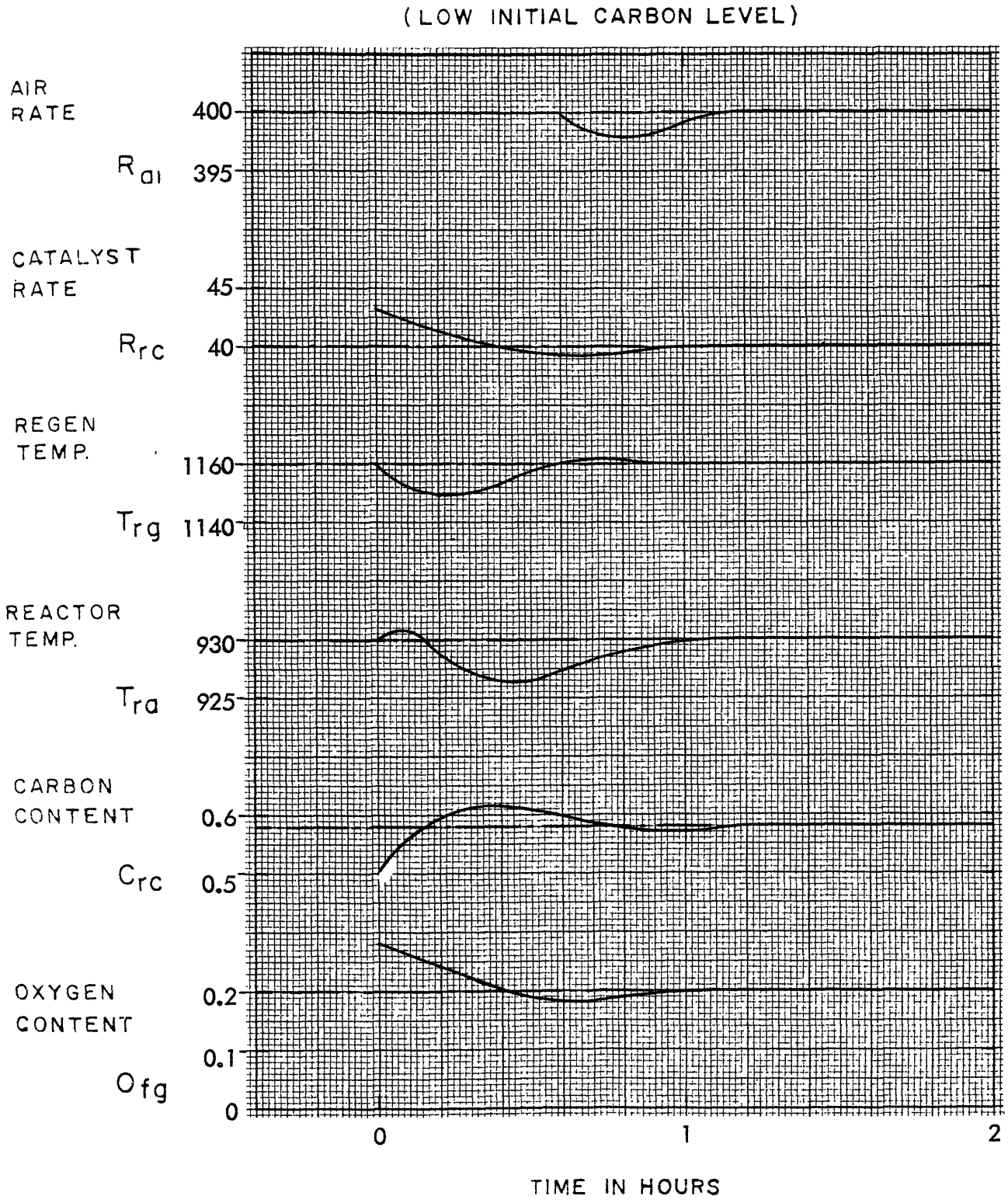

Fig. 5.6 Alternative Control Scheme for Initial Condition No. 2

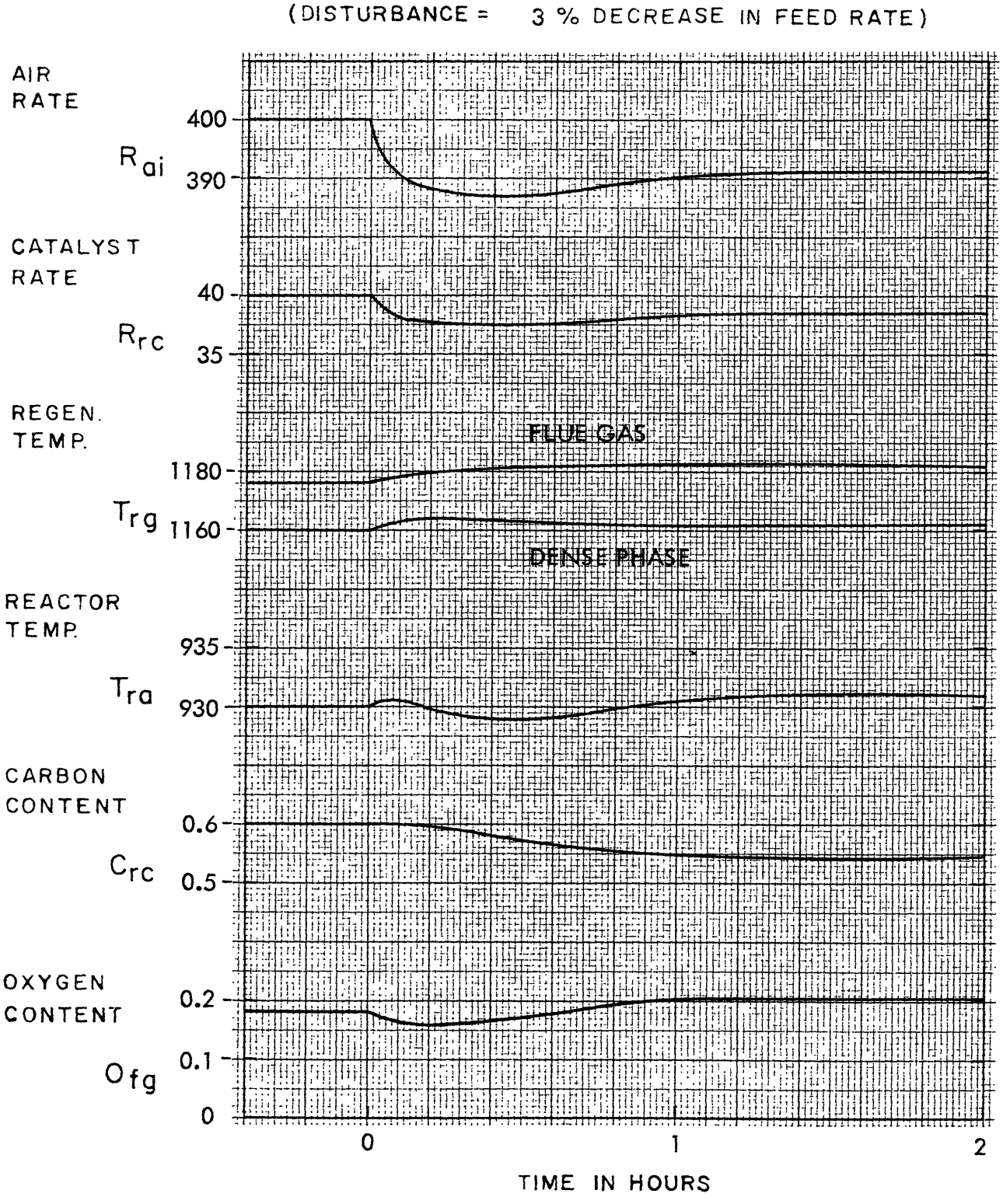

Fig. 5.7 Performances of Alternative Control Scheme (No. 1)

As shown in Fig. 5.7, this system is practically insensitive to this feed rate disturbance. If this figure is compared with Fig. 4.4 (note the difference in time scale) it will be found that this alternative scheme is undoubtedly superior to the conventional one.

Figure 1.15 shows the case where the carbon production is suddenly increased. This dynamic behavior will be explained by the following step-by-step-analysis:

1. The increased carbon production causes the carbon level to increase.

2. The increased carbon level causes the regenerator temperature to increase and simultaneously causes the oxygen level to decrease.

3. The decreased oxygen level causes the catalyst rate to decrease by means of the controller, and simultaneously the increased regenerator temperature causes the air rate to decrease by means of the controller.

4. The decreased catalyst rate compensates for the increased carbon production.

As was shown in Fig. 1.15, this system is practically insensitive to this carbon production disturbance. If this figure is compared with Fig. 1.5, the superiority of this scheme over the conventional one will be reconfirmed.

Figure 5.8 shows the case where the catalyst rate is suddenly decreased. In spite of the blower capacity limitation, which is assumed for the purpose of a conservative test, the performance is fairly satisfactory.

5.4 ANALYSIS OF AN ALTERNATIVE CONTROL STRUCTURE

The objective of this section is to demonstrate the superiority of this alternative control scheme from an information feedback point of view. First, negative feedback loops will be discussed in

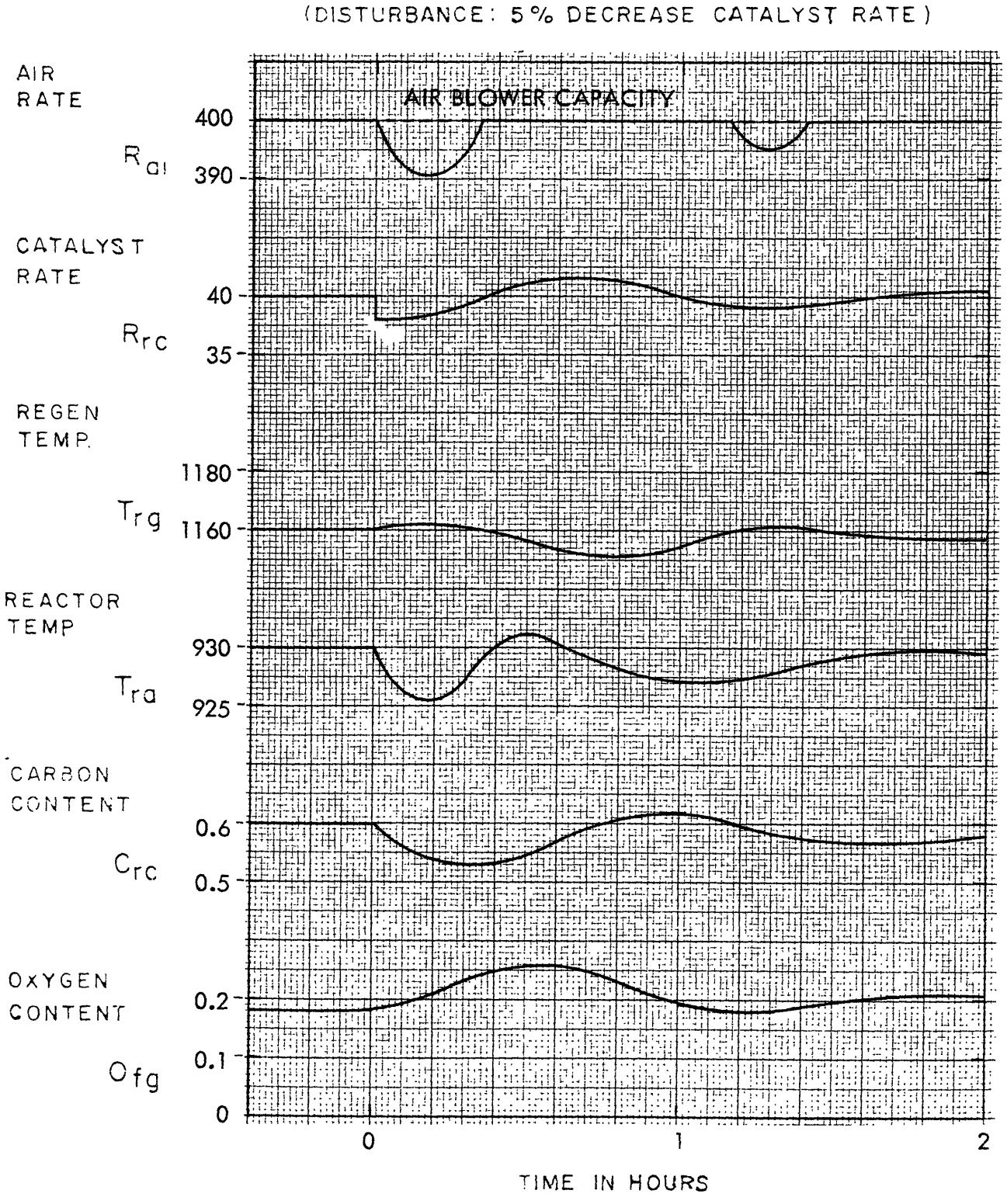

Fig. 5.8 Performances of Alternative Control Scheme (No. 3)

order to understand the real significance of this control scheme. Secondly, positive feedback loops will be discussed and will be shown to have negligible effects on the overall dynamics.

Negative Feedback Loops

As was demonstrated in the previous section, this alternative control scheme is surprisingly stable. From an information feedback point of view, this scheme must have negative feedback loops.

A simplified information feedback structure of this scheme is shown in Fig. 5.9. There are three negative feedback loops, namely A, B, and C. The loop A is just a regenerator temperature control loop and will be explained by the following step by step analysis:

1. An increase in the regenerator temperature causes the air rate to decrease by means of the controller.

2. The decreased air rate causes the regenerator temperature to decrease.

Since the regenerator temperature time constant is relatively small (e.g., order of five min.), the response time of this loop is relatively short and it will be considered as a short-run negative feedback loop.

Loops B and C essentially consist of an oxygen control loop and will be explained by the following step-by-step analysis:

1. An increase in the oxygen level causes the catalyst rate to increase by means of the controller.

2. The increased catalyst rate causes the carbon level to increase because the carbon production is increased, and simultaneously results in the higher reactor temperature which in turn increases the carbon production.

3. The increased carbon level causes the oxygen level to decrease because the conversion of oxygen is increased.

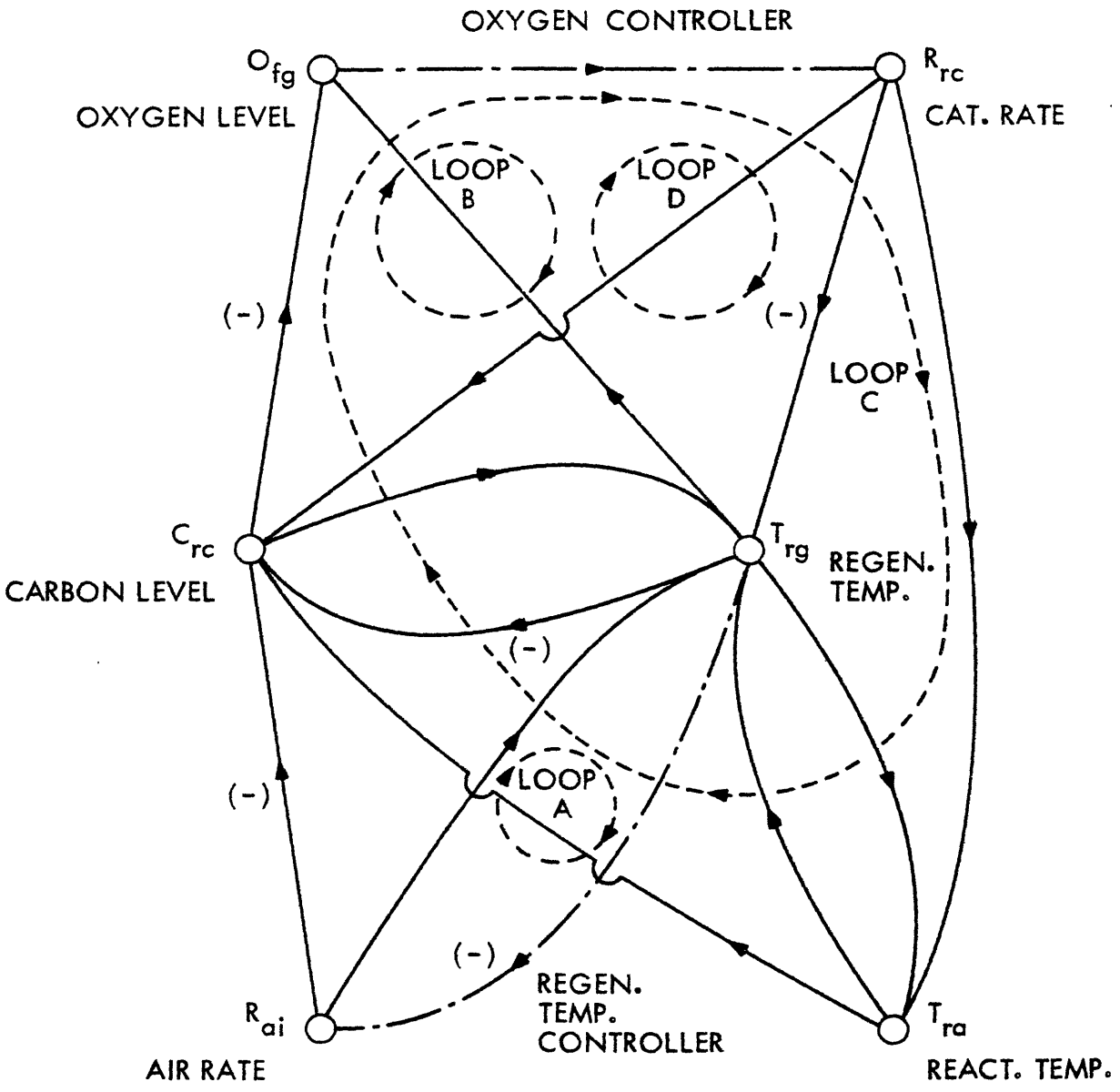

Fig. 5.9 Information Feedback Structure of Alternative Control Scheme

Since the regenerator carbon time constant is relatively high (e.g., order of one hour), the response times of these loops are relatively slow and they will be considered as two long-run negative feedback loops.

Positive Feedback Loops

In Fig. 5.9, there are a few positive feedback loops. The objective of the following discussion is to show that these positive feedback loops are not serious. For example loop D is a positive feedback loop, and will be explained by the following step-by-step analysis.

1. An increase in the oxygen level causes the catalyst rate to increase by means of the controller.

2. The increased catalyst rate causes the regenerator temperature to decrease.

3. The decreased regenerator temperature causes the oxygen level to increase because the conversion of oxygen is decreased.

Since the regenerator temperature time constant is relatively small, this loop will be considered a short-run positive feedback loop. However, since loop A is a short-run negative feedback loop, the regenerator temperature is so stable that the overall effect of loop D is less important than that of loop B and C. The above analysis will become clear if one recalls that a negative feedback loop, in general, works to compensate for a change in any direction, and that therefore, if a negative feedback loop exists in some information flow, then the overall gain of this flow is less than the gain without this negative feedback loop, and that a positive feedback loop is unimportant if its gain is small enough.

Concluding Remarks

The fact that this alternative control scheme, which is an approximate optimal control scheme, has a significant superiority over the conventional one, is partly confirmed by this analysis of information feedback structure. Therefore this optimal control study for the improved control system can be considered satisfactory at least for the problem formulated here.

With this highly satisfactory control scheme with respect to air rate and catalyst rate, it is possible to conduct the research further into adaptive optimizing control schemes, with respect to reactor catalyst holdup, feed preheater temperature and feed rate. This topic will be discussed in Appendix I, together with general concepts for optimal operation of FCC.

CHAPTER VI

DISCUSSION OF RESULTS

6.1 REVIEW OF RESULTS

The objective of this section is to review the main results obtained in Chapters IV and V. The dynamic simulation of the conventional control scheme, the dynamic optimization for unsteady-state initial conditions, and the dynamic simulation of the alternative control scheme will be reviewed in that order.

The computational aspect of dynamic optimization and the control system design aspect of optimal control study will be left for the next section.

Dynamic Simulation of the Conventional Control Scheme

The performance of the conventional control scheme (Fig. 1.3) is demonstrated in Figs. 1.4, 1.5, 4.3 and 4.4 for several forced disturbances and for several unsteady-state initial conditions. The static behavior of this scheme is characterized by:

1. Compensation of the change in the heat requirement.
2. Compensation of the change in the carbon production.

The dynamic behavior of this scheme is characterized by:

1. Extremely high variations in the regenerator and flue gas temperatures.
2. Relatively long periods of oscillation (on the order of three hours).
3. Relatively small damping ratios, in other words, the degree of stability is small.

Dynamic Optimization for Unsteady-State Initial Conditions

Figures 1.9 and 5.1 through 5.5 show solutions of dynamic optimization, for several unsteady-state initial conditions. The dynamic behavior of this optimal system is characterized by:

1. Small variations in the regenerator and flue gas temperatures, and

2. Short response time (on the order of a half hour).

The phase-plane trajectories of optimal control solutions are shown in Fig. 1.10. Optimal control laws are shown by contour lines in Figs. 1.11 and 1.12. The approximate functional relations of these optimal control laws are as follows:

1. The air rate is a decreasing function of regenerator temperature and oxygen level.

2. The catalyst rate is an increasing function of regenerator temperature and oxygen level.

The Dynamic Simulation of the Alternative Control Scheme

The performance of the alternative control scheme (Fig. 1.13) is shown in Figs. 1.14, 1.15, and Figs. 5.6 through 5.8, for several unsteady-state initial conditions and for several forced disturbances. This alternative control scheme is equivalent to a conventional control scheme when a process is in equilibrium--when static conditions prevail. However, its performance is equivalent to that of an optimal control scheme for a dynamic situation--when conditions are changing rapidly.

6.2 DISCUSSION OF RESULTS

The objective of this section is to discuss the computational aspect of dynamic optimization, to discuss the control system design aspect of optimal control study, and to compare the conventional control scheme with the alternative control scheme.

The Computational Aspect of Dynamic Optimization

Numerical solutions of optimal control for unsteady-state initial conditions are demonstrated in Figs. 1.7 through 1.9 and 5.1 through 5.5. The computational aspect will be summarized as follows:

1. The method of steepest ascent of the Hamiltonian was demonstrated to be satisfactory since no dynamic optimization for such a highly nonlinear-multivariable process has been attempted yet.

2. The utilization of penalty functions made it possible to obtain an approximate solution for the dynamic optimization with state variables constrained.

3. The optimal control solutions were relatively insensitive to the total operating period (running time t_1) if it was greater than two hours.

4. The convergence was rapid with respect to the objective function and state variables, but was relatively slow with respect to the control variables, as were recognized by many investigators.[39]

5. The iteration requirement depends on the accuracy needed. For the cases presented, 10 to 20 iterations were necessary.

6. The computing time requirement depends on the number of iterations and on the time step for numerical integration. For the time step of 0.02 hour, one to two min. was necessary with the IBM 7094.

7. The modification algorithm for relaxation parameters, Eq. 2.13, was satisfactory. For the ratio of relaxation parameters, $e_1/e_2 = 10$ was satisfactory.

8. For penalty functions, Eqs. 3.20 and 3.21, $m_1=2$ and $m_2=1$ were satisfactory.

The lack of any other practical and satisfactory computational algorithm makes the steepest ascent method the most pracically important one for the dynamic optimization of complex chemical processes.

This method is therefore recommended for dynamic optimization studies of similar highly nonlinear and multivariable processes.

The Control System Design Aspect of the Optimal Control Study

In phase-plane trajectories (Fig. 1.10) of optimal control solutions, a trajectory starting from any initial condition never crosses a trajectory starting from any other initial condition; in other words, an optimal trajectory is unique and depends only on initial conditions. This is a direct consequence of the principle of optimality.

As shown in Figs. 1.11 and 1.12, optimal control laws are unique functions of state variables. For the problems considered in the study, this is also a direct consequence of the principle of optimality.

An alternative control scheme has been designed as follows: approximate systematically the exact optimal control laws as simply as possible, while testing the satisfactory performance by the use of dynamic simulation of this approximate optimal control system. This design algorithm has the following significant advantages over conventional trial and error methods:

1. This design algorithm is systematic (although not completely scientific) at least when the optimal control laws are to be expanded in a Taylor series.

2. The solution of this design algorithm always exists, at least theoretically, since an exact approximation corresponds to an optimal control law itself, while the conventional trial and error method can not tell whether a solution exists or not at least until a solution is obtained.

3. This design approach provides information to evaluate the desirability of each step of approximation because the ultimate performance due to optimal control is known. The conventional trial and error method, however, cannot evaluate the desirability of each trial, since the ultimate performance is unknown.

Because of the lack of any other scientific and practical design method for highly nonlinear multivariable chemical process control, this design approach is very significant from both a scientific and an engineering point of view.

The Conventional Control Scheme vs. the Alternative Control Scheme

The performance of both the conventional control scheme and the alternative control scheme is described in Sections 4.2 and 5.3, respectively. The structures of these control schemes, from an information feedback point of view, are analyzed in Sections 4.3 and 5.4 respectively.

The alternative scheme is superior to the conventional scheme for the following reasons:

1. The variations for regenerator temperatures and flue gas temperatures are significantly smaller in the former than in the latter. This allows the former to operate at almost maximum regenerator or flue gas temperatures which the safety of a regenerator limits.

2. The damping ratio or the degree of stability is significantly higher in the former than in the latter. This means that the controller tuning is relatively easy for the former and is not trivial but requires great care for the latter.

3. The period of oscillation is significantly shorter in the former than in the latter.

In other words, as a control system the former responds and recovers quickly, while the latter is sluggish and the quick recovery from the upset condition can not be expected.

These dynamic superiorities were confirmed from an information feedback point of view. The latter is inevitably associated with several positive feedback loops the effect of which can not be overlooked. Therefore the poor performance of the conventional control scheme is due to several positive feedback loops which are inevitably associated with the scheme.

CHAPTER VII

CONCLUSIONS

In the course of this work, the following conclusions were drawn.

1. A new approach to the design of a control system for nonlinear multivariable processes was developed in the course of this work. The method was demonstrated for the design of a control system for a hypothetical fluid catalytic cracking unit and resulted in an entirely different control scheme from the one that is typically used in refinery operations. The performance of the new control scheme was demonstrated by dynamic simulation to be significantly better than the conventional system.

2. The new design approach was found to have significant advantages over conventional trial and error methods, because it is systematic, and because it provides information to evaluate the desirability of each design step since the ultimate performance of the system is known from the optimal control theory. With the conventional trial and error method, it is not possible to evaluate the desirability of each trial efficiently, since the ultimate performance is unknown.

3. The method of steepest ascent of the Hamiltonian, with the utilization of penalty functions, was demonstrated to be satisfactory as a computing algorithm for the dynamic optimization of the fluid catalytic cracking unit considered in this study. This method is therefore recommended for dynamic optimization studies of similar highly nonlinear and multivariable processes.

4. Signal flow graphs for the conventional control scheme and the alternative control scheme of fluid catalytic cracking processes were developed, and the dynamic behavior of these control schemes was

analyzed from an information feedback point of view. This analysis gave insight into reasons why the alternative control scheme was significantly better than the conventional one.

5. Several control schemes, which are different from the conventional control scheme, were also simulated and compared with analog computer simulation studies by others.[33] On the basis of this comparison, it was concluded that, although there are various kinds of fluid catalytic cracking processes, the characteristics of their dynamic behavior are quite similar.

APPENDIX A

REACTOR KINETIC MODELS

The purpose of this appendix is to introduce Blanding's catalytic cracking models and Voorhies catalytic carbon forming models, and to unify them into a consistent set of models which can describe the effects of most operating variables satisfactorily for simulation purposes.

Limiting Step in Reaction

The purpose of the following discussion is to show that, in catalytic cracking, mass transfer and diffusion flow transfer are factors of a secondary nature and that reaction kinetics can be approximated as a function of the reactant partial pressure.

Four important processes can be visualized as occurring in any catalytic cracking reaction:

1. Mass transfer of reactants to and from the exterior surface of praticles and the main body of fluid.
2. Diffusion of reactants and products into and out of the pore structure of the catalyst particle.
3. Activated adsorption of reactants and desorption of products.
4. Surface reaction of adsorbed reactants.

If the first process were important, the velocity of flow in the catalyst bed would be critical. Blanding[10] showed that a fivefold variation in velocity made no important difference in the extent of reaction. For reactions in which processes 1 and 2 are controlling, the effect of temperature is generally very small and is present only in so far as the kinetic motion of the reactant molecules is influenced by temperature. Actually, temperature has a pronounced effect on the catalytic cracking reaction.

Particle size exerts a strong effect on reaction rate, when processes 1 and 2 are controlling. Blanding,[10] with considerable experience in the fluid process, has observed no important difference in cracking rates for particles varying from 10 to 100 microns in diameter. Therefore it seems probable that mass transfer and diffusion flow transfer are factors of a secondary nature, and that processes 3 and 4, involving activated adsorption and/or the surface reaction, are controlling. The reaction kinetics can be approximated to be proportional to some power of the reactant partial pressure, since this treatment could be consistent with either of these latter two mechanisms.

Blanding's Catalytic Cracking Models

The purpose of the following discussion is to show that Blanding's models were successfully developed for a pilot plant, and that these models can be utilized for a full-scale plant at least as a basis.

The considerations discussed in the foregoing section suggest that it should be possible to develop a relatively simple expression for characterizing catalytic cracking reaction. Let

A = species reacting.

W_c = weight of catalyst

n_a = number of moles of A present

n_{ao} = original number of moles of A

n_p = number of moles of products

k_1 = constant (also k_2, k_3, m, etc.)

N = total moles of material present, $n_a + n_p$

n_{ac} = number of moles of n_a on catalyst in reactive situation

P_{ra} = reactor pressure

θ_o = residence time of feed gas

f = fraction of A converted; C = 100f = % conversion

Adopting steady-state and plug-flow assumptions for feed gas, consider, first, the general expression for the rate of the reaction of n_a

$$- \frac{dn_a}{d\theta_o} = k_1 n_a \tag{A.1}$$

Equation A.1 is for a first-order reaction which, past experience indicates, might be applicable to a cracking reaction.

For cracking in the presence of a catalyst, Eq. A.1 will not apply, because only the material on or adjacent to the surface influences the reaction rate. For this case, consider that

$$- \frac{dn_a}{d\theta_o} = k_1 (n_{ac}) \tag{A.2}$$

The amount of material on the catalyst in a reactive situation can be assumed to be an adsorbed layer, as

$$n_{ac} = k_2 W_c \left[\frac{n_a P_{ra}}{N}\right]^m \tag{A.3}$$

In this expression it is assumed that the amount adsorbed will be proportional to some power of the partial pressure of the reactant surrounding the catalyst as well as the amount of catalyst present. Substituting Eq. A.3 into Eq. A.2

$$- \frac{dn_a}{d\theta_o} = k_3 W_c \left[\frac{n_a P_{ra}}{N}\right]^m \tag{A.4}$$

It has also been noted from a number of catalytic cracking experiments that the relative number of moles produced per mole of

reactant increases considerably as the reaction proceeds, owing to secondary reactions. According to Blanding,[10] data indicates that, very roughly, for the cracking of a light East Texas gas oil,

$$\frac{n_a}{N} = k_4 \left[\frac{n_a}{n_{ao}}\right]^2 \tag{A.5}$$

Thus, Eq. A.4 might be written

$$- \frac{dn_a}{d\theta_o} = k_5 \left[\frac{n_a}{n_{ao}}\right]^{2m} P_{ra}^m \, W_c \tag{A.6}$$

According to Blanding,[10] pilot plant data, on the average, indicates that

$$- \frac{dn_a}{d\theta_o} = k_6 \left[\frac{n_a}{n_{ao}}\right]^2 \tag{A.7}$$

This suggests that exponent m in Eq. A.6 is approximately equal to 1. Thus

$$- \frac{dn_a}{d\theta_o} = k_5 P_{ra} \, W_c \, \frac{n_a}{n_{ao}}^2 \tag{A.8}$$

Upon integrating for a total bed, substituting 1-f for n_a/n_{ao}

$$\frac{k_5 \, P_{ra} \, W_c \, \theta_o}{n_{ao}} = \frac{f}{1-f} \tag{A.9}$$

It is common practice to express f in terms of percent conversion, C. Also in a catalytic reaction, a residence time of oil vapor is expressed by

$$\theta_o = \frac{k_7 n_{ao}}{R_{tf}/H_{ra}} \tag{A.10}$$

where R_{tf} is a total feed rate and H_{ra} is a reactor catalyst holdup.

Thus, as a final expression, Blanding obtained

$$\frac{K_{cr}P_{ra}}{R_{tf}/H_{ra}} = \frac{C}{100-C} \qquad (A.11)$$

where K_{cr} = cracking velocity constant.

This formula applies to a bed in which the reactants are proceeding through the catalyst bed in "piston flow."

The above expression and the foregoing derivation, together with confirmation of Blanding's results, suggest that the reaction is indeed approximately first order but that in the constant pressure system considered the reactant becomes increasingly diluted with cracked products, thus diminishing the extent of reaction. Thus in effect the apparent order in terms of feed stock processed approaches 2. Actually Eq. A.5 represents a very rough approximation; most feed stocks examined show exponents ranging from 1.6 to 1.9 in the conversion range of practical interest (30 to 80% conversion). However, although the dilution due to increasing moles of reactant might not be sufficient to increase the apparent order to the level of 2, petroleum fractions consist of a large variety of individual hydrocarbons which vary in their relative refractoriness. It might be expected therefore that compounds easiest to crack would crack first, leaving a residue of reactants which becomes increasingly harder to crack. This additional factor also tends to increase the apparent order above 1.

The velocity constant K_{cr} of Eq. A.11 is expected to be a function of the degree of catalyst fouling, which in turn depends on operating variables. Therefore the determination of K_{cr} is postponed until the carbon-forming kinetics are discussed.

Voorhies' Catalytic Carbon Forming Models

The objective of the following discussion is to show that Voorhies models are successfully developed for the catalyst which is

fresh or which activity is completely restored after regenerating to a low residual carbon content, and that they provide basic models for the equilibrium (or reduced activity) catalyst.

The carbonaceous deposit that is an inevitable by-product of catalytic cracking is called "coke," and is generally measured as a percentage by weight of feed or of catalyst. Although the extent of carbon formation in catalytic cracking depends on the type of catalyst, the feed stock, and the operating conditions, it has been found that there is an intrinsic uniformity in the way the amount of carbon deposit on the catalyst increases with time. Certain generalized correlations of striking simplicity and considerable utility have resulted from a study of such data.[74]

There are three types of carbon: catalytic carbon, additive carbon, and strippable carbon. The catalytic carbon is produced in the catalytic reaction. The additive carbon is present in most heavy gas oil and is deposited without catalytic reaction.[3,52] The strippable carbon represents adsorbed and interspersed hydrocarbon gas and liquid remaining with the spent catalyst after the cracking has been accomplished. It is common practice to purge most of the strippable carbon before the catalyst is regenerated. We therefore can assume that the strippable carbon is negligible.[74]

For the catalytic carbon, according to Voorhies,[74] a considerable amount of data shows that the amount of carbon formed on the catalyst is approximately a logarithmic function of the length of time elapsed since the catalyst was freshly regenerated, and that the feed rate has no effect on the extent of carbon formation on the catalyst for a given residence time. Much thought and speculation have been devoted to the question why the amount of carbon deposited on the catalyst for a given residence time should be relatively independent of feed rate. The characteristics of the hydrocarbons in contact with the catalyst are continually changing as the feed stock progresses through the catalyst bed, and also different feed stocks

differ in their carbon-forming tendencies. However, consider what happens as the feed stock passes through the bed of catalyst. It is converted to an increasing extent into (a) gasoline and gas, which have less tendency to carbonize than the original feed, and (b) cycle gas oil, which has more tendency to carbonize than the original feed. To the degree that these two tendencies balance each other, the extent of carbon formation on the catalyst will not differ at any level in the catalyst bed at any given time: this means that the amount of carbon deposited on the catalyst is independent of feed rate within limits.[74]

For a given catalyst, feed stock, temperature, and pressure, Voorhies found experimentally that

$$C_{cat} = A \cdot \theta_c^n \qquad (A.12)$$

where

C_{cat} = catalytic carbon yield on catalyst

A = constant

θ_c = catalyst residence time

n = exponent (0.38-0.53)

Since the rate of carbonization drops off as the percentage of carbon on the catalyst increases, Voorhies postulated that the coke itself is the diffusion barrier, and found that if it is assumed the rate of diffusion is inversely proportional to the amount of carbon, then the power of catalyst residence time is 0.5 which suggests a good concordance with the experimental results.

However, the above hypothesis of Voorhies has several essential discrepancies:

1. The large specific surfaces of cracking catalysts require an extremely large coke deposition to form a monomolecular layer.

2. As described in the section of "Limiting Step in Reaction," the catalytic cracking, which is significantly influenced by carbon production, is not controlled by the pore diffusion.

3. Voorhies found that the carbon formation doubles with an increase in cracking temperature of approximately 190-200°F and this effect of temperature is so strong that the diffusion is unlikely to be controlling.

However, since the catalytic carbon formation depends on the conditions of catalytic active sites (e.g., activity distribution) the models of Voorhies turn out to be meaningful and useful, if we postulate that an apparent (or averaged) activity of catalyst is inversely proportional to the catalytic carbon content of catalyst.

Derivation of Unified Reactor Kinetic Models

The objective of the following discussion is to unify Blanding's catalytic cracking models and catalytic carbon forming models, and to determine the effects of temperature, pressure, and residual carbon on their kinetics.

In commercial plants, it is known that the residual carbon content of catalysts, which was left unburned in the regenerator and is present in the reactor, has significant effect on the selectivity between the catalytic cracking and the carbon formation. Assuming the catalytic carbon formation is (1) inversely proportional to the catalytic carbon content (as assumed by Voorhies), (2) inversely proportional to the residual carbon content (raised to some power n), and (3) directly proportional to the pressure (as Blanding assumed for catalytic cracking), a catalytic carbon forming rate is expressed by:

$$R_{cc} = K_{cc} P_{ra} H_{ra} \qquad (A.13)$$

$$K_{cc} = \frac{k_{cc}}{C_{cat} C_{res}^{n}} \exp\left\{ - \frac{\Delta E_{cc}}{R(T_{ra} + 460)} \right\} \qquad (A.14)$$

where R_{cc} = catalytic carbon forming rate

K_{cc} = velocity constant for catalytic carbon formation

P_{ra} = reactor pressure

H_{ra} = reactor catalyst holdup

C_{cat} = catalytic carbon content of catalyst

C_{res} = residual carbon content of catalyst

ΔE_{cc} = activation energy

k_{cc} and n = constant

If the catalysts in the reactor are uniform, then a steady-state material balance for the catalytic carbon is

$$R_{cc} - R_{rc} C_{cat} = 0 \qquad \text{(A. 15)}$$

where

R_{rc} = catalyst rate

Substituting Eq. A. 13 into Eq. A. 15, and solving for C_{cat}

$$C_{cat} = \left[\frac{k_{cc} P_{ra} \theta_c}{C_{res}^n} \exp \left\{ - \frac{\Delta E_{cc}}{R(T_{ra} + 460)} \right\} \right]^{1/2} \qquad \text{(A. 16)}$$

where $\theta_c = H_{ra}/R_{rc}$ = catalyst residence time

Equation A. 16 can be used to determine the effect of the catalytic carbon on the catalytic cracking as follows. Blanding[10] found that the cracking velocity constant, which is denoted by K_{cr} in Eq. A. 11, is roughly inversely proportional to the 0.5 power of the catalyst residence time. This relationship (see Eq. A. 16) will follow if the catalytic carbon formation, and the catalytic cracking are inversely proportional to the catalytic carbon content. These factors have been noted by Shankland, et. al.[65]

Therefore, assuming the cracking velocity constant is inversely proportional to some power of the residual carbon, the following expression is obtained:

$$K_{cr} = \frac{k_{cr}}{C_{cat}\, C_{res}^{m}} \exp\left\{ - \frac{\Delta E_{cr}}{R(T_{ra} + 460)} \right\} \qquad (A.17)$$

where ΔE_{cr} = activation energy for catalytic cracking

k_{cr} and m = constant

Substituting Eq. A.16 into Eq. A.17

$$K_{cr} = \frac{k_{cr}}{C_{res}^{m}} \left\{ \frac{C_{res}^{n}}{k_{cc} P_{ra} \theta_c} \right\}^{1/2} \exp\left\{ - \frac{(\Delta E_{cr} - \Delta E_{cc}/2)}{R(T_{ra}+460)} \right\} \qquad (A.18)$$

Equation A.18 describes the total effect of temperature on the cracking velocity constant. Blanding[10] reported that

$$\Delta E_{cr} - \Delta E_{cc}/2 \doteq 18,000 \text{ Btu./lb.mole} \qquad (A.19)$$

Furthermore, Eq. A.18 shows that the observed cracking velocity constant is inversely proportional to the 0.5 power of pressure. This fact is also pointed out by Blanding as follows. According to the cracking rate formula, Eq. A.11, the cracking rate is directly proportional to oil partial pressure, and, hence, doubling total pressure should increase the cracking rate in the same proportion as hauling feed rate. However, the above relationship should necessarily apply only instantaneously, and the resultant cumulative effect of pressure in an actual cracking operation should be somewhat different. This would be expected because the cracking rate is higher at higher pressures, and the catalyst should deactivate with time at a greater rate than normal, owing to the greater rate of deposition of carbon resulting from the higher cracking rate. According to Blanding, therefore, actual fluid unit data show that the observed $K_{cr}P_{ra}$ is very closely proportional to the 0.5 power of pressure which is consistent with the above derivation.

Elimination of C_{cat} from Eq. A.14 and A.17 results in

$$K_{cr} = K_{cc} \frac{k_{cr}}{k_{cc} C_{res}^{m-n}} \exp\left\{- \frac{(\Delta E_{cr} - \Delta E_{cc})}{R(T_{ra}+460}\right\} \qquad (A.20)$$

Substituting Eq. A.20 into Eq. A.11, together with Eq. A.13, results in

$$\frac{R_{cc}}{R_{tf}} \frac{k_{cr}}{k_{cc} C_{res}^{m-n}} \exp\left\{- \frac{(\Delta E_{cr} - \Delta E_{cc})}{R(T_{ra}+460)}\right\} = \frac{C}{100-C} \qquad (A.21)$$

Eq. A.21 describes the overall effects of the temperature and the residual carbon on the catalytic carbon yield for a constant conversion level. Oden, et al.[52] reported that, for a commercial plant, these effects are approximately

$$\Delta E_{cr} - \Delta E_{cc} \doteq 9,000 \text{ Btu./lb.mole} \qquad (A.22)$$

and

$$m-n \doteq 0.09 \qquad (A.23)$$

Substituting Eq. A.18 into Eq. A.11

$$\left(\frac{P_{ra} S}{k_{cc}}\right)^{1/2} \frac{k_{cr}}{C_{res}^{m-0.5n}} \exp\left\{- \frac{(\Delta E_{cr} - \Delta E_{cc}/2)}{R(T_{ra}+460)}\right\} = \frac{C}{100-C} \qquad (A.24)$$

where $S = \dfrac{1}{(R_{tf}/H_{ra})^2 \theta_c} = \dfrac{R_{rc}/R_{tf}}{R_{tf}/H_{ra}}$ = cracking severity

Equation A.24 describes the overall effect of the temperature and the residual carbon on conversion for a constant severity. Oden, et al.[52] reported that

$$m - 0.5n \doteqdot 0.12 \tag{A.25}$$

$$\Delta E_{cr} - \Delta E_{cc}/2 \doteqdot 18,000 \text{ Btu./lb.mole}$$

which is surprisingly consistent with Blanding's finding (i.e., Eq. A.19).

Solving Eq. A.19 and A.22 simultaneously

$$\Delta E_{cr} = 27,000 \text{ Btu./lb.mole} \tag{A.26}$$

$$\Delta E_{cc} = 18,000 \text{ Btu./lb.mole} \tag{A.27}$$

Furthermore, the fact that the intrinsic activation energy (i.e., Eq. A.26) is greater than the apparent activation energy (i.e., Eq. A.19) is pointed out by Blanding.[10]

Solving Eq. A.23 and A.25 simultaneously,

$$m = 0.15 \tag{A.28}$$

$$n = 0.06 \tag{A.29}$$

This difference of effects of the residual carbon is explained by the selectivity, which is consistent with the results of Oden, et al.[52]*

Substituting Eq. A.16 into Eq. A.14

$$K_{cc} = \left(\frac{k_{cc}}{P_{ra} \theta_c C_{res}^n} \right)^{1/2} \exp \left\{ - \frac{\Delta E_{cc}/2}{R(T_{ra}+460)} \right\} \tag{A.30}$$

---

* According to H. E. von Rosenberg (Esso Research and Engineering Company, personal communication), the credits for lowering the residual carbon are an improvement in catalyst stability or life and an improvement in the reactor yields. The most important yield improvement is a reduction in carbon yield. This allows an increase in fresh feed or in conversion until the carbon burning limitation of the regenerator is again reached. This fact is consistent with the above derivation.

Eq. A. 30 describes the overall effect of the temperature on the catalytic carbon formation. Voorhies[74] found that, for long period (order of an hour) fixed bed reactors,

$$\Delta E_{cc}/2 = 12,000 \text{ Btu./lb.mole}$$

or

$$\Delta E_{cc} = 24,000 \text{ Btu./lb.mole} \qquad (A.31)$$

The reason for the different results of Eqs. A.27 and A.31 is not clear. However, it may be concluded that the intrinsic activation energy for the catalytic carbon formation is slightly less than that for the catalytic cracking, and that high temperatures result in less carbon yield, which is consistent with the results of Oden, et al.[52]

Final Forms of Kinetic Models

The objective of the following discussion is to summarize the above derivations and to supply a few details useful in completing the models for the simulation study.

The gas oil cracking rate is related to the conversion as follows:

$$R_{oc} = (1.75) D_{ff} R_{ff} C_{ff} \qquad (A.32)$$

where

R_{oc} = gas oil cracking rate

D_{ff} = density of fresh feed

R_{ff} = fresh feed rate

C_{ff} = conversion on fresh feed

(1.75)= (42 gal./bbl.)/(24 hr./day)

The conversion on fresh feed is related to the conversion on total feed as follows:

$$C_{ff} = C_{tf} \frac{R_{tf}}{R_{ff}} = C_{tf} (1+R_r) \qquad (A.33)$$

where C_{tf} = conversion on total feed

R_{tf} = total feed rate

R_r = recycle ratio

Using the relation $100\ C_{tf} = C$, Eq. A.11 is rearranged to

$$C_{tf} = \frac{A}{A+1} \tag{A.34}$$

where $$A = \frac{K_{cr} P_{ra}}{W/H/W_c}$$

Therefore, Eqs. A.32, A.33, A.34, together with Eq. A.17, consist of a complete set of models for the gas oil cracking rate in terms of operating states and variables.

Assuming the strippable carbon production is negligible, the carbon forming rate is expressed by

$$R_{cf} = K_{cc} P_{ra} H_{ra} + F_{tf} R_{tf} \tag{A.35}$$

where R_{cf} = carbon forming rate

F_{tf} = additive carbon forming factor of total feed

Therefore, Eq. A.35, together with Eq. A.14, consists of a complete set of models for the carbon forming rate in terms of operating states and variables.

Estimation of Constants

In the above set of models, the estimation of constants k_{cr}, k_{cc} is necessary to utilize the models for the simulation. These constants are not universally constant but are dependent on the compositions of feeds and the condition of the catalyst. However, since they are not strongly dependent on the operating variables, it can be assumed

that these constants do not vary significantly for the operation of the same unit, and the assumption of their constancy is adequate for the purpose of simulation and control.

The objective of the following discussion is to show a simple method of estimation of constants which are used throughout the study. Assuming that the reactor is operated at a certain probable steady-state condition (e.g., H_{ra} = 60 ton, P_{ra} = 40 psia, T_{ra} = 930°F, R_{tf} = 100,000 bbl./day, R_{rc} = 40 tons/min., C_{ff} = 0.6), together with a certain probable steady-state condition of the regenerator, probable k_{cr} and k_{cc} are determined automatically. Since it is not only difficult but also useless for our purpose of simulation to estimate accurately these constants by purely chemical analysis of feed composition and catalyst condition, the above (a kind of closed-loop) method was used.

APPENDIX B

REGENERATOR KINETIC MODELS

Regeneration of coked or spent catalyst by burning the coke with air is an essential part of the catalytic-cracking process; indeed the capacity of the regenerator for burning the formed coke often limits the rate at which a unit can crack feed. This appendix describes the significance of a regenerator, a literature review of regeneration kinetics, and the construction of models.

Significance of Regenerators

The purpose of the following discussion is to show that a regenerator of FCC is one of the most important parts of FCC from an economic point of view and from a control point of view, and that its models must be constructed with great care in order to utilize them satisfactorily.

There are three main incentives for improving the carbon burning in regenerators. The first is to lower the carbon levels on the catalyst for a given rate of carbon burning and conversion of the oxygen. The low carbon level on the regenerated catalyst would improve the gasoline yield in the reactor for a given conversion level.[52] The second incentive would be to increase the conversion of the oxygen for a given carbon level on the catalyst. This would result in an increase in the total carbon burning rate and so increase the total capacity of a unit, which is usually limited by the regenerator gas velocity or blower capacity. The third incentive is related to the second. By increasing the oxygen conversion, the amount of "afterburning" in the dilute phase could be reduced.

Role of Pore Diffusion

The purpose of the following discussion is to show that the role of pore diffusion in fluidized regenerators is negligible, and that the

pore diffusion mechanism is not necessary to describe the fluidized regenerator kinetics.

The mechanism and kinetics of the burning of carbon from catalysts has not been clearly worked out. It is generally agreed that diffusion rates into the particle, as well as the chemical reaction, play a part. At low temperatures the chemical reaction is controlling, while at high temperatures diffusion is controlling. The various regeneration studies in air at atmospheric pressure indicate that, on a silica-alumina bead catalyst of about 1/8 in. diameter with fine pores (e.g., 50 to 100 Å), diffusion of oxygen begins to become rate limiting at about 900°F (480°C).[76] A clay catalyst with large pores (e.g., half exceeding 2000 Å in diameter) has a higher diffusivity, and oxygen diffusion was not rate limiting even at 1200°F.[16] With the fine particle sizes used in fluidized-bed operations, oxygen diffusion is not rate controlling on silica-alumina or similar catalysts, at least up to 1290°F (700°C).[76]

Carbon on the Catalyst

The purpose of the following discussions is to show that, although the intrinsic kinetics of burning carbon on the catalyst is not completely established yet, one of the most acceptable models for the intrinsic reaction rate would be expected to be first order with respect to carbon and oxygen.

The main complicating features of regeneration are the nature and amount of carbon on the catalyst, its distribution on the surface and within the pores of the catalyst, metal contamination, sintering and catalyst pore size. The intrinsic rate is generally found to be proportional to oxygen concentration, but the nature of the function of the amount of carbon present has varied in different investigations (see Table B.1). The reason for these variations is not clear; in some cases an aging effect may have caused a decrease in carbon activity, or the distribution of carbon atoms on a molecular scale

Table B.1

List of Published Regeneration Kinetics

Literature	Dart et al.[16]	Johnson et al.[35]	Lavrouskii et al.[40]	Aliev et al.[2]	Pansing[56]
Bed Type	Fixed	Fluidized	Fluidized	Fluidized	Fluidized
Bed Size diameter length	 1.25 in. 2 ft.	 2 in. 20 in.		 3 cm. 1 m.	 10 in. 5 ft.
Catalyst Type	Clay Pellet	Clay Si.Al. Si.Mg.	Si.Al.	Si.Al.	
Catalyst Size	4.0-2.4 mm.		100-250 μ 200-500 μ	75 μ	44-79 μ
Superficial velocity, ft./sec.	30-40	0.2		0.16	0.1-0.6
Average O_2, psia.	3.06	0.324-0.676		0.676-3.06	
Initial Carbon Content wt.%	0.83-2.75	0.3		0.6-2.0	
Kinetic Order of Oxygen	1	1	1	1	1
Kinetic Order of Carbon	2	1	1	2	1
Average Temp. °F	850-1200	950-1050		978-1113	965-1075
Activation Energy Btu./lb.mole	47,900	74,000	44,100 55,600	53,000	63,000

into clumps may well have varied in different studies. In studies made in a fixed bed, it is evident that considerable temperature gradients may have occurred axially and radially in the bed which make a precise interpretation of the results impossible.

In an industrial operation with a high-area catalyst, the initial coke concentration will generally be less than about 5 wt. %, which is equivalent to considerably less than a monolayer. If the carbon atoms were indeed all exposed and all equally reactive, the intrinsic reaction rate would be expected to be first order with respect to carbon.[61]

The coke generally contains considerable hydrogen, but the hydrogen is removed in the initial stages of the reaction, leaving a carbon skeleton on the catalyst. Thus the principal reaction of concern is the gasification of carbon. For a given catalyst, there seems to be little variation in the burning rates of coke deposited from different hydrocarbon reactions, although the reaction-velocity constant for carbon deposited from high-sulphur feeds is higher than from low-sulphur feeds.[56] Also a decline in reactivity on aging has been reported.[35] Little difference is found between reactivity of carbon on silica-alumina, silica-magnesia, clay, silica gel, and other cracking catalysts containing no transition metals,[35] although the low-activity catalysts show a higher reaction-velocity constant than does the high-activity catalyst.[56] The presence of chromia in the xerogel, however, increases the burning rate, and other transition metals will presumably also catalyze carbon combustion, as may also some potassium compounds. Most workers report the intrinsic activiation energy for carbon burnoff to be above 63,000 to 66,000 Btu./lb.mole.

Effects of Steam

The purpose of the following discussion is to show that, although the effect of steam gasification reaction can not be overlooked, one of the most acceptable models for the intrinsic carbon burning

reaction rate is still first order with respect to carbon and oxygen, providing that the variation of steam content is negligible.

Contacting Gas and Solid

The purpose of the following discussion is to show that the contacting of gas and solid is a particular phenomenon for fluid process, that it is the most essential factor which governs the efficiency or performance of regenerators, and that it is essential to include this phenomenon in the regenerator model as accurately as possible in order to describe the difference in the performance of different regenerators.

Contacting of the solid with the regenerating gas is, of course, important. Apparently very little work has been done on this effect in fludized regenerators. The analysis of fluidized beds is made complex by the fact that the gas flows through the bed by two paths.[78] One is in the form of gas "bubbles" which have relatively low solid-to-gas ratios and shorter residence time than the average. The other path is through the interstices of the dense phase, which involves a longer residence time and much higher ratios of solids to gas. The linear velocity at which gas flows through the dense phase corresponds approximately to that which produces incipient fluidization. Any excess gas flow goes up as bubbles. Thus the fraction of the total gas flowing in the form of bubbles increases as total gas flow rate is increased above that required for incipient fluidization; but this fraction is also a function of particle size and particle size distribution. As the bubbles rise, they grow by seepage from the surrounding dense phase, the rate of which is likewise a function of particle size and of size distribution. Higher gas velocities or finer catalysts will increase the distance between particles and so the resistance to diffusion from the "bubble" phase to the dense phase will be less. The coefficient of mass transfer has been reported to be a function of some powers of the mass velocity of the gas and the average particle diameter.[56]

Pansing's Regenerator Models

The purpose of the following discussion is to show the successful development of Pansing's regenerator for a pilot plant. Although they are not completely accurate for a full-scale regenerator, they still remain one of the most acceptable models because they embody both the intrinsic regeneraton kinetics and also the gas-solid contacting phenomenon.

During burning of coke, oxygen must be transferred from the air stream to the surface of the catalyst. Burning rate may as well be limited by diffusion from the air stream to the surface as by reaction on the surface. In a fixed bed, the resistance to diffusion occurs in a stagnant film surrounding the individual catalyst particles. In a fluidized bed however, much of the gas passes through the catalyst in the form of pseudobubbles or pockets and relatively little flows through the interstices between the more densely packed particles.[26] Much of the catalyst can receive oxygen only by diffusion or mass transfer of gas from the bubbles. Resistance to mass transfer can be combined with reaction kinetics to develop an equation for the overall rate of reaction.

The concentration of carbon on the catalyst can be considered uniform throughout a fluidized bed, because the rate of catalyst mixing is rapid.[26] The gas flow can be assumed unidirectional, because bypassing or short-circuiting of gas in a fluidized bed is far more pronounded than back mixing.[26] Gas bypassing causes the oxygen concentration to vary across the horizontal cross section of the regenerator, but an average oxygen concentration can be assumed to exist at a given vertical level.

The rate of reaction of carbon is assumed to be first order with respect to the concentration of carbon on the catalyst,[35,40] and partial pressure of oxygen.[2,16,35,40,54] A stoichiometric expression for regeneration is, in general, as follows:

$$\text{Coke (C, H)} + O_2 \rightarrow CO + CO_2 + H_2O$$

where stoichiometric coefficients are not specified. For the stoichiometric ratio of carbon and oxygen, Pohlenz[57] found that it is almost constant with the deviation of the same order as the accuracy of the measurements. He speculates that a catalyst with high hydrogen-producing activity reduced hydrogen content of the coke, but in the oxidized state catalyzes the oxidation of CO to CO_2, thus causing increased ratios of CO_2/CO, and that the stoichiometric ratio is nearly constant, independent of the CO_2/CO ratio. Assuming that carbon and oxygen must react in some stoichiometric ratio, the rate of reaction of oxygen r_r in moles/hr./lb. of catalyst can be expressed as

$$r_r = k_r C_r p_i \tag{B.1}$$

where the proportionality constant relating the rates of carbon and oxygen reactions is contained in k_r, the specific reaction-velocity constant in moles/hr./atm./lb. The term C_r is the fraction of carbon on regenerated catalyst, and p_i is the partial pressure of oxygen in interstices of catalyst in atm. The rate of oxygen transfer depends upon the pressure gradient of the oxygen from the interior of the bubbles to the interstices of the catalyst. Thus r_d, the rate of oxygen diffusion from bubbles to catalyst in moles/hr./lb. of catalyst, can be expressed as

$$r_d = k_d (p - p_i) \tag{B.2}$$

where k_d is the coefficient of mass transfer in moles/hr./atm./lb. and p is the partial pressure of oxygen in bubbles in atm. At steady-state conditions, the overall rate of reaction must equal the rate of oxygen transfer or rate of surface reaction. Thus, after equating Eqs. B.1 and B.2, solving for p_i, and substituting this expression in Eq. B.1, one can express the overall rate of reaction r, in moles/hr./lb. of catalyst, as

$$r = \frac{p}{\frac{1}{k_d} + \frac{1}{k_r C_r}} \tag{B.3}$$

A material balance on oxygen across a differential length of regenerator may be written

$$F\, dN = -r\, dW \tag{B.4}$$

where F is the feed rate of gas in lb./hr., N is the oxygen concentration in the gas in lb. moles/lb. feed, and W is the weight of catalyst in lb. If Eq. B.3 is substituted in Eq. B.4, and the total moles of reactants and products is considered constant, the resulting equation may be integrated from the inlet to the outlet oxygen concentration to give

$$-\frac{W}{F} = \frac{N_t}{P}\left(\frac{1}{k_d} + \frac{1}{k_r C_r}\right) \ell n\ \frac{N}{N_o} \tag{B.5}$$

where N_t is the total moles gas/lb. of feed to the regenerator, P is the total pressure in atm, and N_o is the inlet oxygen concentration in lb.moles/lb. feed. The quantity $F N_t/W$ is defined as the space velocity S and equals the moles of gas fed to the regenerator/hr./lb. of catalyst. The quantity N/N_o is the fraction of inlet oxygen unconverted in the regenerator and is defined as f. If these terms are introduced in Eq. B.5, it may be rearranged to give

$$-\frac{PC_r}{S \ell nf} = \frac{C_r}{k_d} + \frac{1}{k_r} \tag{B.6}$$

Significant variables are thus related in terms of a specific reaction-velocity constant and coefficient of mass transfer.

Equation B.6 could be used to evaluate the specific reaction-velocity constant k_r from regeneration data if values of k_d were

available. Although some data on mass transfer in fluidized beds exist, there are no data on particles in the 0-to 100-μ range. Hence the coefficient of mass transfer can be assumed to be a function of some powers of mass velocity of gas and the average particle diameter. Higher gas velocity or finer catalysts will increase the distance between particles and so the resistance to diffusion will be less. Thus the coefficient of mass transfer k_d may be expressed as

$$k_d = \frac{1}{a} \frac{G^m}{D_p^n} \tag{B.7}$$

where a is a proportionality constant, m and n are unknown exponents, G is the gas mass velocity in the regenerator in lb./hr./sq.ft., and D_p is the average particle diameter in μ. Equation B.7 can be substituted in Eq. B.6 to give

$$-\frac{PC_r}{S\ell nf} = a \frac{C_r D_p^n}{G^m} + \frac{1}{k_r} \tag{B.8}$$

which represents a straight line of slope a and intercepts $1/k_r$ when $-PC_r/(S\ell nf)$ is plotted against $C_r D_p^n/G^m$. Both k_r and a can be evaluated from regeneration data if suitable values of m and n can be obtained.

From extensive pilot plant data, Pansing[56] found that

$$m = 2,\ n = 1.5,\ a = 146$$

or

$$-\frac{PC_r}{S\ell nf} = 146 \frac{C_r D_p^{1.5}}{G^2} + \frac{1}{k_r} \tag{B.9}$$

and that an activation energy is about 63,000 Btu./lb. mole. However, Pansing found that the correlation has proved less useful when applied to commercial units, where such interfering factors as afterburning

and partial combustion in large transfer lines are more difficult to control. Equation B.9 usually gives lower reaction velocity constants than are observed in the pilot plant. Reaction-velocity constants developed from pilot plant data contain a factor that represents the extent of participation of the catalyst in the reaction. In commercial units, where the regenerator may be 30 ft. in diam., part of the catalyst may be ineffective because of nonuniform gas distribution in the fluidized bed.

The above discussion suggests that the principal discrepancy between the performances of pilot plant and commercial units comes from the efficiency of gas-solid contacting which is characterized by a of Eqs. B.7 or B.8. Therefore it is expected that if the commercial plant data are arranged to estimate the apparent (or spacially averaged) constant a for mass transfer coefficient, then the resulting models are more useful.

Afterburning

The purpose of the following discussion is to show that the "afterburning" or oxidation of carbon monoxide to carbon dioxide in the regenerator lean phase is one of the most important control problems from the regenerator safety point of view and from the control system design point of view, that the extent of afterburning is observed by the temperature rise in the regenerator lean phase or the differential temperature across the cyclones, and that the extent of afterburning is mainly expressed in terms of oxygen content in lean phase and regenerator temperature.

The large amount of combustible carbon monoxide in the flue gases sometimes leads to afterburning in the disengaging space and cyclones of fluid regenerators. Such fires are put out by means of steam or water, and the best safeguard seems to keep the excess air low (oxygen below 0.5 to 1 percent in the flue gas), and to keep

the regenerator temperature low (below about 1130°F).*[49] At higher regenerator temperatures, the temperature rise between dense and dilute phases or dense phase and flue gas is a very sensitive indicator of the oxygen content of the gas leaving the dense phase.**[57]

Derivation of Simplified Models

The objective of the following discussion is to derive a mathematically compact set of models which can be readily utilized for the simulation and control studies. Assuming that a stoichiometric ratio of oxygen and carbon is constant, a steady-state material balance for oxygen can be expressed by

$$R_{cb} = \frac{R_{ai}}{C_1}(21-O_{fg})/(100) \qquad (B.10)$$

where R_{cb} = coke burning rate

R_{ai} = air rate

O_{fg} = mol % oxygen in flue gas

C_1 = stoichiometric coefficient

Arranging Eq. B.5, O_{fg} is expressed by

$$O_{fg} = 21 \exp\left\{ - \frac{P_{rg}H_{rg}/R_{ai}}{1/K_{od}+(100)/K_{or}C_{rc}} \right\} \qquad (B.11)$$

---

* It is reported that, for a fluid unit operated at the low regenerator temperature of 1,050°-1,055°F, afterburning problems could never be experienced and it could be operated at almost any oxygen level, but that, operating this unit at 1,100°F regenerator temperature, the danger of afterburning exists anytime with above 1.5% oxygen.[55]

** It is reported that, for a fluid regenerator, the amount of air is controlled through a vernier bypass value by a temperature differential between the dense bed and the flue gas, that the temperature setting for a 60°F spread is sufficient for a good catalyst cleanup, and the corresponding excess oxygen in the flue gas is about 0.2-0.4%.[55]

where P_{rg} = regenerator pressure

H_{rg} = regenerator holdup

K_{od} = oxygen diffusion coefficient

K_{or} = oxygen reaction coefficient

C_{rc} = wt. % carbon on regenerated catalyst

Assuming that the average particle diameter is constant, Eq. B.7 is modified to

$$K_{od} = C_2 R_{ai}^2 \tag{B.12}$$

where C_2 is a constant.

Assuming that an Arrhenius type of temperature factor is held, K_{or} is expressed by

$$K_{or} = C_3 \exp\left\{\frac{\Delta E_{or}}{R(1100+460)} - \frac{\Delta E_{or}}{R(T_{rg}+460)}\right\} \tag{B.13}$$

where C_3 = constant

ΔE_{or} = activation energy of oxygen reaction

T_{rg} = regenerator temperature

R = gas law constant

As far as the afterburning is concerned, assuming that the temperature rise caused by afterburning is directly proportional to the oxygen level, the following expression is obtained:

$$T_{fg} = T_{rg} + C_4 O_{fg} \tag{B.14}$$

where T_{fg} = flue gas temperature

C_4 = constant

Estimation of Constants

In the above set of models, the estimation of constants C_1, C_2, C_3, and C_4 is necessary to utilize the models for the simulation. These constants are not universally constant but depend on the specific operating conditions. However, since they are not strongly dependent on the operating variables, it can be assumed that these constants do not vary significantly for the operation of the same unit, and the assumption of their constancy is adequate for the purpose of simulation and control.

The purpose of the following discussion is to show a simple example of the estimation of constants which is used throughout the study. Assuming that the carbon is oxidized to the same amount of carbon monoxide and carbon dioxide as follows:

$$2C + \frac{3}{2} O_2 \rightarrow CO + CO_2$$

C_1 is estimated by

$$C_1 = 2.0 \text{ (lb. oxygen/lb. carbon)} \qquad \text{(B.15)}$$

Pansing[56] found that

$$k_r \text{ (at } 1429^{\circ}F) = 2.0 \text{ (lb. mole oxygen/hr. atm. lb. carbon)}$$

which, assuming the activation energy of 63,000 Btu./lb. mole, is equivalent to

$$k_r \text{ (at } 1100^{\circ}F) = 12.8 \text{ (lb. mole oxygen/hr. atm. lb. catalyst, fractional carbon)}$$

or

$$= (12.8)(2,000)/(14.7)$$

$$\doteq 1,800 \text{ (lb. mole oxygen/hr. psia, ton carbon)}$$

or equivalently

$$C_3 = (1,800)(32)/(1000) = 57.5 \text{ (M lb. oxygen/hr. psia, ton of carbon)} \qquad \text{(B.16)}$$

If the regenerator efficiency is such that

$$O_{fg} = 0.2\,(\%) \text{ at} \begin{cases} H_{rg} = 200 \text{ (ton)},\ P_{rg} = 25 \text{ (psia)},\ T_{rg} = 1{,}160^{\circ}F \\ C_{rc} = 0.6\,(\%),\ R_{ai} = 400 \text{ (M lb./hr.)} \end{cases}$$

then a direct calculation of Eq. B.11 results in

$$C_2 \doteq 5.0 \times 10^{-6} \qquad \text{(B.17)}$$

Finally, if 0.2 % of O_{fg} corresponds to $20^{\circ}F$ of temperature rise, then

$$C_4 = 100\ (^{\circ}F/\%\ \text{oxygen}) \qquad \text{(B.18)}$$

APPENDIX C

DYNAMIC MODELS AND CONTROL MODELS

There can be various kinds of dynamic mathematical models of FCC, from the highly sophisticated ones to the very simple ones, depending on their intended use. It is a very hard thing to determine what level of model sophistication is necessary and adequate to use them satisfactorily before starting the simulation. Answers will be given only after the simulation is completed and only after the result is found satisfactory judging by the engineering common sense. This study is also not the exception. Most of the assumptions introduced in the study were too difficult to justify completely at least before starting the simulation. However after completing the simulation, it was found that these assumptions are adequate at least for the purposes of the study.

Therefore the purpose of the following discussion is to show the basis of the study, and to describe a simple form of controller models.

General Assumptions for Dynamic Models

Simplified dynamic models can be obtained by isolating the reactor and regenerator systems from the fractionator and the feed preheater. Furthermore, the following idealizations are thought to be necessary and adequate in the interest of simplicity:

1. Riser cracking is negligible.
2. Thermal cracking is negligible.
3. Air riser burning is negligible.
4. Reactor catalyst and regenerator catalyst are uniformly mixed.
5. Catalyst addition, withdrawal, and entrainment are negligible.
6. Heat loss from reactor and regenerator walls are negligible.
7. Stripper holdup, reactor and regenerator standpipe and cone holdups are negligible.

8. Properties (i.e., density, specific heat) of streams and beds are uniform and constant.
9. Process steam, spray water, and torch oil are negligible.
10. Parameters such as heat of cracking, heat of regeneration, and heat of vaporizations are constant.
11. Heats of adsorption of coke and steam on catalyst are negligible.

Reactor Material Balances

There are five materials which have significant roles in the reactor, namely catalyst, total carbon, catalytic carbon, residual carbon, and oil vapor. Since the residence time of oil vapor is normally an order of 10 sec. which is much smaller than those of other materials, it can be assumed that the oil vapor passes through the reactor bed instantaneously with no time lag. This hypothesis allows us to utilize the Blanding's catalytic cracking models which were developed for the above situation. Therefore, it is not necessary to take a material balance for the oil vapor here, since it was done in the development of reactor kinetic models.

Since there are no source and sink for the catalyst and the residual carbon, material balances for them are simply "accumulation = input-output" as follows:

$$dH_{ra}/dt = (60)(R_{rc}-R_{sc}) \qquad (C.1)$$

$$d(H_{ra}C_{res})/dt = (60)(R_{rc}C_{rc}-R_{sc}C_{res}) \qquad (C.2)$$

where

H_{ra} = reactor catalyst hold up

C_{res} = residual carbon

C_{rc} = carbon on regenerated catalyst

R_{rc} = regenerated catalyst rate

R_{sc} = spent catalyst rate

(60) = (60 min./hr.)

Since there is no sink for the total carbon, and neither sink nor input for the catalytic carbon, material balances for them are simply "accumulation = production + input-output"

$$d(H_{ra}C_{sc})/dt = (50)R_{cf} + (60)(R_{rc}C_{rc} - R_{sc}C_{sc}) \qquad (C.3)$$

$$d(H_{ra}C_{cat})/dt = (50)R_{cc}H_{ra} - (60)R_{sc}C_{cat} \qquad (C.4)$$

where C_{sc} = carbon on spent catalyst

C_{cat} = catalytic carbon

R_{cf} = carbon forming rate

R_{cc} = catalytic carbon forming rate per unit of catalyst

(50) = (1000/M)(100 %/1)/(2000 lb./ton)

Reactor Heat Balance

Although there are no heat sources for the reactor, there are two heat inputs, namely feed streams and regenerated catalyst; two heat outputs, namely oil vapor and spent catalyst; and two heat sinks, namely heat of vaporization and heat of cracking. After rearranging, a reactor heat balance is expressed by

$$S_c d(H_{ra}T_{ra})/dt = (60)S_c(R_{rc}T_{rg} - R_{sc}T_{ra})$$

$$-(.875)S_f\{D_{ff}R_{ff}(T_{ra} - T_{fp}) + D_{rf}R_{rf}(T_{ra} - T_{rf})\}$$

$$-(.875)\Delta H_{fv}\{D_{ff}R_{ff} + D_{rf}R_{rf}\} - (.5)\Delta H_{cr}R_{oc} \qquad (C.5)$$

where S_c = specific heat of catalyst

S_f = specific heat of feed

T_{ra} = reactor temperature

T_{rg} = regenerator temperature

T_{fp} = feed preheater temperature

T_{rf} = recycle feed temperature

R_{ff} = fresh feed rate

R_{rf} = recycle feed rate

R_{co} = oil cracking rate

ΔH_{fv} = heat of vaporization

ΔH_{cr} = heat of cracking

D_{ff} = density of fresh feed

D_{rf} = density of recycle feed

(.875) = (42 gal./bbl.)(1000/M)/(24 hr./day)(2000 lb./ton)

(.5) = (1000/M)/(2000 lb./ton)

Regenerator Material Balances

There are three materials which have significant roles in the regenerator, namely catalyst, carbon, and air. Since the residence time of air is normally an order of 10 sec., which is much smaller than those of other materials, it can be assumed that the air passes through the regenerator bed instantaneously with no time lag. This hypothesis allows us to utilize the Pansing's regeneration models which were developed for the above situation. Therefore it is not necessary to take a material balance for the air here, since it was done in the development of regenerator kinetic models.

Since there is neither source nor sink for the catalyst, and since there is no source for the carbon, material balances for them are

$$d H_{rg}/dt = (60)(R_{sc} - R_{rc}) \qquad (C.6)$$

$$d(H_{rg}C_{rc})/dt = (60)(R_{sc}C_{sc} - R_{rc}C_{rc}) - (50)R_{cb} \qquad (C.7)$$

where H_{rg} = regenerator catalyst holdup

R_{cb} = carbon burning rate

Regenerator Heat Balance

Although there is no heat sink for the regenerator, there are two heat inputs, namely air and spent catalyst; two heat outputs, namely air and regenerated catalyst; and a heat source, namely heat of regeneration. After rearranging, a regenerator heat balance is expressed by

$$S_c d(H_{rg}T_{rg}) = (.5)\Delta H_{rg}R_{cb} - (60)S_c(R_{rc}T_{rg} - R_{sc}T_{ra}) - (.5)S_a R_{ai}(T_{rg} - T_{ai}) \qquad (C.8)$$

where ΔH_{rg} = heat of regeneration

S_a = specific heat of air

T_{ai} = air inlet temperature

Pressure Balances

The variations of pressure in FCC affect the catalyst circulation mechanism, the cracking, and the regeneration. Since the effects on the cracking and the regeneration are relatively small, the pressure in the reactor and regenerator kinetic models can be assumed constant. However, since the effect on the catalyst circulation mechanism is not so simple, it is necessary to evaluate the relation between them. If the catalyst slide value is not used to control a certain variable (e.g., catalyst holdup, bed temperature, etc.) automatically, then the effect of the pressure variations on the catalyst rate will become extremely

large since the pressure difference across the slide valve determines the catalyst rate. However, if the catalyst slide valve is used to control a certain variable automatically, then the effect of the pressure variations on the catalyst rate will become extremely small since the controlled variable has a greater role to determine the catalyst rate than has the pressure difference between the slide valve. In the latter situation, the pressure variations affect the apparent controller gain between the catalyst rate and the controlled variable rather than on the catalyst rate directly. Most of the commercial FCC hold this situation (e.g., the spent catalyst slide valve is used to control the reactor holdup automatically, and the regenerated catalyst slide valve is used to control the reactor temperature automatically).

These closed-loop structures with respect to the catalyst rate were assumed throughout the study. Therefore the accurate determinations of the pressure variations and their effects on the catalyst circulation mechanism were neither necessary nor useful for simulation of controlled FCC. However, it should be noted that this pressure balance is not particularly difficult to analyze and simulate if one constructs systematically the functional relationship between the material flows and the pressure drop for risers, standpipes, slide valves, dense beds, dilute phases, grids (distributors) and gas lines.

Estimation of Physical Constants

Although some of the physical constants for catalytic crackers are not well known, the following values were used throughtout the study:

S_c = specific heat of catalyst = 0.25 Btu./lb.^{o}F (Ref. 49, p.789)

S_a = specific heat of air = 0.27 Btu./lb.^{o}F at 1200^{o}F, 1 atm. (Perry, Chem. Eng. H.B. p. 3-127)

S_f = specific heat of feed gas oil $\doteq$ (725-500)/300 Btu./lb.^{o}F (Ref. 49, p. 170)

ΔH_{cr} = heat of cracking $\doteq$ 200 Btu./lb.cracked (Ref. 49, p. 795 or Ref. 15, p. 114)

ΔH_{fv} = heat of feed vaporization $\doteq$ 500-425 Btu./lb.(Ref. 49 p. 170)

ΔH_{rg} = heat of regeneration $\doteq$ 13,000 Btu./lb. carbon (Ref.49, p. 789 and p. 792, or Ref. 57, p. 128)

D_{ff} = density of gas oil $\doteq$ 7.30 lb./gal.

D_{co} = density of cycle oil $\doteq$ 7.38 lb./gal.

$D_{g\ell}$ = density of gasoline $\doteq$ 6.40 lb./gal.

} (Ref.49, p.778)

D_{rf} = density of recycle oil $\doteq D_{co}$

Activation energies are discussed in Appendix A and B.

Control Models

Throughout the study, the controllers were assumed to have the following idealized properties:

1. Measuring delay is negligible.
2. Controller functions are perfectly proportional and/or integral.
3. Control valve delay is negligible.
4. Control variables are idealized quantity (e.g., air rate in M lb./hr., catalyst rate in tons/min., etc.)
5. Controlled variables are an idealized quantity (e.g., holdup in tons, oxygen content in %, etc.)
6. Saturation of control variables is pure, in other words, can be described by an inequality.

A basic model for any controller therefore is expressed by

$$\Delta u = K_p(x-x_s) + K_I \int_0^t (x-x_s)dt \qquad (C.9)$$

where Δu = incremental control variable

x = controlled variable

x_s = set point

K_p = proportional gain

K_I = integral gain

Controller Tunings

Controller tunings were done essentially by a trial and error method with the use of dynamic simulation. The following tunings were used throughout the study:

1. Conventional control scheme:

   a. reactor temperature vs. catalyst rate

   $$K_p = -0.2 \text{ and } K_I = -0.1$$

   b. oxygen level vs. air rate

   $$K_p = -20 \sim -40 \text{ and } K_I = -5 \sim -10$$

2. Alternative control scheme:

   a. regenerator temperature vs. air rate

   $$K_p = -1 \sim -4$$

   b. oxygen level vs. catalyst rate

   $$K_p = 20 \sim 40 \text{ and } K_I = 40 \sim 80$$

3. Flue gas temperature control scheme:

   a. reactor temperature vs. catalyst rate

   $$K_p = -0.5 \text{ and } K_I = -2 \sim -10$$

b. flue gas temperature vs. air rate

$$K_p = -4 \sim -6$$

APPENDIX D

DYNAMIC SIMILARITIES OF FCC CONTROL SYSTEMS

The basic ideas of the simulation study of an idealized hypothetical FCC are (1) although there are various kinds of FCC, the dynamic behavior of their controlled systems have, to a great extent, common characteristics which might be called "dynamic similarities of FCC control systems," and therefore (2) the results obtained for an FCC can be generalized, to a certain extent, to most of the FCC.

Although there are few published reports on dynamic behavior of any FCC control systems, Hicks, et al.[32] fortunately reported their analog computer simulation study of an Atlantic's Orthoflow type FCC. In spite of the differences in capacity, size, configuration, and mechanism between their FCC and our hypothetical FCC, the comparison of dynamic behavior can provide a basis to support items 1 and 2.

Therefore, the purpose of this appendix is to demonstrate the dynamic similarities of FCC control systems and to provide a basis to support items 1 and 2.

Differences in Conditions

In order to emphasize the dynamic similarity it is better, first, to show the differences in operating conditions. Although the exact operating conditions of the Atlantic's FCC are not reported, it is apparently operated at different conditions (e.g., reactor and regenerator temperatures and holdups, feed rate, air rate, catalyst rate, carbon levels, oxygen levels, feed compositions, etc.) from ours. Furthermore, their mechanical conditions such as regenerator efficiency (i.e., mass transfer coefficient), lean phase residence time which affects afterburning, and catalyst valve differential pressures are different from ours. Other differences will be in the control

systems such as tuning of controllers, air vent saturation, pressure control systems, and level control systems.

Considering the above differences, the dynamic similarities, which will be followed, will become clear.

Reactor and Flue Gas Temperature Control Systems

Hicks, et al.[32] describes their control systems of Atlantic's Orthoflow type FCC as follows. Figure D.1 depicts the equivalent control systems of our hypothetical FCC. Catalyst flows via regenerated catalyst stand pipe into the reactor on reactor temperature control. During the cracking reaction, coke production results in a buildup of carbon on the catalyst. Following steam stripping of hydrocarbons from the spent catalyst, it is returned to the regenerator to burn off this accumulation. The flow from the reactor vessel is controlled by reactor level.

Regeneration air is supplied from blowers to rejuvenate the spent catalyst. Vernier control of this air rate is provided by a "trim-air vent" actuated by the flue-duct temperature. When the carbon level on the catalyst decreases, residual oxygen becomes available to burn some of the CO in the flue gas to CO_2, increasing the heat release and raising the flue-duct temperature. The trim-air control then removes a small amount of air from the regenerator, suppressing the afterburning.

If a small amount of excess oxygen is normally present to sustain some afterburning, an increased coke load to the regenerator will activate the trim air in a reverse manner as the primary coke burning tends to snuff out the afterburn.

Figure D.2 compares the dynamic behavior of these control systems when the reactor temperature set point is suddenly decreased. This dynamic behavior will be explained by the following step-by-step analysis:

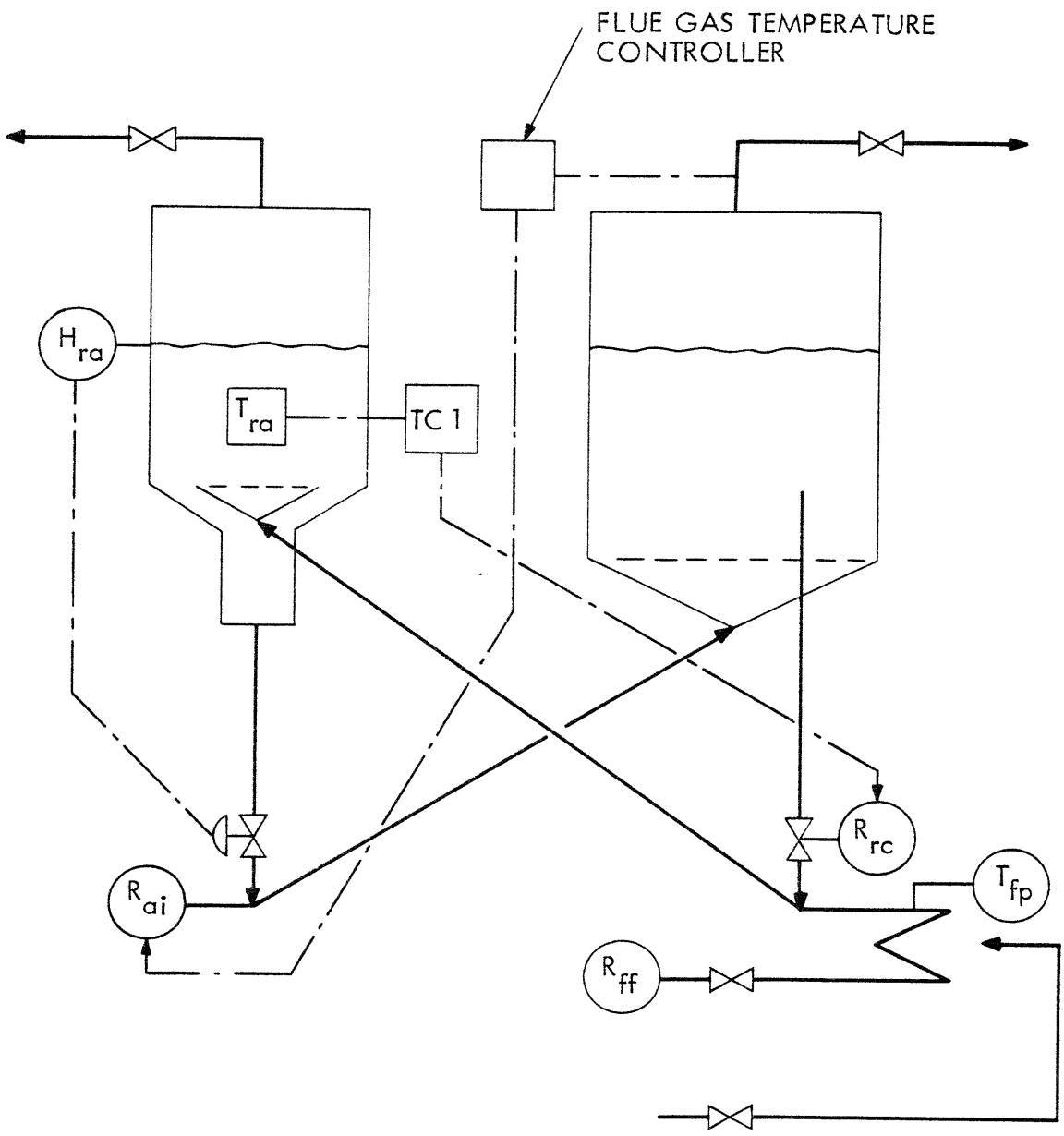

Fig. D.1 Flue Gas Temperature Control Scheme of FCC

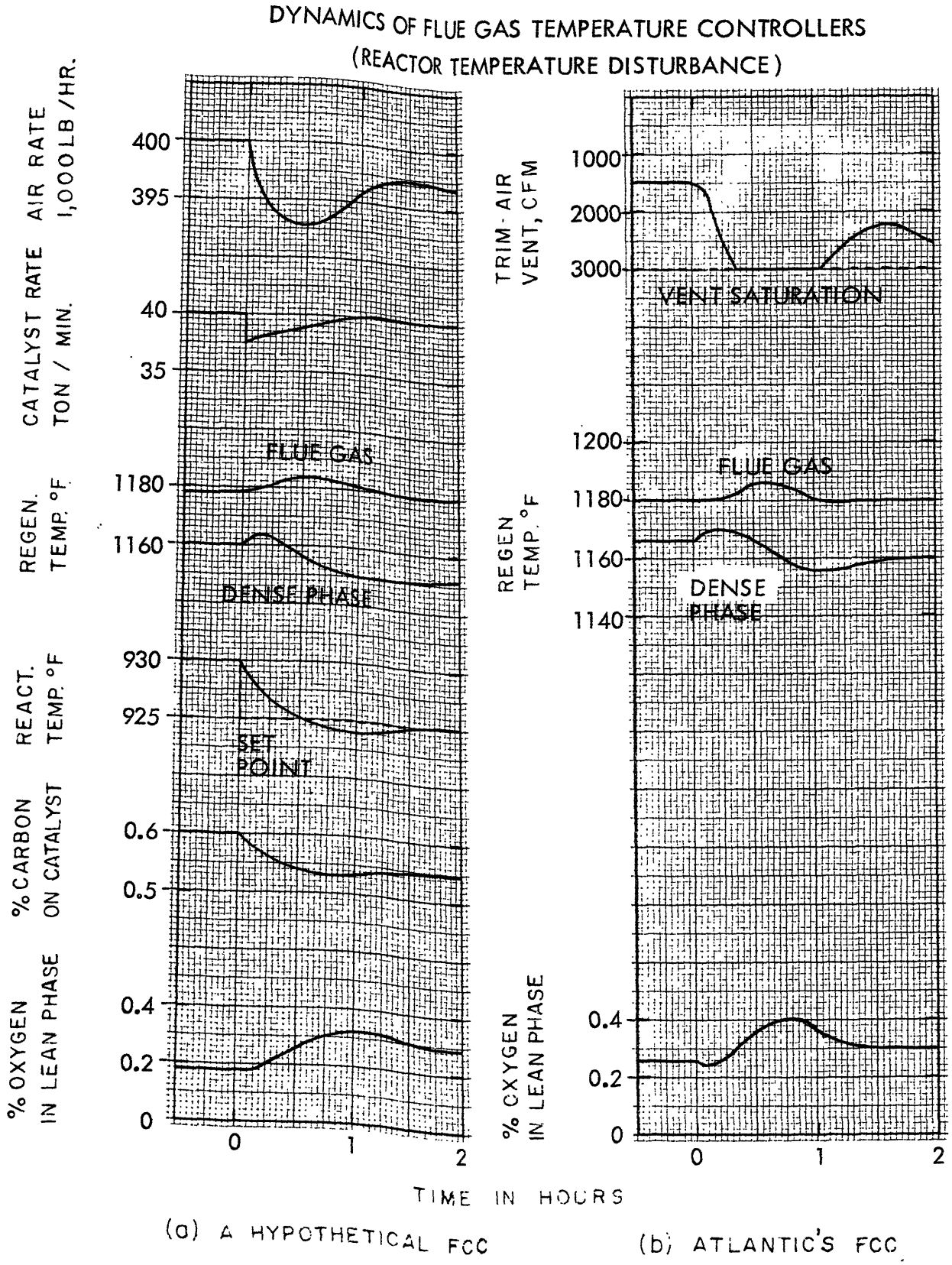

Fig. D.2 Dynamic Similarities (No. 1) of FCC Control Systems

1. The reactor temperature set point is decreased.

2. The reactor temperature controller decreases the catalyst rate.

3. The carbon content starts to decrease because of less carbon production due to lower reactor temperature and catalyst rate. Simultaneously the lower catalyst rate increases the regenerator temperature and the flue gas temperature which, in turn, reduces the air rate by means of the controller.

4. The oxygen level and the flue gas temperature start to increase because of the lower carbon content.

5. The decreased air rate compensates for the decreased carbon production, and the carbon content and the oxygen content tend to level off.

Although the Atlantic's FCC data are not complete with respect to the reactor temperature and the carbon content, there are significant similarities for the dynamic behavior of the air rate, the regenerator, and the flue gas temperatures, and the oxygen content.

The dynamic behavior of these control systems when the catalyst rate is suddenly decreased (by a certain probable mechanism such as pressure variations) is shown in Fig. D.3 for a poor tuning of the reactor temperature controller and in Fig. D.4 for a better tuning. The dynamic behavior will be explained by the following step-by-step analysis:

1. The catalyst rate is suddenly decreased.

2. The reduced catalyst rate reduces the reactor temperature and the carbon content, and increases the regenerator and the flue gas temperatures.

3. The reduced reactor temperature accelerates the carbon content to decrease and increases the catalyst rate by means of the controller. Simultaneously the increased flue gas temperature decreases the air rate by means of the controller.

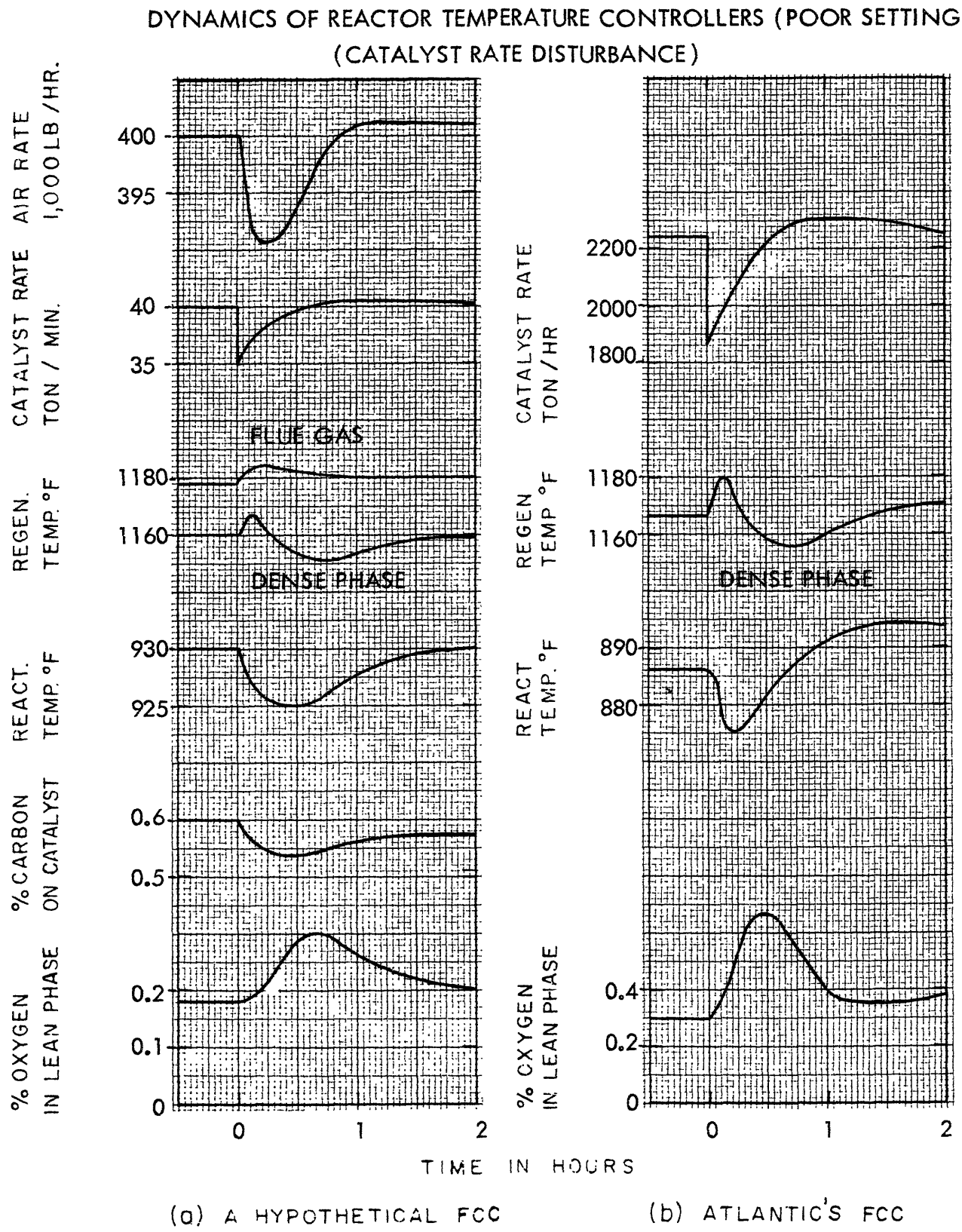

Fig. D.3 Dynamic Similarities (No. 2) for FCC Control Systems

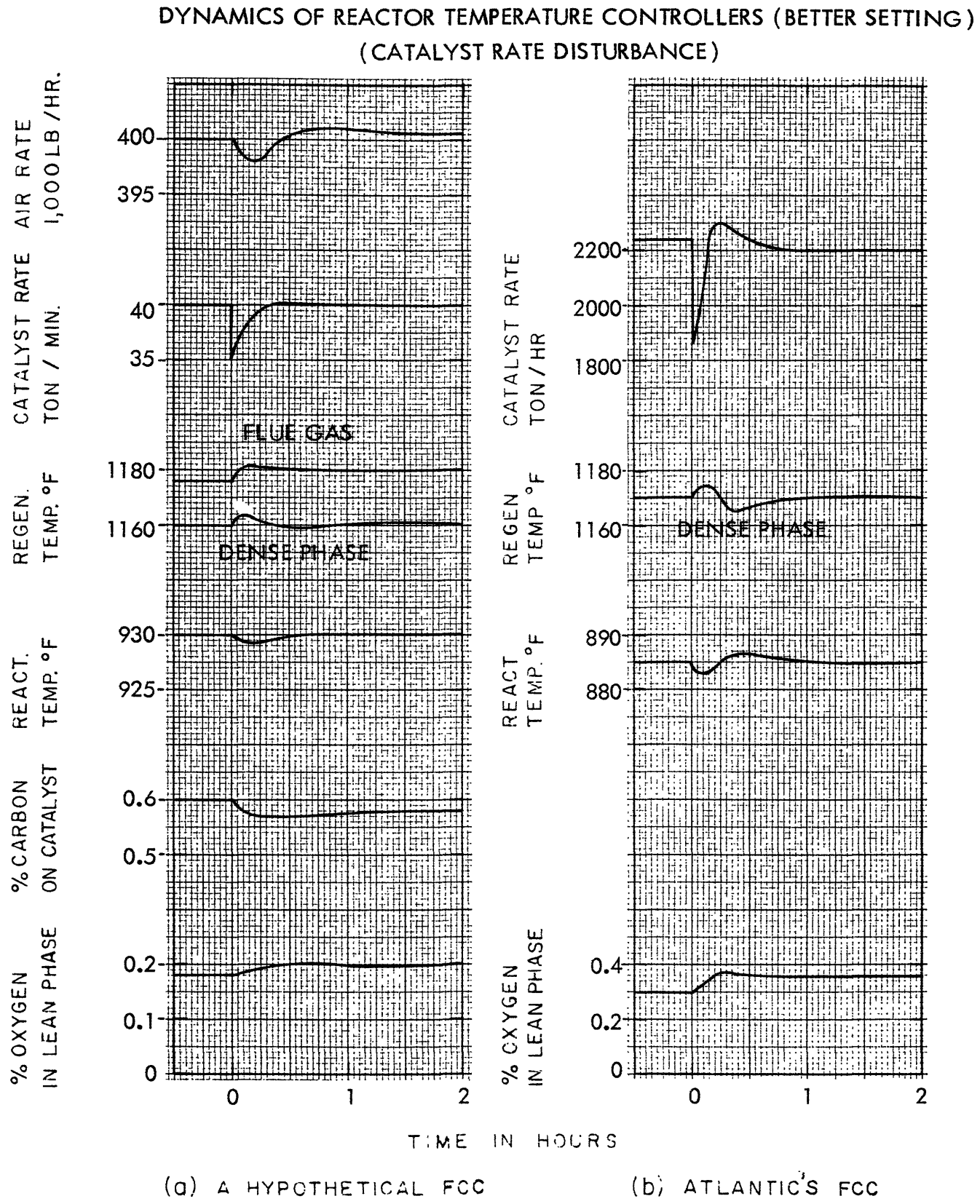

Fig. D.4 Dynamic Similarities (No. 3) of FCC Control Systems

4. The reduced air rate reduces the carbon burning rate and the heat release rate, which in turn reduces the regenerator and the flue gas temperature and the reactor temperature, which accelerates the catalyst rate to restore. Simultaneously the reduced carbon content results in the high oxygen level.

Although the Atlantic's FCC data are not complete with respect to the air rate and the carbon content, there are significant similarities for the dynamic behavior of the catalyst rate, the reactor and the regenerator temperatures, and the oxygen content.

Alternative Oxygen Control Systems

Hicks, et al.[32] describes their study for an alternative oxygen control system* of Atlantic's Orthoflow type FCC as follows. Figure D.5 depicts the equivalent control system of our hypothetical FCC. Through work with the model, they confirmed the importance of reactor temperature on the generation of coke in the reactor. A few degrees change in reactor temperature could compensate for a fairly large change in the coke-producing tendency of the gas-oil charge to the reactor.** Thus, one suggested control scheme was to

---

* Since, as an oxygen control system, the control by the air rate is more conventional than the control by the catalyst rate, we call the latter "an alternative oxygen control system" throughout the study.

** This statement made by Hicks, et al. is not completely adequate, and it requires some interpretation. In the reactor temperature control system, which is manipulated by the catalyst rate, the coke production is governed not only by the reactor temperature but also by the catalyst rate, and the effect of the latter can not be overlooked. Moorman[46] and Pohlenz[57] clearly reported that the effect of the reduced catalyst rate, while keeping the reactor temperature constant, is a significant reduction in the coke production. Therefore, it is adequate to restate that a slight change in the catalyst rate, together with the resulting change in the reactor temperature, could compensate for a fairly large change in the coke-producing tendency of the gas-oil charge to the reactor.

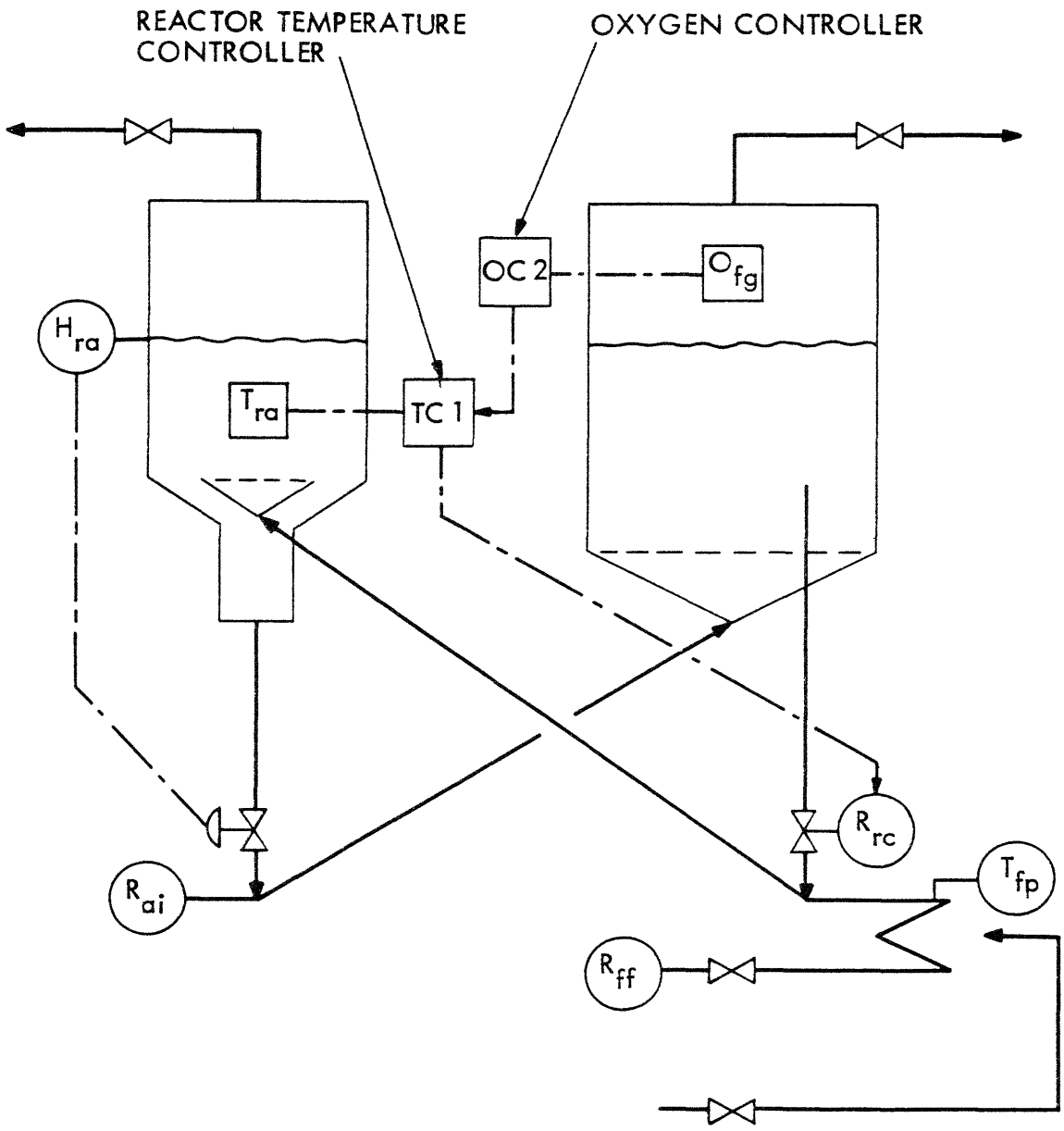

Fig. D.5 A Cascaded Control System of FCC

retain the present controls on catalyst flow, but manipulate the set point of the reactor temperature controller to hold constant excess oxygen in the regenerator. A measure of the excess oxygen leaving the dense phase is the temperature rise due to afterburning in the lean phase or across the cyclones, so that ΔT was selected as the variable to be measured and controlled.

Since the real function of this cascaded controller is to manipulate the catalyst rate in order to control the oxygen level, a direct oxygen controller, where the catalyst rate is directly manipulated, is used as a basis for the comparison for our hypothetical FCC.

Figure D.6 compares the dynamic behavior of these control systems when the carbon production is suddenly increased (by a certain probable mechanism such as the feed composition variations). This dynamic behavior will be explained by the following step-by-step analysis:

1. The reduced carbon production increases the carbon content temporarily, which in turn reduces the oxygen content and increases the regenerator temperature as the carbon burning rate increases.

2. The reduced oxygen content reduces the catalyst rate by means of the controller, which in turn reduces the reactor temperature and increases the regenerator temperature.

3. The reduced catalyst rate and the resulting reduced reactor temperature reduce the carbon production to an original level.

Although the Atlantic's FCC data are not complete with respect to the catalyst rate and the carbon content, there are significant similarities in the dynamic behavior of the reactor and regenerator temperatures and the oxygen content.

Figure D.7 compares the same systems when the carbon production is suddenly decreased. In this case, the step-by-step analysis

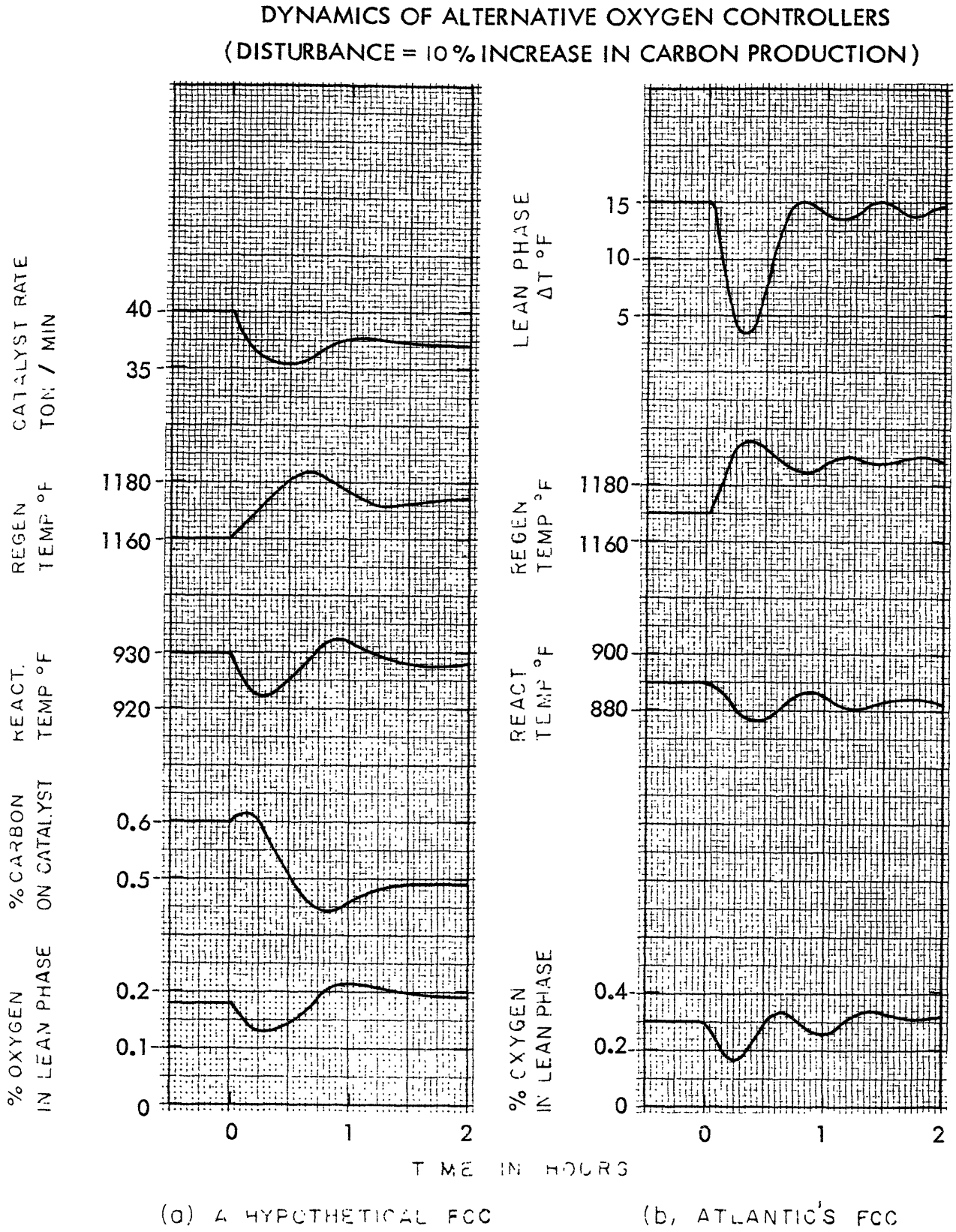

Fig. D.6 Dynamic Similarities (No. 4) for FCC Control Systems

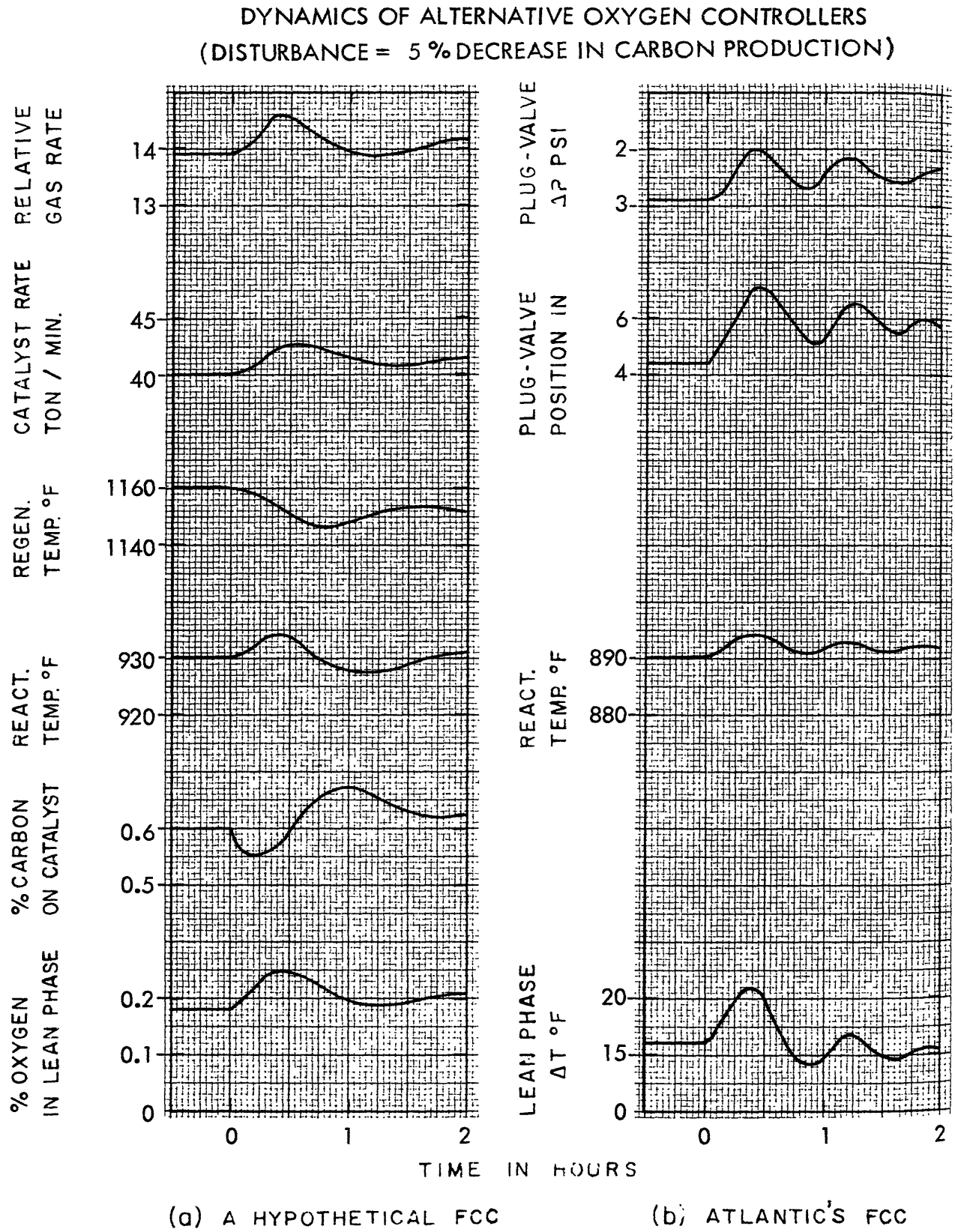

Fig. D.7 Dynamic Similarities (No. 5) of FCC Control Systems

will not be repeated since it is essentially the reverse of the previous case. Instead, in this case, a comparison is made for the gas production rate and the differential pressure of the catalyst valve. When the gas compressors are running at capacity, the compressor suction pressure increases with increasing gas flow. This causes the reactor pressure to increase and the differential pressure across the regenerated catalyst valve to decrease.

Although the Atlantic's FCC data are not complete with respect to the gas production rate, there are significant similarities for the dynamic behavior of the gas production rate and the catalyst valve differential pressure.

It should be noted that the object of this appendix is just to demonstrate the dynamic similarities of these control systems, and that we do not intend to support the performance of these control systems here, and that critical evaluation of this performance is presented in the next appendix.

APPENDIX E

ANALYSIS OF VARIOUS INCOMPLETE CONTROL SYSTEMS

The control systems, which were studied by Hicks, et al.,[32] namely (1) reactor and flue gas temperature control systems, and (2) alternative oxygen control systems, were apparently satisfactory from the dynamic point of view, since, as was demonstrated in the previous appendix, most of the transient phenomena caused by various disturbances decay in a few hours, and it was possible to maintain the reactor and the flue gas temperatures or the oxygen level nearly constant.

However, they are still far from satisfactory from a safety point of view. In short, these control systems do not have complete information feed back with respect to the variables which really govern the regenerator safety, namely regenerator temperature and oxygen level or carbon level.

Therefore the purpose of this appendix is to demonstrate the critical performance of these "incomplete" control systems and to provide a basis for the evaluation of the control systems.

Reactor Temperature Control System

One of the simplest control systems is merely the control of reactor temperature by the catalyst rate. Since this control system does not have any information feedback with respect to the regenerator temperature and the oxygen content it is not difficult to see that this control system is subject to various upsets such as excessive afterburning and/or excessive carbon buildup phenomena for certain disturbances.

Figure E.1 shows the performance of this control system when the feed rate is suddenly decreased. The dynamic behavior is explained by the following step-by-step analysis:

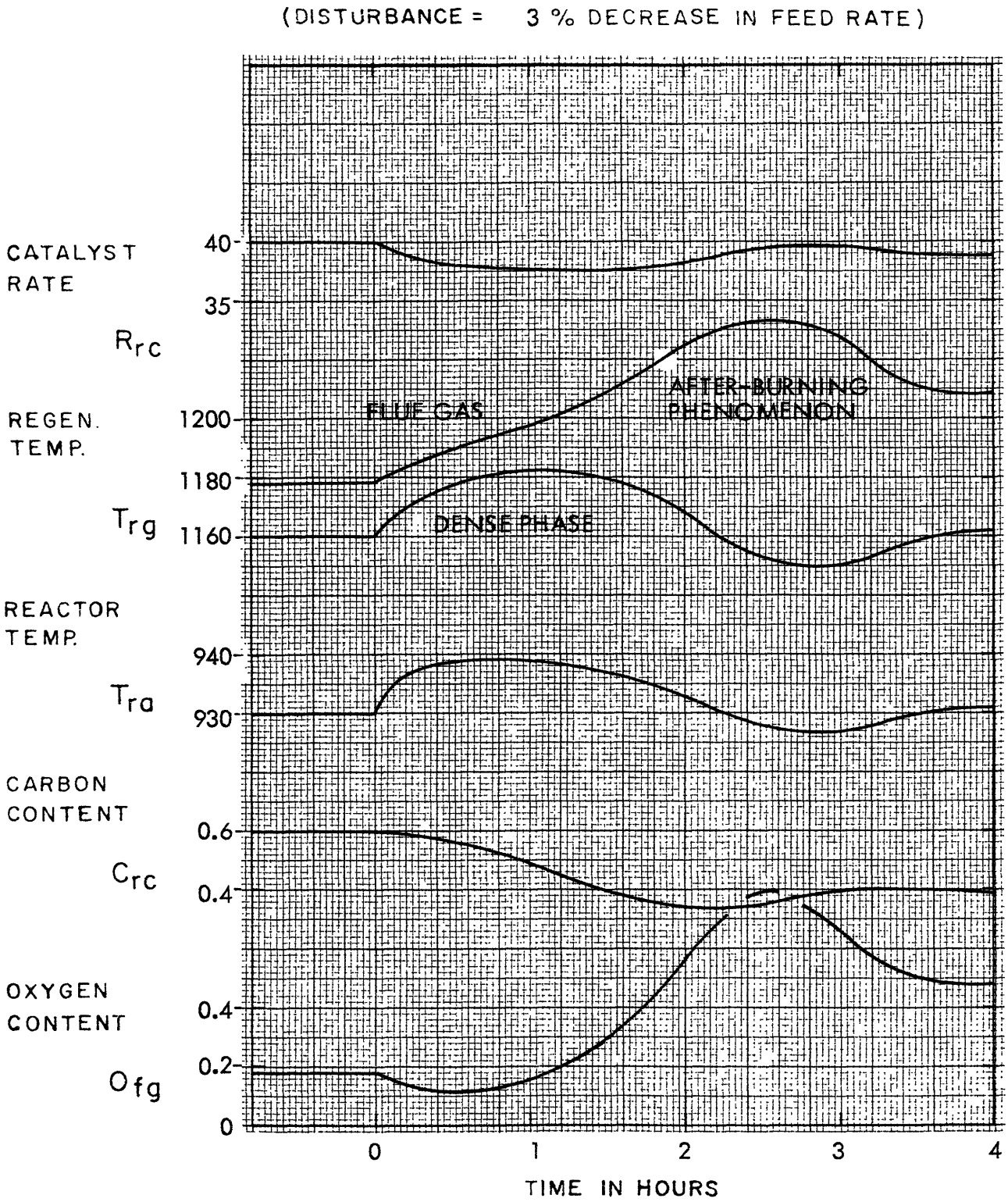

Fig. E.1 Performances of Reactor Temp. Control System

1. The reduced feed rate increases the reactor and the regenerator temperatures.

2. The increased reactor temperature reduces the catalyst rate, by means of the controller, which in turn accelerates the regenerator temperature to increase.

3. The increased regenerator temperature burns off the carbon to a lower level, which in turn results in the excessive afterburning and excessive flue gas temperature.

The main disadvantage of this control system is that it can not recover this flue gas temperature to an original level, since the air rate is held constant in spite of the reduced heat requirement resulting from the reduced feed rate.

Reactor and Flue Gas Temperature Control Scheme

In order to overcome the deficiency of the previous control system, Hicks, et al.[32] added the flue gas temperature control by the air rate to the original reactor temperature controller. Figures E.2 and E.3 demonstrate the performance of these control systems when the feed rate is suddenly reduced or increased. It is not difficult to see how the air rate is changed to compensate for the changes in the heat requirement. Any change in the flue gas temperature resulting from the feed rate change actuates the air rate in such a manner as to keep the flue gas temperature nearly constant.

Unfortunately the above situation is rarely practical, since the air rate is limited by the blower capacity which can not be expected to increase significantly. Figure E.4 demonstrates the performance when the feed rate is suddenly increased and when the air rate has only one percent excess capacity. Failing to compensate for the change in the heat requirement, the regenerator temperature is accelerated to decrease by means of the reactor temperature controller. The reduced burning rate, which is due to the lower regenerator temperature,

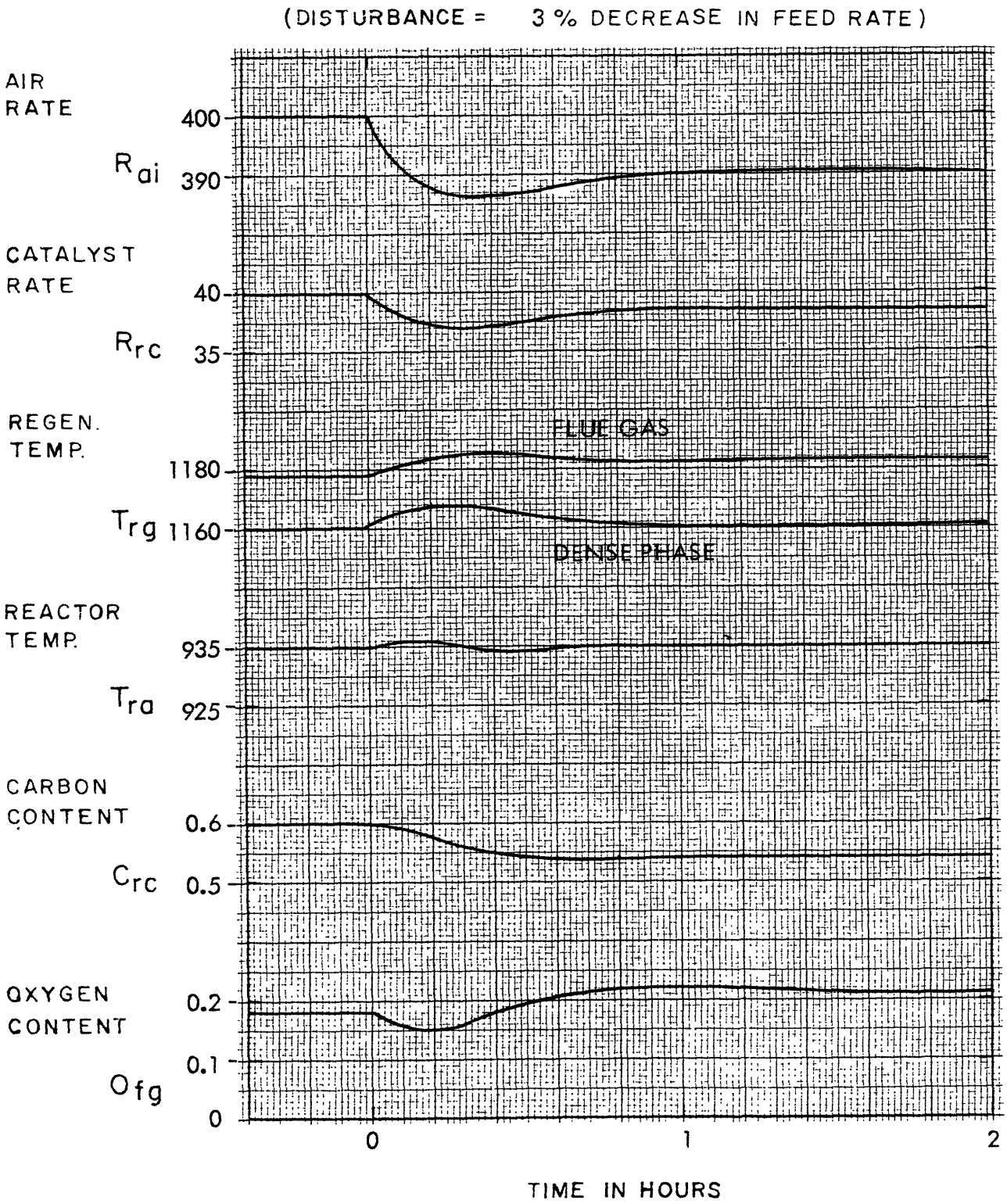

Fig. E.2 Performances of Flue Gas Temp. Control Scheme (No. 1)

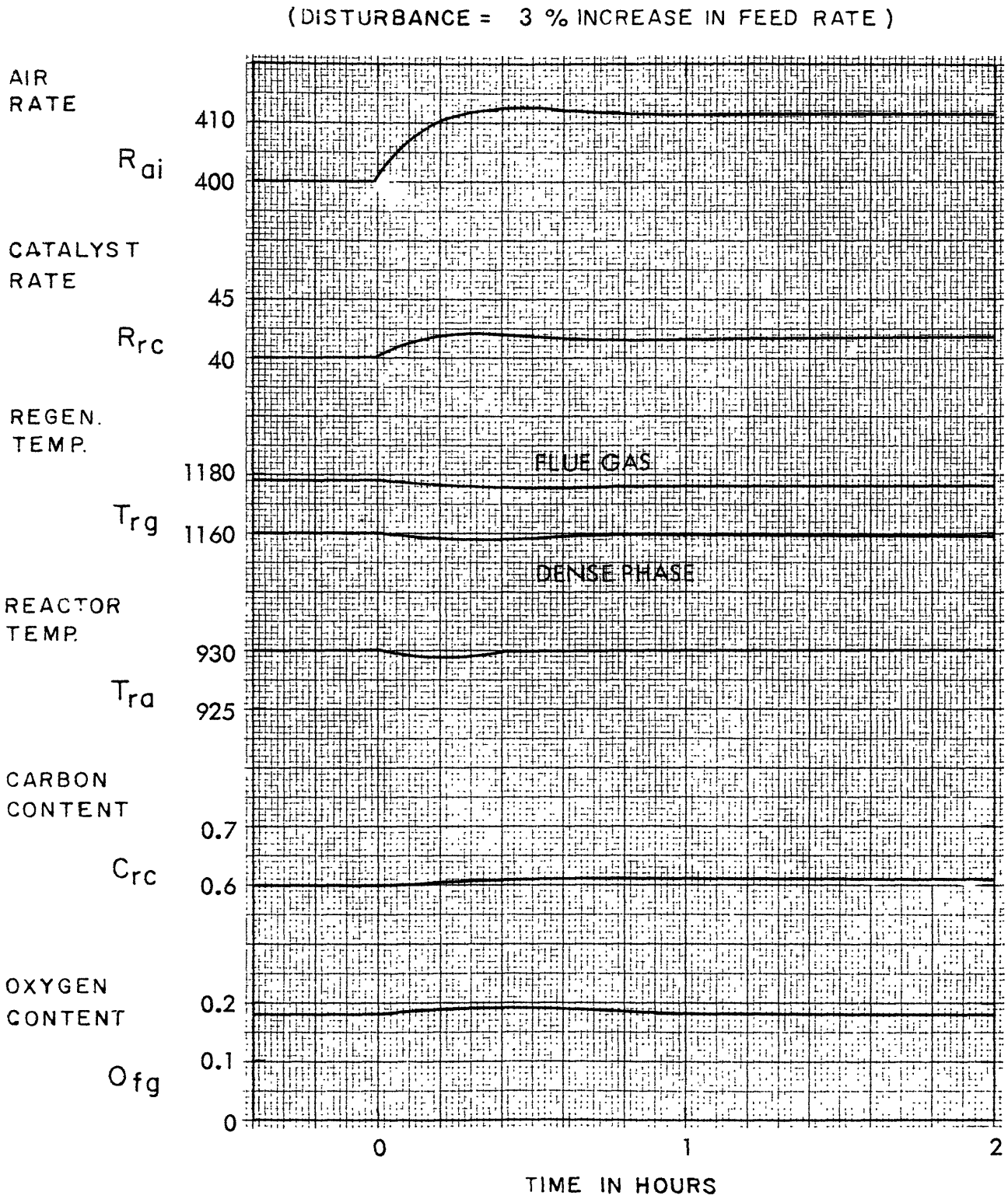

Fig. E.3 Performances of Flue Gas Temp. Control Scheme (No. 2)

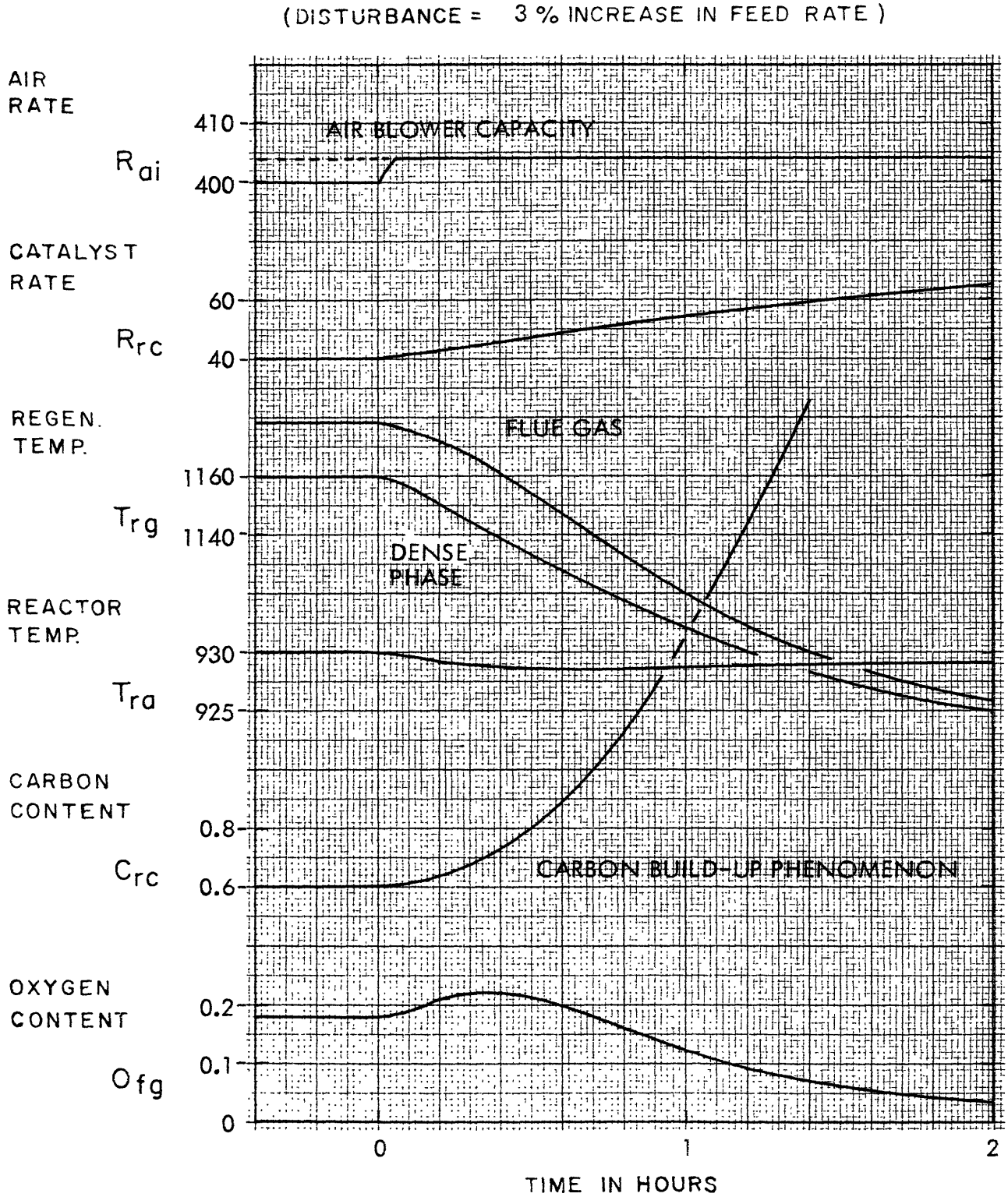

Fig. E.4 Performances of Flue Gas Temp. Control Scheme (No. 3)

and the increased carbon production rate, which is due to the higher catalyst rate, accelerate the carbon build-up phenomenon.

This carbon build-up phenomenon can be said to be the characteristic of control systems which do not have any information feedback with respect to the oxygen level. The following example will make the above statement clear. Figure E.5 shows what happens when the carbon production is suddenly increased. Although the resulting increase in the reactor and the flue gas temperatures are quickly recovered by means of controllers, the oxygen content continues to decrease and the carbon level continues to build up, since the flue gas temperature controller can compensate for the change in heat requirement; but it can not compensate for the change in carbon production. Figure E.6 shows what happens when the carbon production is suddenly reduced. In this case, the carbon burn-off, reversal phenomenon to the carbon build-up, saturates at a certain level because of the nonlinearity. However, if the blower capacity is limited, then the carbon build-up can occur, as Fig. E.7 and Fig. E.8 show.

In summary, the main disadvantages of the reactor and the flue-gas temperatures control systems are that they can not compensate for the change in carbon production and even the change in heat requirement when the blower capacity is limited. In fact, Hicks et al.[32] evaluate their control systems as saying that "hands-off operation for (only) six to eight hours is frequently possible."

Alternative Oxygen Control System

In order to overcome the deficiency of the previous control systems, Hicks et al.[32] studied an alternative oxygen control system where essentially the catalyst rate is manipulated to compensate for the change in carbon production. A typical example is already demonstrated in Fig. D.6 of the previous appendix where the carbon production is suddenly increased. Although this system can compensate for the change in carbon production, it can not compensate for the change in

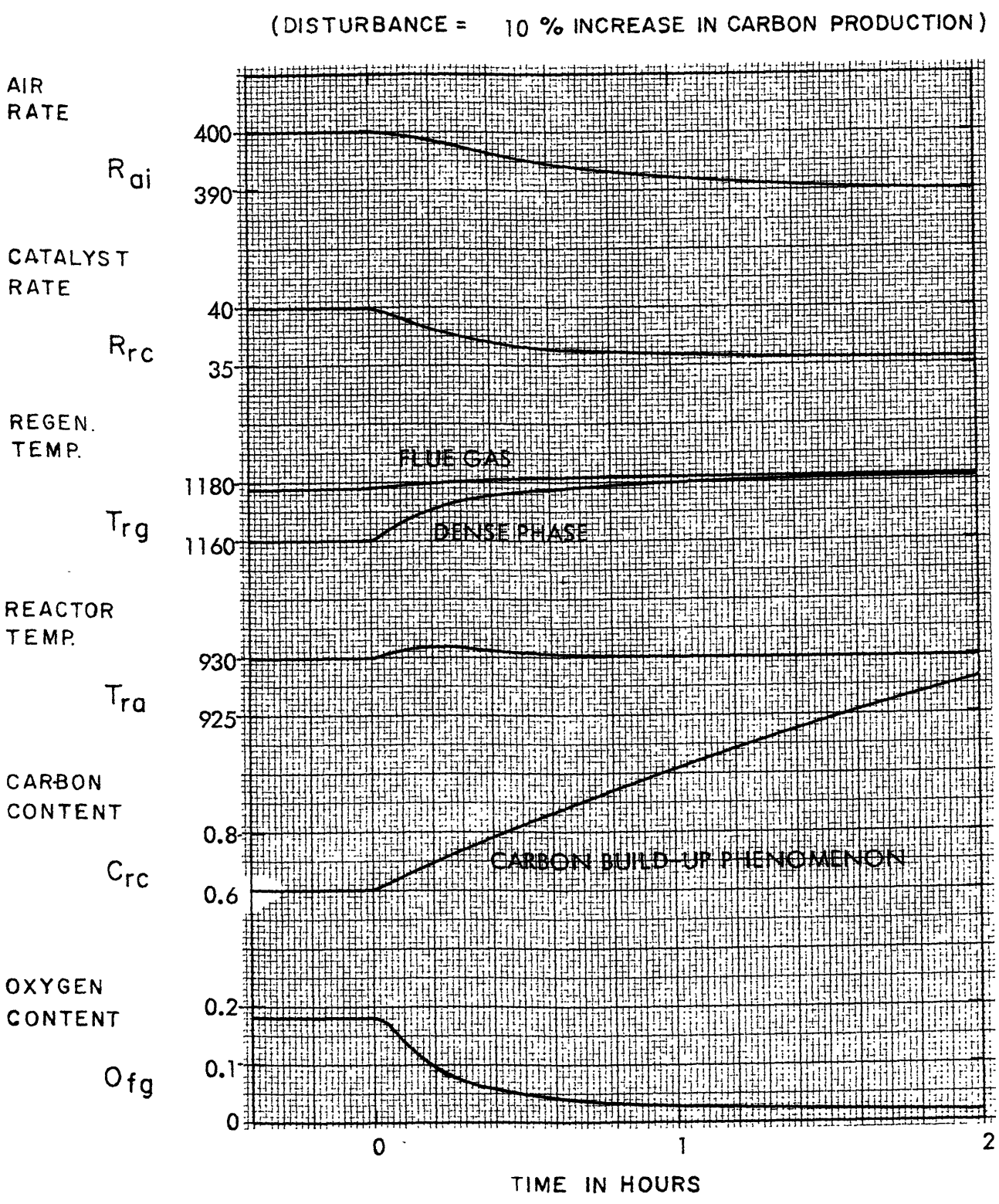

Fig. E.5 Performances of Flue Gas Temp. Control Scheme (No. 4)

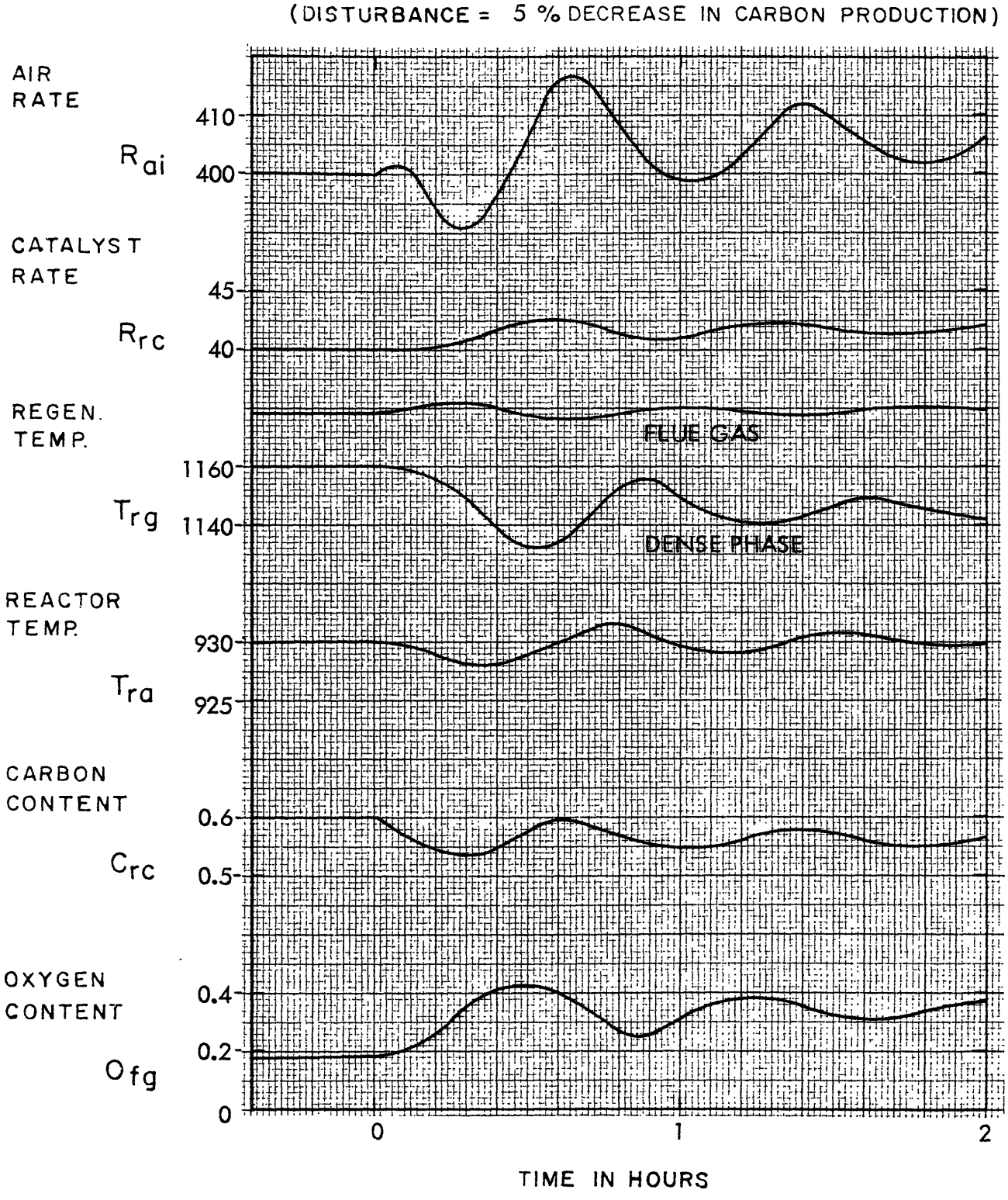

Fig. E.6 Performances of Flue Gas Temp. Control Scheme (No. 5)

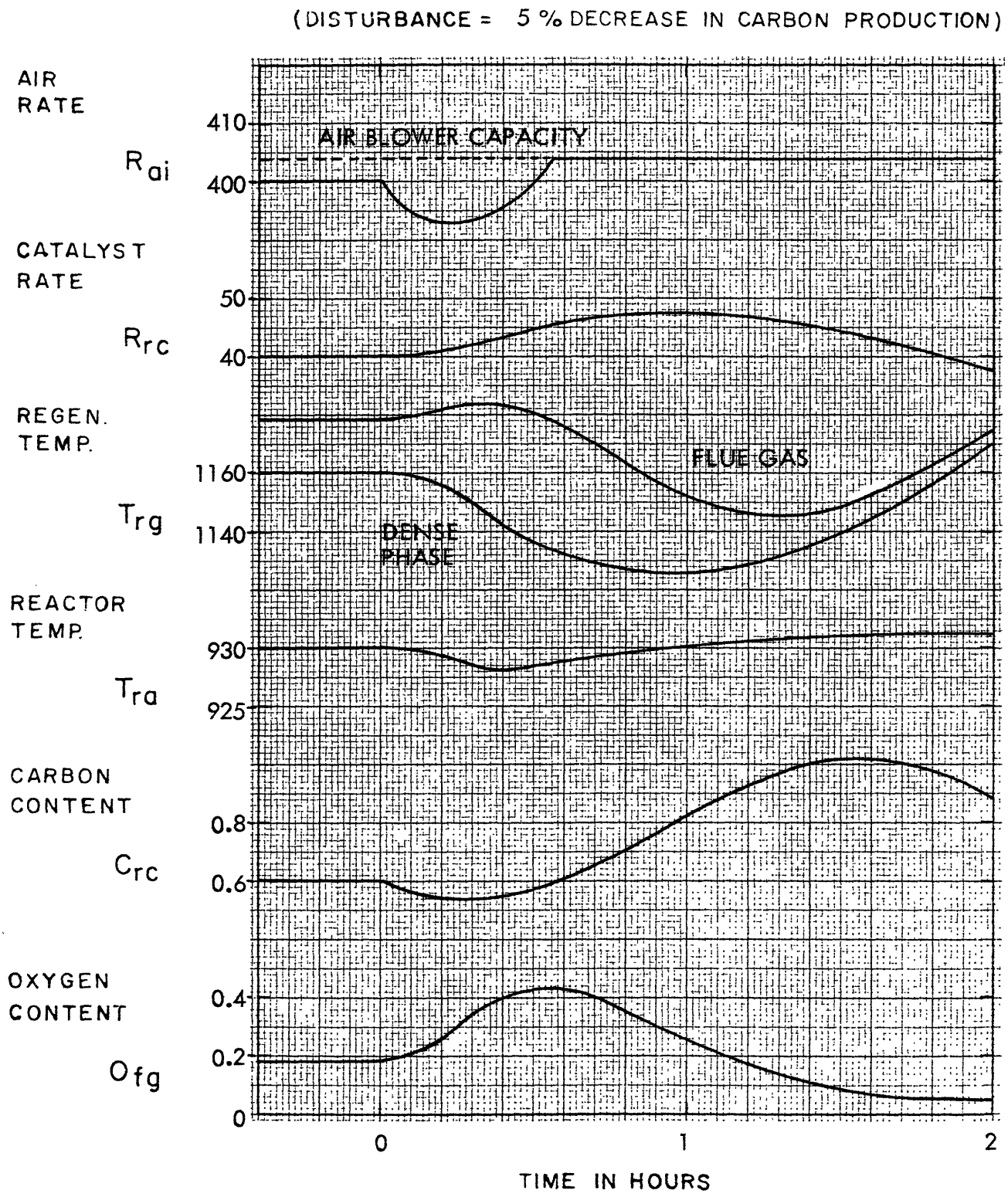

Fig. E.7 Performances of Flue Gas Temp. Control Scheme (No. 6)

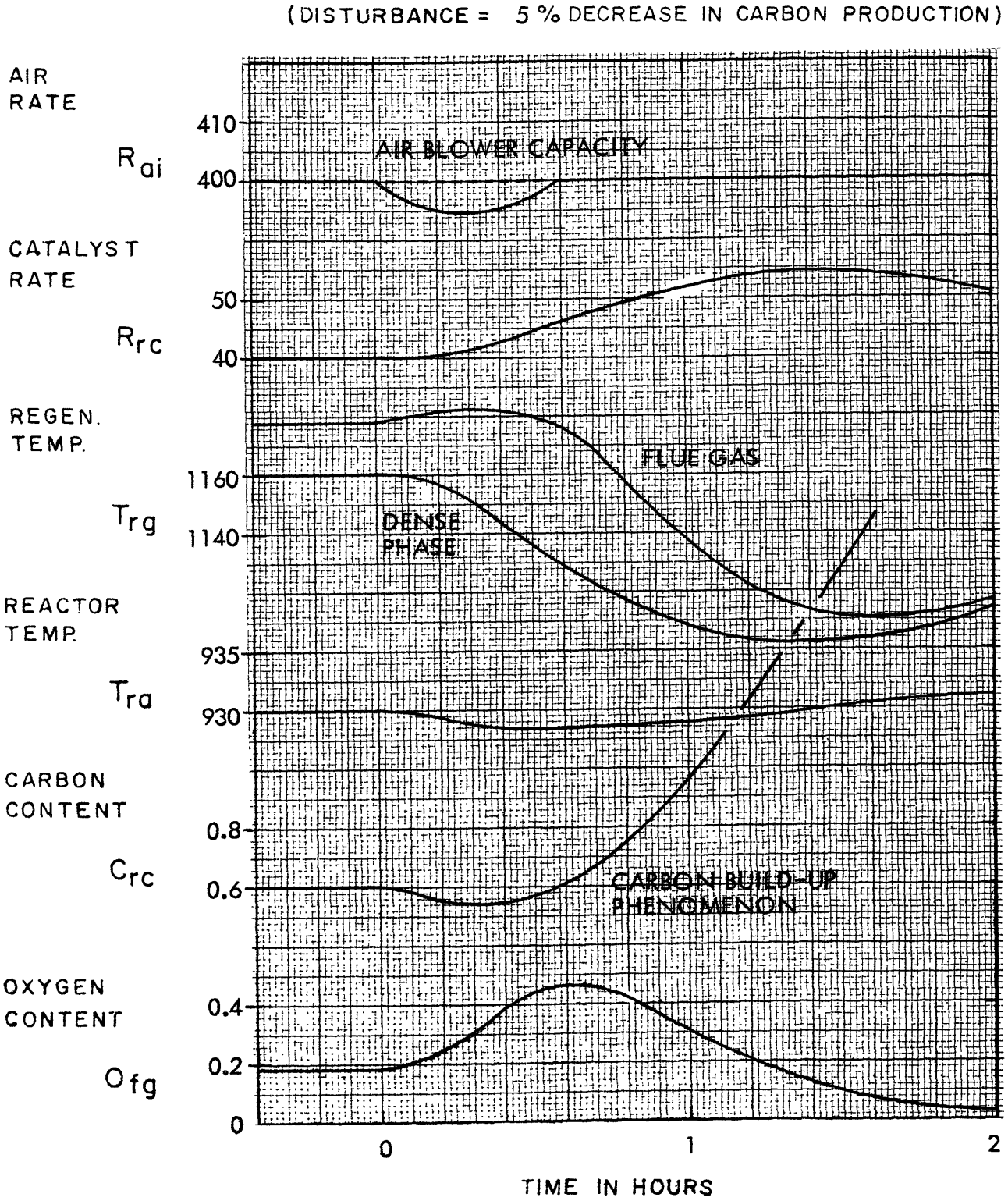

Fig. E.8 Performances of Flue Gas Temp. Control Scheme (No. 7)

heat requirement. In other words, since this system does not have any information feedback with respect to the regenerator temperature, the resulting variations in the regenerator temperature can be a main cause for upsets. As was shown in Fig. D.6, the excessively high regenerator and flue-gas temperatures can not recover by themselves.

Figure E.9 shows the performances when the feed rate is suddenly decreased. The dynamic behavior will be explained by the following step-by-step-analysis:

1. The reduced feed rate increases the reactor and regenerator temperatures.

2. The increased regenerator temperature reduces the oxygen level by means of increased conversion of oxygen, which in turn reduces the catalyst rate by means of the controller.

3. The reduced catalyst rate accelerates the regenerator temperature to increase.

As was shown in Fig. E.9, although the oxygen level is recovered to an original level, the regenerator and the flue gas temperatures remain at excessively high levels.

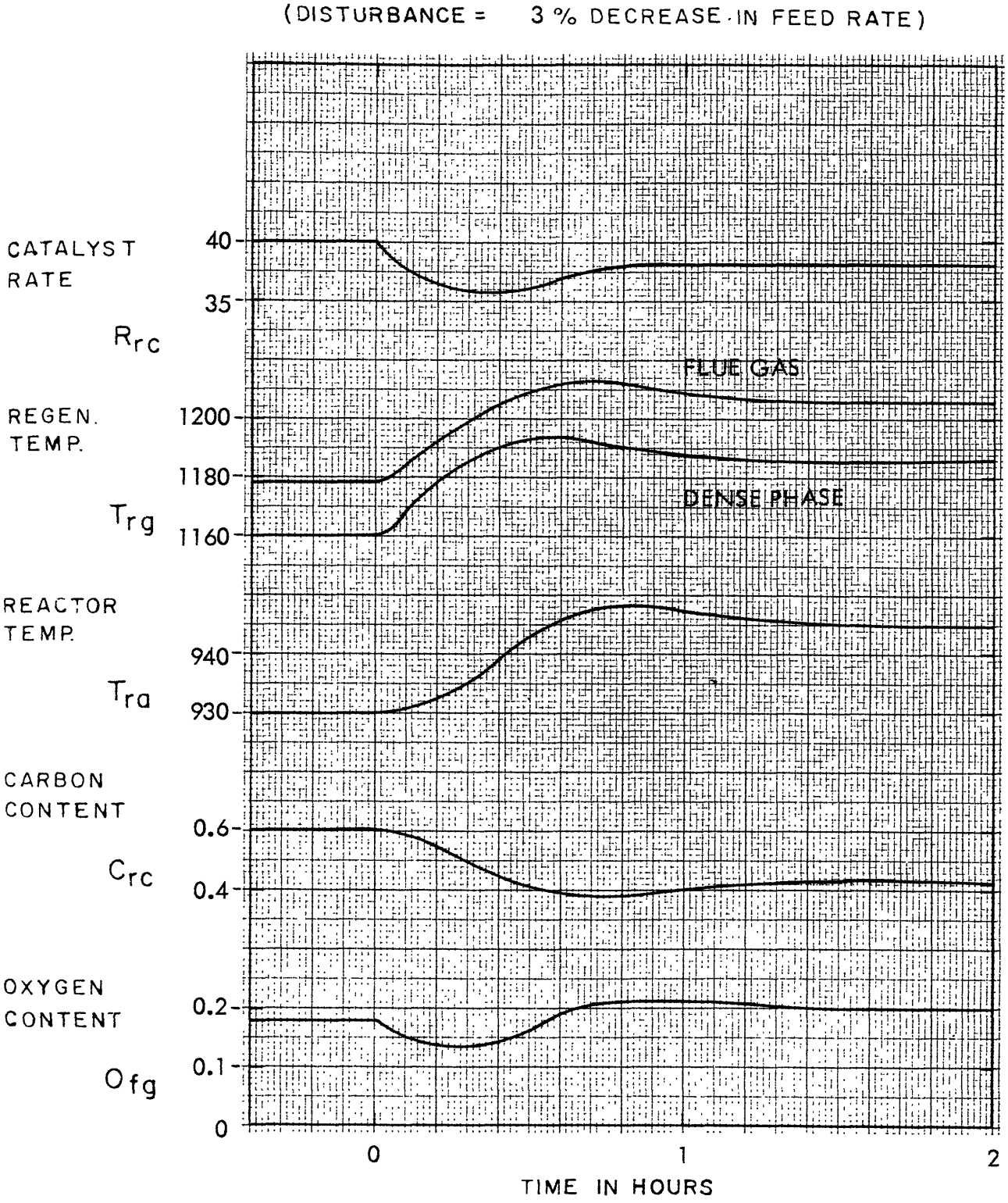

Fig. E.9 Performances of Alternative Oxygen Control System

APPENDIX F

ECONOMIC, YIELD, AND SAFETY MODELS

In order to formulate an optimization problem of FCC, it is necessary to define an objective function and several constraints on dependent variables. Obviously there does not exist any objective function which is valid and adequate for all purposes. Therefore the objectives of the following discussions are to derive a simple example of objective function and, together with the yield and safety model, to provide a basis for the formulation of the optimization problem.

Economic Models

The underlying objective in operating an FCC is to realize maximum profitability. Because of the nature of the process, the plant management might conclude that maximum profitability is synonymous with maximum product value. As far as the operation of the unit which was already constructed is concerned, organization costs, which are due to expenses for directive personnel, physical equipment, and other services or facilities, are relatively independent of the rate of production. If the unit is operated at almost full capacity, then operating costs (excluding raw material costs) or utility costs such as fuel gas, steam, and catalysts are relatively constant. Determining economic factors which govern the operation of the unit include the price structure of products and of raw materials, and market structure (e.g., gasoline demand, fuel oil demand, etc.). Which structure, price or market, is really controlling the operation depends on the situation confronted by the refinery. Here a simplifying, but still realistic, assumption is introduced: the refinery operations are production-limited rather than market-limited. In other words, the price structure is a predominant economic factor which really governs the operation of the unit. In fact, most of the incentives for the improved operation of FCC are found in this situation.[12, 25, 37, 62]

Product value is defined as the sum of the flow rates of all of the product streams multiplied by their respective unit values, expressed for example in dollars per barrel,with the corresponding value of the plant feed subtracted from the sum. In the interest of simplicity, some of the streams will be combined. All unit values and combined unit values may be considered adjustable parameters which can be adjusted from the measurements of flow ratios and stream qualities if desired. Typical unit values will be 4.59 for gasoline, 3.68 for light cycle oil, 3.61 for polymerization unit feed, 2.97 for decant oil, 2.97 for fuel oil equivalent fuel gas, and 3.15 for fresh feed.[17] In the interest of simplicity, light cycle oil and decant oil may be combined to be "cycle oil," and polymerization unit feed and fuel gas are combined to be "gas" since their combined unit values (or yield ratios) are relatively insensitive to operational changes.

Simplifying the product structure such that a fresh feed is converted into gas, gasoline, cycle oil, and coke, which has zero unit value, the following economic objective function is derived:

$$P_{gr} = \int_0^t \frac{R_{ff}}{(24)} \{(42) D_{ff} Y_{gs} P_{gs} + Y_{g\ell} P_{g\ell} + Y_{co} P_{co} - P_{ff}\} \, dt \qquad (F.1)$$

where

P_{gr} = gross profit

P_{gs} = price of gas

$P_{g\ell}$ = price of gasoline

P_{co} = price of cycle oil

P_{ff} = price of fresh feed

R_{ff} = fresh feed rate

D_{ff} = density of fresh feed

Y_{gs} = gas yield

$Y_{g\ell}$ = gasoline yield

Y_{co} = cycle oil yeild

(24) = (24 hr./day)

(42) = (42 gal./bbl.)

Yield Models

The usual investigation for product distribution on a given feed involves holding the reactor temperature, recycle ratio, and catalyst activity constant, and then changing space velocity or catalyst rate to change conversion over the range of 40 to 80 percent. The gasoline vs. conversion relation demonstrates the importance of recycle ratio on gasoline yield at a given conversion.[57,69] If the cracking severity is sufficient to produce high conversion per pass (i.e., little or no recycle), gasoline yield actually decreases with increasing conversion due to cracking of the gasoline into gas before the products leave the reaction zone. Therefore, there exists an optimal conversion which produces maximum gasoline yield for a sufficiently low recycle rate. Although it is possible to construct a curve-fitting type model from the above characteristics of gasoline yield, it may be desirable to develop an analytical model for the purpose of generality.

Blanding[10] found that a cracking rate of a reactant is nearly proportional to its partial pressure and that the higher the molecular weight, the higher the cracking velocity constant. Therefore, consider the following simple models:

$$A \xrightarrow{r_a} aB + \text{gas} + \text{coke} \qquad \text{(F.2)}$$

$$B \xrightarrow{r_b} \text{gas} + \text{coke} \qquad \text{(F.3)}$$

where A = gas oil as a reactant

a = (hypothetical) stoichiometric coefficient

B = gasoline as a reactant

r_a = cracking rate for A

r_b = cracking rate for B

Assuming that the cracking rate of a reactant is a function of its concentration, and that reactants pass through the bed as a "plug flow,"

$$dn_a/d\theta_o = -r_a(n_a) \tag{F.4}$$

$$dn_b/d\theta_o = ar_a(n_a) - r_b(n_a) \tag{F.5}$$

where n_a = No. of moles of A present

n_b = No. of moles of B present

θ_o = residence time of feed stream

Dividing Eq. F.5 by Eq. F.4 results in

$$dn_b/dn_a = -a + r_b(n_b)/r_a(n_a) \tag{F.6}$$

Define the gasoline recracking intensity by

$$I_{g\ell} = \{r_b(n_b)/n_b\}/\{r_a(n_a)/n_a\} \tag{F.7}$$

which characterizes the tendency of gasoline cracking relative to that of gas oil cracking. Since the molecular weight of gasoline is smaller than that of gas oil, the gasoline recracking intensity is expected to be less than one.

Substituting Eq. F. 7 into Eq. F. 6,

$$dn_b/dn_a = -a + I_{g\ell}\, n_b/n_a \tag{F.8}$$

integration of Eq. F.8 results in

$$\frac{n_b}{n_{ao}} = \frac{a}{1-I_{g\ell}} \left\{ \left(\frac{n_a}{n_{ao}} \right)^{I_{g\ell}} - \frac{n_a}{n_{ao}} \right\} \qquad (F.9)$$

where n_{ao} = original number of moles of A. In the above idealized situation, it is possible to express conversion and gasoline yield by

$$C_{tf} = C_{ff}/(1+R_r) = 1-n_a/n_{ao} \qquad (F.10)$$

$$Y_{g\ell} = (n_b/n_{ao})(1+R_r) \qquad (F.11)$$

where C_{tf} = fractional conversion on total feed

C_{ff} = fractional conversion on fresh feed

R_r = recycle ratio

Substituting Eqs. F.10 and F.11 into Eq. F.9, a gasoline yield is expressed by

$$Y_{g\ell} = (1+R_r)\left\{ \frac{F_{g\ell}}{1-I_{g\ell}} (1-C_{tf})^{I_{g\ell}} - (1-C_{tf}) \right\} \qquad (F.12)$$

where $F_{g\ell}$ = gasoline yield factor of catalyst (=a).

Figure F.1 shows a typical relation between gasoline yield and conversion for no recycle. It is clearly observed that there exists an optimal conversion which produces maximum gasoline yield, which in turn depends on the gasoline recracking intensity. Therefore the gas oil cracking is characterized by the consecutive nature of reaction step. Figure F.2 shows the relation for recycle. As the recycle ratio increases, an optimal conversion shifts to the higher level, which is a very realistic phenomenon. Unknown parameters, $F_{g\ell}$ and $I_{g\ell}$, will be estimated from any realistic data. Using the data of Pohlenz,[57] $F_{g\ell} = 1.0$ and $I_{g\ell} = 0.9$ were used throughout the study.

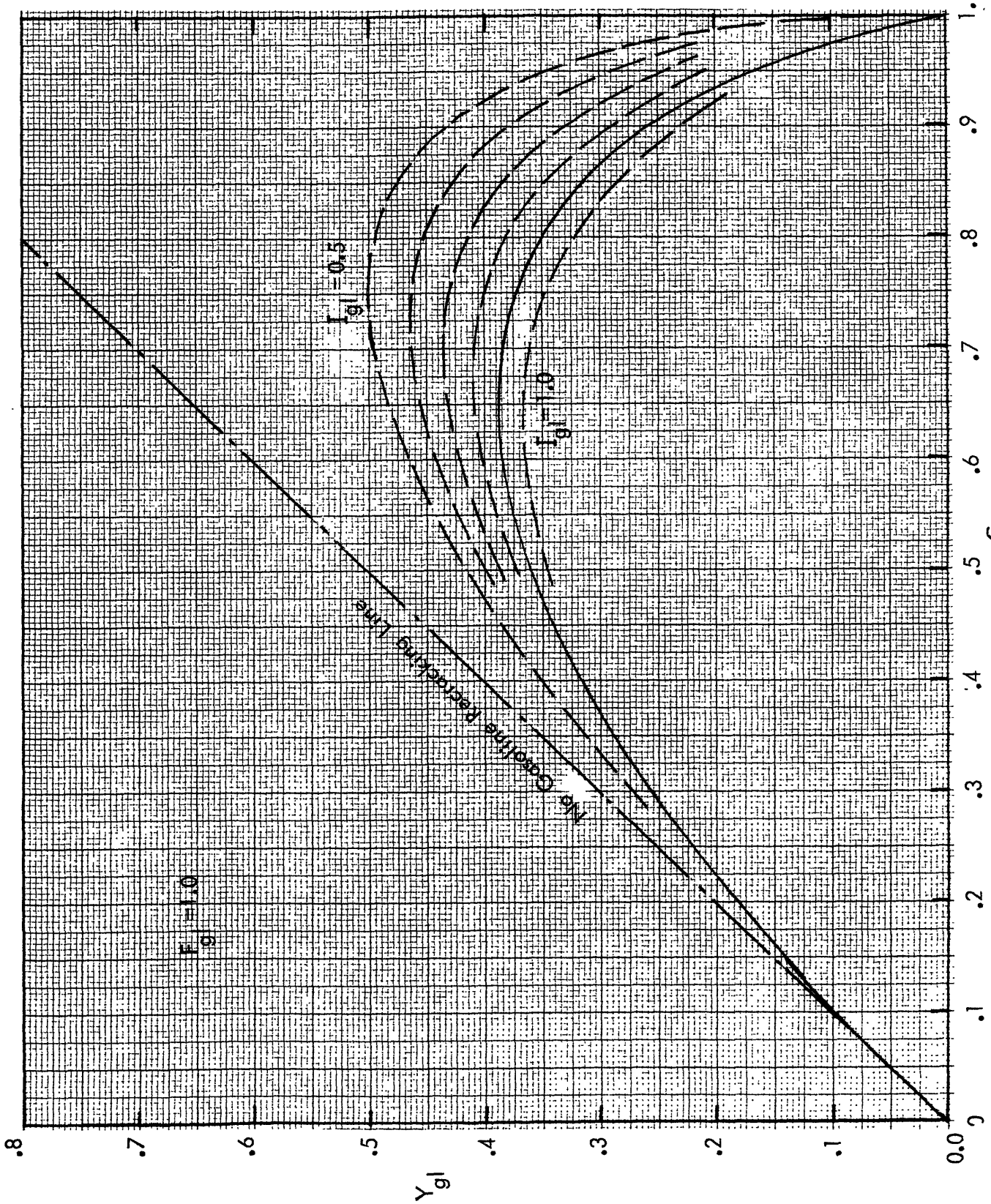

Fig. F.1 Gasoline Yield without Recycle

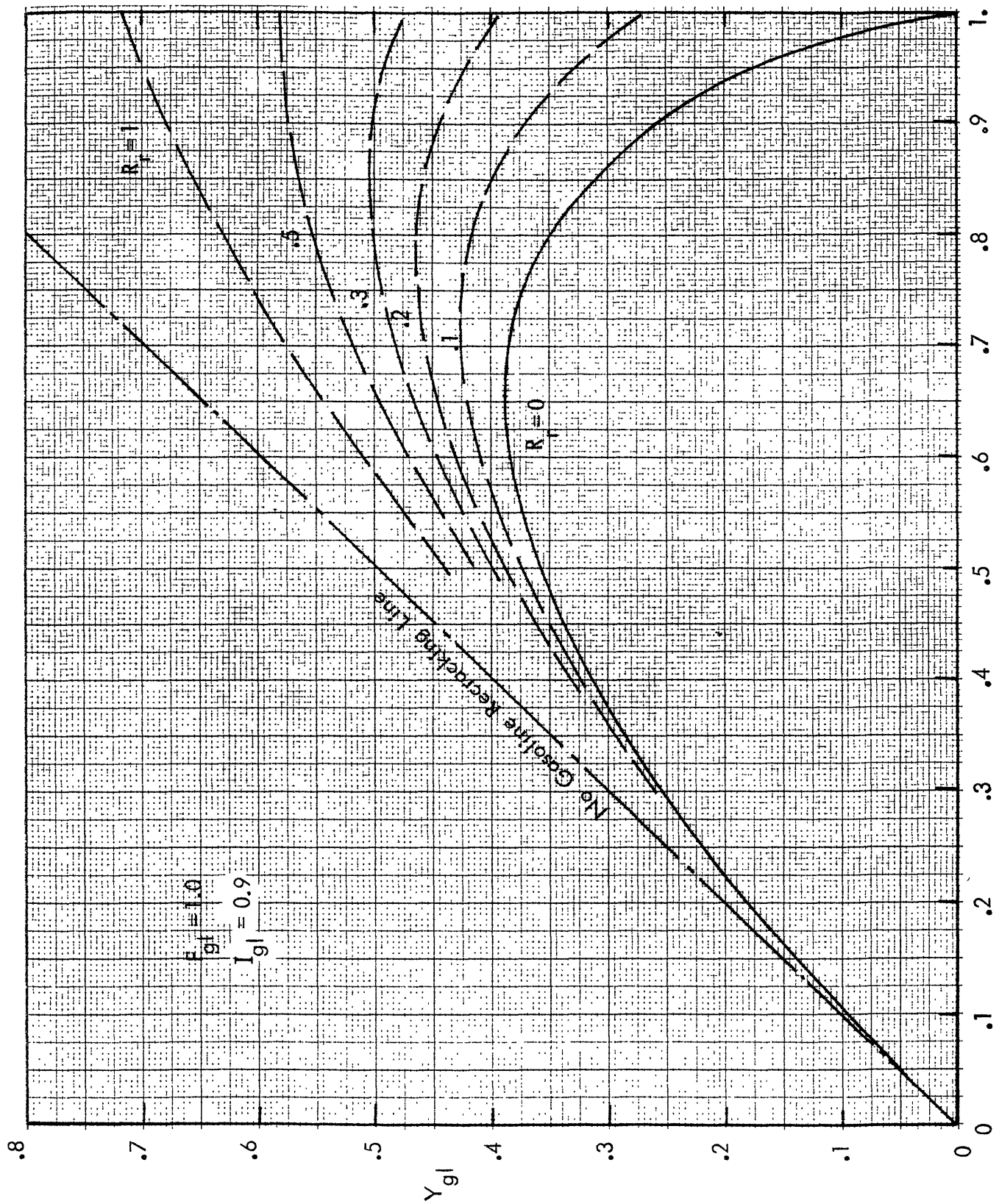

Fig. F.2 Gasoline Yield with Recycle

A cycle oil yield is quite simple, since it corresponds to unconverted gas oil, and is expressed by

$$Y_{co} = 1-C_{ff} \qquad (F.13)$$

A coke yield is related to the carbon forming rate as follows:

$$Y_{ck} = (.571)\, R_{cf}/R_{ff}D_{ff} \qquad (F.14)$$

where (.571) = (24 hr./day)/(42 gal./bbl.)

Assuming that the rest of the gas oil goes to gas completely from the material balance of products, a gas yield is expressed by

$$Y_{gs} = 1-Y_{g\ell}\, D_{g\ell}/D_{ff} - Y_{co}D_{co}/D_{ff} - Y_{ck} \qquad (F.15)$$

Equations F.12, F.13, F.14, and F.15 consist of a complete set of yield models, and together with Eq. F.1 they complete an economic objective function.

Safety Models

Optimization problems require not only an economic objective function but also the identification of constraints on dependent variables. Several constrained dependent variables require particular consideration in the operation of FCC. They are the reactor and regenerator temperatures, which are subject to upper bounds for reasons of safety. The flue gas oxygen level is of critical importance. It should be kept below maximum level in order to ensure that excessive combustion of carbon monoxide will not take place in the cyclone separator of the regenerator. Also the carbon content in the catalyst must be kept below a certain level. According to Smith,[64] excessively high carbon on the regenerated catalyst leads to low catalyst activity, high coke make, and low selectivity to gasoline; and excessively high carbon on the spent catalyst leads to high surface temperatures

during regeneration and more rapid permanent deactivation of the catalyst. Also a capacity limitation of the down stream processing units may affect the operation.

Among the several constraints on dependent variables, the ones on regenerator temperature and on oxygen level are primarily important.* In fact, the reactor temperature is normally observed far below its safety limit.** Therefore, although not always sufficient, the study assumed that the principal safety models are expressed by the following inequalities:

$$T_{rg} \leq (T_{rg})_{max} \tag{F.16}$$

$$O_{fg} \leq (O_{fg})_{max} \tag{F.17}$$

where $(T_{rg})_{max}$ = allowable maximum regenerator temperature

$(O_{fg})_{max}$ = allowable maximum oxygen level.

---

* The regenerator temperature is normally limited by 1,150°F for carbon-steel cyclones and by 1,200°F for stainless-steel or other alloy cyclones.[51] The oxygen level is normally limited by 0.2-0.4 percent depending on the conditions.

** The reactor temperature is normally limited not by its own safety, but by the maximum regenerator temperature. Other factors might be alkylation capacity, gas-compressor capacity, etc.[51]

APPENDIX G

FORMULATION OF OPTIMAL CONTROL PROBLEMS

The following are brief descriptions of the optimal control problem and the theorem on which the study is based. The maximum principle of Pontryagin was formulated to solve the class of problems to which this study was restricted. More rigorous and mathematical manipulations will be found elsewhere (see Refs. 6 and 58).

The Optimal Control Problem

In recent years great attention has been given to the theory of optimal control.[6, 39, 58, 60] The theory supposes that a plant can be described by a set of ordinary differential equations

$$\dot{\underline{x}} = \underline{f}(\underline{x}, \underline{u}, t) \qquad (G.1)$$

where $\underline{x}$ represents a vector of state variables (dependent variables) and $\underline{u}$ represents a vector of control variables (independent variables). An objective functional (or performance criterion), which may consist of profit, cost, or other artificial measures of performance of operating the plant from time $t = 0$ to $t = t_1$, is given by

$$J(\underline{u}, \underline{x}_0, \underline{x}_1, t_o, t_1) = K(\underline{x}_0, \underline{x}_1) + \int_{t_0}^{t_1} L(\underline{x}, \underline{u}, t)dt \qquad (G.2)$$

where

K = arbitrary function

L = arbitrary function

$\underline{x}_0$ = vector of initial condition

$\underline{x}_1$ = vector of final condition

t_0 = initial time

t_1 = final time

Optimal control theory asks how $\underline{u}$ should be chosen as a function of t, $t_0 \leq t \leq t_1$, in order to make the objective functional J a maximum (or a minimum). The control vector $\underline{u}$ is often restricted to lie in a closed bounded region U.

Necessary Conditions for Optimality

Once the problem has been suitably posed, the optimal control can be derived by the mathematical techniques such as the maximum principle of Pontryagin.[58] First, the problem of optimizing an objective functional, Eq. G.2, while observing Eq. G.1 as constraints, can be reduced to the problem of optimizing the following Lagrangean functional with respect to $\underline{x}_1$ and $\underline{u}$.

$$\mathcal{L}(\underline{x}, \underline{p}, \underline{u}, \underline{x}_0, \underline{x}_1, \underline{p}_0, \underline{p}_1, t_0, t_1) = J(\underline{u}, \underline{x}_0, \underline{x}_1, t_0, t_1) + \int_{t_0}^{t_1} \underline{p}'\{\underline{f}(\underline{x}, \underline{u}, t) - \dot{\underline{x}}\}\, dt \qquad (G.3)$$

where $\underline{p}$ represents a vector of costate variables (or Lagrange multipliers). Rearranging the second term of Eq. G.3 by integrating by parts reduces Eq. G.3 to

$$\mathcal{L}(\underline{x}, \underline{p}, \underline{u}, \underline{x}_0, \underline{x}_1, \underline{p}_0, \underline{p}_1, t_0, t_1) = K(\underline{x}_0, \underline{x}_1) + \int_{t_0}^{t_1} H(\underline{x}, \underline{p}, \underline{u}, t)dt$$

$$+\underline{p}'(t_0)\underline{x}(t_0) - \underline{p}'(t_1)\underline{x}(t_1) + \int_{\underline{p}(t_0)}^{\underline{p}(t_1)} \underline{x}'d\underline{p} \qquad (G.4)$$

where $$H(\underline{x}, \underline{p}, \underline{u}, t) = L(\underline{x}, \underline{u}, t) + \underline{p}'\underline{f}(\underline{x}, \underline{u}, t) \qquad (G.5)$$

which is called a "Hamiltonian function."

The necessary condition for $\mathcal{L}$ to be extremal with respect to $\underline{x}$, is obtained by resetting the variation of $\mathcal{L}$ with respect to $\underline{x}$ to zero as follows:

$$\delta\mathcal{L}(\underline{x}) = \int_{t_0}^{t_1} (\partial H/\partial \underline{x} + \dot{\underline{p}})\,\delta\underline{x}\, dt = 0$$

or $$\dot{\underline{p}} = -\partial H/\partial x \qquad (G.6)$$

The variations of $\mathcal{L}$ with respect to $\underline{x}_0$ and $\underline{x}_1$ are

$$d\mathcal{L}/d\underline{x}_0 = dK/d\underline{x}_0 + \underline{p}(t_0) \qquad (G.7)$$

$$d\mathcal{L}/d\underline{x}_1 = dK/d\underline{x}_1 - \underline{p}(t_1) \qquad (G.8)$$

If $\underline{x}_0$ or $\underline{x}_1$ is free, then the necessary condition for $\mathcal{L}$ to be extremal with respect to $\underline{x}_0$ or $\underline{x}_1$ is obtained by setting Eqs. G.7 or G.8 to zero.

The variations of $\mathcal{L}$ with respect to t_0 and t_1 are

$$d\mathcal{L}/d\,t_0 = -H(t_0) \qquad (G.9)$$

$$d\mathcal{L}/d\,t_1 = H(t_1) \qquad (G.10)$$

If t_0 or t_1 is free, then the necessary condition for $\mathcal{L}$ to be extremal with respect to t_0 or T_1 is obtained by setting Eqs. G.9 or G.10 to zero.

The variation of $\mathcal{L}$ with respect to $\underline{u}$ is

$$\delta\mathcal{L}(\underline{u}) = \int_{t_0}^{t_1} (\partial H/\partial \underline{u})' \delta \underline{u} \, dt \qquad (G.11)$$

Therefore the necessary condition for $\mathcal{L}$ to be extremal with respect to u_i is

$$\partial H/\partial u_i = 0 \qquad (G.12)$$

or u_i is on the boundary. Equation G.11 is the basis of the method of steepest ascent of the Hamiltonian.

Fixed Time, Free End Problem

The problem is to determine the control $\underline{u}$ which maximizes the objective functional

$$J(\underline{u}, \underline{x}_1) = K(\underline{x}_1) + \int_0^{t_1} L(\underline{x}, \underline{u}, t) \, dt \qquad (G.13)$$

under the following conditions:

1. The state equations are Eq. G.1.
2. Initial conditions are specified by $\underline{x}(0) = \underline{x}_0$.
3. End conditions are not specified, but are free.

The maximum principle for this problem is: In order that $\underline{u}$ be optimal for the problem stated above, it is necessary that a vector function $\underline{p}$ exists such that:

1. $\underline{p}$ is a solution of the costate equations, Eq. G.6, satisfying the boundary conditions Eq. G.8

2. The Hamiltonian function, Eq. G.5, has an absolute maximum as a function of $\underline{u}$, i.e.,

$$\max_{\underline{u}} H(\underline{x}, \underline{p}, \underline{u}, t) = H^* \qquad \text{(G.14)}$$

APPENDIX H

STRUCTURE OF OPTIMAL FEEDBACK CONTROL LAWS

An optimal feedback control structure is derived from the principle of optimality: an optimal policy has the property that whatever the previous state and previous decision are, the remaining decision must constitute an optimal policy with respect to the state resulting from the previous decision.

Consider a time-invariant system

$$\dot{\underline{x}} = \underline{f}(\underline{x}, \underline{u}) \tag{H.1}$$

$$\underline{y} = \underline{g}(x) \tag{H.2}$$

with a time-invariant objective functional

$$J(\underline{u}) = \int_{t_0}^{t_1} L(\underline{x}, \underline{u})\,dt \quad \text{with} \quad \underline{x}(t_0) = \underline{x}_0 \tag{H.3}$$

Principle of Optimality

Express the optimal control solution for Eq. H.3 by

$$\underline{u} = \underline{u}_1^* (\underline{x}_0,\ t_1 - t) \tag{H.4}$$

$$\underline{x} = \underline{x}^* (\underline{x}_0,\ t_1 - t) \tag{H.5}$$

where $t_0 \leq t \leq t_1$. Now consider a new optimal control problem where an objective function is expressed by

$$J(\underline{u}) = \int_{t}^{t_1} L(\underline{x}, \underline{u})\,d\tau \quad \text{with} \quad \underline{x}(t) = \underline{x}^* (\underline{x}_0, t_1 - t) \tag{H.6}$$

Then, according to the principle of optimality,

$$\underline{u}^*(\underline{x}_0, t_1-\tau) = \underline{u}^*\{\underline{x}^*(\underline{x}_0, t_1-t), t_1-\tau\}$$

where $t \leq \tau \leq t_1$. (H.7)

Especially setting $\tau = t$, Eq. H.7 is reduced to

$$\underline{u}^*(\underline{x}_0, t_1-t) = \underline{u}^*\{\underline{x}^*(\underline{x}_0, t_1-t), t_1-t\} \quad \text{(H.8)}$$

If t_1 is an infinity, then Eq. H.8 is further reduced to, for $0 \leq t \ll t_1$,

$$\underline{u}^*(\underline{x}_0) \doteq \underline{u}^*\{\underline{x}^*(\underline{x}_0)\}$$

or simply $$\underline{u}^* = \underline{u}^*(\underline{x}^*) \quad \text{(H.9)}$$

Therefore, optimal control solutions Eqs. H.4 and H.5 are related to each other along the optimal trajectory, as follows:

$$\underline{u} = \underline{h}_1(\underline{x}) \quad \text{(H.10)}$$

This is a so-called optimal feedback control structure.

Optimal Feedback Control Law

In order to construct a practical optimal feedback control law, it is necessary to express the control law in terms of measurable variables $\underline{y}$ rather than state variables $\underline{x}$. This can be done using Eq. H.2. Assuming the existence and uniqueness of the inverse function, the control law results in an optimal feedback control law as follows:

$$\underline{u} = \underline{h}_2(\underline{y}) \quad \text{(H.11)}$$

Kalman's Optimal Linear Regulator

As an example of optimal feedback control, Kalman's linear regulator will be described. The basic results for this problem are as

follows: Consider the linear system

$$d\underline{x}/dt = \underline{A}\,\underline{x} + \underline{B}\,\underline{u} \tag{H.12}$$

and the cost functional

$$J(\underline{u}) = \int_0^\infty (\underline{x}'\underline{Q}\,\underline{x} + \underline{u}'\underline{R}\,\underline{u})\, dt \tag{H.13}$$

with the assumptions that the matrices $\underline{Q}$ and $\underline{R}$ are positive definite. Then, the optimal control $\underline{u}^*$ which minimizes the cost functional Eq. H.13 exists, is unique, and is given by the equation

$$\underline{u}^* = -\underline{R}^{-1}\,\underline{B}'\,\underline{K}\underline{x} \tag{H.14}$$

where $\underline{K}$ is the symmetric and positive definite solution of the matrix algebraic equation

$$-\underline{K}\,\underline{A} - \underline{A}'\underline{K} + \underline{K}\,\underline{B}\,\underline{R}^{-1}\underline{B}'\underline{K}' - \underline{Q} = 0 \tag{H.15}$$

As shown in Eq. H.14, the above results can be used to design optimal linear feedback systems.

The principal disadvantages of the Kalman's method, when it is applied to chemical process control, are expected to be as follows:

1. It is frequently found that a chemical process is difficult to express in the form of Eq. H.12 because of high nonlinearities and cross multiplications of variables. Therefore, the method is always subject to critical evaluation with respect to the range where the assumption of linearization is valid.

2. It is frequently found that an objective function of chemical process is difficult to express in the quadratic form of Eq. H.13, since the former is affected by profitability and plant safety in a complex manner.

3. It is frequently found that some of the variables in a chemical process can not be measured continuously or at least instantaneously. Therefore, the Kalman's method, which assumes complete freedom for the selection of variables, has a serious limitation.

APPENDIX I

GENERAL CONCEPTS FOR OPTIMAL OPERATIONS OF FCC

Some aspects of optimal operations of FCC are briefly described here in order to support the basic issue of "optimal control of FCC;" that is, "to what conditions are we controlling the FCC optimally?"

Determination of steady-state optimal condition of FCC is, in general, a problem of nonlinear programming which has many independent variables and many dependent variables with many constraints to be observed. Although some nonlinear programming problems with relatively few independent variables can be solved by means of "hill climbing" or "steepest ascent," these techniques are by themselves, generally not the most efficient way for optimization of FCC. Repetition of linearization and linear programming[12,25,37,62] or combined repetition of linear programming and steepest ascent[63] have been used with some success.

Although the optimal conditions of FCC can be determined at least numerically and iteratively, these optimal conditions are not fully understood nor interpreted yet qualitatively. The purpose of this Appendix is as follows:

1. To interpret the optimal conditions qualitatively.
2. To derive several useful criteria for optimal operations.

Throughout this Appendix the following variables are not taken into consideration in the interest of simplicity:

1. Catalyst addition rate
2. Reactor pressure
3. Reactor steam rate
4. Fractionator adjustment or recycle feed rate
5. Down stream processing capacity such as alkylation.

Therefore, all discussion in this Appendix must be considered conditional.

Problem Formulation

Utilizing all reactor kinetic and yield equations, a steady-state profit rate (P_s) can be expressed by

$$P_s = P_s[T_{ra}, C_{rc}, R_{rc}, H_{ra}, R_{ff}] \tag{I.1}$$

Similarly, a gas rate to compressor is expressed by

$$R_{gs} = R_{gs}[T_{ra}, C_{rc}, R_{rc}, H_{ra}, R_{ff}] \tag{I.2}$$

Steady-state carbon balance is

$$R_{cf} - R_{cb} = 0 \tag{I.3}$$

where
$$R_{cf} = R_{cf}[T_{ra}, R_{rc}, H_{ra}, R_{ff}] \tag{I.4}$$

$$R_{cb} = R_{cb}[R_{ai}, O_{fg}] \tag{I.5}$$

$$O_{fg} = O_{fg}[C_{rc}, T_{rg}, R_{ai}] \doteq O_{fg}[C_{rc}, T_{rg}] \tag{I.6}$$

(where the direct effect of R_{ai} on O_{fg} is limited unless the performance of fluidization changes significantly.)

From a reactor heat balance, a reactor temperature is expressed by

$$T_{ra} = T_{ra}[T_{rg}, C_{rc}, R_{rc}, H_{ra}, T_{fp}, R_{ff}]$$

$$\doteq T_{ra}[T_{rg}, R_{rc}, T_{fp}, R_{ff}] \tag{I.7}$$

where direct effects of C_{rc} and H_{ra} on T_{ra} are limited since "heat of cracking" is relatively small.

From a regenerator heat balance, a catalyst circulation rate is expressed by

$$R_{rc} = R_{rc}[T_{ra}, T_{rg}, R_{cb}, R_{ai}] \doteq R_{rc}[T_{ra}, T_{rg}, R_{cb}] \qquad (I.8)$$

where the direct effect of R_{ai} on R_{rc} is limited since "specific heat of air" is relatively small.

Constraints for independent variables are

$$R_{ai} \leq (R_{ai})_{max} \text{ (blower capacity limit)} \qquad (I.9)$$

$$(H_{ra})_{min} \leq H_{ra} \leq (H_{ra})_{max} \qquad (I.10)$$

(grid and cyclone efficiency consideration)

$$T_{fp} \leq (T_{fp})_{max} \text{ (gas firing capacity)} \qquad (I.11)$$

$$R_{ff} \leq (R_{ff})_{max} \text{ (feed stock or upper stream capacity)} \qquad (I.12)$$

Constraints for dependent variables are

$$T_{rg} \leq (T_{rg})_{max} \text{ (regenerator safety)} \qquad (I.13)$$

$$O_{fg} \leq (O_{fg})_{max} \text{ (regenerator safety)} \qquad (I.14)$$

$$R_{gs} \leq (R_{gs})_{max} \text{ (gas compressor capacity)} \qquad (I.15)$$

We have five apparently independent variables, i.e., R_{ai}, R_{rc}, H_{ra}, T_{fp}, and R_{ff}. Therefore the problem is essentially a "five-parameter maximization problem."

Mathematically, eliminating T_{ra}, T_{rg}, C_{rc}, O_{fg}, R_{cf}, and R_{cb} from Eqs. I.1, I.3 through I.8, the profit rate is expressed by

$$P_s = P_s[R_{ai}, R_{rc}, H_{ra}, T_{fp}, R_{ff}] \qquad (I.16)$$

The problem is: maximize Eq. I.16 while observing constraints Eq. I.9 through Eq. I.15.

Now we are ready to derive several optimal operating criteria. We know that the optimal points of continuous function lie on the peaks or

on the boundaries. If our functions are such that the optimal points lie only on the boundaries, then five of seven constraints Eq. I.9 through Eq. I.15 must be satisfied on the boundaries.

The following optimal operating criteria are the results of the steady state simulation study, where marginal profitability are evaluated for each operating condition in order to determine which boundary the optimal condition is located. This simulation study was essentially conducted with the use of an adaptive optimizing scheme, the design of which will be discussed later.

Optimal Operating Criterion I

If the following conditions are satisfied:

1. gas compressor capacity is not limiting,
2. feed preheater is not limiting,

then the optimal conditions are

1. air blower capacity is max,
2. oxygen level is max,
3. regenerator temperature is max,
4. reactor catalyst holdup is min,
5. feed rate is max.

In order to interpret this criterion, R_{rc} and T_{fp} of Eq. I.16 are replaced by apparently independent variables T_{rg} and O_{fg} as follows:

$$P_s = P_s[R_{ai}, O_{fg}, T_{rg}, H_{ra}, R_{ff}] \qquad (I.17)$$

Let us examine each issue of the criterion by taking partial derivatives.

$$(1) \quad (\partial P_s/\partial R_{ai})_{O_{fg}, T_{rg}, H_{ra}, R_{ff}} > 0 \qquad \begin{matrix}\text{(order of (\$10/hr.)/} \\ \text{(10 M lb./hr.) for} \\ \text{100 M bbl./day capacity.)}\end{matrix} \qquad (I.18)$$

This implies that the higher the carbon burning capacity, the more cracking occurs.

$$(2) \quad (\partial P_s/\partial O_{fg})_{R_{ai}, T_{rg}, H_{ra}, R_{ff}} > 0 \quad \begin{matrix}(\text{order of } (\$5/\text{hr.})/ \\ (.05\%))\end{matrix} \tag{I.19}$$

This implies that the higher the oxygen level, the higher the gasoline vs. coke ratio, since the resultant low carbon level improves the selectivity.

$$(3) \quad (\partial P_s/\partial T_{rg})_{R_{ai}, O_{fg}, H_{ra}, R_{ff}} > 0 \quad \begin{matrix}(\text{order of } (\$7/\text{hr.})/ \\ (5^{\circ}\text{F}))\end{matrix} \tag{I.20}$$

This implies that the higher the regenerator temperature, the higher the gasoline vs. coke ratio, since the resultant low catalyst circulation rate improves the yield.

$$(4) \quad (\partial P_s/\partial H_{ra})_{R_{ai}, O_{fg}, T_{rg}, R_{ff}} > 0 \quad \begin{matrix}(\text{order of } -(\$7/\text{hr.})/ \\ (2 \text{ ton}))\end{matrix} \tag{I.21}$$

This implies that the lower the reactor catalyst level, the higher the gasoline vs. coke ratio, since the resultant high reactor temperature improves the yields.

$$(5) \quad (\partial P_s/\partial R_{ff})_{R_{ai}, O_{fg}, T_{rg}, H_{ra}} > 0 \quad \begin{matrix}(\text{order of } (\$70/\text{hr.})/ \\ (3 \text{ M bbl./day}))\end{matrix} \tag{I.22}$$

This implies that the higher the feed rate, the more cracking occurs.

Optimal Operating Criterion II

If the following conditions are satisfied:

1. gas compressor capacity is not limiting,
2. regenerator temperature is not limiting,

then the optimal conditions are:

1. air blower capacity is max,
2. oxygen level is max,
3. feed preheater is max,
4. reactor catalyst holdup is max,
5. feed rate is max.

In order to interpret this criterion, R_{rc} of Eq. I.16 is replaced by the apparently independent variable O_{fg} as follows:

$$P_s = P_s[R_{ai}, O_{fg}, T_{fp}, H_{ra}, R_{ff}] \tag{I.23}$$

Examination of each issue of the criterion is similar to that of "Criterion I," except as seen in items (3) and (4) as follows:

$$(3) \quad (\partial P_s/\partial T_{fp})_{R_{ai}, O_{fg}, H_{ra}, R_{ff}} > 0 \quad \begin{matrix}(\text{order of } (\$12/\text{hr.})/ \\ 10^{\circ}\text{F})\end{matrix} \tag{I.24}$$

This implies that the higher the feed preheater temperature, the higher the gasoline vs. coke ratio, since the resultant low catalyst circulation rate improves the yield.

$$(4) \quad (\partial P_s/\partial H_{ra})_{R_{ai}, O_{fg}, T_{fp}, R_{ff}} > 0 \quad \begin{matrix}(\text{order of } (\$2/\text{hr.})/ \\ (5 \text{ ton})\end{matrix} \tag{I.25}$$

Optimal Operating Criterion III

If the following conditions are satisfied:

1. air blower capacity is not limiting,
2. feed preheater is not limiting,

then the optimal conditions are

1. gas compressor capacity is max,
2. regenerator temperature is max,
3. oxygen level is max,
4. reactor catalyst holdup is min,
5. feed rate is max.

In order to interpret this criterion, R_{ai}, R_{rc}, and T_{fp} of Eq. I.16 are replaced by apparently independent variables R_{gs}, T_{rg}, and O_{fg} as follows:

$$P_s = P_s [R_{gs}, O_{fg}, T_{rg}, H_{ra}, R_{ff}] \tag{I.26}$$

Examination of each issue of the criterion is similar to that of "Criterion I," except as seen in item 1 as follows:

(1) $(\partial P_s/\partial R_{gs})_{O_{fg}, T_{rg}, H_{ra}, R_{ff}} > 0$ (order of ($30/hr.)/(2 M bbl.-equivalent/day))

This implies that the cracked gas has more value than the gas oil. (I.27)

Optimal Operating Criterion IV

If the following conditions are satisfied:

1. air blower capacity is not limiting,
2. regenerator temperature is not limiting,

then the optimal conditions are

1. gas comperssor capacity is max,
2. oxygen level is max,
3. feed preheater is max,
4. reactor catalyst holdup is max,
5. feed rate is max.

In order to interpret this criterion, R_{ai}, R_{rc} of Eq. I:16 are replaced by apparently independent variables R_{gs}, O_{fg} as follows:

$$P_s = P_s[R_{gs}, O_{fg}, T_{fp}, H_{ra}, R_{ff}] \qquad (I.28)$$

Examination of each issue of the criterion is similar to that of "Criterion II or III."

Use of Optimal Operating Criteria

The above criteria are idealized ones in the sense that it is assumed other mechanical conditions, such as catalyst circulation rate or gas velocity in the reaction vessels, are not limiting. Except for these limitations, the criteria provide the main goal of the adaptive otpimizing system, which keeps the criteria automatically in the face of unknown disturbances. This adaptive control system should be the final goal of the optimal control study.

An adaptive optimizing scheme for Criterion I is shown in Fig. I.1. This scheme essentially consists of the alternative control scheme developed in the study and an additional loop which regulates the regenerator temperature by the feed preheat temperature. If the air rate is manipulated by a proportional control, where the equilibrium point corresponds to the maximum regenerator temperature and the maximum air rate and where the preheater temperature is manipulated by an integral control, then this scheme is found by the use of dynamic simulation to be satisfactory in the sense that after any forced disturbance occurs this scheme can keep the optimal Criterion I always. For other criteria, similar studies were

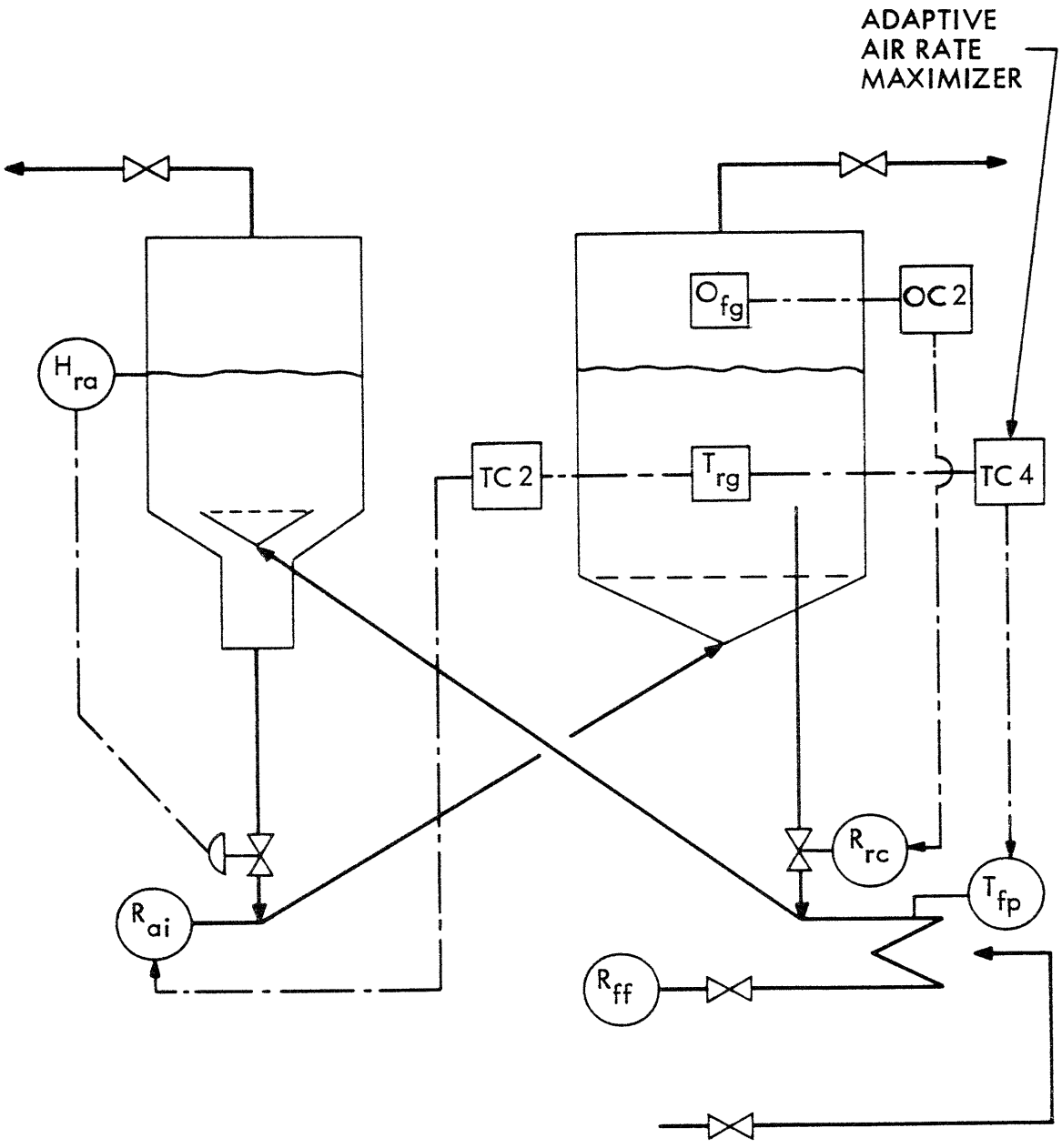

Fig. I.1 AnAdaptive Optimizing Scheme of FCC (Criterion I

done and found to be satisfactory,* but a critical evaluation of these adaptive optimizing schemes is obviously outside of the scope of this study.

---

* For Criterion II, an oxygen control by catalyst rate was used. For Criterion III, an optimizing scheme was used consisting of (1) oxygen control by catalyst rate, (2) regenerator temperature control (proportional) by air rate, (3) gas rate control (integral) by air rate, and (4) regenerator temperature control (integral) by feed preheater temperature. For Criterion IV, an optimizing scheme was used consisting of (1) oxygen control by catalyst rate, (2) regenerator temperature control (proportional) by air rate, and (3) gas rate control (cascade, integral) by regenerator temperature set point.

APPENDIX J

QUANTITATIVE COMPARISON OF CONTROL SYSTEM PERFORMANCE

This appendix provides additional data to evaluate the performance of the conventional control scheme and the alternative control scheme. In Sections 4.2 and 5.3, these control schemes were evaluated qualitatively. A quantitative evaluation of these control schemes helps to explain the relation between the objective function used to compute the optimal control policy and the quantitative performance observed in the simulated system.

Any objective function is at best an approximate representation of what one believes to be a realistic performance criterion. In this investigation the gross profit based on stream values was selected as a realistic criterion for evaluating the economic performance of the system. The total performance of the system will be judged satisfactory, however, only if all constraints are satisfied (i.e., regenerator temperature and oxygen content of the flue gas are within allowable limits). Therefore, the problem was formulated as an optimization problem with constraints where constraints were replaced by penalty functions of sufficient magnitudes. In this formulation, the objective function is not just the gross profit but consists of the gross profit and penalty functions.

Ideally, the penalty function should reflect the real economic penalty associated with violating a constraint. For example, the cost of exceeding the allowable regenerator temperature should be related to the increased probability of a regenerator failure. In practice, however, it is virtually impossible to obtain quantitative estimates of the probabilities of failure and it is even more difficult to assign costs associated with injury or loss of life by personnel. As a result, the penalty functions must be selected somewhat artificially.

The resulting performance of the system determined by dynamic optimization should be insensitive to the exact form of the penalty functions provided that the penalty is large enough to offset any economic advantage that might be gained by operating the process outside the constraints. The relative value of the objective function achieved for different operating conditions can be used to rank the performance of the system and, hence, select the best set of conditions. But numerical values of the objective function per se have no physical or economic significance.

In the light of the preceding qualifications, the following data will be useful to evaluate the performance of two control schemes in terms of the objective function. Figure J.1 supplements the results shown in Fig. 1.4, where the conventional control scheme was simulated for the perturbed initial condition. Although the instantaneous gross profit rate (P_{ig}) oscillates around the steady-state optimal level, the two penalty functions (P_{e1} and P_{e2}) penalized the objective function (L) and the resulting poor performance is apparent. Figure J.2 supplements results shown in Fig. 1.9, where the dynamic optimization was obtained for the same initial condition. Since the two penalty functions are negligibly small, for the optimal control the objective function remains at a highest level. The difference in performance between Figs. J.1 and J.2 is evident. Figure J.3 supplements the results shown in Fig. 1.14, where the alternative control scheme was simulated for the same initial condition. One can see easily that the performance of the alternative control scheme is quite close to that of the optimal control.

If step-type disturbances are introduced to the process, the comparison of performance is more complicated, since the disturbances may change the optimal steady-state operating conditions. Figure J.4 supplements the results shown in Fig. 1.5, where the conventional control scheme was simulated for a step increase in the rate of carbon production. Although the instantaneous gross profit rate oscillates around a level slightly lower than the previous steady-state optimal

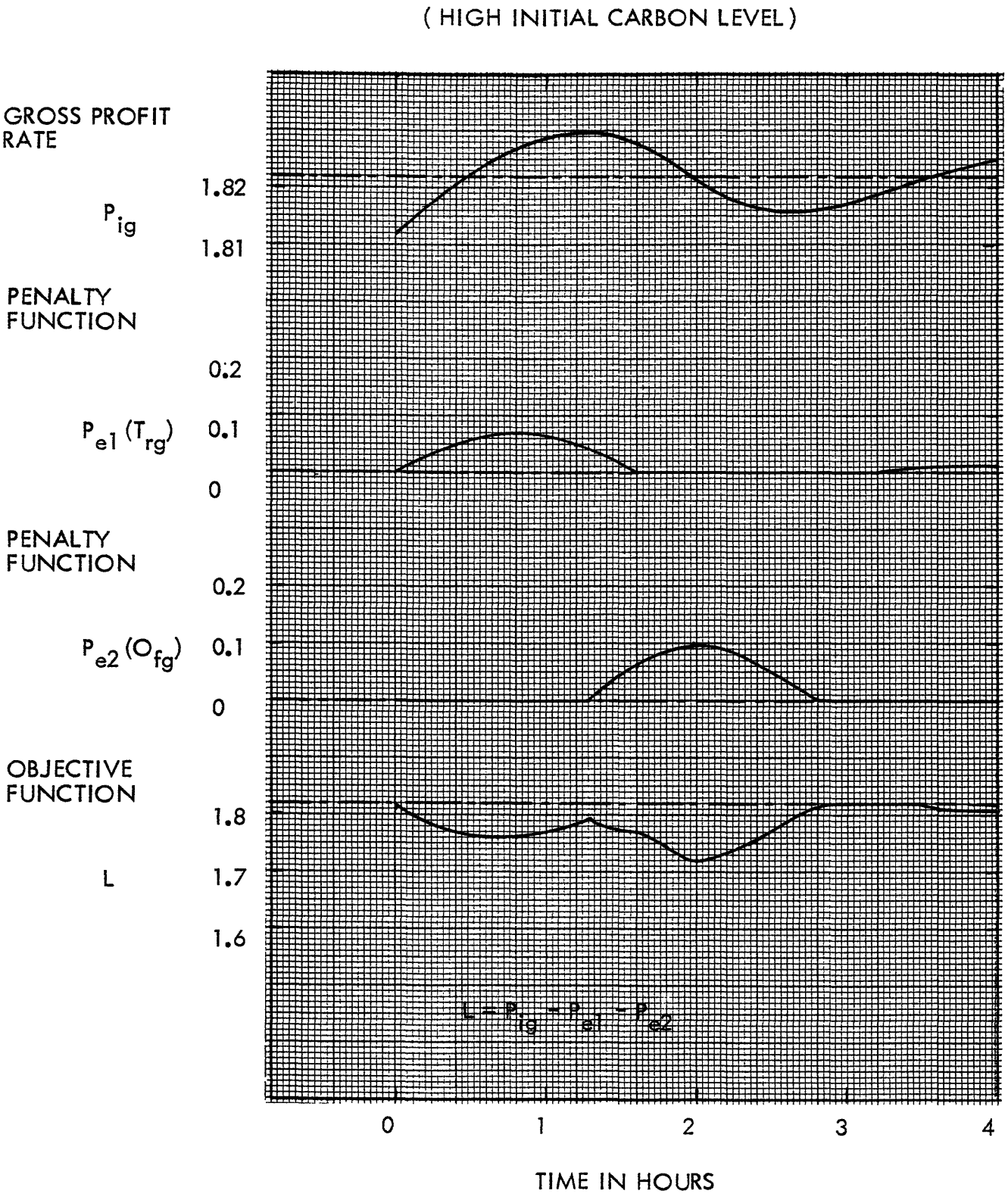

Fig. J.1 Conventional Control Scheme for Initial Condition No. 1

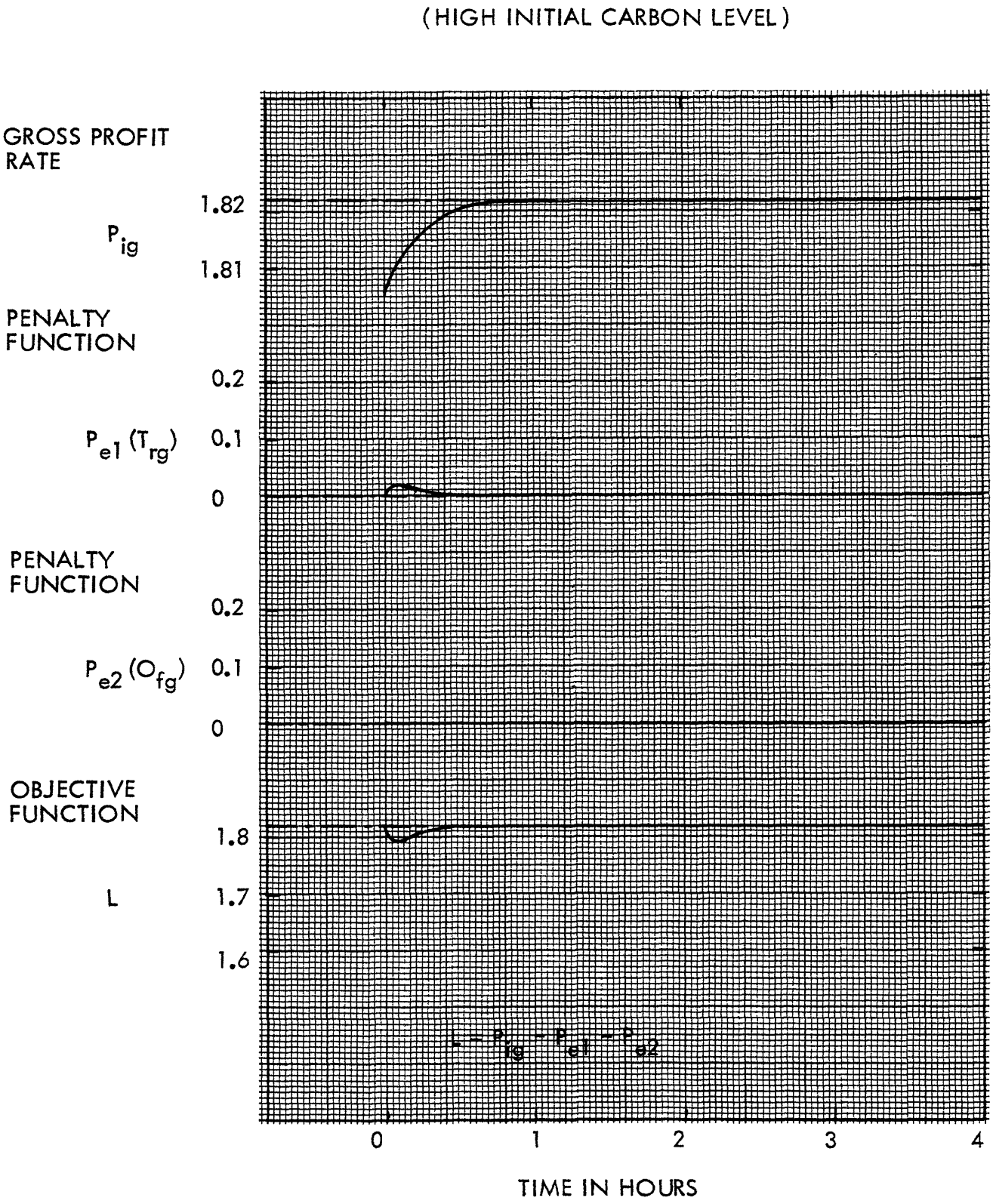

Fig. J.2 Optimal Control Scheme for Initial Condition No. 1

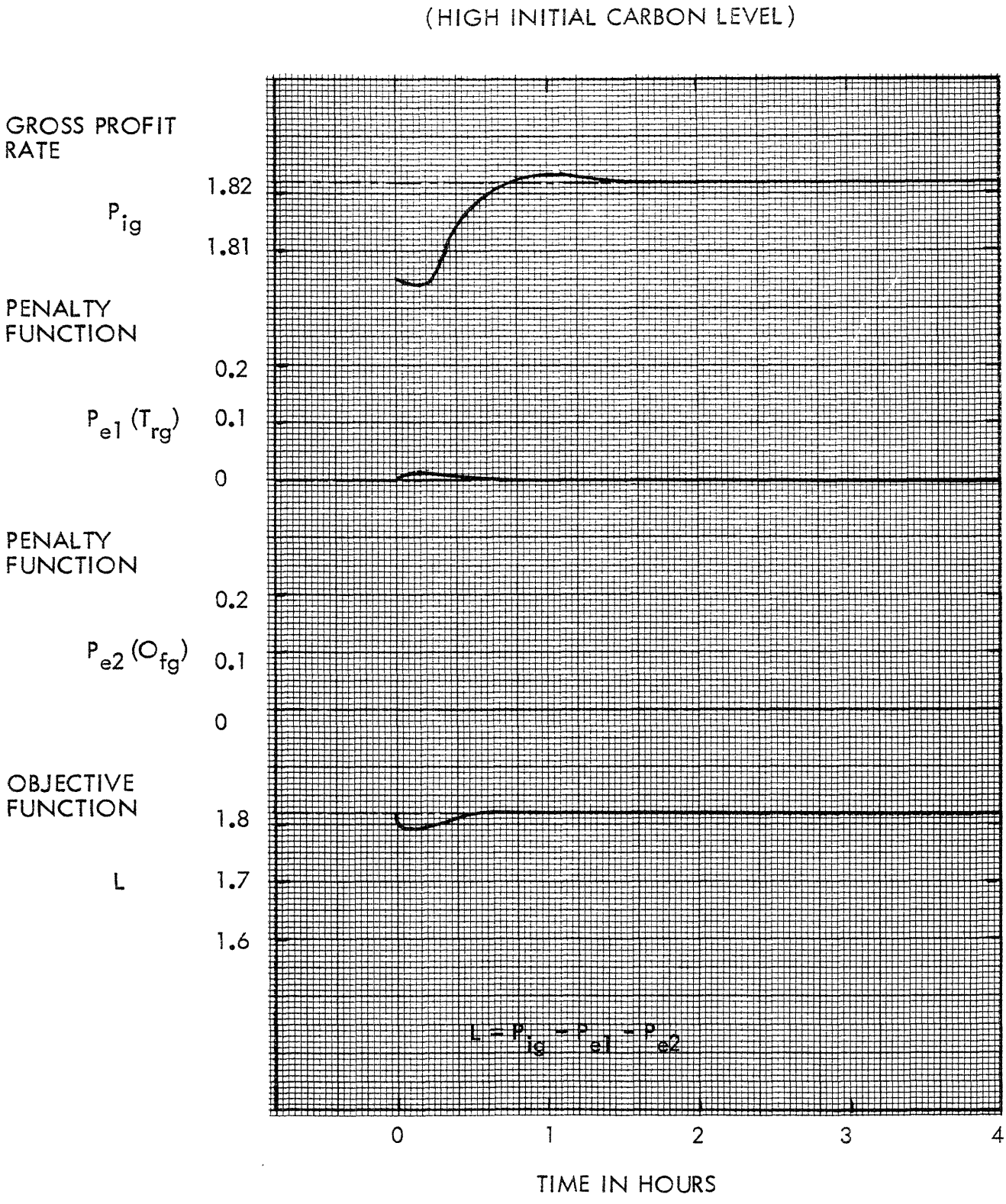

Fig. J.3 Alternative Control Scheme for Initial Condition No. 1

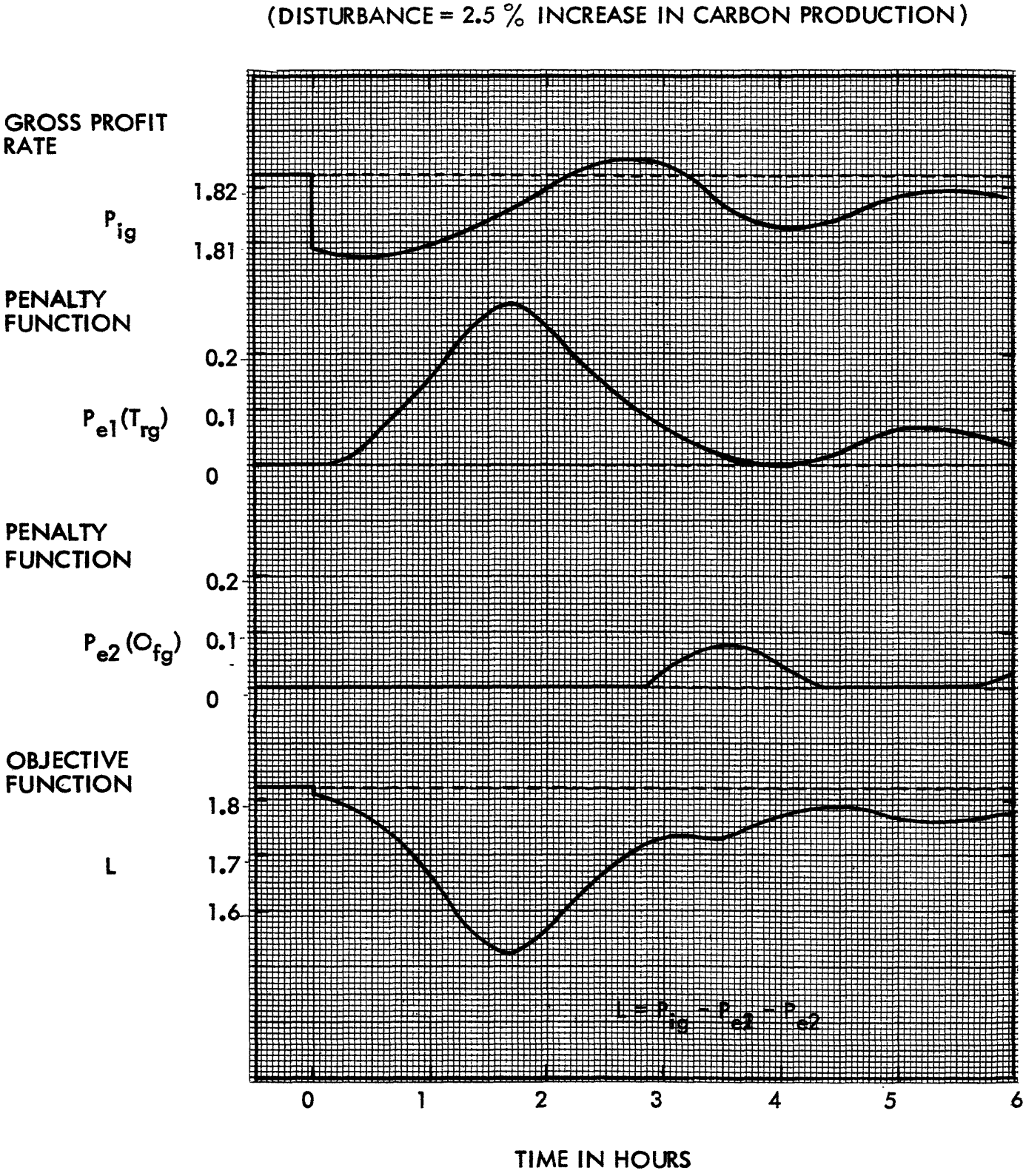

Fig. J.4 Performances of Conventional Control Scheme (No. 2)

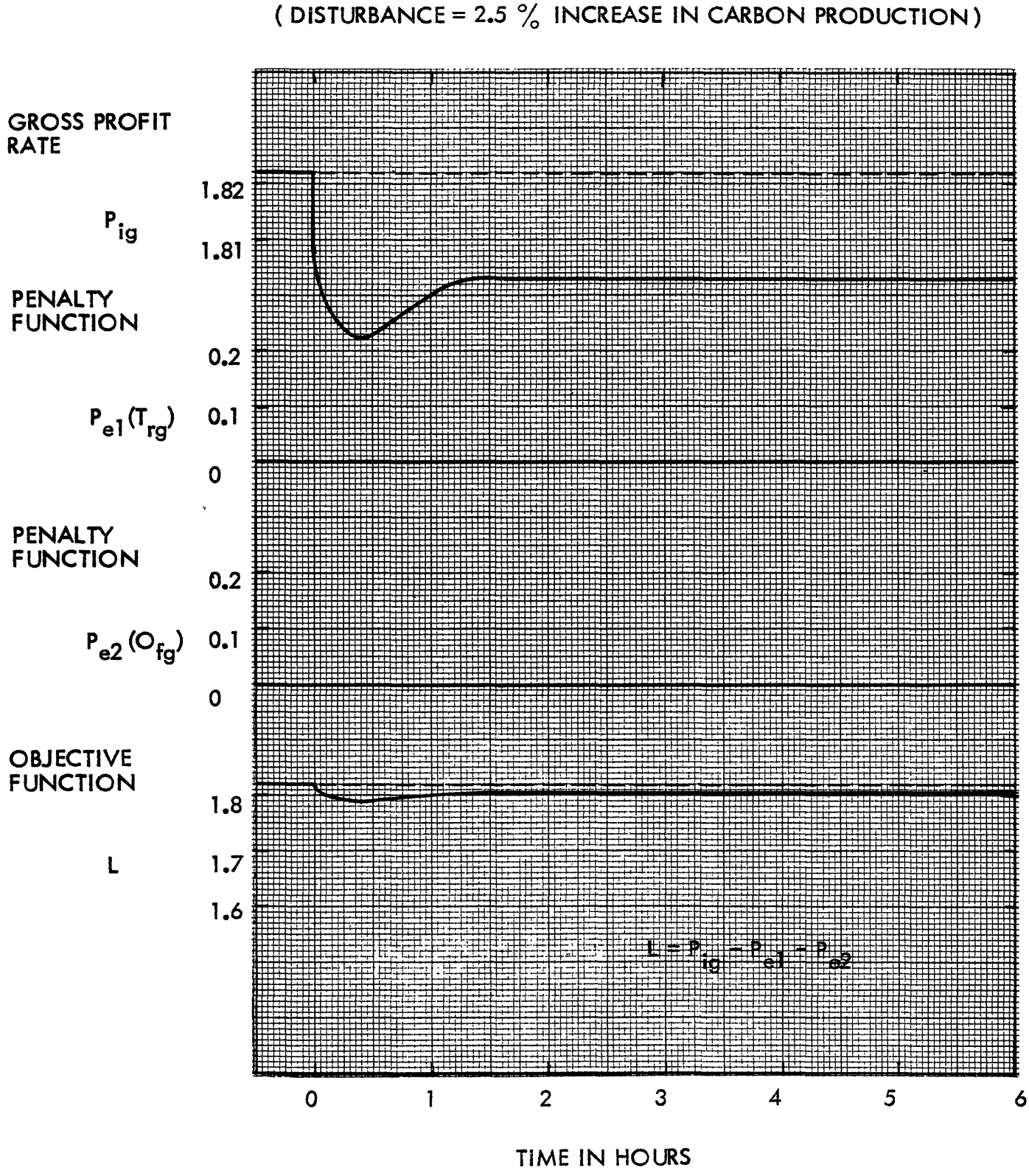

Fig. J.5 Performance of Alternative Control Scheme (No. 2)

level, the two penalty functions penalized the objective function and the resulting poor performance is apparent. Figure J.5 supplements the results shown in Fig. 1.15, where the alternative control scheme was simulated for the same disturbance. Since the two penalty functions are negligibly small, in this case the objective function remains at a highest level. The difference in performance between Figs. J.4 and J.5 is evident.

The conclusion that the alternative control scheme is better than the conventional control scheme is consistent with the relative values of the objective function achieved for each scheme.

APPENDIX K

NOMENCLATURE

A_1	Constant for R_{oc} introduced in Eq. 3.17	
A_2	Constant for R_{cf} introduced in Eq. 3.18	
C	Conversion introduced in Eq. A.11	%
C_1	Stoichiometric coefficient defined by Eq. B.15	lb. oxygen/lb. coke
C_2	Coefficient for K_{od} defined by Eq. B.17	(M lb. oxygen/ hr., psia, ton of cat.)(hr./ M lb.)^2
C_3	Coefficient for K_{or} defined by Eq. B.16	M lb. oxygen/ hr, psia, ton of coke
C_4	Coefficient for T_{fg} defined by Eq. B.18	^{o}F/% oxygen
C_{cat}	Catalytic carbon on spent catalyst	wt. %
C_{ff}	Conversion on fresh feed	vol. fract.
C_{rc}	Carbon on regenerated catalyst	wt. %
C_{res}	Residual carbon on spent catalyst	wt. %
C_{sc}	Carbon (total) on spent catalyst	wt. %
C_{tf}	Conversion on total feed	vol. fract.
D_{co}	Density of cycle oil	lb./gal.
D_{ff}	Density of fresh feed	lb./gal.
$D_{g\ell}$	Density of gasoline	lb./gal.
D_{rf}	Density of recycle feed	lb./gal.
e_i	i-th relaxation parameter introduced in Eq. 2.12	

NOMENCLATURE (Contd.)

f_i	i-th function of $\underline{x}$ and $\underline{u}$ introduced in Eq. 2.6	
$F_{g\ell}$	Gasoline yield factor introduced in Eq. F.12	
F_{tf}	Coke formation factor of total feed introduced in Eq. A.35	$\frac{\text{(M lb. carbon/hr)}}{\text{(M bbl/day)}}$
g_i	i-th function of $\underline{x}$ introduced in Eq. G.3	
H	Hamiltonian function defined by Eq. 2.9	
H_{ra}	Reactor catalyst holdup	ton
H_{rg}	Regenerator catalyst holdup	ton
$I_{g\ell}$	Gasoline recracking intensity defined by Eq. F.7	
J	Objective functional defined by Eq. 2.5	
K_{cc}	Velocity constant for catalytic carbon formation defined by Eq. A.14	
k_{cc}	Constant for K_{cc}	
K_{cr}	Velocity constant for catalytic cracking defined by Eq. A.17	
k_{cr}	Constant for K_{cr}	
K_I	Integral controller gain	
K_{od}	Oxygen diffusion coefficient	M lb. oxygen/ ton cat., psia, hr.
K_{or}	Oxygen reaction coefficient	M lb. oxygen/ ton coke, psia, hr.
K_P	Proportional controller gain	
L	Integrand of J	
M	1,000	

NOMENCLATURE (Contd.)

O_{fg}	Oxygen in flue gas	mol.%
p_i	i-th costate variable introduced in Eq. 2.9	
P_{co}	Price of cycle oil	$/bbl.
P_1	Penalty function defined by Eq. 3.20	
P_2	Penalty function defined by Eq. 3.21	
P_{ff}	Price of fresh feed	$/bbl.
$P_{g\ell}$	Price of gasoline	$/bbl.
P_{gr}	Gross profit	M$
P_{gs}	Price of gas	$/lb.
P_{ra}	Reactor pressure	psia
P_{rg}	Regenerator pressure	psia
P_s	Steady state profit rate expressed by Eq. I.1	
R	Gas law constant	
R_r	Recycle ratio	
R_{ai}	Air rate	M lb./hr.
R_{cb}	Coke burning rate	M lb./hr.
R_{cc}	Catalytic carbon forming rate defined by Eq. A.13.	
R_{cf}	Coke (total) forming rate	M lb./hr.
R_{ff}	Fresh feed rate	M bbl./day
R_{oc}	Gas oil cracking rate	M lb./hr.
R_{rc}	Regenerated catalyst rate	ton/min.
R_{rf}	Recycle feed rate	M bbl./day

NOMENCLATURE (Contd.)

R_{sc}	Spent catalyst rate	ton/min.
R_{tf}	Total feed rate	M bbl./day
S_a	Specific heat of air	Btu./lb., ^oF
S_c	Specific heat of catalyst	Btu./lb., ^oF
S_f	Specific heat of feed	Btu./lb., ^oF
T_{ai}	Air inlet temperature	^oF
T_{fg}	Flue gas temperature	^oF
T_{fp}	Fresh feed preheater temperature	^oF
T_{ra}	Reactor temperature	^oF
T_{rf}	Recycle feed temperature	^oF
T_{rg}	Regenerator temperature	^oF
t	Time	hr
u_i	i-th control variable	
u_i^*	i-th optimal control variable	
u_i^s	i-th optimal control variable in steady state	
$W/H/W_c$	Weight hourly space velocity introduced in Eq. A.11	
x_i	i-th state variable	
x_i^*	i-th optimal state variable	
x_i^s	i-th optimal state variable in steady state	
y_i	i-th function of state variables defined by Eq. H.2	
Y_{ck}	Coke yield on fresh feed	wt. fract.
Y_{co}	Cycle oil yield on fresh feed	vol. fract.

NOMENCLATURE (Contd.)

$Y_{g\ell}$	Gasoline yield on fresh feed	vol. fract.
Y_{gs}	Gas yield on fresh feed	wt. fract.
$\Delta E'_{cc}$	Activation energy (intrinsic) of catalytic carbon formation	Btu./lb. mole
$\Delta E'_{cc}$	Activation energy (apparent) of catalytic carbon formation	Btu./lb. mole
$\Delta E'_{cr}$	Activation energy (intrinsic) of catalytic cracking	Btu./lb. mole
$\Delta E'_{cr}$	Activation energy (apparent) of catalytic cracking	Btu./lb. mole
ΔE_{or}	Activation energy of oxygen reaction	Btu./lb. mole
ΔH_{cr}	Heat of cracking	Btu./lb.
ΔH_{fv}	Heat of feed vaporization	Btu./lb.
ΔH_{rg}	Heat of regeneration	Btu./lb.
θ_c	Residence time of catalyst	
θ_o	Residence time of gas oil	

APPENDIX L

LITERATURE CITATIONS

1. Abbott, M. D., Archibald, R. C., Dorn, R. W., "How Hydrogen Improves Cat Cracker Feed," Oil Gas J., 56, p. 144, May 19, 1958.

2. Aliev, V. S., Al'tman, N. B., Kasinova, N. P., "Some Relationships in the Burning of Coke, Deposited on Finely Divided Silica-Alumina Catalyst, in a Stationary Fluidized Bed," Azerbaidzhan, Neftyanoe Khoz., No. 10, pp. 27-31, 1956.

3. Andrews, J. M., "Cracking Characteristics of Catalytic Cracking Units," Ind. Eng. Chem., 51, 4, p. 507, April, 1959

4. Andrews, J. A., Barr, W. E., Wills, J. B., "How Phillips Collects Complete FCC-Unit Data," Oil Gas J., 60, pp. 93-95, July 23, 1962.

5. Appleby, W. G., Gibson, J. W., Good, G. M., "Coke Formation in Catalytic Cracking," Ind. Eng. Chem. PD & D, 1, 2, p. 162, April, 1962.

6. Athans, M., Falb, P. L., Optimal Control-An Introduction to the Theory and its Applications, McGraw-Hill, 1966.

7. Bailey, W. A., Morse, N. L., "Cat Cracking's Luster Undimmed," Oil Gas J., 64, pp. 110-114, March 14, 1966.

8. Bell, H. S., American Petroleum Refining, D. van Nostrand Co., 1959.

9. Binford, J. S., "Kinetics of the Oxidation of Graphite," Advances in Chemistry Series, ACS, No. 20, 1958.

10. Blanding, F. H., "Reaction Rates in Catalytic Cracking of Petroleum," Ind. Eng. Chem., 45, p. 1186, June, 1953.

11. Bondi, A., Miller, R. S., Schlaffer, W. G., "Rapid Deactivation of Fresh Cracking Catalyst," Ind. Eng. Chem., PD & D, 1, 3, pp. 196-203, July, 1962.

12. Chien, G. K. L., Computer Control in Process Industries, Chap. 20 in "Leondes," C. T. (ed) Computer Control Systems Technology, McGraw-Hill, 1961.

LITERATURE CITATIONS (Contd.)

13. Crawford, P. B., Cunningham, W. A., "Carbon Formation in Cat. Cracking," Petroleum Refiner, p. 169, Jan., 1956.

14. Daniels, L. S., "Fluid-Catalyst Technique," Petroleum Refiner, 25, 9, pp. 435-442, 1946.

15. Dart, J. C., Oblad, A. G., "Heat of Cracking and Regeneration in Catalytic Cracking," Chem. Eng. Prog., 45, 2, p. 110, Feb., 1949.

16. Dart, J. C., Savage, P. T., Kirkbride, C. G., "Regeneration Characteristics of Clay Cracking Catalyst," Chem. Eng. Prog., 45, 2, pp. 102-110, Feb., 1949.

17. Demmel, E. J., Perrela, A. V., Stover, W. A., Shambaugh, J. P., "Cat-Cracking Catalysts Show Savings," Oil Gas J., 64, pp. 178-180, May 16, 1966.

18. Demmel, E. J., Perrella, A. V., Stover, W. A., Shambaugh, J. P.,"Save with New Cracking Catalysts," HP/PR, 45, 5, pp. 145-148, May, 1966.

19. Emmett, P. H., (ed), Catalysis, Vol. 6, Reinhold Pub., 1958.

20. Enos, J. L., Petroleum Progress and Profits-a History of Process Innovation, M.I.T. Press, 1962.

21. Farrar, G. L., "Computer Control Comes of Age," Oil Gas J., 61, pp. 77-100, October 28, 1963.

22. Farrar, G. L., "Computer Control in the Oil Industry," Oil Gas J., 62, pp. 89-114, October 26, 1964.

23. Farrar, G. L., "Computer Control in the Oil Industry," Oil Gas J, 63, p. 92, Oct. 25, 1965.

24. Frank-Kamenetskii, D. A., Diffusion and Heat Exchange in Chemical Kinetics, Princeton Univ. Press, 1955.

25. Gandsey, L. J., "Two-Way Communication Between Operators and Computers," Chem. Eng. Prog., 61, 10, p. 93, October, 1965.

26. Gilliland, E. R., Mason, E. A., Oliver, R. C., "Gas Flow Patterns in Beds of Fluidized Solids," Ind. Eng. Chem., 45, pp. 1177-1185, June, 1953.

LITERATURE CITATIONS (Contd.)

27. Gould, L. A., Chemical Process Control, to be published, 1967.

28. Greensfelder, et al., "Catalytic Cracking of Pure Hydrocarbons," Ind. Eng. Chem., 37, pp. 514, 983, 1038, 1168, 1945.

29. Handlos, A. E., Kunstman, R. W., Schissler, D. O., "Gas Mixing Characteristics of a Fluid Bed Regenerator," Ind. Eng. Chem., 49, 1, pp. 25-30, Jan., 1957.

30. Hansford, R. C., "AMechanism of Catalytic Cracking," Ind. Eng. Chem., 39, pp. 849-852, 1947.

31. Heldman, et al., "Two-Stage Fluid Cat. Cracking," Oil Gas J., p. 230, May 21, 1956.

32. Hicks, R. C., Worrell, G. R., Durney, R. J., "Analog-Digital Cat-Cracking-Model Development," Oil Gas J., pp. 97-105, Jan. 24, 1966.

33. Horn, F., Troltenier, U., "Über den optimalen Temperaturverlauf im Reaktionsrohr," Chem. Ing. Tech., 32, pp. 382-393, 1960.

34. "Humble Bolsters Confidence in Future of Catalytic Cracking," Oil Gas J., p. 54, Aug. 23, 1965.

35. Johnson, M. F. L., Mayland, H. C., "Carbon Burning Rates of Cracking Catalyst in the Fluidized State," Ind. Eng. Chem., 47, pp. 127-132, Jan., 1955.

36. Kalman, R. E., "Contributions to the Theory of Optimal Control," Bol. Soc. Mat. Mex., 5, pp. 102-109, 1960.

37. Kane, E. D., Lewis, C. D., Schuyten, H., Beck, R. D., "Computer Control of an FCC Unit," Natl. Petrol. Refiners' Assoc. Computer Conf., Tech Paper 62-38, 1962.

38. Kipiniak, W., Dynamic Optimization and Control-A Variational Approach, M.I.T. Press and Wiley, 1961.

39. Kurihara, H., "Optimal Control of Stirred-Tank Chemical Reactors," Report ESL-R-267, Electronic Systems Laboratory, M.I.T., May, 1966.

LITERATURE CITATIONS (Contd.)

40. Lavrouskii, K. P., Rozental, A. L., "The Kinetics of the Regeneration of Powdered Catalysts," Izv. Akad. (Tekh.) No. 6, pp. 140-148, 1955.

41. Leva, Fluidization, McGraw-Hill, 1959.

42. Luyben, W. L., Lamb, D. E., "Feedforward Control of a Fluidized Catalytic Reactor Regenerator System," Chem. Eng. Prog. Symp. Series, 59, 46, 1963.

43. MacDonald, M., "Automatic Control of a Fluid Catalytic Cracking Unit," Pet. Refiner, p. 87, Oct., 1946.

44. May, "Fluidized-Bed Reactor Studies," Chem. Eng. Prog., 55, pp. 49-56, Dec., 1959.

45. Mills, "Aging of Cracking Catalyst-Loss of Selectivity," Ind. Eng. Chem., 42, pp. 182-187, 1950.

46. Moorman, J. W., "What is the Effect of Feed Preheat, Part 5," Oil Gas J., p. 68, Jan. 10, 1955.

47. Murphree, et al., "Improved Fluid Process," Trans. A.I.Ch.E, 41, p. 19, 1945.

48. Murphree, E. V., Brown, C. L., Fischer, H.G.M., Gohr, E. J., Sweeney, W. J., "Fluid Catalyst Process (Catalytic Cracking of Petroleum)," Ind. Eng. Chem., 35, pp. 768-773, 1943.

49. Nelson, W. L., Petroleum Refinery Engineering, McGraw-Hill, 1958.

50. Nelson, W. L., "Circulation Control in Fluid Process," Oil Gas J., p. 120, Apr. 14, 1949.

51. "NPRA Panel Discusses Cat-Cracking Techniques," Oil Gas J., pp. 108-113, Aug. 1, 1966.

52. Oden, E. C., Granberry, T. S., "Propane Deasphalted Gas Oil as Catalytic Cracking Feed Stock," Ind. Eng. Chem., 44, p. 896, 1952.

53. Olsen, C. R., Sterba, M. J., "Effect of Reactor Temperature on Product Distribution and Product Quality in Fluid Cat. Cracking," Chem. Eng. Prog., pp. 692-700, Nov., 1949.

LITERATURE CITATIONS (Contd.)

54. Panchenkov, G. M., Golovanov, N. V., Kinetics of Regeneration of Alumina-Silicate Catalysts-Reaction Mechanism of Oxidation of Coke on Alumina-Silicate Catalysts," Izv. Akad. (Tekh.) No. 3, pp. 384-394, 1952.

55. "Panel Fields Searching Questions on Cat-Cracking Technology," Oil Gas J., 63, p. 95, Aug. 2, 1965.

56. Pansing, W. F., "Regeneration of Fluidized Cracking Catalysts," A.I.Ch.E.J., 2, 1, pp. 71-74, March, 1956.

57. Pohlenz, J. B., "How Operational Variables Affect Fluid Catalytic Cracking," Oil Gas J., p. 124, April 1, 1963.

58. Pontryagin, L. S., Boltyanskii, V., Gamkredize, R., Mischenko, E., The Mathematical Theory of Optimal Processes, Interscience Publishers, Inc., 1962.

59. Pugh, A. L., DYNAMO Users Manual, M.I.T. Press, Cambridge, Mass., 1961.

60. Rosenbrock, H. H., Storey, C., Computational Techniques for Chemical Engineers, Pergamon Press, 1966.

61. Satterfield, C. N., Sherwood, T. K., The Role of Diffusion in Catalysis, Addison-Wesley, 1963.

62. Savas, E. S., Computer Control of Industrial Processes, McGraw-Hill, 1965.

63. Schrage, R. W., "Optimizing a Catalytic Cracking Operation by the Method of Steepest Ascents," Presented at the Pittsburgh Meeting of A.I.Ch.E., Sept., 9-12, 1956.

64. Schulman, B. L., "Building a Mathematical Model for Catalyst Regeneration in Fixed Beds," Ind. Eng. Chem, 55, 12, pp. 44-49, Dec., 1963.

65. Shankland, R. V., Schmitkons, G. E., "Determination of Activity and Selectivity of Cracking Catalyst," Proc. Am. Petrol. Inst., 27, Part III, p. 57, 1947.

66. Singer, E., Todd, D. B., Gunn, V. P., "Catalyst Mixing Patterns in Commercial Catalytic Cracking Units," Ind. Eng. Chem., 49, 1, pp. 11-19, Jan., 1957.

LITERATURE CITATIONS (Contd.)

67. Sittig, M., "Catalytic Cracking Techniques in Review," Pet. Refiner, pp. 263-316, Sept., 1952.

68. Sittig, M., "Fluidized Solids," Chem. Eng., pp. 219-231, May, 1953.

69. Smith, W. M., "Advances in Fluid Catalytic Cracking," to be presented at the 7th World Petroleum Congress, Mexico City, April, 1967.

70. Stormont, D. H., "What's Ahead for Cat Cracking," Oil Gas J., 62, p. 78, Aug., 17, 1964.

71. Stormont, D. H., "Data Logging Computers Help Study of Fluid Cat Cracker Operation," Oil Gas J., 61, pp. 142-144, Nov. 18, 1963.

72. Stormont, D. H., "Fluid Cracker Revamp Ups Gasoline Output," Oil Gas J., 62, p. 87, Feb. 24, 1964.

73. Todd, D. B., Wilson, W. B., "Stack Loss of Catalyst from Commercial Catalytic Cracking Units," Ind. Eng. Chem., 49, 1, pp. 20-24, Jan, 1957.

74. Voorhies, A. Jr., "Carbon Formation in Catalytic Cracking," Ind. Eng. Chem., 37, p. 318, 1945.

75. Weekman, V. W., Harter, M. D., Marr, G. R., "Hybrid Computer Simulation of a Moving-Bed Catalyst Regenerator," Presented at A.I.Ch.E. 59th National Meeting, Columbus, Ohio, May 18, 1966.

76. Weisz, P. B., "Intra-particle Diffusion in Catalytic Systems," Chem. Eng. Prog. Symp. Series, 55, 25, p. 29, 1959.

77. Zabrouskii, Hydrodynamics and Heat Transfer in Fludized Bed, M.I.T. Press, 1966.

78. Zenz, F. A., Othmer, D. F., Fluidization and Fluid Particle Systems, Reinheld, New York, 1960.

APPENDIX L

BIOGRAPHICAL NOTE

Hirofumi Kurihara was born July 14, 1940, in Hiroshima Pref., Japan. He entered Tokyo University in April, 1959, and graduated with a Kogakushi in Applied Physics in March, 1963. From April, 1963, he was working with Toa Nenryo Kogyo, Japan, until he took an educational relief in July, 1964. In September, 1964, he entered the Massachusetts Institute of Technology, where he received his Master of Science degrees in Chemical Engineering and Electrical Engineering in June, 1966.

He performed research on distillation column control systems during the summer of 1965 at the Esso Research and Engineering Company, in Florham Park, New Jersey, and on fluid catalytic cracking processes during the summer of 1966, in Baytown, Texas.